Quantifying Sex and Asexuality Using an Ancestral Recombination Graph (ARG) Approach



Tymoteusz Pieszko

St Cross College

University of Oxford

A thesis submitted for the degree of

Doctor of Philosophy

Michaelmas 2025

Declaration

Unless explicitly stated, I declare that all code, analyses, and written material presented in this thesis were created by me. The AI language model ChatGPT Edu (developed by OpenAI) was used for code debugging and refactoring, occasional editing of written text, and for writing the original draft of this declaration. ChatGPT did not generate any original analyses or research content. All outputs from the AI were critically reviewed, verified, and incorporated solely at my discretion.

The work has not been submitted for any degree or professional qualification except as specified.

Tymoteusz Pieszko, Michaelmas 2025

Acknowledgements

I would like to express my sincerest gratitude to my supervisors, Tim Barraclough and Jerome Kelleher, for the many, many hours we spent discussing our research, and for their unwavering support in helping me develop my ideas. Tim, Jerome, I hope you both know how much I have learned from you – thank you!

I would also like to thank all members of the Barraclough and Kelleher groups, especially Reuben Nowell for his expert bioinformatics advice, Yan Wong and Shing Zhan for fun occasional chats, and, most of all, Chris Wilson for sharing his infectious passion for bdelloid rotifers. And thank you for Dorset and France, Chris!

Thank you to all my friends from Oxford and beyond – Lingchen Huang, Alena Chemulova, Michael Berson, Saba Ishrat, Vrinda Jariwala, Robert Lu, Aavika Dhanda, Bil Todorova, Will Paine, Andrew Spires, Joris Alkemade, Teja Dandu, Prarthana Agrawal, Elisa Mogollón Pérez, Daniel Cazares López, Cédric Lood, Jacob Wilde, Claire Marr, Martyna Krupińska, Haaziquah Tahir, Szymon Kość, Franek Bryk (to the Polish guys – so glad to have known you since high school!), and Carla Wagener (for always being my Brother).

Finally, two very special acknowledgements. To my Parents – for enabling me to get where I am today. To Chio – for her support, our adventures in the UK, Perú, Poland, and for being simply the best.

Abstract

Although many testable hypotheses have been proposed, biologists still do not know why sexual reproduction exists. Sex is often portrayed as one of the major unresolved problems in evolutionary science. Intuitively, asexuality, the vertical transfer of genetic material from parent to offspring, appears to be a much simpler and effective mode of propagation. In this thesis, I focus on an essential prerequisite for testing hypotheses of sex – the methodology for reconstructing histories of sexual and asexual reproduction from DNA sequence data. Specifically, I use the lens of ancestral recombination graphs (ARGs) to distinguish and quantify genealogical signatures of sex from those of recombination occurring asexually. In Chapter 1, I introduce my ARG-based analytical framework and use biologically-realistic models of asexuality that include recombination via gene conversion or crossing-over to demonstrate its advantages over standard approaches. Concurrently, I develop a framework for the signatures expected across a range of asexuality–sex scenarios. Building on this foundation, in Chapter 2, I develop a new ARG-inspired approach for genealogical analysis, explicitly tailored to the problem of reproductive history reconstruction. Finally, in Chapter 3, I apply my methodology to genomic datasets for two species of bdelloid rotifers – a group famous for their asexuality, yet recently the subject of debate over presumed signatures of cryptic sex. The results are consistent with an asexual mode of reproduction. Throughout this research, I highlight issues of technical artefacts and uncertainty, which are critical to consider in systems where sex may occur only rarely, while other forms of recombination can be common. Collectively, my DPhil work provides the foundation for improved and flexible methodology of reproductive mode reconstruction from DNA sequence data, addressing a critical gap in the field.

Contents

General Introduction **1**
Sex, asexuality and recombination 3
Detecting and quantifying sex and asexuality 9
Ancestral recombination graphs of reproductive history 20
Bdelloid rotifers as a study system 22
References 28
Supplement to General Introduction **40**
Chapter 1: Detecting and quantifying rare sex in natural populations **57**
Abstract 58
Introduction 59
Results 64
Discussion 79
Methods 83
Acknowledgments 87
References 88
Supplement to Chapter 1 ..... **97**
Supplementary Text 1: Models of asexuality with asyngamous recombination 98
Supplementary Text 2: Simulation pipeline 105
Supplementary Text 3: Comparison of MP and CF models 107
Supplementary Text 4: Comparison of genealogical inference with IQ-TREE and SINGER 108
Supplementary Text 5: $\boldsymbol{K}$, a statistic to measure the signal of reproductive mode from unphased, genome-wide SNPs. 110
Supplementary Figures 115
Supplementary Tables 132
References 137
Chapter 2: A parsimony-based approach to genealogical analysis of reproductive mode **139**
Introduction 140
Methods 144
Results 146
Discussion 151
References 153
Supplement to Chapter 2 ..... **156**

Supplementary Figures 157
References 159
Chapter 3: Asexual divergence in epibiotic bdelloid rotifers of the genus *Rotaria*.... 160
Abstract 161
Introduction 162
Results 166
Discussion 179
Materials and Methods 181
References 185
Supplement to Chapter 3 190
Supplementary Figures 191
Supplementary Tables 199
References 205
General Discussion 206
In the grip of summaries 207
Selection and the genomic landscape of reproduction 208
Improved simulation-based inference 211
What's next for bdelloid rotifers? 212
References 212

General Introduction



——————————— O ———————————

Tymoteusz Pieszko

——————————— O ———————————

Contributions

➔ Above: Antonie van Leeuwenhoek's bdelloid rotifer from a letter to Hendrik van Bleyswijk, dated 9th February 1702.

➔ A classical chapter of which I am the sole author. The introduction to bdelloid rotifers is partly based on my contributions to a published review article (see Supplement):

- Wilson, C.G., Pieszko, T., Nowell, R.W. and Barraclough, T.G. (2024). Recombination in bdelloid rotifer genomes: asexuality, transfer and stress. *Trends in Genetics*, DOI: 10.1016/j.tig.2024.02.001.

The ability to reproduce defines life. In eukaryotes, reproductive modes can be broadly classified as sexual or asexual. Sex – defined by meiosis (a reductional cell division) and ploidy restoration through syngamy (the fusion of cells produced in two distinct meiotic divisions) – underlies eukaryotic life cycle diversity. Meiosis and syngamy separate the haploid (post-meiosis) and diploid (post-syngamy) phases of the cycles, whose relative lengths vary across the group. In many unicellular eukaryotes (e.g., the green alga *Chlamydomonas*; Harris, 2001), fungi (e.g., Ascomycota; Amses et al., 2022) and some land plants (e.g., mosses), the haploid phase predominates, comprising multiple asexual generations or a long-lived multicellular stage. At the other end of the spectrum, sex in its most familiar form is known from the vascular plants and animals, where the diploid generation reproduces through ephemeral haploid spores (plants) or gametes (animals). Asexual reproduction, in turn, encompasses diverse forms of propagation without ploidy reduction: from mitotic binary fission in (haploid or diploid) 'protists' (Sherwood et al., 2014), production of unreduced eggs / seeds (e.g., in parthenogenetic animals), to budding (e.g., *Hydra*; Tannreuther, 1909), whole-body fission (e.g., planarian flatworms; Malinowski et al., 2017) and fragmentation (algae, land plants). Variation in the modes of reproduction, its causes and consequences, has long been a major focus of ecological and evolutionary science.

This thesis aims to develop a general framework for reconstructing the histories of sexual and asexual reproduction from population genomic data. In the General Introduction, after outlining the issues of reproductive evolution in eukaryotes (*Why is sex so common and yet some organisms abandon it?*), I provide an overview of the present approaches to reconstructing past reproduction from sequence data. I posit that the lack of methodological developments has limited progress in the broader field of reproductive mode evolution and argue that this gap can be most naturally addressed using the concept of ancestral recombination graphs (ARGs). Finally, I introduce bdelloid rotifers, a class of semi-aquatic

micrometazoans (in)famous for their presumed long-term asexuality, as an ideal system to test my proposed analytical framework.

Sex, asexuality and recombination

The origins of meiosis and syngamy are unclear, with hypotheses that differentially emphasise the role of meiotic machinery in DNA repair (Bernstein et al., 1988; Hörandl & Speijer, 2018) or the evolutionary benefits of cycling ploidy (Cavalier-Smith, 2002; Lenormand et al., 2016). It is nonetheless generally accepted that the last eukaryotic common ancestor (LECA) was sexual (Cavalier-Smith, 2002), as evidenced by the presence of homologues of genes associated with meiosis (the 'meiosis toolkit'; Hofstatter et al., 2020), plasmogamy (gamete fusion) and karyogamy (nuclear fusion) across the major eukaryotic radiations (Hofstatter & Lahr, 2019; Speijer et al., 2015). This does not imply, however, that we are close to a thorough understanding of the distribution and diversity of sexual cycles, especially in groups where most reproductive cell divisions are mitotic, such as the 'protists' and fungi. In the protists, a sexual cycle is usually inferred indirectly: for example, meiosis and syngamy have been directly observed in only 20% of the known free-living lineages, most of the rest being unculturable (Rizos et al., 2024). While sex appears fairly widespread in fungi (e.g., approx. half of Ascomycota have long been known to produce sexual spores; Reynolds & Taylor, 1993), the fungal life cycles are highly diverse, with sex frequency varying from very rare *(e.g., in Saccharomyces cerevisiae*; Bennett & Turgeon, 2016) to very frequent (e.g., in the plant pathogen *Sclerotinia*; Nieuwenhuis & James, 2016), and a vast range of the number of mating types, i.e., the classes of compatibility for syngamy (up to over 20,000, as in the wood-degrading fungus *Schizophyllum commune*; Kothe, 1996). In addition, fungi employ parasexual cycles, where cell fusion is followed by chromosome loss during vegetative propagation without meiosis (Bennett & Turgeon, 2016; Mishra et al., 2021). The parasexual cycle of the pathogen *Candida albicans*, for instance, was only documented in the last two decades (Mishra et al., 2021), and it is unclear if a similar process occurs outside of the laboratory (Nieuwenhuis &

James, 2016), hinting at underexplored diversity. The situation is more clear-cut in animals and plants, where frequent or even obligate sexual reproduction with two sexes is the norm; in fact, the discovery of parthenogenesis by von Siebold (1856) was initially likened to a hypothetical ‘exception to the law of gravitation’ (Churchill, 1979). It is estimated that less than 1% of animals are obligate parthenogens (Vrijenhoek, 1998; White, 1973; van der Kooi et al., 2017) and a similar proportion of angiosperms are obligate apomicts (i.e., reproduce through unreduced seeds; Mogie, 1992; Van Dijk, 2009).

The persistence of sex across the eukaryotic tree of life strongly indicates that it confers fundamental benefits. Obligate asexual taxa with a well-validated status (e.g., through extensive fieldwork and experimentation, as in many all-female squamates; Barley & Cole, 2025) tend to appear as ‘twigs’ on the phylogeny (Williams, 1975; Schwander & Crespi, 2009), a pattern typically interpreted as arising from high rates of extinction and limited long-term evolutionary potential (Avise, 2008). It was not until relatively late, however, that the paradox in the success of sexuality was pointed out by Maynard Smith (1971), who noted that a lineage of parthenogenetic females should easily invade a sexual population, doubling in frequency each generation, known as the ‘twofold cost of sex’ (Maynard Smith, 1978). While this cost rests on the assumption of anisogamy and may be mitigated if males contribute additional resources to offspring (e.g., through parental care; Lehtonen et al., 2012), meiosis itself is an energy-consuming and lengthy process. In single-celled eukaryotes, meiosis may require from five to 100 times the duration of mitosis (Lehtonen et al., 2012; Lewis Jr, 1983), implying a demographic disadvantage of at least 1 : 8 (4 vs 2^5 offspring). The mitotic population might continue growing, while a new meiotic division will only be initiated upon encountering a compatible cell (or a mate in animals; Lehtonen et al., 2012). Furthermore, syngamy is no guarantee of future success, since meiotic recombination breaks down allele combinations that allowed their parents to reproduce (Feldman, 1972). Indeed, one might wonder why sexuality did not disappear in distant geological epochs.

So, what benefits does sexual reproduction confer, as strong as to maintain it in spite of its manifold costs? Some of the foundational theoretical works include those of Fisher (1930), Muller (1932, 1964) and Hill and Robertson (1966). Although differing in emphasis, all these authors considered the effects of recombination on evolutionary rates. Fisher (1930) and Muller (1932) observed that recombination combines beneficial alleles arising in different genetic backgrounds, that would otherwise co-occur only through rare sequential mutation. A later addition by Muller (1964) was a similar argument for the restoration of genotypes carrying few deleterious alleles, otherwise irreversibly lost ('Muller's ratchet'). Hill and Robertson (1966), on the other hand, modelled how chance associations between alleles interfere with their selective response: the quicker an association is broken down by recombination, the more efficient the response of an allele. That these works describe different facets of the same effect of 'selective (Hill-Robertson) interference' (Otto, 2021) was realised by Felsenstein (1974), who concluded his synthesis with an argument for how, under recurrent environmental change, recombination facilitates the removal and the fixation of deleterious and beneficial variation, respectively. One such source of environmental change in nature is the 'Red Queen dynamics' (a metaphor sourced from Lewis Carroll's *Through the Looking-Glass*) of antagonistic coevolution between hosts and parasites (Van Valen, 1973; Bell, 1982). Following a general analysis of recombination rates under fluctuating selection (Charlesworth, 1976), the idea that parasite-imposed selection favours sex (Jaenike, 1978) was explicitly modelled by Hamilton (1980), who showed that sexuality gains an advantage through the generation of rare, parasite-resistant genotypes. Though many alternative hypotheses have since been proposed (Kondrashov, 1993), selective interference (Otto, 2021) and the Red Queen hypothesis (Lively, 2010) are generally regarded as the most potent answers to the 'sex question' (jointly reviewed by Hartfield & Keightley, 2012; Otto, 2009). What unites the theoretical work on this topic is that the maintenance of sex is typically investigated by contrasting recombining and non-recombining (clonally-reproducing) haploids (but see, for example, Otto (2003), for the benefits of segregation in diploids).

One complication that has been almost universally neglected is that asexual reproduction is commonly accompanied by homologous recombination, contradicting the strictly clonal picture. I call such recombination ‘asyngamous recombination’ (Fig. 1) – that is, recombination uncoupled from syngamy – to differentiate it from the common notion of ‘sexual recombination’ (Felsenstein, 1974). Asyngamous recombination occurs in the diploid phase, when homologous chromosomes have the opportunity to pair (Fig. 1A). Depending on whether non-sister or sister chromatids co-segregate (outcomes B-G in Fig. 1), asyngamous recombination induces or protects from the loss of heterozygosity (LOH), respectively. Indirect evidence of asyngamous recombination is seen in the generally low intragenomic divergence in predominantly asexual taxa, except those of hybrid origin (Jaron et al., 2021). Perhaps its best documented pathways are associated with mitotic reproduction in the yeast *S. cerevisiae*. A double-strand break (DSB) during budding in *S. cerevisiae* can be repaired through homologous recombination, with a crossover (CO) or non-crossover (NCO) resolution (both associated with localised gene conversion), or through non-homologous end joining (NHEJ) (Symington et al., 2014; Jinks-Robertson & Petes, 2021). Under the standard mitotic co-segregation of non-sister chromatids, a recombinant locus (Fig. 1A) has a $\frac{1}{2}$ chance of undergoing LOH (outcomes B-E), while heterozygosity is maintained otherwise. On a genome-wide scale, different molecular pathways can lead to mosaic LOH, including interstitial tracts (from < 100 bp to megabase-scale LOH in the middle of chromosomes) and terminal tracts (generally kilobase to megabase-scale LOH at chromosome ends) (Vijayan et al., 2025; Dutta et al., 2021). Another fungal type of asyngamous recombination occurs with intra-tetrad mating (Zakharov, 2005), as observed in *S. cerevisiae* and other Ascomycota (e.g., *Neurospora tetrasperma*; Meunier et al., 2018) and Basidiomycota (e.g., *Microbotryum violaceum*; Hood & Antonovics, 2000). Here, a meiotic division is followed by the fusion of haploid cells (e.g., spores within an ascus in ascomycetes), with a theoretical $\frac{1}{3}$ chance of LOH at both recombinant and non-recombinant

loci (outcomes B-G) that is modulated by the spatial organisation and mating-type compatibility of meiotic products (Zakharov, 2005).

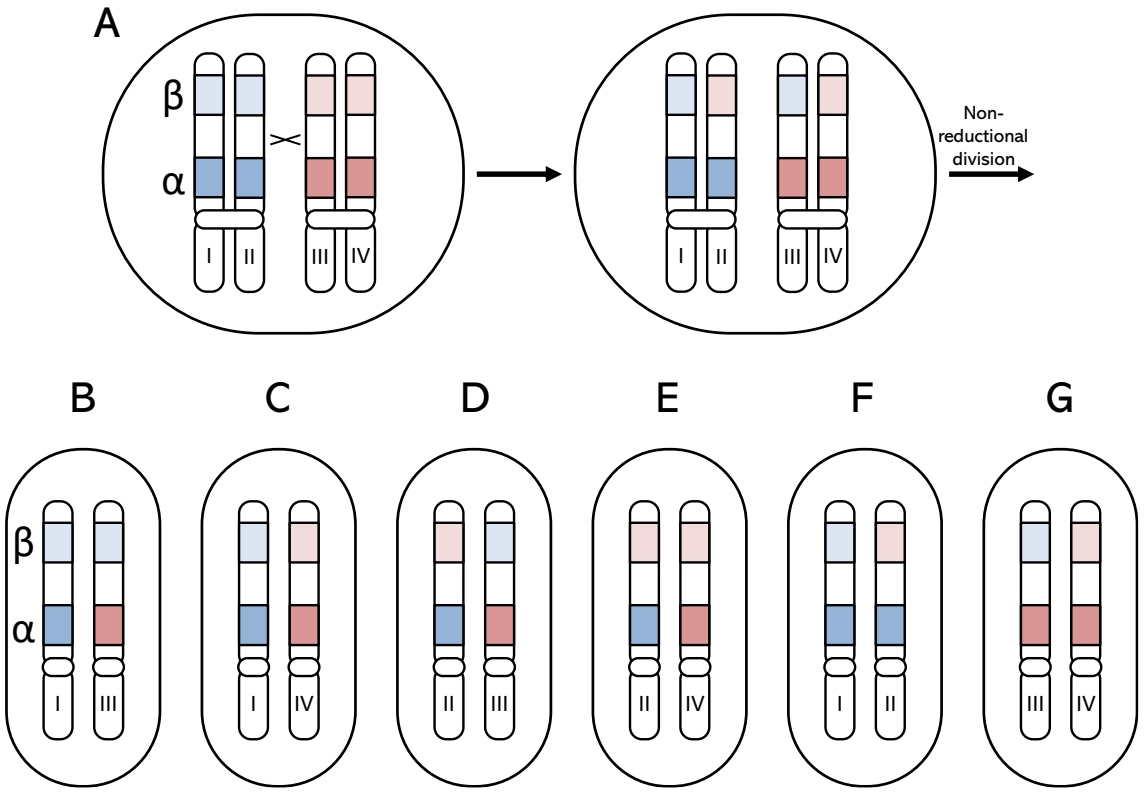


Fig. 1. Asexual chromatid segregation modulates the consequences of recombination: a two-locus example with a single crossover (CO). (A) A CO between loci α and β leads to a recombinant configuration at the CO-distal locus β, followed by a non-reductional (mitotic or meiotic) cell division. (B-G) The six theoretically possible combinations of chromatids in a non-reduced gamete. Random pairing with equiprobable outcomes B-G results in a $\frac{1}{3}$ chance of LOH (non-simultaneously) at either locus. If only non-sister chromatids co-segregate (B-E), as in mitotic and certain forms of meiotic asexuality ('central fusion automixis'; Suomalainen et al., 1987), a $\frac{1}{2}$ chance of LOH at locus β is expected, with no LOH at locus α. If only sister chromatids co-segregate (F and G), as in certain forms of meiotic asexuality ('terminal fusion automixis'; Suomalainen et al., 1987), LOH is avoided at locus β but occurs at locus α. See Stenberg and Saura (2009) for cytological diagrams of how ploidy is restored in different forms of non-reductional meiosis.

In animals, reminiscent of intra-tetrad mating are the non-reductional meiotic pathways of broadly-defined automixis (Suomalainen et al., 1987; but see Blanc et al., 2025 for a harsh critique of this term). In some taxa (e.g., *Drosophila mangabeirai*; Murdy & Carson, 1959; or

the mayfly *Ephoron shigae*; Sekiné & Tojo, 2010), sister chromatids co-segregate, leading to immediate genome-wide LOH unless heterozygosity is rescued by recombination (outcomes F and G). Several taxa where parthenogenesis was originally described as non-recombining and mitotic (e.g., the water flea Daphnia pulex; Zaffagnini & Sabelli, 1972; or bdelloid rotifers; Hsu, 1956b; Hsu, 1956a) have, in turn, been found to employ meiotic pathways with the co-segregation of non-sister chromatids (Hiruta et al., 2010; Terwagne et al., 2022). It has recently been argued that meiotic pathways may, in fact, be the sole mechanism of animal parthenogenesis, with the concept of 'mitotic parthenogenesis' arising from misinterpreted cytological observations (Blanc et al., 2025).

Beyond the precise cytology of asexual pathways, signatures of asyngamous recombination have been documented across eukaryotes ranging from protists (e.g., diatoms; Bulankova et al., 2021), through parthenogenetic animals (with a particularly rich *Daphnia* literature; e.g., Keith et al., 2016; Flynn et al., 2017), to fruit crops propagated by cuttings (e.g., pineapple; Chen et al., 2019). Of note, mitotic recombination is frequently implicated in cancers, for example, when LOH leads to loss of function of tumour-suppressor genes, conveying a selfish advantage to cancer cells (Luo et al., 2000). While asyngamous recombination and LOH have been portrayed as important evolutionary forces in asexuals (e.g., *S. cerevisiae*; Peter et al., 2018; or human-pathogenic yeasts; Diogo et al., 2009; Gusa & Jinks-Robertson, 2019), as supported by plastic responses to stress (e.g., Bulankova et al., 2021; Forche et al., 2011), the subject has received relatively little theoretical attention. Indeed, asyngamous recombination could (partly) alleviate the negative consequences of asexuality with respect to the behaviour of both beneficial and deleterious mutations (Mandegar & Otto, 2007; Engelstädter, 2017; Kopčak & Hartfield, 2024). For the present work, however, the important point is that sequence diversity patterns in asexuals, especially obligate asexuals, might be largely shaped by asyngamous recombination.

Detecting and quantifying sex and asexuality

Influential authors often refer to sex as an ‘enigma’ (Hartfield & Keightley, 2012; Otto, 2009), whose ‘embarrassing existence’ (West et al., 1999) is the ‘Queen of Problems in evolutionary biology’ (Bell, 1982). It indeed appears likely that no universal explanation of sex exists, with multiple factors operating simultaneously or on a case-by-case basis (Neiman et al., 2017; West et al., 1999). Nonetheless, the questions of ‘why’, ‘when’ and ‘to what extent’ remain pertinent. An appealing approach is to study genomic datasets for natural populations, aiming to link the observed sequence diversity patterns (e.g., signatures of inefficient selection; Jaron et al., 2021) with known reproductive mode. In an ideal world, such information would be known from natural history observations. Since these do not exist for most taxa, the key first step is to use the genomic dataset to reconstruct the reproductive history itself.

In Table 1, I collated 25 case studies that reconstruct reproductive mode from patterns of sequence diversity, mostly genome-wide SNPs. Rather than an exhaustive search, I performed a broad taxonomic survey of the literature, aiming to develop an understanding of the questions of interest, the analytical approaches employed, and the challenges and potential issues in the relevant literature. Having identified asyngamous recombination as an overlooked force in asexuals, I only included organisms sampled in the diploid (or higher ploidy) phase. By necessity, this focus excluded a number of asexual taxa, including haploid protists (Gibson, 2021), fungi (Nieuwenhuis & James, 2016) and plants with gametophyte-dominant life cycles (e.g., Sandler et al., 2023). Overall, the major goal of these studies is the detection and quantification of rare genetic exchange in (typically miniscule) groups that are difficult to study in natural conditions. These groups range from those where the mechanisms of sexual reproduction are well-characterised (e.g., *Saccharomyces* or the diatom *Thalassiosira pseudonana*) to those where meiosis and syngamy have not been observed (e.g., the intestinal parasite *Giardia duodenalis* or bdelloid rotifers). Across this

breadth of systems, I distinguished two approaches that are routinely used in conjunction to reconstruct histories of sexual and asexual reproduction.

Table. 1. Reconstructing histories of sex and asexuality using DNA sequence data. I collated representative studies for diploid taxa from across the major eukaryotic groups (protists, fungi, plants and animals). For each study, I report results with respect to within and between-locus diversity ('the diversity-summary approach') as well as SNP or tree-based arguments used to support specific reproductive histories ('the genealogical approach'). Unless specified otherwise, the analyses are based on genome-wide SNPs from multiple (> 2) re-sequenced genomes. Abbreviations used: HWE – Hardy-Weinberg equilibrium, asex. – asexual, σ – per-generation rate of sex, het. – heterozygosity, inds – individuals.

Taxon	Study	Deviation from HWE?	Linkage disequilibrium (LD)	Genealogical analysis	Interpretation
Protists					
Diatoms (Bacillariophyceae) – a class of single-celled, typically facultative asexual algae (Krueger-Hadfield, 2024)					
Thalassiosira pseudonana	Koester et al. (2018)	Het. excess in an asex. strain + LOH of up to 320 kb	Few recombination breakpoints in an asex. strain	NA	Origin of an asex. strain linked to ancestral inbreeding
Leishmania – a genus of parasitic excavates, agents of leishmaniosis; meiosis and syngamy unknown, but genetic exchange (through unknown means) observed in the lab (Akopyants et al., 2009; Ferreira et al., 2022)					
L. aethiopica	Hadermann et al. (2023)	F_{IS}= 0.03 (after removing near-identical genomes) + LOH of up to > 1 Mb	Decay (r^2 of 0.60 → 0.20)	A genotype-based phylogenetic network to identify the origin of hybrids	History of hybridisation, sex, but also frequent LOH during asexuality
L. braziliensis	Van den Broeck et al. (2020)	F_{IS} = -0.11 (but mode at 0) + rare LOH	NA	SNP analysis (e.g., PCA), genotype trees to identify hybrids	History of sex and hybridisation with *L. peruviana* (see below)
L. peruviana	Van den Broeck et al. (2020)	F_{IS} = -0.54	NA	As for *L. brasiliensis*	Hybrids with *L. brasiliensis*

L. donovani	Franssen et al. (2020)	Five-fold variation in het. between strains	Decay (r^2 of 0.80 → 0.20) or no decay depending on the sub-population	SNP analysis + kDNA¶ trees to identify hybrids	History of inbreeding (low-het. strains) and hybridisation (high-het. strains)
L. infantum (of the *L. donovani* complex)	Rogers et al. (2014)	F_{IS} = 0.88	One crossover per 2.3 Mb per generation	Haplotype trees to identify a parent of putative hybrids	Hybridisation with an unknown strain, then sex (and inbreeding) at $\sigma \approx 1.33 \times 10^{-5}$
Trypanosoma – a genus of parasitic excavates, agents of Chagas disease; meiosis and gametes observed in *T. brucei* (Peacock et al., 2014)					
T. brucei gambiense	Weir et al. (2016)	Median per-SNP F_{IS} = -1 + LOH of up to 2 Mb	'Complete genetic linkage'	Haplotype trees showing Meselson effect	Obligate asexuality
T. cruzi	Berry et al. (2019)	Negative mode of per-SNP F_{IS} + LOH of up to 468 kb	NA	NA	Clonality + inbreeding inferred from long-range LOH
T. cruzi	Schwabl et al. (2019)	F_{IS} 'near 0' (but clonal clusters also present)	Decay (r^2 of 0.80 → 0.15) or no decay depending on the sub-population	Haplotype tree incongruence	'Panmixia'; frequent sex up to $\sigma \approx 3.0 \times 10^{-3}$
Entamoeba and *Giardia* – genera of human-pathogenic protists without known sexual cycles (Weedall & Hall, 2015); in the excavate *Giardia*, an asyngamous process of diplomixis (a fusion of two nuclei within a cyst) has been documented (Capewell et al., 2021)					
E. histolytica	Weedall et al. (2012)	NA	Four-gamete test for recombination (Hudson & Kaplan, 1985)	NA	Cryptic sex
G. duodenalis	Lasek-Nesselquist et al. (2009)	Very low het.	Four-gamete test (see above)	Genotype tree incongruence	Cryptic sex

Fungi					
Yeasts (Basidiomycota) – single-celled fungi such as the facultative sexual *Saccharomyces* (Murphy & Zeyl, 2010) and the human-pathogenic *Candida* with a parasexual cycle (Mishra et al., 2021)					
S. paradoxus	Johnson et al. (2004); Tsai et al. (2008)	F_{IS} = 0.98	Decay (r^2 of 0.40 → 0.15)	NA	$\sigma \approx 10^{-3}$ (94% intra-tetrad mating, 5% selfing, 1% outcrossing)
S. cerevisiae	Magwene et al. (2011)	Elevated het. compared to a laboratory strain, but high F_{IS} (0.44 – 0.95)	NA	NA	Mitotic recombination with LOH since outcrossing 50,000 gens ago ($\sigma \approx 3.33 \times 10^{-5}$)
C. albicans	Wang et al. (2018)	LOH of up to > 50 kb	NA	Patterns of hybridisation in IBD blocks and mtDNA trees	Frequent LOH and parasexual genetic exchange
Plants (embryophytes)					
Duckweed *Spirodela polyrhiza*	Ho et al. (2019)	F_{IS} = 0.04	Decay (r^2 of 0.60 → 0.15)	NA	$\sigma \approx 10^{-2}$
Animals					
Placozoan *Trichoplax adherens* – embryos (unclear if fertilised) and a single (!) sperm cell were observed (Eitel et al., 2011)	Signorovitch et al. (2005)	NA	NA	Putative allele sharing patterns at 7 loci (without tree inference)	Cryptic sex
Fungus-growing ant *Mycocepurus smithii*	Rabeling et al. (2011)	F_{IS} = -1.00 in some, up to 0.03 in other populations	NA	NA	218 / 234 colonies asexual; cryptic sex in others

Nematodes (Nematoda) – a speciose phylum (> 25,000 spp.) that includes some of the most prominent crop pests, the asexually-reproducing root-knot nematodes *Meloidogyne* (Castagnone-Sereno & Danchin, 2014)					
Mesorhabditis belari – sperm required for egg development (Grosmaire et al., 2019)	Blanc et al. (2023)	F_{IS} = -0.02	LD lost within 100 bp (LDhelmet analysis; Chan et al., 2012)	NA	At most very rare sex; het. maintained through co-segregation of recombinant non-sister chromatids (cytological analysis)
The rice root-knot nematode *Meloidogyne graminicola*	Phan Thi et al. (2025)[§]	LOH of up to > 100 kb; tracts shared between isolates	Decay (r^2 of 0.98 → 0.13); four-gamete test for recombination (Hudson & Kaplan, 1985)	NA	Predominant asexuality, cryptic sex
Oribatid mites (Oribatida) – a mite order with many independent transitions to asexuality (Norton & Palmer, 1991), though males are known even in putative obligate asexuals (Taberly, 1988)					
Oppiella nova	Brandt et al. (2021)	F_{IS} = -0.33; but 2/9 inds with lower het. than a sexual relative	NA	69 / 223 haplotype trees topologically closer to Meselson effect than to clustering by population	Long-term asexuality with lineage-heterogenous LOH
Platynothrus peltifer	Öztoprak et al. (2025)	Excess of heterozygous sites	NA	> 96% of haplotype trees showing Meselson effect	Long-term asexuality (20 million years)

Stick insects (Phasmatodea) – an insect order where 80 out of 3,500 species are documented facultative or putative obligate asexuals (Schwander et al., 2025)					
Timema spp. (eight populations) - males known (Schwander et al., 2013; Vickery & Sandoval, 2001, 1999), parthenogenesis leads to genome-wide LOH (Jaron et al., 2022)	Freitas et al. (2023)	Six populations with low and two with higher het.	High in six populations, decay in two populations (r^2 ≈ 0.75 → 0.2, but variable between chromosomes)	NA	Rare cryptic sex in two populations previously thought obligate asexual
Bacillus spp. – mostly facultative sexuals with various mechanisms of parthenogenesis (Larose et al., 2023; White, 1973)	Lavanchy et al. (2024)	Het. lower than expected given inferred hybridisations	NA	SNP analysis to identify hybrids	Multiple hybrid lineages, LOH post-hybridisation (or other explanations for low het.)
Bdelloid rotifers (Bdelloidea) – a class within the superphylum Gnathifera (Vasilikopoulos et al., 2024), where no males have been ever observed; see *Bdelloid rotifers as a study system*.					
Adineta vaga	Vakhrusheva et al. (2020)	F_{IS} = -0.03	r^2 of 1.0 → 0.2	Allele sharing in > 12% of haplotype trees (eight inds) + putative hybrids (three inds)	Sex (among eight inds) + hybridisation (three individuals)
Macrotrachela quadricornifera	Laine et al. (2022)	NA	NA	Identical haplotypes in 315 out of the 622 segments phased in 2 inds	Sex – sampled inds related as 'half siblings or double first cousins'

¶ Kinetoplast DNA from the single mitochondrion of excavates (Shapiro & Englund, 1995).
§ Preprint.

The diversity-summary approach

The origins of the ‘diversity-summary’ approach can be traced back to the early 1990s, when the availability of genetic markers stimulated interest in the prevalence of clonality in microorganisms (Tibayrenc et al., 1991; Maynard Smith et al., 1993). A clonal model of diploid asexuality makes clear predictions for the patterns of diversity within and across loci. First, independent evolution of the two haplomes (i.e., homologous genome copies) should lead to excess divergence within as opposed to between genomes. Known as the ‘Meselson effect’ (Mark Welch & Meselson, 2000; Butlin, 2002; White, 1973), this prediction states that asexual genomes should harbour unusual levels of heterozygosity or, at minimum, exceed the Hardy-Weinberg (HW) expectation for the proportion of heterozygous genotypes. The second prediction is that all sites across the genome evolve in strict linkage, as originally envisaged by Fisher (1930) and Muller (1932). In practical terms, a particular pattern of genotypes at locus 1 should be equally correlated with that at locus 10 as at locus 100. In contrast, recombination occurring between these loci would dissipate the correlation in a phenomenon of linkage disequilibrium (LD) decay. Taken together, the diversity-summary approach (as summarised by, e.g., Halkett et al., 2005) quantifies genetic exchange (e.g., *Is sex absent, rare or frequent?*) as a deviation from the clonal expectation for patterns of genetic diversity.

The studies in Table 1 apply different variants of the diversity-summary approach. Some invoke relative differences in heterozygosity between the sequenced genomes to support specific evolutionary hypotheses. Franssen et al. (2020), for instance, used heterozygosity differences among multiple genomes of parasitic excavates from the *Leishmania donovani* complex to identify groups of putative hybrids. In *Leishmania*, while hybrid lineages were generated during coinfection in laboratory conditions (Akopyants et al., 2009; Ferreira et al., 2022), meiosis and gametes remain unknown, and the prevalence of the hypothesised sexual cycle in natural conditions is unclear (Catta-Preta & Sacks, 2025). Similarly, Magwene et al. (2011) used elevated heterozygosity in wild *S. cerevisiae* isolates as

evidence of outcrossing and estimated its timing from LOH tracts presumed to have accumulated since. A commonly reported metric (14 / 25 of studies) is the inbreeding coefficient F_{IS} of Wright (1949), which takes negative values if the HW expectation is broken due to excess heterozygosity, and vice versa. Despite the clonal expectation, only 5 / 14 of studies recovered significantly negative F_{IS} in their focal asexuals, with values ≈ 0 in some groups where gametes and mating are unknown (e.g., in some *Leishmania* or the bdelloid rotifer *Adineta vaga*). On the other hand, $F_{IS} > 0$ and / or the presence of LOH tracts are differentially interpreted as evidence of inbreeding (e.g., in the asexual strain of the diatom *Thalassiosira pseudonana*) or an asyngamous process (e.g., in *C. albicans*), with contrasting interpretations of similar patterns even in the same system (e.g., of 'patchy' heterozygosity in *Leishmania*; see Franssen et al., 2020; Hadermann et al., 2023). Whenever examined (15 / 25 of studies), evidence of recombination was reported, as typically (8 / 15 of studies) measured with the between-genotype correlation coefficient r^2 (Rogers & Huff, 2009). Nonetheless, whether asyngamous recombination could drive these high-level patterns (i.e., beyond identifiable LOH tracts) was rarely considered explicitly. Instead, asyngamous recombination mechanisms were often downplayed as 'rare' or 'short-range' (Berry et al., 2019; Koester et al., 2018; Lasek-Nesselquist et al., 2009; Rogers et al., 2014; Van den Broeck et al., 2020; Weedall et al., 2012; Phan Thi et al., 2025), without evidence.

Arguments from within and across-locus diversity can be formalised to quantify sex. Tsai et al. (2008) used mutation and recombination-derived estimates of the effective population size N_θ and N_ρ, respectively, to compute the relative frequencies of meiotic and mitotic cell divisions in *S. cerevisiae*. Central to their logic is the assumption that only meiotic divisions contribute to LD decay – and thus, that there is no recombination during the asexual, mitotic phase – whereas both types of cell divisions contribute to within-locus diversity. Notwithstanding this limitation, obtaining N_θ and N_ρ requires independent estimates of the per-base, per-generation rates of mutation and recombination, which are unavailable for most taxa. Moreover, while Tsai et al. used sequence diversity around the *S. cerevisiae*

mating type locus *MAT* to quantify the frequency of selfing and intra-tetrad mating, similar information is typically lacking. Especially in animals, the distinction between sexual inbreeding and recombining asexuality is of primary importance, since the former requires the production of both female and male gametes, which is a precondition for outcrossing. It hence appears that the diversity-summary approach might be challenging to extend and fully incorporate asyngamous recombination, though further theoretical work on some of the open threads (e.g., Stoeckel & Masson, 2014) would be most welcome.

The genealogical approach

Because information loss is inherent in summaries, one can attempt to reconstruct the specific events that generated the observed genotypes. Since clonality predicts concerted evolution at all sites in a genome, the 'genealogical approach' analyses deviations from such a shared history to infer sexual events. A basic version of this approach uses SNP-sharing patterns to reconstruct putative sexual crosses (often loosely termed 'hybridisations') at the origin of asexual lineages, for example by matching SNPs in the focal lineage to candidate parent lineages. Such analyses can be performed when genetic exchange is thought rare overall, as in *Leishmania* (Franssen et al., 2020; Van den Broeck et al., 2020) or *C. albicans* (Wang et al., 2018), or when hybrid and parent populations are known to co-occur, as in *Bacillus* stick insects (Lavanchy et al., 2024). The argument can be made more explicit with the inference of genotype-based phylogenetic trees, where an intermediate placement points to a hybrid origin (e.g., Hadermann et al., 2023), and further supported by analysis of organelle genomes (e.g., Wang et al., 2018; Van den Broeck et al., 2020). Finally, topological variation among trees for different nuclear loci (i.e., 'incongruence', as often discussed in the context of gene tree-species tree conflict; Steenwyk et al., 2023) has been generally interpreted as indicating a sexual history (see, for instance, the commentary of Birky Jr, 2010a, on the findings in *G. duodenalis*).

The genealogical approach is potentially the most powerful when the two haplotypes per locus are recovered as separate tips in a tree. Birky Jr. (1996) was first to note that 'a

remarkable consequence' of clonal evolution would be the clustering of haplotypes from different individuals in a bisymmetric pattern – a tree formulation of the Meselson effect – with the tree root in the sexual ancestor (Fig. 2A). Different forms of recombination result in different subtree prune-and-regraft (SPR) operations to this 'clonal scaffold'. Asyngamous recombination can either result in a reciprocal exchange of tips (or larger subtrees, if operating at internal branches) or their LOH-induced clustering (Fig. 2B). Assuming no other processes affect tree topologies, all the remaining SPR operations can be attributed to genetic exchange. Already at the level of three individuals, however, a total of 945 rooted, bifurcating trees (Felsenstein, 1978) would need to be classified as 'asexuality-compatible' or 'sex-specific'. To circumvent this problem, two putative sex-specific topological patterns have been considered. On the one hand, the clustering of both haplotypes per genome by sub-population of origin has been interpreted, as in any standard sexual system, as evidence of population sub-division with pervasive gene flow within sub-populations (Brandt et al., 2021; but note an essentially identical pattern is expected if asyngamous recombination is pervasive within asexual sub-populations; Fig. 2C). On the other hand, the so-called 'allele sharing' pattern, or the clustering of haplotypes from one individual with haplotypes from two different individuals (Fig. 2D), has been taken as a specific signature of an outcrossing event (Vakhrusheva et al., 2020; Signorovitch et al., 2015). Probing for patterns of both kinds has been used as a method of detecting cryptic sexuality (e.g., Brandt et al., 2021; Vakhrusheva et al., 2020).

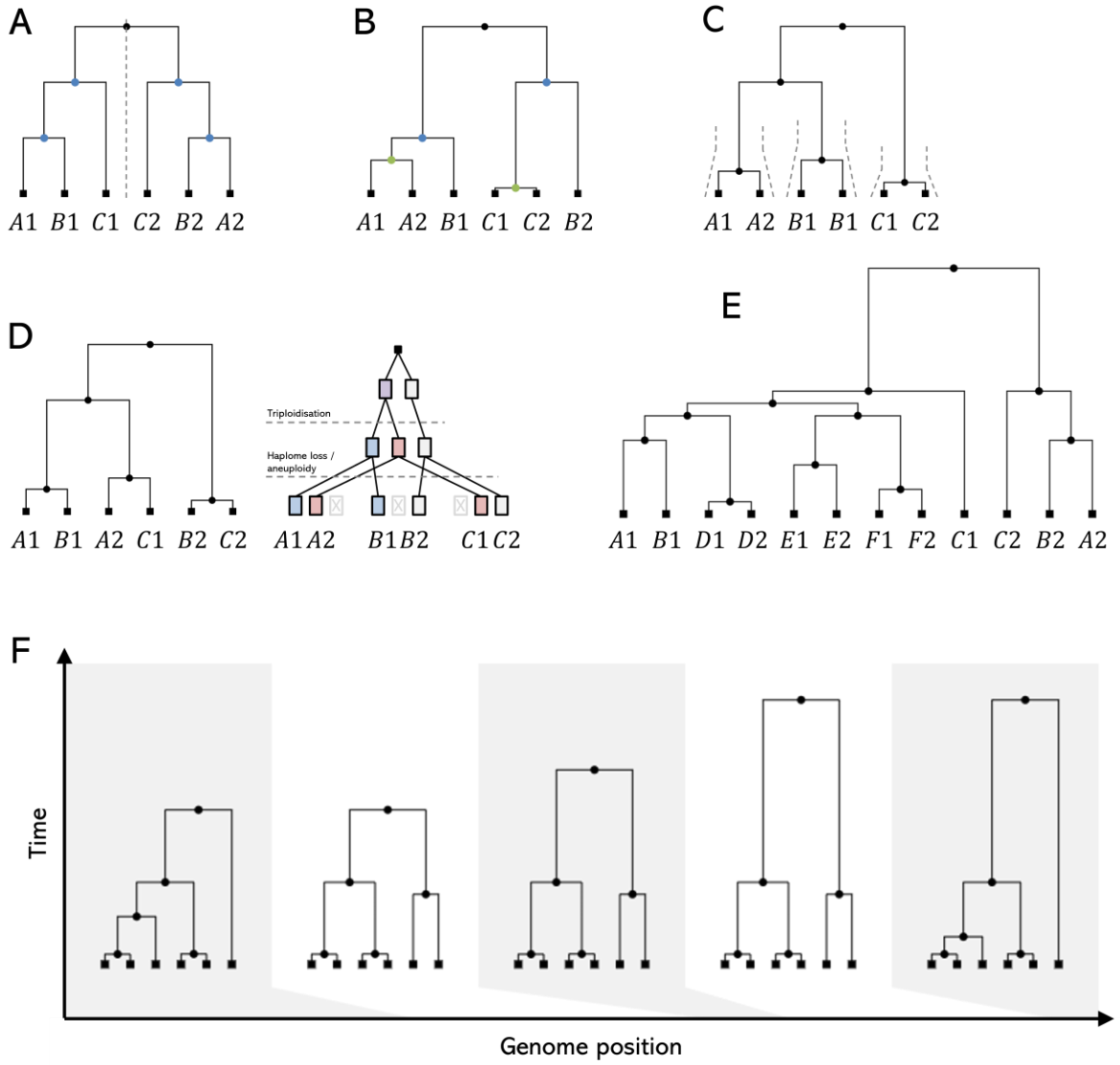


Fig. 2. Genealogical relationships and reproductive mode. The trees are shown for individuals A-F, each with haplotypes 1 and 2. (A) Topological Meselson effect under clonality; blue nodes correspond to splits between asexual lineages. (B) Asyngamous LOH at terminal branches (green nodes) brings haplotypes together within individuals. (C) Clustering of haplotypes by population of origin: sex (Brandt et al., 2021) or asyngamous recombination? (D) The 'allele sharing' pattern: sex (Vakhrusheva et al., 2020) or triploidisation followed by loss of homologous copies (right)? (E) Half of haplotypes cluster with a different population: hybridisation (see Fig. 2B in Rogers et al., 2014; Fig. 7 in Vakhrusheva et al., 2020) or asexuality with lineage-heterogenous LOH? (F) An ARG represented as a sequence of local trees: a sexual example simulated with msprime v1.3.2 (Baumdicker et al., 2022). Each tree describes a local non-recombining genealogy.

Haplotype analyses remain uncommon, largely because of the difficulty of obtaining high-quality haplotype-resolved data (Richards, 2018). An early genome-wide analysis by Weir et al. (2016) found evidence of independent, parallel haplotype evolution in the human-

infectious *Trypanosoma brucei gambiense* (Table 1), seemingly confirming the conviction that the Meselson effect is a hallmark of obligate asexuality (Butlin, 2002). That the situation is in fact more complex is illustrated by the animal literature, where two recent haplotype-based analyses yielded strikingly different conclusions: that of pervasive Meselson effect and ancient asexuality in the oribatid mite *Platynothrus peltifer* (Öztoprak et al., 2025), and of 'allele sharing', interpreted as arising from cryptic sex, in the all-female bdelloid rotifer *Adineta vaga* (Vakhrusheva et al., 2020). While I return later to a fuller discussion of this latter study's findings, here I highlight the most significant ways that genealogical approaches could be improved. At present, genealogical analyses are typically qualitative (but see Ruderfer et al., 2006), aimed to distinguish between the alternative asexual and facultative sexual scenarios as a binary trait. There are several possible pitfalls to this approach. At the most fundamental level, it is unclear what constitutes reliable evidence of sex when a large number of trees are inferred against a heterogenous background of asyngamous processes. The concept of 'sex-specificity' itself requires excluding processes such as gene duplication and loss, aneuploidy and whole-genome ploidy cycles (Fig 2D; very frequent in, e.g., *Leishmania*; Dujardin et al., 2014), and horizontal gene transfer (common in single-celled eukaryotes, e.g., Peck et al., 2024; Habig et al., 2024). Fitting sexual hypotheses to data poses a broader risk of confirmation bias: for instance, lineage-heterogenous LOH can easily generate patterns resembling hybridisation (Fig. 2E). All of these challenges could be addressed by establishing a quantitative link between genealogy and the history of sex, asexuality and asyngamous recombination.

Ancestral recombination graphs of reproductive history

In this thesis, I develop a framework for quantifying sex and asexuality using an approach based on ancestral recombination graphs (ARGs) to summarise haplotype histories. The concept of ARGs is rooted in the theory of coalescence developed in the 1980s (Kingman, 1982; Hudson, 1983, 1990) to describe the formation of haplotype genealogies as a backwards-in-time process: from the extant haplotypes to the most recent common ancestor

(MRCA) of the sample. An ARG was originally defined as a realisation of the process of coalescence with recombination (Griffiths & Marjoram, 1997; Hudson, 1983), where lineages coalesce or split due to recombination until an MRCA is reached for each locus. The thus-defined ARG long remained a purely theoretical construct – primarily because the joint reconstruction of the history of coalescence and recombination, from among an unimaginable number of possibilities, is a computationally difficult problem (Nielsen et al., 2025). Nonetheless, the last decade has seen rapid progress in ARG reconstruction, with methods such as ARGweaver (Rasmussen et al., 2014) and the very recent SINGER (Deng et al., 2025) that approximate the coalescent with recombination by sampling from the posterior distribution of the Sequential Markov Coalescent model, alongside others, employing heuristic strategies to increase scalability (e.g., Kelleher et al., 2019; Speidel et al., 2019; Schaefer et al., 2021). In practice, a major conceptual advance of an ARG approach over classical tree-based methods is that local genealogies and recombination breakpoints are reconstructed (and analysed) jointly. Unfortunately, ARG thinking has not yet gained popularity in the broader field of evolutionary genomics, remaining largely confined to human genomics and disease-focused applications (Nielsen et al., 2025; Lewanski et al., 2024; Brandt et al., 2024).

The ARG has been described as the ‘holy grail of statistical population genetics’ (Hubisz & Siepel, 2020). An accurately reconstructed ARG is the best record of the evolutionary history that can possibly be extracted from the extant sequences. If available, such record can serve as the basis for further study of processes such as demography (Fan et al., 2025; Osmond & Coop, 2024; Wohns et al., 2022) and selection (Hejase et al., 2022; Stern et al., 2019). Here, I determine and quantify features of the ARG with respect to asexuality, asyngamous recombination and sex. I explore approaches to estimating recombination breakpoints – using a model-based (Chapter 1) and a parsimony-based approach (Chapter 2) – as an answer to the heterogenous signal that can be expected from the prevalence of asyngamous recombination in asexual systems (Table 1). In my work, I draw on several recent

developments in the field. For instance, I analyse ARGs in the succinct tree sequence (or 'tree sequence' for short; Fig. 2F) format, which enables seamless analysis of local genealogies in Python (while explicitly encoding linkage disequilibrium between neighbouring trees; see Kelleher et al., 2016; Whitehouse et al., 2024 for details). Moreover, I construct forwards-in-time models (Haller et al., 2019) of asexuality with asyngamous recombination, which I use to simulate the first (to my knowledge) ARGs under an exhaustive space of obligate and facultative asexual scenarios (Chapter 1; but see Hartfield et al., 2018, for a coalescent simulator of facultative asexual genealogies). Building on the newly gained understanding of the genealogical signatures of reproductive modes, I develop a parsimony-based, recombination-aware approach for reproductive history analysis (Chapter 2). Throughout the thesis, but especially in Chapter 3, my focus is on the arguably most famous and recently controversial group of asexual animals – the 'scandalous' (Maynard Smith, 1986) bdelloid rotifers.

Bdelloid rotifers as a study system[1]

'Here we see again the inconceivable possibilities … innate in such small creatures which escape our sight […]' – van Leeuwenhoek (1702)

After adding water to some dry dirt collected from a gutter, the Dutch microscopist Antonie van Leeuwenhoek observed 'animalcules' rolled-up into ovals which, within half an hour, stretched out their bodies and started swimming around (van Leeuwenhoek, 1702). These ovals, known as 'tuns' or sometimes 'xerosomes', were the dormant forms of microscopic invertebrates later identified as bdelloid rotifers (from Greek *bdella* or leech, for their leech-like movements; Hudson, 1884). The ubiquity of bdelloids in ephemeral freshwater habitats like moss or lichen (Ricci, 1987), where even a patch the size of a coin may harbour hundreds of individuals less than half millimetre long, made them a fond study subject of 19th century naturalists (Davis, 1873). By 1886, Hudson and Gosse noted a 'strange fact' about

[1] Section partly based on *Recombination in bdelloid rotifer genomes: asexuality, transfer and stress* by Wilson et al. (2024) (see Supplement).

bdelloids: no males had been seen, despite ‘a century and half of observation’ (Hudson & Gosse, 1886). Another century and half later, this strange fact holds for each of the 460 described species (Donner, 1965; Mark Welch et al., 2009; Segers, 2007), and despite direct observations of hundreds of thousands of individuals (Birky Jr, 2010b). With an estimated crown age of at least 50 million years (Segers, 2007; Tang et al., 2014), bdelloid rotifers are the oldest and largest clade of animals that lack a described sexual cycle.

The recognition of the paradox of sex stimulated interest in putative cases of long-term obligate asexuality (Maynard Smith, 1986; Judson & Normark, 1996; Normark et al., 2003). The reasoning was that lineages which have persisted without sex over evolutionary timescales could shed light on asexuality’s negative consequences that they had somehow managed to circumvent. Among the metazoans, the status of ‘ancient asexuals’ was most avidly argued for darwinulid ostracods (Martens et al., 2003; Schön et al., 2009; Butlin et al., 1998), the brine shrimp *Artemia parthenogenetica* (Baxevanis et al., 2006; Browne, 1992), oribatid mites (Heethoff et al., 2009; Maraun et al., 2004) and, finally, bdelloid rotifers. Apart from being the strongest candidates to the title (males were discovered in all the other groups; Taberly, 1988; Smith et al., 2006; Boyer et al., 2021), bdelloid rotifers possess unusual features of biology that could compensate for the lack of sex. Their ability to undergo dormancy upon desiccation (anhydrobiosis), as witnessed by van Leeuwenhoek, has been speculated to function as an ecological escape mechanism from Red Queen co-evolutionary dynamics (Ladle et al., 1993). This idea was verified experimentally by Wilson and Sherman (2010), who showed that the lethal fungal parasite *Rotiferophthora angustispora* is less resistant to desiccation than its bdelloid host *Habrotrocha elusa*, which can also disperse with wind (as ‘tuns’) to establish fungus-free populations (Wilson & Sherman, 2010). Moreover, already the early sequencing attempts revealed that over 8% of bdelloid genes have been transferred horizontally from non-metazoans, including bacteria, fungi, and plants (Gladyshev et al., 2008). Later work has shown these genes are implicated in DNA repair (Hecox-Lea & Mark Welch, 2018; Nicolas et al., 2023), silencing of

transposable elements (TEs) (Nowell et al., 2021) and / or gene regulation via epigenetic DNA modification (Rodriguez et al., 2022), long-chain fatty acid biosynthesis (Ribes-Navarro et al., 2023), freezing tolerance (Raymond, 2025) and, indeed, defence from fungal pathogens (Nowell et al., 2024). Taken together, one could imagine a scenario in which an unusual lifestyle combined with horizontally acquired evolutionary novelty enabled the asexual success of the bdelloid clade.

The last 25 years of bdelloid rotifer research have been marked by various attempts to confirm their obligate asexual status using sequence data. An early finding of highly divergent gene copies in four bdelloid species was initially interpreted as arising from long-term clonal reproduction (Mark Welch & Meselson, 2000). Later studies, however, revealed that bdelloid genomes are of degenerate tetraploid nature, with gene copies that arose via an ancient whole-genome duplication before the divergence of bdelloid families (Hur et al., 2009; Mark Welch et al., 2008). Similarly, the apparent paucity of TEs in five species, and the absence of class I retrotransposons in particular, was presented as additional evidence of bdelloid asexuality (Arkhipova & Meselson, 2000). If present, the vertically-transmitted class I retrotransposons could accumulate through a ratchet-like mechanisms, driving a non-recombining lineage extinct (Dolgin & Charlesworth, 2006; Wright & Finnegan, 2001). However, this finding was also overturned by later studies which revealed that bdelloid genomes harbour a diverse array of TEs, including class I retrotransposons (Gladyshev & Arkhipova, 2007, 2010; Gladyshev et al., 2007). Finally, the first bdelloid genome assembly of *Adineta vaga* contained rearrangements apparently incompatible with meiotic chromosome pairing and segregation (Flot et al., 2013). None of the subsequent bdelloid genomes (Nowell et al., 2018; Nowell et al., 2021), including a new, chromosome-scale *A. vag*a assembly (Simion et al., 2021), confirmed this finding, suggesting the reported rearrangements were an artefact of the first assembly.

With mostly diploid karyotypes (Mark Welch & Meselson, 1998), heterozygosity (≈ 0.05% - 4.5%; Nowell et al., 2018; Simion et al., 2021) within the range of values known from sexual

taxa (e.g., Mackintosh et al., 2019; Romiguier et al., 2014), and with a diverse TE landscape (Nowell et al., 2021), bdelloid genomes lack the characteristics classically predicted for clonal taxa (Normark et al., 2003; Jaron et al., 2021). The long-held assumption of bdelloid clonality (Ricci, 2017) originated from cytological studies in *Philodina roseola* (Hsu, 1956b) and *Habrotrocha tridens* (Hsu, 1956a), which reported that non-reduced eggs are produced without synapsis of homologous chromosomes. Already the first *A. vaga* genome assembly (Flot et al., 2013), however, showed an excess of identity tracts consistent with asyngamous recombination, while the later chromosome-level assembly (total length of ≈ 100 Mb) harboured LOH tracts of up to 4.5 Mb (Simion et al., 2021). While these observations would be entirely consistent with a mitotic process and the findings of Hsu (1956b, 1956a), a modern cytological analysis of *A. vaga* oogenesis revealed chromosome pairing and putative chiasmata (as in the prophase of meiosis), followed by the co-segregation of non-sister chromatids (Terwagne et al., 2022). Most recently, Houtain et al. (2024) studied the accumulation of LOH in *A. vaga* using a mutation accumulation-like design. Over the course of over 75 generations, the propagated lineages accumulated a diversity of LOH tracts, including short-range LOH (up to several kb; putative gene conversion events), long-range terminal LOH (up to several Mb; consistent with a single crossover) and interstitial LOH (consistent with two simultaneous crossovers). Overall, Houtain et al. (2024) estimated that LOH in *A. vaga* occurs at a spontaneous rate of 3.24×10^{-4} per-site, per-generation, i.e., at least four orders of magnitude higher than the typical rates of mutation (Wang & Obbard, 2023).

Two recent genealogical analyses claimed to resolve our picture of the bdelloid reproductive system. First, Vakhrusheva et al. (2020) inferred trees for 303 haplotype-resolved genomic segments obtained for eight wild-sampled *A. vaga* individuals, together spanning approx. 0.3% of their reference assembly. In over 12% of the trees, they found that *'two haplotypes of at least one individual had their reciprocal closest counterparts in two different individuals'* (Vakhrusheva et al., 2020), the allele sharing pattern, with further cross-locus incongruence

of haplotype relationships. The authors also analysed three additional *A. vaga* individuals, which clustered together by one of their haplotypes in the majority of the segments, with the remaining haplotypes interspersed within those of the other eight individuals (Vakhrusheva et al., 2020). The study concluded that the recovered patterns are best explained by a history of facultative sex and a hybridisation event ancestral to the three additional individuals(Vakhrusheva et al., 2020). Second, a pattern similarly akin to genetic exchange was found by Laine et al. (2022) in two individuals of *Macrotrachela quadricornifera*, a species from a different bdelloid order. In this study, 315 out of the 622 analysed segments (together spanning less than 4% of the reference assembly) contained near-identical haplotypes. Because the remaining regions were more divergent, the authors inferred that the studied individuals originated from a recent bout of sex and were related as *'half siblings or double first cousins'* (Laine et al., 2022).

The issue presents a twofold challenge. If confirmed, these findings undermine centuries of close observation (van Leeuwenhoek, 1702; Hudson & Gosse, 1886; Wesenberg-Lund, 1923; Donner, 1965; Segers, 2007; Birky Jr, 2010b). Conversely, a negative verification poses a major challenge to methodologies applied routinely across the broader field (Table 1). The three possible resolutions are as follows:

(1) If bdelloid rotifers do produce males, they must be either exceedingly rare, produced only under specific conditions, or have been taxonomically misassigned. Alternatively, male function in a putative bdelloid hermaphrodite could be highly reduced, anatomically unusual or expressed only transiently. Monogonont rotifers are facultative parthenogens that live in overlapping habitats to bdelloids. Their males are reduced in size but bear a morphological similarity to females of their species, and they have been comprehensively described by rotifer taxonomists (Hudson & Gosse, 1886; Ricci & Melone, 1998; Wesenberg-Lund, 1923). The single account of a possible sighting of a bdelloid male was in a mixed wild sample also containing monogonont rotifers, and framed very cautiously *('With great hesitation I venture to remark…'*): two animals resembling monogonont males were seen swimming among a

dense population of bdelloids (Wesenberg-Lund, 1923), but were not isolated or drawn, leaving open the possibility that they were, in fact, monogonont males. While negative evidence is not conclusive, the extensive history of rotifer sampling across aquatic and semiterrestrial habitats makes it difficult to suggest new ways to test the cryptic male hypothesis directly (but see Laine et al., 2022).

(2) Another hypothesis is that bdelloid rotifers might exchange or transfer genes within populations in alternative ways that are distinct from outcrossing. For example, perhaps horizontal transfer between homologous loci occurs by uptake of exogenous DNA (for example, during DNA repair after desiccation; Gladyshev et al., 2008) or via vectors such as mobile elements (analogous to transformation and transduction, respectively, in bacteria; Arnold et al., 2022). This hypothesis was initially prompted by the discovery of high levels of HGT from non-metazoan sources (Gladyshev et al., 2008), though whether HGT within populations would occur by similar means is unknown. Evidence to assess this possibility directly is currently lacking – one such putative pattern (Debortoli et al., 2016) was shown to have arisen through cross-contamination (Wilson et al., 2018) – and I know of no successful transformation experiments with bdelloids to date. Frequent HGT might be expected to generate a patchwork of allele sharing-like patterns at restricted sets of loci rather than the genome-wide shuffling or sharing expected through outcrossing (Laine et al., 2022). Other alternative mechanisms might include parasexual exchange as in fungi (Mishra et al., 2021), but this would require a haploid life stage, thus far unknown in bdelloids. All these hypotheses are speculative at present. Nonetheless, even heterodox ideas should be considered, given the puzzle of the missing males.

(3) The final possibility is that both outcrossing and genetic exchange are absent in bdelloid rotifer populations, and signatures interpreted in this light have other explanations. These could include biological mechanisms (Fig. 2) as well as technical artefacts, unavoidable when multiple tests are performed. Moreover, both studies reporting allele sharing patterns analysed only a fraction of the genome, so that biases in assembly, variant calling, filtering

and phasing could influence some results. How does biased genome sampling affect different genealogical signatures? How strong is the signal of asyngamous recombination in the recovered genealogies? Do the observed patterns fit those predicted by cryptic sex, or do they require other biological mechanisms? As long as these questions remain outstanding, alternative explanations for the reported ‘sex signatures’ cannot be ruled out.

In Chapter 3, I reconstruct haplotype trees for two species of bdelloid rotifers and apply my novel method of quantifying reproductive histories. Apart from the obvious biological interest in the bdelloid reproductive system, the present research constitutes a case of bridging two distinct and largely hermetic areas of research. On the one hand, outstanding claims about bdelloid rotifers, whether concerning non-canonical forms of genetic exchange (Signorovitch et al., 2015; Debortoli et al., 2016) or other extraordinary features (Shmakova et al., 2021), often gain quick acceptance in the wider community (e.g., Schwander, 2016). Interestingly, workers are similarly eager to accept that rotifers *'cannot be considered as effectively asexual'* (Archetti, 2022) since cryptic sex has been *‘documented’* (Molinier et al., 2025). Such an attitude echoes a long history of competitive claims of ancient asexuality (Öztoprak et al., 2025; Brandt et al., 2021; Schwander et al., 2011; Mark Welch & Meselson, 2000; Martens et al., 2003) – the idea that *my asexual is more asexual than yours* – which, with hindsight, is hardly productive for the field. On the other, while the theory and tools for reconstructing reticulate evolutionary relationships exist, their integration into the current lines of inquiry has to be preceded by 'a step back' from routine approaches. The present research will hopefully pave the way for further applications of ARG thinking to non-model reproductive systems – bdelloid rotifers, on the other hand, will remain interesting whether they are or are not obligate and ancient asexuals.

References

Akopyants, N. S., Kimblin, N., Secundino, N., Patrick, R., Peters, N., Lawyer, P., Dobson, D. E., Beverley, S. M., & Sacks, D. L. (2009). Demonstration of genetic exchange during cyclical development of Leishmania in the sand fly vector. *Science*, *324*(5924), 265–268.

Amses, K. R., Simmons, D. R., Longcore, J. E., Mondo, S. J., Seto, K., Jerônimo, G. H., Bonds, A. E., Quandt, C. A., Davis, W. J., & Chang, Y. (2022). Diploid-dominant life cycles characterize the early evolution of Fungi. *Proceedings of the National Academy of Sciences*, *119*(36), e2116841119.

Archetti, M. (2022). Evidence from automixis with inverted meiosis for the maintenance of sex by loss of complementation. *Journal of Evolutionary Biology*, *35*(1), 40–50.

Arkhipova, I., & Meselson, M. (2000). Transposable elements in sexual and ancient asexual taxa. *Proceedings of the National Academy of Sciences*, *97*(26), 14473–14477.

Arnold, B. J., Huang, I.-T., & Hanage, W. P. (2022). Horizontal gene transfer and adaptive evolution in bacteria. *Nature Reviews Microbiology*, *20*(4), 206–218.

Avise, J. C. (2008). Reproduction by the Chaste: Parthenogenesis. In *Clonality: The Genetics, Ecology, and Evolution of Sexual Abstinence in Vertebrate Animals*. Oxford University Press. https://doi.org/10.1093/acprof:oso/9780195369670.003.0003

Barley, A. J., & Cole, C. J. (2025). Speciation by hybridization: the mind-boggling nature, educational, and research value of the largest group of unisexual vertebrates. *Bioscience*, *75*(4), 331–341.

Baumdicker, F., Bisschop, G., Goldstein, D., Gower, G., Ragsdale, A. P., Tsambos, G., Zhu, S., Eldon, B., Ellerman, E. C., & Galloway, J. G. (2022). Efficient ancestry and mutation simulation with msprime 1.0. *Genetics*, *220*(3), iyab229.

Baxevanis, A. D., Kappas, I., & Abatzopoulos, T. J. (2006). Molecular phylogenetics and asexuality in the brine shrimp Artemia. *Molecular phylogenetics and evolution*, *40*(3), 724–738.

Bell, G. (1982). *The masterpiece of nature: the evolution and genetics of sexuality*. Routledge.

Bennett, R. J., & Turgeon, B. G. (2016). Fungal sex: the Ascomycota. *Microbiology spectrum*, *4*(5), 10.1128/microbiolspec. funk–0005–2016.

Bernstein, H., Hopf, F., & Michod, R. (1988). Is meiotic recombination an adaptation for repairing DNA, producing genetic variation, or both. *The evolution of sex*, 139–160.

Berry, A. S., Salazar-Sanchez, R., Castillo-Neyra, R., Borrini-Mayori, K., Chipana-Ramos, C., Vargas-Maquera, M., Ancca-Juarez, J., Naquira-Velarde, C., Levy, M. Z., & Brisson, D. (2019). Sexual reproduction in a natural Trypanosoma cruzi population. *PLoS neglected tropical diseases*, *13*(5), e0007392.

Birky Jr, C. W. (2010a). Giardia sex? Yes, but how and how much? *Trends in parasitology*, *26*(2), 70–74.

Birky Jr, C. W. (2010b). Positively negative evidence for asexuality. *Journal of Heredity*, *101*, S42–S45. https://doi.org/10.1093/jhered/esq014

Birky Jr., C. W. (1996). Heterozygosity, heteromorphy, and phylogenetic trees in asexual eukaryotes. *Genetics*, *144*(1), 427–437.

Blanc, C., Saclier, N., Le Faou, E., Marie-Orleach, L., Wenger, E., Diblasi, C., Glemin, S., Galtier, N., & Delattre, M. (2023). Co-segregation of recombinant chromatids maintains genome-wide heterozygosity in an asexual nematode. *bioRxiv*, 2023.2003. 2017.533182.

Blanc, C. S., Delattre, M., & Van Doninck, K. (2025). Cracking the meiotic secrets behind animals asexuality When cytology seduces genomics to decode asexual meiosis. *Journal of Evolutionary Biology*, voaf045.

Boyer, L., Jabbour-Zahab, R., Mosna, M., Haag, C. R., & Lenormand, T. (2021). Not so clonal asexuals: Unraveling the secret sex life of Artemia parthenogenetica. *Evolution Letters*, *5*(2), 164–174.

Brandt, A., Tran Van, P., Bluhm, C., Anselmetti, Y., Dumas, Z., Figuet, E., François, C. M., Galtier, N., Heimburger, B., & Jaron, K. S. (2021). Haplotype divergence supports long-term asexuality in the oribatid mite Oppiella nova. *Proceedings of the National Academy of Sciences*, *118*(38), e2101485118.

Brandt, D. Y., Huber, C. D., Chiang, C. W., & Ortega-Del Vecchyo, D. (2024). The promise of inferring the past using the ancestral recombination graph. *Genome Biology and Evolution*, *16*(2), evae005.

Browne, R. A. (1992). Population genetics and ecology of Artemia: insights into parthenogenetic reproduction. *Trends in ecology & evolution*, *7*(7), 232–237.
Bulankova, P., Sekulić, M., Jallet, D., Nef, C., Van Oosterhout, C., Delmont, T. O., Vercauteren, I., Osuna-Cruz, C. M., Vancaester, E., & Mock, T. (2021). Mitotic recombination between homologous chromosomes drives genomic diversity in diatoms. *Current Biology*, *31*(15), 3221–3232. e3229.
Butlin, R. (2002). The costs and benefits of sex: new insights from old asexual lineages. *Nature Reviews Genetics*, *3*(4), 311–317.
Butlin, R., Schön, I., & Martens, K. (1998). Asexual reproduction in nonmarine ostracods. *Heredity*, *81*(5), 473–480.
Capewell, P., Krumrie, S., Katzer, F., Alexander, C. L., & Weir, W. (2021). Molecular epidemiology of Giardia infections in the genomic era. *Trends in parasitology*, *37*(2), 142–153.
Castagnone-Sereno, P., & Danchin, E. (2014). Parasitic success without sex–the nematode experience. *Journal of Evolutionary Biology*, *27*(7), 1323–1333.
Catta-Preta, C. M., & Sacks, D. L. (2025). Genetic Exchange in Leishmania: Understanding the Cryptic Sexual Cycle. *Annual Review of Microbiology*, *79*.
Cavalier-Smith, T. (2002). Origins of the machinery of recombination and sex. *Heredity*, *88*(2), 125–141.
Chan, A. H., Jenkins, P. A., & Song, Y. S. (2012). Genome-wide fine-scale recombination rate variation in Drosophila melanogaster. *PLoS Genetics*, *8*(12), e1003090.
Charlesworth, B. (1976). Recombination modification in a fluctuating environment. *Genetics*, *83*(1), 181–195.
Chen, L.-Y., VanBuren, R., Paris, M., Zhou, H., Zhang, X., Wai, C. M., Yan, H., Chen, S., Alonge, M., & Ramakrishnan, S. (2019). The bracteatus pineapple genome and domestication of clonally propagated crops. *Nature genetics*, *51*(10), 1549–1558.
Churchill, F. B. (1979). Sex and the single organism: biological theories of sexuality in mid-nineteenth century. *Studies in history of biology*, *3*, 139–177.
Davis, H. (1873). A new Callidina: with the result of experiments on the desiccation of rotifers. *The Monthly Microscopical Journal*, *9*(5), 201–209.
Debortoli, N., Li, X., Eyres, I., Fontaneto, D., Hespeels, B., Tang, C. Q., Flot, J.-F., & Van Doninck, K. (2016). Genetic exchange among bdelloid rotifers is more likely due to horizontal gene transfer than to meiotic sex. *Current Biology*, *26*(6), 723–732.
Deng, Y., Nielsen, R., & Song, Y. S. (2025). Robust and accurate Bayesian inference of genome-wide genealogies for hundreds of genomes. *Nature genetics*, 1–12.
Diogo, D., Bouchier, C., d'Enfert, C., & Bougnoux, M.-E. (2009). Loss of heterozygosity in commensal isolates of the asexual diploid yeast Candida albicans. *Fungal Genetics and Biology*, *46*(2), 159–168.
Dolgin, E. S., & Charlesworth, B. (2006). The fate of transposable elements in asexual populations. *Genetics*, *174*(2), 817–827.
Donner, J. (1965). *Ordnung Bdelloidea (Rotatoria, Radertiere)*. Akademie-Verlag.
Dujardin, J.-C., Mannaert, A., Durrant, C., & Cotton, J. A. (2014). Mosaic aneuploidy in Leishmania: the perspective of whole genome sequencing. *Trends in parasitology*, *30*(12), 554–555.
Dutta, A., Dutreux, F., & Schacherer, J. (2021). Loss of heterozygosity results in rapid but variable genome homogenization across yeast genetic backgrounds. *eLife*, *10*, e70339.
Eitel, M., Guidi, L., Hadrys, H., Balsamo, M., & Schierwater, B. (2011). New insights into placozoan sexual reproduction and development. *PLoS One*, *6*(5), e19639.
Engelstädter, J. (2017). Asexual but Not Clonal: Evolutionary Processes in Automictic Populations. *Genetics*, *206*(2), 993–1009. https://doi.org/10.1534/genetics.116.196873
Fan, C., Cahoon, J. L., Dinh, B. L., Ortega-Del Vecchyo, D., Huber, C. D., Edge, M. D., Mancuso, N., & Chiang, C. W. (2025). A likelihood-based framework for demographic inference from genealogical trees. *Nature genetics*, 1–10.

Feldman, M. W. (1972). Selection for linkage modification: I. Random mating populations. *Theoretical population biology*, *3*(3), 324–346.
Felsenstein, J. (1974). The evolutionary advantage of recombination. *Genetics*, *78*(2), 737–756.
Felsenstein, J. (1978). The number of evolutionary trees. *Systematic zoology*, *27*(1), 27–33.
Ferreira, T. R., Inbar, E., Shaik, J., Jeffrey, B. M., Ghosh, K., Dobson, D. E., Beverley, S. M., & Sacks, D. (2022). Self-hybridization in Leishmania major. *MBio*, *13*(6), e02858–02822.
Flot, J.-F., Hespeels, B., Li, X., Noel, B., Arkhipova, I., Danchin, E. G., Hejnol, A., Henrissat, B., Koszul, R., & Aury, J.-M. (2013). Genomic evidence for ameiotic evolution in the bdelloid rotifer Adineta vaga. *Nature*, *500*(7463), 453–457.
Flynn, J. M., Chain, F. J., Schoen, D. J., & Cristescu, M. E. (2017). Spontaneous mutation accumulation in Daphnia pulex in selection-free vs. competitive environments. *Molecular Biology and Evolution*, *34*(1), 160–173.
Forche, A., Abbey, D., Pisithkul, T., Weinzierl, M., Ringstrom, T., Bruck, D., Petersen, K., & Berman, J. (2011). Stress alters rates and types of loss of heterozygosity in Candida albicans. *MBio*, *2*(4), 10.1128/mbio. 00129–00111.
Franssen, S. U., Durrant, C., Stark, O., Moser, B., Downing, T., Imamura, H., Dujardin, J.-C., Sanders, M. J., Mauricio, I., & Miles, M. A. (2020). Global genome diversity of the Leishmania donovani complex. *eLife*, *9*, e51243.
Freitas, S., Parker, D. J., Labédan, M., Dumas, Z., & Schwander, T. (2023). Evidence for cryptic sex in parthenogenetic stick insects of the genus Timema. *Proceedings of the Royal Society B*, *290*(2007), 20230404.
Gibson, W. (2021). The sexual side of parasitic protists. *Molecular and Biochemical Parasitology*, *243*, 111371.
Gladyshev, E. A., & Arkhipova, I. R. (2007). Telomere-associated endonuclease-deficient Penelope-like retroelements in diverse eukaryotes. *Proceedings of the National Academy of Sciences*, *104*(22), 9352–9357.
Gladyshev, E. A., & Arkhipova, I. R. (2010). Genome structure of bdelloid rotifers: shaped by asexuality or desiccation? *Journal of Heredity*, *101*(suppl_1), S85–S93.
Gladyshev, E. A., Meselson, M., & Arkhipova, I. R. (2007). A deep-branching clade of retrovirus-like retrotransposons in bdelloid rotifers. *Gene*, *390*(1-2), 136–145.
Gladyshev, E. A., Meselson, M., & Arkhipova, I. R. (2008). Massive horizontal gene transfer in bdelloid rotifers. *Science*, *320*(5880), 1210–1213.
Griffiths, R. C., & Marjoram, P. (1997). An ancestral recombination graph. *Institute for Mathematics and its Applications*, *87*, 257.
Grosmaire, M., Launay, C., Siegwald, M., Brugière, T., Estrada-Virrueta, L., Berger, D., Burny, C., Modolo, L., Blaxter, M., & Meister, P. (2019). Males as somatic investment in a parthenogenetic nematode. *Science*, *363*(6432), 1210–1213.
Gusa, A., & Jinks-Robertson, S. (2019). Mitotic recombination and adaptive genomic changes in human pathogenic fungi. *Genes*, *10*(11), 901.
Habig, M., Grasse, A. V., Müller, J., Stukenbrock, E. H., Leitner, H., & Cremer, S. (2024). Frequent horizontal chromosome transfer between asexual fungal insect pathogens. *Proceedings of the National Academy of Sciences*, *121*(11), e2316284121.
Hadermann, A., Heeren, S., Maes, I., Dujardin, J.-C., Domagalska, M. A., & Van den Broeck, F. (2023). Genome diversity of Leishmania aethiopica. *Frontiers in Cellular and Infection Microbiology*, *13*, 1147998.
Halkett, F., Simon, J.-C., & Balloux, F. (2005). Tackling the population genetics of clonal and partially clonal organisms. *Trends in ecology & evolution*, *20*(4), 194–201.
Haller, B. C., Galloway, J., Kelleher, J., Messer, P. W., & Ralph, P. L. (2019). Tree-sequence recording in SLiM opens new horizons for forward-time simulation of whole genomes. *Molecular ecology resources*, *19*(2), 552–566.
Harris, E. H. (2001). Chlamydomonas as a model organism. *Annual review of plant biology*, *52*(1), 363–406.

Hartfield, M., & Keightley, P. D. (2012). Current hypotheses for the evolution of sex and recombination. *Integrative zoology*, *7*(2), 192–209.
Hartfield, M., Wright, S. I., & Agrawal, A. F. (2018). Coalescence and linkage disequilibrium in facultatively sexual diploids. *Genetics*, *210*(2), 683–701.
Hecox-Lea, B. J., & Mark Welch, D. B. (2018). Evolutionary diversity and novelty of DNA repair genes in asexual Bdelloid rotifers. *BMC evolutionary biology*, *18*, 1–25.
Heethoff, M., Norton, R. A., Scheu, S., & Maraun, M. (2009). Parthenogenesis in oribatid mites (Acari, Oribatida): evolution without sex. In *Lost sex: the evolutionary biology of parthenogenesis* (pp. 241–257). Springer.
Hejase, H. A., Mo, Z., Campagna, L., & Siepel, A. (2022). A deep-learning approach for inference of selective sweeps from the ancestral recombination graph. *Molecular Biology and Evolution*, *39*(1), msab332.
Hiruta, C., Nishida, C., & Tochinai, S. (2010). Abortive meiosis in the oogenesis of parthenogenetic Daphnia pulex. *Chromosome Research*, *18*, 833–840.
Ho, E. K., Bartkowska, M., Wright, S. I., & Agrawal, A. F. (2019). Population genomics of the facultatively asexual duckweed Spirodela polyrhiza. *New Phytologist*, *224*(3), 1361–1371.
Hofstatter, P. G., & Lahr, D. J. (2019). All eukaryotes are sexual, unless proven otherwise: Many so-called asexuals present meiotic machinery and might be able to have sex. *BioEssays*, *41*(6), 1800246.
Hofstatter, P. G., Ribeiro, G. M., Porfírio-Sousa, A. L., & Lahr, D. J. (2020). The Sexual Ancestor of all Eukaryotes: A Defense of the “Meiosis Toolkit” A Rigorous Survey Supports the Obligate Link between Meiosis Machinery and Sexual Recombination. *BioEssays*, *42*(9), 2000037.
Hood, M. E., & Antonovics, J. (2000). Intratetrad mating, heterozygosity, and the maintenance of deleterious alleles in Microbotryum violaceum (= Ustilago violacea). *Heredity*, *85*(3), 231–241.
Hörandl, E., & Speijer, D. (2018). How oxygen gave rise to eukaryotic sex. *Proceedings of the Royal Society B: Biological Sciences*, *285*(1872), 20172706.
Houtain, A., Derzelle, A., Llirós, M., Hespeels, B., Nicolas, É., Simion, P., Virgo, J., Lenormand, T., Hallet, B., & Van Doninck, K. (2024). Transgenerational chromosome repair in the asexual bdelloid rotifer *Adineta vaga*. *bioRxiv*, 2024.2001.2025.577190. https://doi.org/10.1101/2024.01.25.577190
Hsu, W. S. (1956a). Oogenesis in Habrotrocha tridens (Milne). *The Biological Bulletin*, *111*(3), 364–374.
Hsu, W. S. (1956b). Oogenesis in the Bdelloidea rotifer Philodina roseola Ehrenberg. *Cellule*, *57*, 283–296.
Hubisz, M., & Siepel, A. (2020). Inference of ancestral recombination graphs using ARGweaver. In *Statistical population genomics* (pp. 231–266). Springer US New York, NY.
Hudson, C. (1884). An Attempt to re-classify the Rotifers. *Journal of cell science*, *2*(95), 335–356.
Hudson, C. T., & Gosse, P. H. (1886). *The Rotifera or Wheel-Animalcules* (Vol. 1). Longmans, Green & Co.
Hudson, R. R. (1983). Properties of a neutral allele model with intragenic recombination. *Theoretical population biology*, *23*(2), 183–201.
Hudson, R. R. (1990). Gene genealogies and the coalescent process. *Oxford surveys in evolutionary biology*, *7*(1), 44.
Hudson, R. R., & Kaplan, N. L. (1985). Statistical properties of the number of recombination events in the history of a sample of DNA sequences. *Genetics*, *111*(1), 147.
Hur, J. H., Van Doninck, K., Mandigo, M. L., & Meselson, M. (2009). Degenerate tetraploidy was established before bdelloid rotifer families diverged. *Molecular Biology and Evolution*, *26*(2), 375–383.
Jaenike, J. (1978). An hypothesis to account for the maintenance of sex within populations. *Evol. theory*, *3*, 191–194.

Jaron, K. S., Bast, J., Nowell, R. W., Ranallo-Benavidez, T. R., Robinson-Rechavi, M., & Schwander, T. (2021). Genomic features of parthenogenetic animals. *Journal of Heredity*, *112*(1), 19–33.

Jaron, K. S., Parker, D. J., Anselmetti, Y., Tran Van, P., Bast, J., Dumas, Z., Figuet, E., François, C. M., Hayward, K., & Rossier, V. (2022). Convergent consequences of parthenogenesis on stick insect genomes. *Science Advances*, *8*(8), eabg3842.

Jinks-Robertson, S., & Petes, T. D. (2021). Mitotic recombination in yeast: what we know and what we don't know. *Current opinion in genetics & development*, *71*, 78–85.

Johnson, L. J., Koufopanou, V., Goddard, M. R., Hetherington, R., Schäfer, S. M., & Burt, A. (2004). Population genetics of the wild yeast Saccharomyces paradoxus. *Genetics*, *166*(1), 43–52.

Judson, O. P., & Normark, B. B. (1996). Ancient asexual scandals. *Trends in ecology & evolution*, *11*(2), 41–46.

Keith, N., Tucker, A. E., Jackson, C. E., Sung, W., Lledó, J. I. L., Schrider, D. R., Schaack, S., Dudycha, J. L., Ackerman, M., & Younge, A. J. (2016). High mutational rates of large-scale duplication and deletion in Daphnia pulex. *Genome research*, *26*(1), 60–69.

Kelleher, J., Etheridge, A. M., & McVean, G. (2016). Efficient coalescent simulation and genealogical analysis for large sample sizes. *PLOS Computational Biology*, *12*(5), e1004842.

Kelleher, J., Wong, Y., Wohns, A. W., Fadil, C., Albers, P. K., & McVean, G. (2019). Inferring whole-genome histories in large population datasets. *Nature genetics*, *51*(9), 1330–1338.

Kingman, J. F. (1982). On the genealogy of large populations. *Journal of applied probability*, *19*(A), 27–43.

Koester, J. A., Berthiaume, C. T., Hiranuma, N., Parker, M. S., Iverson, V., Morales, R., Ruzzo, W. L., & Armbrust, E. V. (2018). Sexual ancestors generated an obligate asexual and globally dispersed clone within the model diatom species Thalassiosira pseudonana. *Scientific Reports*, *8*(1), 10492.

Kondrashov, A. (1993). Classification of hypotheses on the advantage of amphimixis. *Journal of Heredity*, *84*(5), 372–387.

Kopčak, D., & Hartfield, M. (2024). How do self-fertilising and facultative sexual populations differ in mutation accumulation? *bioRxiv*, 2024.2008. 2030.610445.

Kothe, E. (1996). Tetrapolar fungal mating types: sexes by the thousands. *FEMS microbiology reviews*, *18*(1), 65–87.

Krueger-Hadfield, S. A. (2024). Let's talk about sex: Why reproductive systems matter for understanding algae. *Journal of Phycology*, *60*(3), 581–597.

Ladle, R. J., Johnstone, R. A., & Judson, O. P. (1993). Coevolutionary dynamics of sex in a metapopulation: escaping the Red Queen. *Proceedings of the Royal Society of London. Series B: Biological Sciences*, *253*(1337), 155–160.

Laine, V. N., Sackton, T. B., & Meselson, M. (2022). Genomic signature of sexual reproduction in the bdelloid rotifer Macrotrachella quadricornifera. *Genetics*, *220*(2), iyab221.

Larose, C., Lavanchy, G., Freitas, S., Parker, D. J., & Schwander, T. (2023). Facultative parthenogenesis: a transient state in transitions between sex and obligate asexuality in stick insects? *Peer Community Journal*, *3*.

Lasek-Nesselquist, E., Welch, D. M., Thompson, R. C. A., Steuart, R. F., & Sogin, M. L. (2009). Genetic exchange within and between assemblages of Giardia duodenalis. *Journal of Eukaryotic Microbiology*, *56*(6), 504–518.

Lavanchy, G., Brandt, A., Bastardot, M., Dumas, Z., Labédan, M., Massy, M., Toubiana, W., Tran Van, P., Luchetti, A., & Scali, V. (2024). Evolution of alternative reproductive systems in Bacillus stick insects. *Evolution*, *78*(6), 1109–1120.

Lehtonen, J., Jennions, M. D., & Kokko, H. (2012). The many costs of sex. *Trends in ecology & evolution*, *27*(3), 172–178.

Lenormand, T., Engelstädter, J., Johnston, S. E., Wijnker, E., & Haag, C. R. (2016). Evolutionary mysteries in meiosis. *Philosophical Transactions of the Royal Society B: Biological Sciences*, *371*(1706), 20160001.

Lewanski, A. L., Grundler, M. C., & Bradburd, G. S. (2024). The era of the ARG: An introduction to ancestral recombination graphs and their significance in empirical evolutionary genomics. *PLoS Genetics*, *20*(1), e1011110.

Lewis Jr, W. M. (1983). Interruption of synthesis as a cost of sex in small organisms. *The American Naturalist*, *121*(6), 825–833.

Lively, C. M. (2010). A review of Red Queen models for the persistence of obligate sexual reproduction. *Journal of Heredity*, *101*(suppl_1), S13–S20.

Luo, G., Santoro, I. M., McDaniel, L. D., Nishijima, I., Mills, M., Youssoufian, H., Vogel, H., Schultz, R. A., & Bradley, A. (2000). Cancer predisposition caused by elevated mitotic recombination in Bloom mice. *Nature genetics*, *26*(4), 424–429.

Mackintosh, A., Laetsch, D. R., Hayward, A., Charlesworth, B., Waterfall, M., Vila, R., & Lohse, K. (2019). The determinants of genetic diversity in butterflies. *Nature Communications*, *10*(1), 3466.

Magwene, P. M., Kayıkçı, Ö., Granek, J. A., Reininga, J. M., Scholl, Z., & Murray, D. (2011). Outcrossing, mitotic recombination, and life-history trade-offs shape genome evolution in Saccharomyces cerevisiae. *Proceedings of the National Academy of Sciences*, *108*(5), 1987–1992.

Malinowski, P. T., Cochet-Escartin, O., Kaj, K. J., Ronan, E., Groisman, A., Diamond, P. H., & Collins, E.-M. S. (2017). Mechanics dictate where and how freshwater planarians fission. *Proceedings of the National Academy of Sciences*, *114*(41), 10888–10893.

Mandegar, M. A., & Otto, S. P. (2007). Mitotic recombination counteracts the benefits of genetic segregation. *Proceedings of the Royal Society B: Biological Sciences*, *274*(1615), 1301–1307.

Maraun, M., Heethoff, M., Schneider, K., Scheu, S., Weigmann, G., Cianciolo, J., Thomas, R. H., & Norton, R. A. (2004). Molecular phylogeny of oribatid mites (Oribatida, Acari): evidence for multiple radiations of parthenogenetic lineages. *Experimental & applied acarology*, *33*(3), 183–201.

Mark Welch, D. B., Mark Welch, J. L., & Meselson, M. (2008). Evidence for degenerate tetraploidy in bdelloid rotifers. *Proceedings of the National Academy of Sciences*, *105*(13), 5145–5149.

Mark Welch, D. B., & Meselson, M. (2000). Evidence for the evolution of bdelloid rotifers without sexual reproduction or genetic exchange. *Science*, *288*(5469), 1211–1215.

Mark Welch, D. B., Ricci, C., & Meselson, M. (2009). Bdelloid rotifers: progress in understanding the success of an evolutionary scandal. In I. Schön, K. Martens, & P. Dijk (Eds.), *Lost sex: the evolutionary biology of parthenogenesis* (pp. 259–279). Springer.

Mark Welch, J. L., & Meselson, M. (1998). Karyotypes of bdelloid rotifers from three families. Rotifera VIII: A Comparative Approach: Proceedings of the VIIIth International Rotifer Symposium, held in Collegeville, Minn., USA, 22–27 June 1997,

Martens, K., Rossetti, G., & Horne, D. J. (2003). How ancient are ancient asexuals? *Proceedings of the Royal Society of London. Series B: Biological Sciences*, *270*(1516), 723–729.

Maynard Smith, J. (1971). The origin and maintenance of sex. In *Group selection* (pp. 163–175). Routledge.

Maynard Smith, J. (1978). *The evolution of sex*. Cambridge University Press.

Maynard Smith, J. (1986). Evolution: contemplating life without sex. *Nature*, *324*(6095), 300–301.

Maynard Smith, J., Smith, N. H., O'Rourke, M., & Spratt, B. G. (1993). How clonal are bacteria? *Proceedings of the National Academy of Sciences*, *90*(10), 4384–4388.

Meunier, C., Hosseini, S., Heidari, N., Maryush, Z., & Johannesson, H. (2018). Multilevel selection in the filamentous ascomycete Neurospora tetrasperma. *The American Naturalist*, *191*(3), 290–305.

Mishra, A., Forche, A., & Anderson, M. Z. (2021). Parasexuality of Candida species. *Frontiers in Cellular and Infection Microbiology*, *11*, 796929.
Mogie, M. (1992). *The evolution of asexual reproduction in plants*. Springer.
Molinier, C., Clément, C., Calzan, H., Lenormand, T., & Haag, C. R. (2025). Rare sexual reproduction by females of “obligate parthenogenetic” lineages of Daphnia cf. pulex. *Journal of Evolutionary Biology*, voaf044.
Murdy, W., & Carson, H. (1959). Parthenogenesis in Drosophila mangabeirai Malog. *The American Naturalist*, *93*(873), 355–363.
Murphy, H. A., & Zeyl, C. W. (2010). Yeast sex: surprisingly high rates of outcrossing between asci. *PLoS One*, *5*(5), e10461.
Neiman, M., Lively, C. M., & Meirmans, S. (2017). Why sex? A pluralist approach revisited. *Trends in ecology & evolution*, *32*(8), 589–600.
Nicolas, E., Simion, P., Guérineau, M., Terwagne, M., Colinet, M., Virgo, J., Lingurski, M., Boutsen, A., Dieu, M., & Hallet, B. (2023). Horizontal acquisition of a DNA ligase improves DNA damage tolerance in eukaryotes. *Nature Communications*, *14*(1), 7638.
Nielsen, R., Vaughn, A. H., & Deng, Y. (2025). Inference and applications of ancestral recombination graphs. *Nature Reviews Genetics*, *26*(1), 47–58.
Nieuwenhuis, B. P., & James, T. Y. (2016). The frequency of sex in fungi. *Philosophical Transactions of the Royal Society B: Biological Sciences*, *371*(1706), 20150540.
Normark, B. B., Judson, O. P., & Moran, N. A. (2003). Genomic signatures of ancient asexual lineages. *Biological Journal of the Linnean Society*, *79*(1), 69–84.
Norton, R., & Palmer, S. (1991). The distribution, mechanisms and evolutionary significance of parthenogenesis in oribatid mites. In *The Acari: Reproduction, development and life-history strategies* (pp. 107–136). Springer.
Nowell, R. W., Almeida, P., Wilson, C. G., Smith, T. P., Fontaneto, D., Crisp, A., Micklem, G., Tunnacliffe, A., Boschetti, C., & Barraclough, T. G. (2018). Comparative genomics of bdelloid rotifers: Insights from desiccating and nondesiccating species. *PLoS biology*, *16*(4), e2004830.
Nowell, R. W., Rodriguez, F., Hecox-Lea, B. J., Mark Welch, D. B., Arkhipova, I. R., Barraclough, T. G., & Wilson, C. G. (2024). Bdelloid rotifers deploy horizontally acquired biosynthetic genes against a fungal pathogen. *Nature Communications*, *15*(1), 5787.
Nowell, R. W., Wilson, C. G., Almeida, P., Schiffer, P. H., Fontaneto, D., Becks, L., Rodriguez, F., Arkhipova, I. R., & Barraclough, T. G. (2021). Evolutionary dynamics of transposable elements in bdelloid rotifers. *eLife*, *10*, e63194.
Osmond, M., & Coop, G. (2024). Estimating dispersal rates and locating genetic ancestors with genome-wide genealogies. *eLife*, *13*, e72177.
Otto, S. P. (2003). The advantages of segregation and the evolution of sex. *Genetics*, *164*(3), 1099–1118.
Otto, S. P. (2009). The evolutionary enigma of sex. *The American Naturalist*, *174*(S1), S1–S14.
Otto, S. P. (2021). Selective interference and the evolution of sex. *Journal of Heredity*, *112*(1), 9–18.
Öztoprak, H., Gao, S., Guiglielmoni, N., Brandt, A., Zheng, Y., Errbii, M., Bednarski, V., Becker, C., Becker, K., & Borgschulte, L. (2025). Chromosome-scale genome dynamics reveal signatures of independent haplotype evolution in the ancient asexual mite Platynothrus peltifer. *Science Advances*, *11*(4), eadn0817.
Peacock, L., Bailey, M., Carrington, M., & Gibson, W. (2014). Meiosis and haploid gametes in the pathogen Trypanosoma brucei. *Current Biology*, *24*(2), 181–186.
Peck, L. D., Llewellyn, T., Bennetot, B., O’donnell, S., Nowell, R. W., Ryan, M. J., Flood, J., de la Vega, R. C. R., Ropars, J., & Giraud, T. (2024). Horizontal transfers between fungal Fusarium species contributed to successive outbreaks of coffee wilt disease. *PLoS biology*, *22*(12), e3002480.

Peter, J., De Chiara, M., Friedrich, A., Yue, J.-X., Pflieger, D., Bergström, A., Sigwalt, A., Barre, B., Freel, K., & Llored, A. (2018). Genome evolution across 1,011 Saccharomyces cerevisiae isolates. *Nature*, *556*(7701), 339–344.

Phan Thi, N., Danchin, E. G., Koutsovoulos, G. D., Rancurel, C., Vermeire, M.-l., Besnard, G., & Bellafiore, S. (2025). Genomic rearrangements promote diversification of a facultative meiotic parthenogenetic nematode pest (Meloidogyne graminicola). *bioRxiv*, 2025.2003. 2020.644268.

Rabeling, C., Gonzales, O., Schultz, T. R., Bacci Jr, M., Garcia, M. V., Verhaagh, M., Ishak, H. D., & Mueller, U. G. (2011). Cryptic sexual populations account for genetic diversity and ecological success in a widely distributed, asexual fungus-growing ant. *Proceedings of the National Academy of Sciences*, *108*(30), 12366–12371.

Rasmussen, M. D., Hubisz, M. J., Gronau, I., & Siepel, A. (2014). Genome-wide inference of ancestral recombination graphs. *PLoS Genetics*, *10*(5), e1004342.

Raymond, J. A. (2025). A horizontally transferred bacterial gene aids the freezing tolerance of Antarctic bdelloid rotifers. *Proceedings of the National Academy of Sciences*, *122*(10), e2421910122.

Reynolds, D. R., & Taylor, J. W. (1993). *The fungal holomorph: mitotic, meiotic and pleomorphic speciation in fungal systematics*.

Ribes-Navarro, A., Kabeya, N., Castro, L. F. C., Gomes-dos-Santos, A., Fonseca, M. M., Alberts-Hubatsch, H., Hontoria, F., Navarro, J. C., & Monroig, Ó. (2023). Examination of gammarid transcriptomes reveals a widespread occurrence of key metabolic genes from epibiont bdelloid rotifers in freshwater species. *Open Biology*, *13*(10), 230196.

Ricci, C. (2017). Bdelloid rotifers:‘sleeping beauties’ and ‘evolutionary scandals’, but not only. *Hydrobiologia*, *796*(1), 277–285.

Ricci, C., & Melone, G. (1998). Dwarf males in monogonont rotifers. *Aquatic Ecology*, *32*(4), 361–365.

Ricci, C. N. (1987). Ecology of bdelloids: how to be successful. Rotifer Symposium IV: Proceedings of the Fourth Rotifer Symposium, held in Edinburgh, Scotland, August 18–25, 1985,

Richards, S. (2018). Full disclosure: Genome assembly is still hard. *PLoS biology*, *16*(4), e2005894.

Rizos, I., Frada, M. J., Bittner, L., & Not, F. (2024). Life cycle strategies in free-living unicellular eukaryotes: Diversity, evolution, and current molecular tools to unravel the private life of microorganisms. *Journal of Eukaryotic Microbiology*, *71*(6), e13052.

Rodriguez, F., Yushenova, I. A., DiCorpo, D., & Arkhipova, I. R. (2022). Bacterial N4-methylcytosine as an epigenetic mark in eukaryotic DNA. *Nature Communications*, *13*(1), 1072.

Rogers, A. R., & Huff, C. (2009). Linkage disequilibrium between loci with unknown phase. *Genetics*, *182*(3), 839–844.

Rogers, M. B., Downing, T., Smith, B. A., Imamura, H., Sanders, M., Svobodova, M., Volf, P., Berriman, M., Cotton, J. A., & Smith, D. F. (2014). Genomic confirmation of hybridisation and recent inbreeding in a vector-isolated Leishmania population. *PLoS Genetics*, *10*(1), e1004092.

Romiguier, J., Gayral, P., Ballenghien, M., Bernard, A., Cahais, V., Chenuil, A., Chiari, Y., Dernat, R., Duret, L., & Faivre, N. (2014). Comparative population genomics in animals uncovers the determinants of genetic diversity. *Nature*, *515*(7526), 261–263.

Ruderfer, D. M., Pratt, S. C., Seidel, H. S., & Kruglyak, L. (2006). Population genomic analysis of outcrossing and recombination in yeast. *Nature genetics*, *38*(9), 1077–1081.

Sandler, G., Agrawal, A. F., & Wright, S. I. (2023). Population genomics of the facultatively sexual liverwort Marchantia polymorpha. *Genome Biology and Evolution*, *15*(11), evad196.

Schaefer, N. K., Shapiro, B., & Green, R. E. (2021). An ancestral recombination graph of human, Neanderthal, and Denisovan genomes. *Science Advances*, *7*(29), eabc0776.

Schön, I., Rossetti, G., & Martens, K. (2009). Darwinulid ostracods: Ancient asexual scandals or scandalous gossip? In *Lost sex: the evolutionary biology of parthenogenesis* (pp. 217–240). Springer.

Schwabl, P., Imamura, H., Van den Broeck, F., Costales, J. A., Maiguashca-Sánchez, J., Miles, M. A., Andersson, B., Grijalva, M. J., & Llewellyn, M. S. (2019). Meiotic sex in Chagas disease parasite Trypanosoma cruzi. *Nature Communications*, *10*(1), 3972.

Schwander, T. (2016). Evolution: the end of an ancient asexual scandal. *Current Biology*, *26*(6), R233–R235.

Schwander, T., & Crespi, B. J. (2009). Twigs on the tree of life? Neutral and selective models for integrating macroevolutionary patterns with microevolutionary processes in the analysis of asexuality. *Molecular Ecology*, *18*(1), 28–42.

Schwander, T., Crespi, B. J., Gries, R., & Gries, G. (2013). Neutral and selection-driven decay of sexual traits in asexual stick insects. *Proceedings of the Royal Society B: Biological Sciences*, *280*(1764), 20130823.

Schwander, T., Henry, L., & Crespi, B. J. (2011). Molecular evidence for ancient asexuality in Timema stick insects. *Current Biology*, *21*(13), 1129–1134.

Schwander, T., Soldini, L., Boisseau, R. P., Mérel, V., Toubiana, W. S., & Lavanchy, G. (2025). On the Repeated Evolution of Parthenogenesis in Stick Insects.

Segers, H. (2007). Annotated checklist of the rotifers (Phylum Rotifera), with notes on nomenclature, taxonomy and distribution. *Zootaxa*, *1564*(1), 1–104–101–104.

Sekiné, K., & Tojo, K. (2010). Automictic parthenogenesis of a geographically parthenogenetic mayfly, Ephoron shigae (Insecta: Ephemeroptera, Polymitarcyidae). *Biological Journal of the Linnean Society*, *99*(2), 335–343.

Shapiro, T. A., & Englund, P. T. (1995). The structure and replication of kinetoplast DNA. *Annual Review of Microbiology*, *49*, 117–144.

Sherwood, R. K., Scaduto, C. M., Torres, S. E., & Bennett, R. J. (2014). Convergent evolution of a fused sexual cycle promotes the haploid lifestyle. *Nature*, *506*(7488), 387–390.

Shmakova, L., Malavin, S., Iakovenko, N., Vishnivetskaya, T., Shain, D., Plewka, M., & Rivkina, E. (2021). A living bdelloid rotifer from 24,000-year-old Arctic permafrost. *Current Biology*, *31*(11), R712–R713.

Signorovitch, A., Hur, J., Gladyshev, E., & Meselson, M. (2015). Allele sharing and evidence for sexuality in a mitochondrial clade of bdelloid rotifers. *Genetics*, *200*(2), 581–590.

Signorovitch, A. Y., Dellaporta, S. L., & Buss, L. W. (2005). Molecular signatures for sex in the Placozoa. *Proceedings of the National Academy of Sciences*, *102*(43), 15518–15522.

Simion, P., Narayan, J., Houtain, A., Derzelle, A., Baudry, L., Nicolas, E., Arora, R., Cariou, M., Cruaud, C., & Gaudray, F. R. (2021). Chromosome-level genome assembly reveals homologous chromosomes and recombination in asexual rotifer Adineta vaga. *Science Advances*, *7*(41), eabg4216.

Smith, R. J., Kamiya, T., & Horne, D. J. (2006). Living males of the 'ancient asexual'Darwinulidae (Ostracoda: Crustacea). *Proceedings of the Royal Society B: Biological Sciences*, *273*(1593), 1569–1578.

Speidel, L., Forest, M., Shi, S., & Myers, S. R. (2019). A method for genome-wide genealogy estimation for thousands of samples. *Nature genetics*, *51*(9), 1321–1329.

Speijer, D., Lukeš, J., & Eliáš, M. (2015). Sex is a ubiquitous, ancient, and inherent attribute of eukaryotic life. *Proceedings of the National Academy of Sciences*, *112*(29), 8827–8834.

Steenwyk, J. L., Li, Y., Zhou, X., Shen, X.-X., & Rokas, A. (2023). Incongruence in the phylogenomics era. *Nature Reviews Genetics*, *24*(12), 834–850.

Stenberg, P., & Saura, A. (2009). Cytology of Asexual Animals. In (pp. 63–74). Springer Netherlands. https://doi.org/10.1007/978-90-481-2770-2_4

Stern, A. J., Wilton, P. R., & Nielsen, R. (2019). An approximate full-likelihood method for inferring selection and allele frequency trajectories from DNA sequence data. *PLoS Genetics*, *15*(9), e1008384.

Stoeckel, S., & Masson, J.-P. (2014). The exact distributions of F IS under partial asexuality in small finite populations with mutation. *PLoS One*, *9*(1), e85228.
Suomalainen, E., Saura, A., & Lokki, J. (1987). *Cytology and evolution in parthenogenesis*. CRC Press.
Symington, L. S., Rothstein, R., & Lisby, M. (2014). Mechanisms and regulation of mitotic recombination in Saccharomyces cerevisiae. *Genetics*, *198*(3), 795–835.
Taberly, G. (1988). Researchs on the thelytokous parthenogenesis of two species of Oribatid mites-Trhypochthonius tectorum (Berlese) and Platynothrus peltifer (Koch). 4. Observations on atavic males. *Acarologia*, *29*(1), 95–107.
Tang, C. Q., Obertegger, U., Fontaneto, D., & Barraclough, T. G. (2014). Sexual species are separated by larger genetic gaps than asexual species in rotifers. *Evolution*, *68*(10), 2901–2916.
Tannreuther, G. W. (1909). Budding in hydra. *The Biological Bulletin*, *16*(4), 210–214.
Terwagne, M., Nicolas, E., Hespeels, B., Herter, L., Virgo, J., Demazy, C., Heuskin, A.-C., Hallet, B., & Van Doninck, K. (2022). DNA repair during nonreductional meiosis in the asexual rotifer Adineta vaga. *Science Advances*, *8*(48), eadc8829.
Tibayrenc, M., Kjellberg, F., Arnaud, J., Oury, B., Brenière, S. F., Dardé, M.-L., & Ayala, F. J. (1991). Are eukaryotic microorganisms clonal or sexual? A population genetics vantage. *Proceedings of the National Academy of Sciences*, *88*(12), 5129–5133.
Tsai, I. J., Bensasson, D., Burt, A., & Koufopanou, V. (2008). Population genomics of the wild yeast Saccharomyces paradoxus: quantifying the life cycle. *Proceedings of the National Academy of Sciences*, *105*(12), 4957–4962.
Vakhrusheva, O. A., Mnatsakanova, E. A., Galimov, Y. R., Neretina, T. V., Gerasimov, E. S., Naumenko, S. A., Ozerova, S. G., Zalevsky, A. O., Yushenova, I. A., Rodriguez, F., Arkhipova, I. R., Penin, A. A., Logacheva, M. D., Bazykin, G. A., & Kondrashov, A. S. (2020). Genomic signatures of recombination in a natural population of the bdelloid rotifer Adineta vaga. *Nature Communications*, *11:6421*. https://doi.org/10.1038/s41467-020-19614-y
Van den Broeck, F., Savill, N. J., Imamura, H., Sanders, M., Maes, I., Cooper, S., Mateus, D., Jara, M., Adaui, V., & Arevalo, J. (2020). Ecological divergence and hybridization of Neotropical Leishmania parasites. *Proceedings of the National Academy of Sciences*, *117*(40), 25159–25168.
van der Kooi, C. J., Matthey-Doret, C., & Schwander, T. (2017). Evolution and comparative ecology of parthenogenesis in haplodiploid arthropods. *Evolution Letters*, *1*(6), 304–316.
Van Dijk, P. (2009). Apomixis: Basics for non-botanists. In *Lost sex: the evolutionary biology of parthenogenesis* (pp. 47–62). Springer.
van Leeuwenhoek, A. (1702). Letter to Hendrik van Bleyswijk, dated 9th February 1702. In: Digitale Bibliotheek voor de Nederlandse Letteren.
Van Valen, L. (1973). Body size and numbers of plants and animals. *Evolution*, 27–35.
Vasilikopoulos, A., Herlyn, H., Fontaneto, D., Wilson, C. G., Nowell, R. W., Flot, J.-F., Barraclough, T. G., & Van Doninck, K. (2024). Whole-genome analyses converge to support the Hemirotifera hypothesis within Syndermata (Gnathifera). *Hydrobiologia*, 1–32.
Vickery, V. R., & Sandoval, C. P. (1999). Two new species of Timema (Phasmatoptera: Timematodea: Timematidae), one parthenogenetic, in California. *Journal of Orthoptera Research*, 45–47.
Vickery, V. R., & Sandoval, C. P. (2001). Descriptions of three new species of Timema (Phasmatoptera: Timematodea: Timematidae) and notes on three other species. *Journal of Orthoptera Research*, *10*(1), 53–61.
Vijayan, N., Joshi, S., Sarath, P., & Nishant, K. T. (2025). Loss of Heterozygosity associated with ubiquitous environments in yeast. *PLoS Genetics*, *21*(5), e1011692.
von Siebold, C. T. E. (1856). *Wahre Parthenogenesis bei Schmetterlingen und Bienen. Ein Beitrag zur Fortpflanzungsgeschichte der Thiere, etc*.
Vrijenhoek, R. C. (1998). Animal clones and diversity. *Bioscience*, *48*(8), 617–628.

Wang, J. M., Bennett, R. J., & Anderson, M. Z. (2018). The genome of the human pathogen Candida albicans is shaped by mutation and cryptic sexual recombination. *MBio*, *9*(5), 10.1128/mbio. 01205–01218.
Wang, Y., & Obbard, D. J. (2023). Experimental estimates of germline mutation rate in eukaryotes: a phylogenetic meta-analysis. *Evolution Letters*, *7*(4), 216–226.
Weedall, G. D., Clark, C. G., Koldkjaer, P., Kay, S., Bruchhaus, I., Tannich, E., Paterson, S., & Hall, N. (2012). Genomic diversity of the human intestinal parasite Entamoeba histolytica. *Genome biology*, *13*(5), R38.
Weedall, G. D., & Hall, N. (2015). Sexual reproduction and genetic exchange in parasitic protists. *Parasitology*, *142*(S1), S120–S127.
Weir, W., Capewell, P., Foth, B., Clucas, C., Pountain, A., Steketee, P., Veitch, N., Koffi, M., De Meeûs, T., & Kaboré, J. (2016). Population genomics reveals the origin and asexual evolution of human infective trypanosomes. *eLife*, *5*, e11473.
Wesenberg-Lund, C. (1923). *Contributions to the Biology of the Rotifera*. A.F. Høst og Søn.
West, Lively, & Read, A. (1999). A pluralist approach to sex and recombination. *Journal of Evolutionary Biology*, *12*(6), 1003–1012.
White, M. J. D. (1973). *Animal cytology & evolution* (3rd ed.). Cambridge University Press.
Whitehouse, L. S., Ray, D. D., & Schrider, D. R. (2024). Tree sequences as a general-purpose tool for population genetic inference. *Molecular Biology and Evolution*, *41*(11), msae223.
Williams, G. C. (1975). *Sex and evolution*. Princeton University Press.
Wilson, C. G., Nowell, R. W., & Barraclough, T. G. (2018). Cross-contamination explains “inter and intraspecific horizontal genetic transfers” between asexual bdelloid rotifers. *Current Biology*, *28*(15), 2436–2444. e2414.
Wilson, C. G., & Sherman, P. W. (2010). Anciently asexual bdelloid rotifers escape lethal fungal parasites by drying up and blowing away. *Science*, *327*(5965), 574–576.
Wohns, A. W., Wong, Y., Jeffery, B., Akbari, A., Mallick, S., Pinhasi, R., Patterson, N., Reich, D., Kelleher, J., & McVean, G. (2022). A unified genealogy of modern and ancient genomes. *Science*, *375*(6583), eabi8264.
Wright, S. (1949). The genetical structure of populations. *Annals of eugenics*, *15*(1), 323–354.
Wright, S., & Finnegan, D. (2001). Genome evolution: sex and the transposable element. *Current Biology*, *11*(8), R296–R299.
Zaffagnini, F., & Sabelli, B. (1972). Karyologic observations on the maturation of the summer and winter eggs of Daphnia pulex and Daphnia middendorffiana. *Chromosoma*, *36*(2), 193–203.
Zakharov, I. (2005). Intratetrad mating and its genetic and evolutionary consequences. *Russian Journal of Genetics*, *41*(4), 402–411.

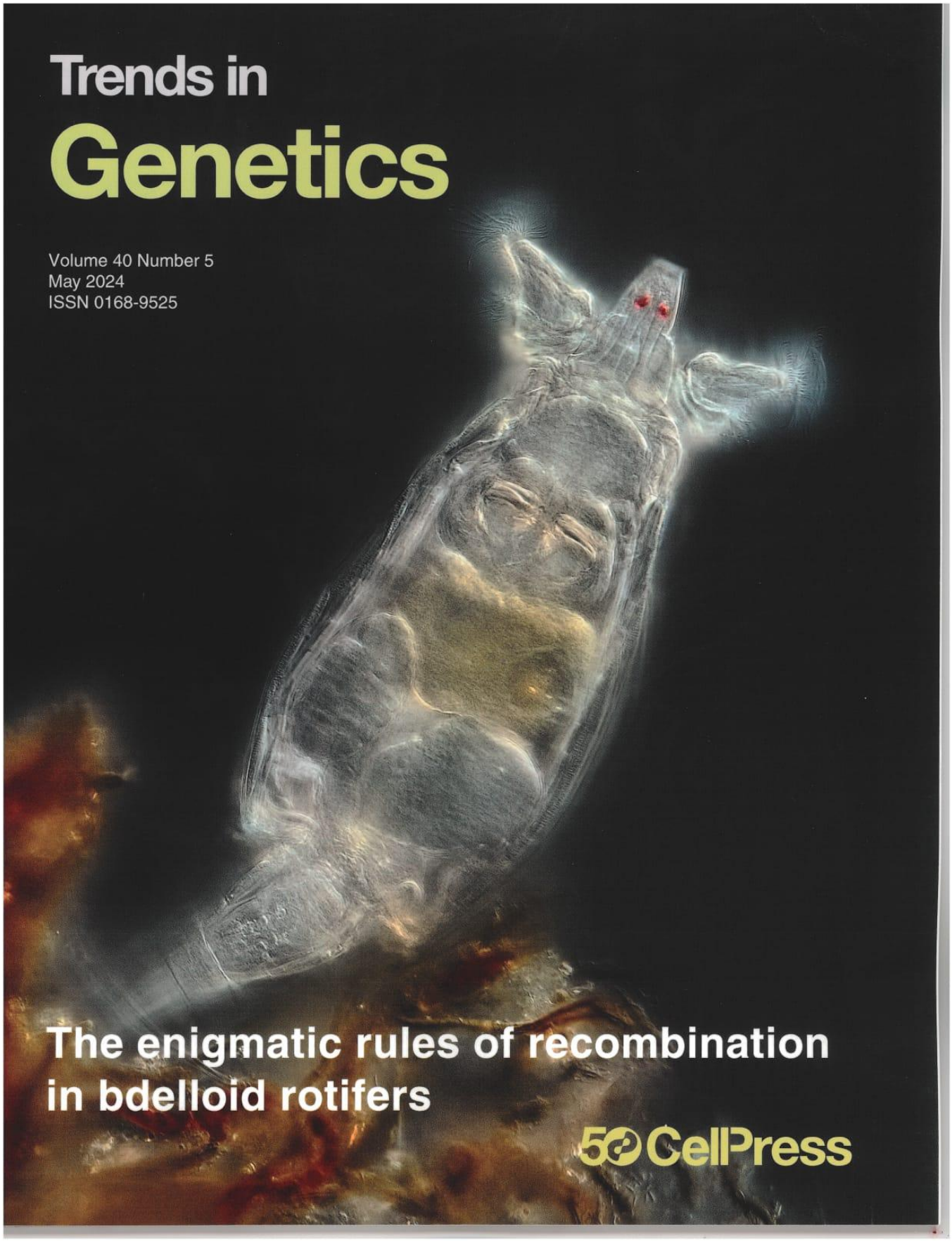
Supplement to General Introduction



——————————— O ———————————

Tymoteusz Pieszko

——————————— O ———————————


Trends in
Genetics
Volume 40 Number 5
May 2024
ISSN 0168-9525
The enigmatic rules of recombination in bdelloid rotifers
CellPress

CellPress
OPEN ACCESS

Trends in
Genetics

Review

Recombination in bdelloid rotifer genomes: asexuality, transfer and stress

Christopher G. Wilson,[1,*] Tymoteusz Pieszko,[1] Reuben W. Nowell,[2,3] and Timothy G. Barraclough[1]

Bdelloid rotifers constitute a class of microscopic animals living in freshwater habitats worldwide. Several strange features of bdelloids have drawn attention: their ability to tolerate desiccation and other stresses, a lack of reported males across the clade despite centuries of study, and unusually high numbers of horizontally acquired, non-metazoan genes. Genome sequencing is transforming our understanding of their lifestyle and its consequences, while in turn providing wider insights about recombination and genome organisation in animals. Many questions remain, not least how to reconcile apparent genomic signatures of sex with the continued absence of reported males, why bdelloids have so many horizontally acquired genes, and how their remarkable ability to survive stress interacts with recombination and other genomic processes.

What are bdelloid rotifers and why study their genomes?

Early genome sequencing focused on a small set of model organisms, chosen to represent major branches of the tree of life, in an initial search for general rules that govern genome organisation and evolution. As genomes are sequenced from an expanding array of taxa [1], it has become clear that these rules can vary strikingly among organisms. Consequently, diverse taxa from distinct phylogenetic clades might provide interesting cases for investigating particular genomic processes. The limiting step now is often not sequencing a genome, but knowing enough about the life history, ecology, and cellular biology of the organism to interpret genomic patterns.

Bdelloid rotifers have long attracted interest as a case that seems to push the limits of metazoan biology, initially in terms of ecology and reproduction, and more recently with respect to genomics. These microscopic invertebrates, typically <0.5 mm long, are common worldwide in freshwater and especially ephemeral habitats such as the water film on mosses and lichens [2], where even a patch the size of a coin may harbour hundreds of individuals (Figure 1A). Discovered by Antonie van Leeuwenhoek in the 1670s [3,4], over 460 species are now known, comprising a monophyletic clade within the phylum Rotifera (and superphylum Gnathifera [5]) with an estimated crown age of at least 50 million years [6,7]. By 1886, Hudson and Gosse noted a 'strange fact' about bdelloids: no males had been seen, despite 'a century and half of observation' [8]. Another century and half later, this strange fact remains [9,10], despite direct observation of hundreds of thousands of individuals [11] and the discovery of males in other putative '**ancient asexual**' (see Glossary) groups [12–14]. As the largest clade of animals that lack known males, they have sometimes been called an '**evolutionary scandal**' [15–17] because they seem to challenge theories for the adaptive benefits of sexual reproduction [18].

Aside from the strange lack of males, bdelloid rotifers have drawn interest for their extraordinary stress tolerance, especially in relation to desiccation and radiation [19–22]. After adding water to some dry dirt collected from a gutter, van Leeuwenhoek observed 'animalcules' rolled-up into ovals which, within 30 min, stretched out their bodies and started swimming around [23].

Highlights

Bdelloid rotifer genomes show signatures of asyngamous recombination leading to loss of heterozygosity. This has been hypothesised to occur via chromosome pairing during egg formation through a meiosis-like but non-reductional process.

Evidence of genetic exchange in bdelloid populations requires further validation in our view.

Around 10% of bdelloid genes have been acquired horizontally from other kingdoms of life; the mechanisms and consequences of high horizontal gene transfer (HGT) prevalence remain to be confirmed by functional and comparative studies.

Bdelloids tolerate desiccation and radiation stress, and appear to repair the resulting DNA double-strand breaks by different mechanisms in the soma versus germline; other aspects of stress tolerance remain to be investigated.

Links between parthenogenesis, desiccation tolerance and horizontal gene transfer have been hypothesised, but several key steps remain to be tested.

[1]Department of Biology, University of Oxford, 11a Mansfield Road, Oxford OX1 3SZ, UK
[2]Institute of Ecology and Evolution, Ashworth Laboratories, Charlotte Auerbach Road, Edinburgh EH9 3FL, UK
[3]Biological and Environmental Sciences, School of Natural Sciences, University of Stirling, Stirling FK9 4LA, UK

*Correspondence:
chris.wilson@biology.ox.ac.uk
(C.G. Wilson).

© 2024 The Authors. Published by Elsevier Ltd. This is an open access article under the CC BY license (http://creativecommons.org/licenses/by/4.0/).

Trends in Genetics

CellPress
OPEN ACCESS

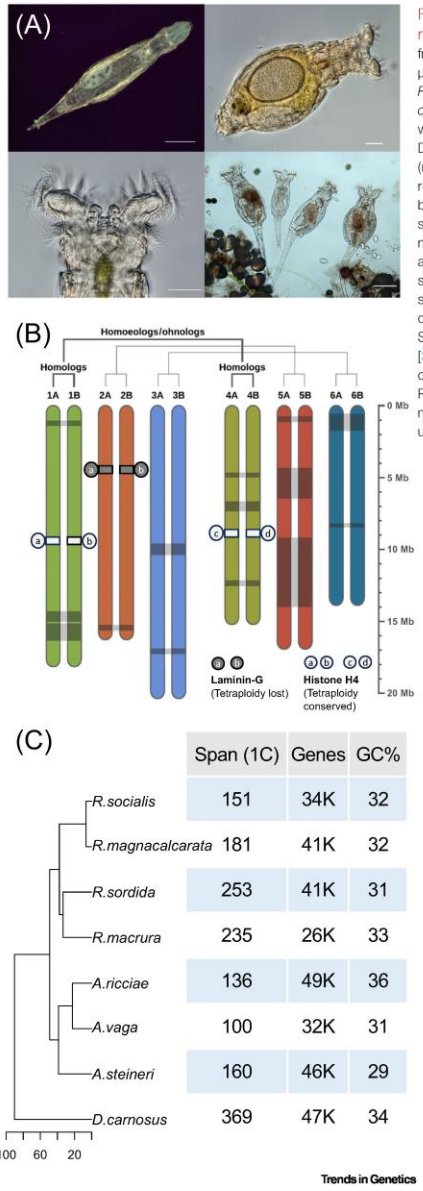


Figure 1. (A) Micrographs of some bdelloid rotifers used in genomic studies. Clockwise from top left (scale bar length): *Adineta vaga* (30 µm), *Macrotrachela quadricornifera* (25 µm), *Rotaria macruca* (50 µm), and *Didymodactylos carnosus* (25 µm). *A. vaga* by C. Wilson, others with permission by M. Plewka (plingfactory.de). (B) Degenerate tetraploidy of the *A. vaga* genome (modified from [36]). Shading indicates regions of loss of heterozygosity (LOH) between diploid chromosomes. Other bdelloid species may have different chromosome numbers. Examples of genes retaining all four ancestral copies versus just two copies are shown. (C) Phylogeny and comparative genomic statistics for species of bdelloid rotifers with crude date calibration in millions of years (based on [7]). Span indicates the haploid assembly size [34,36,71], number of predicted protein-coding genes (×1000), and GC content. References discuss uncertainties in span and gene number owing to fragmented assemblies and uneven haplotype collapse in most species.

Glossary

Allele sharing: a class of allele relationships postulated as incompatible with obligate asexuality: for example, a tree topology where alleles of an individual cluster with alleles of two other individuals.
Ancient asexual: groups proposed to have lacked sexual reproduction for extended evolutionary periods, typically exceeding 100 000 years. Estimates of lineage age and evidence of truly obligate asexuality are subject to debate and uncertainty.
Anhydrobiosis: the phenomenon by which an organism can survive desiccation. In bdelloids, this can occur at any life stage, with adults contracting into dormant 'tuns' that revive and resume reproduction on rehydration.
Asyngamous recombination: recombination occurring within a parthenogenetic line of descent, without the fusion of gametes (syngamy). This could include gene conversion or crossing over, either mitotic or associated with an abortive meiosis.
Degenerate tetraploidy: the signal of ancient genome duplication or hybridisation, such that genes group into homologous pairs, which then further pair into divergent ohnologs (duplication scenario) or homoeologs (hybridisation scenario) (Figure 1). The scenario in bdelloids is possibly unknowable given the long time since this unique event.
DNA double-stranded breaks (DSBs): both DNA strands are broken in close enough proximity that the double helix is cut in two. Caused by ROS resulting from desiccation, IR exposure, and other stressors, or by enzymes during meiosis and other cellular processes.
Evolutionary scandal: from a quote about bdelloid rotifers by Maynard Smith (1986): a 'scandal' because these rotifers seem to contradict evolutionary theories predicting extinction for obligate asexuals.
Genetic exchange: any process that brings together genetic material from different individuals, leading to 'reshuffling' of genotypes. It encompasses sexual reproduction in the form of outcrossing and other mechanisms (e.g., parasexuality or near HGT).
Genetic system: the way that genetic information is organised and transmitted between generations.
HGTc: HGT candidate gene, defined as a gene showing closer protein sequence similarity to non-metazoan sequences

CellPress OPEN ACCESS

Trends in Genetics

These ovals, known as 'tuns' or sometimes 'xerosomes', were bdelloid rotifers in the state of **anhydrobiosis**, a form of dormancy they undergo frequently and repeatedly in nature for weeks at a time, apparently without severe fitness consequences [24]. In both the desiccated and hydrated state, bdelloids can tolerate massive doses of ionising radiation (IR), making them of potential interest for space research [21,25]. Desiccation and radiation both result in cellular and DNA damage which bdelloids can resist or repair to an unusual degree [26–28]. With respect to radiation and probably other stressors, the extreme resilience of bdelloid rotifers matches or exceeds that of tardigrades [19], although their media profile has yet to catch up.

Together, these features sparked interest in genomic signatures and mechanisms that might reflect the unusual lifestyles of bdelloids. DNA sequencing began in 2000 with attempts to test early genetic predictions of ancient asexuality [29,30]. The first transcriptomes and a genome assembly arrived a decade later [31–33], followed by comparative genomics [34,35], a chromosome-scale assembly (Figure 1B) [36], and population genomic data by the 2020s [35,37,38]. Bdelloid genome assemblies range from 135 to 369 Mb in estimated haploid span and contain between 25 000 and 50 000 predicted protein-coding genes [34,35] (Figure 1C). All bdelloid genomes so far sequenced display a signature of **degenerate tetraploidy**: while genes group into homologous pairs with relatively low divergence (0.03–4.5%) (Figure 1B), many but not all homologs group further into pairs of distantly related copies called homoeologs (or ohnologs) that typically show >30% sequence divergence at the protein level, consistent with an ancient hybridisation (or duplication) event. The chromosomal assembly of *Adineta vaga* has six diploid pairs of homologous and colinear chromosomes that also group into three homoeologous sets. Over 30% of coding genes are present in four copies across two pairs of homoeologous chromosomes [36] (Figure 1B), while other genes have lost one homeologous pair.

Genomic investigations revealed yet another 'strange fact' about bdelloids. Over 8% of their genes appear to have been acquired via **horizontal gene transfer (HGT)** from non-metazoans, including bacteria, fungi, and plants [31,34,36,39,40]. This level (Figure 2A) is much higher than that reported in other animals [41], and includes genes with biochemical functions that animals normally lack [32,42].

The combination of (i) potential long-term asexuality, (ii) stress tolerance (especially DNA repair capabilities), and (iii) high levels of HGT makes bdelloids a fascinating system for investigating how and why DNA is recombined in animals. How does their natural history relate to their **genetic system** and its functional and evolutionary consequences? Do they possess genetic mechanisms that other animals lack? This review discusses key research questions and opportunities in bdelloid genomics. We outline the latest findings and how they relate to the aforementioned three strange facts. Given the challenges in connecting genomic patterns in bdelloids to their presumed lifestyle (Box 1), we evaluate mechanisms and scenarios without making prior assumptions about the bdelloid genetic system. Recent work has brought substantial advances, but major questions remain to be resolved. The contributions of bdelloid rotifers to understanding **recombination** and DNA repair now extend well beyond their original 'claim to fame' as ancient asexuals, although that remains an important topic of active research. Work on this unusual group is indeed shedding light on the 'inconceivable possibilities' [23] of life as an animal.

How can we reconcile the absence of males with genomic signatures of sex?

Early research on bdelloid genomes sought to test classical predictions of long-term obligate asexuality [17,43]: for instance, that former diploid alleles inherited from a sexual common ancestor should diverge over time in the absence of segregation and recombination (Box 2). Later work looked for signatures of **genetic exchange** within populations, such as **incongruence** in

than to any metazoan sequences, thus inferred to be horizontally transferred. The 'candidate' flag acknowledges that alternative explanations may exist (e.g., differential loss or convergent evolution).

Horizontal gene transfer (HGT): the acquisition of genetic material via processes other than vertical descent from parent to offspring that results in reticulate evolution. 'Distant' HGT describes transfers between distantly related donor and recipient lineages (e.g., from a bacterium to an animal). 'Near' HGT describes transfers between more closely related lineages (e.g., within populations).

Incongruence: differences in branching order (topology) between loci or different copies at a single locus, which is unexpected in strictly clonal populations, but might occur by asyngamous recombination or genetic exchange.

Outcrossing: sexual reproduction involving the mating of unrelated individuals.

Recombination: any process that forms a new DNA molecule with sequences from previously different DNA molecules. Also used in an evolutionary context for the generation of new allele combinations within populations, as can arise through outcrossing or gene transfer. We use the molecular definition to distinguish between asyngamous processes and sexual reproduction.

Trends in Genetics

CellPress
OPEN ACCESS

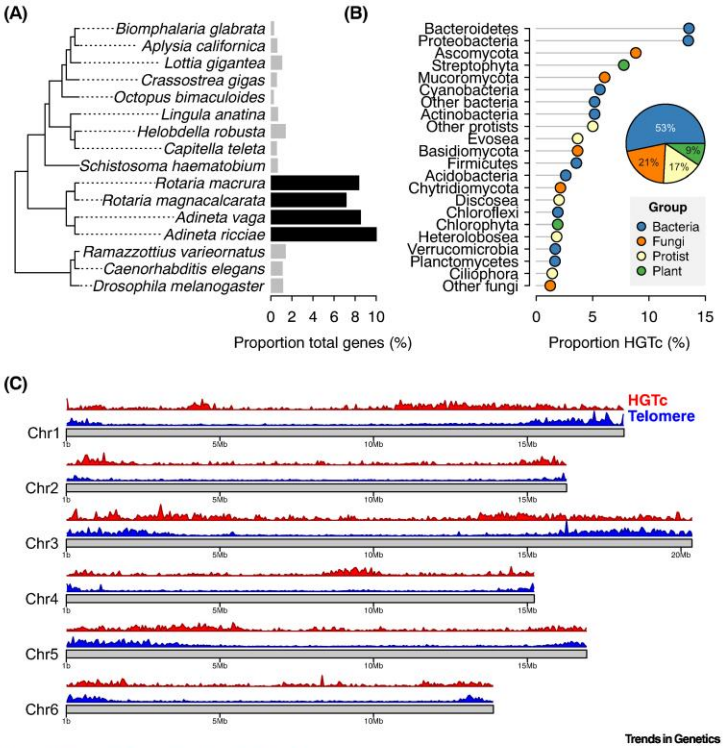


Figure 2. Horizontal gene transfer in bdelloids. (A) The percentage of genes identified as horizontally acquired from non-metazoa for a suite of animal taxa. Values for bdelloid species *Adineta vaga*, *A. ricciae*, *Rotaria macrura*, and *R. magnacalcarata* are shown with black bars. All values are taken from [34] except those for *A. vaga* [36]. (B) The proportion of horizontal gene transfer candidate (HGTc) genes attributed to different donor taxa, based on best Basic Local Alignment Search Tool match. Bacteria (blue) are most frequent, followed by fungi (orange) and plants (green). (C) The density of HGTcs (shown in red) and telomeric repeats (TGTGGG, blue) in 50 kb sliding windows along the six chromosomes of the *A. vaga* chromosomal scale haploid assembly.

genealogical relationships among loci. Despite considerable effort, however, the bdelloid genetic system has been surprisingly difficult to pin down, and several signatures reported as positive evidence either for obligate asexuality or for genetic exchange were later reinterpreted (Box 1).

At present, many features of bdelloid genomes do not seem obvious outliers when compared with sexual groups. With homologous chromosome pairs [36,44], most meiosis genes present [31,34], a diverse landscape of transposable elements (TEs) [35,45–47], heterozygosity, and other population genetic parameters within the range of sexual species [34,37], so far there is no positive genomic evidence of bdelloid ancient asexuality. Yet, these features do not constitute clear evidence for the presence of sex either. In particular, recombination between homologs within an individual has long been documented via gene conversion or larger-scale mechanisms [48,49], which must be accounted for in predictions and tests. For instance, this can explain the

CellPress OPEN ACCESS

Trends in Genetics

Box 1. Genomic patterns in bdelloid rotifers have been reinterpreted over time

The challenges of applying older sequencing and assembly techniques to tiny non-model animals mean that several early results have later been overturned. Nuclear protein-coding sequences [30] initially seemed to show that bdelloid genera shared two deeply divergent lineages of each gene, interpreted as pairs of former alleles that had ceased to segregate and recombine millions of years ago when sex was lost in a common ancestor. Later, these divergent copies were found to result from an ancient genome duplication or hybridisation [48], with each present in paired, locally collinear, functionally diploid copies (Figure 1B in main text). In 2013, the pioneering first bdelloid genome (for *A. vaga)* appeared to show chromosomal rearrangements incompatible with meiotic pairing [31], but later long-read and *in situ* hybridisation data revealed these as assembly artefacts and resolved the same genome as six pairs of homologous chromosomes [36]. Bdelloids were initially reported to lack vertically transmitted long interspersed nuclear elements (LINE)-like and *gypsy-like* TEs, as predicted by some models of asexual evolution [29], but such elements were uncovered in later surveys [35], while evidence from other taxa has questioned the link between TEs and reproductive mode (e.g., [1,81]).

Evidence for mechanisms of genetic exchange within or between species has been similarly inconsistent. Three *Macrotrachela* lineages from distant locations seemed to show linked inheritance at multiple loci in a strikingly symmetrical pattern of allele sharing [82], interpreted as evidence of recent sexual ancestry involving non-canonical meiosis. However, genomic reanalysis of the same isolates [38] clarified that close relationships are limited to two lineages, whereas the third is closely related at only a small number of loci, four of which were initially sampled by chance. Finally, a report of inter- and intraspecific HGTs between individuals in the genus *Adineta* [83] was found to be explainable by accidental cross-contamination during sample processing [63]. In many cases, clues to the eventual reinterpretation were present in the original work as inconsistencies that required supplementary explanations beyond the main predictions, and whose importance only became clear with hindsight.

lack of deep divergence between homologous alleles without requiring the shuffling of chromosomes through fusion of gametes (syngamy) during sexual **outcrossing** (Box 2).

Progress in cytology has helped clarify how such **asyngamous recombination**, defined as recombination occurring in a parthenogenetic lineage, could shape bdelloid genomes. Although the whole class was long regarded as apomictic [10,50], recent work suggests that parthenogenesis in *A. vaga* involves a form of abortive meiosis [27,36]. This includes a non-reductional meiosis I with homologous chromosome pairing [27]. In theory, pairing could provide the opportunity for recombination between homologous chromosomes at multiple scales [36]. This could lead to loss of heterozygosity and decay of linkage disequilibrium over long genome tracts, as observed in laboratory resequencing and population samples [36,37], even when occurring in a single germline inherited parthenogenetically from mother to daughter. Evidence is now emerging to assess experimentally the mechanisms and consequences of interactions between homologous chromosomes [51].

Some recently reported genetic signatures in wild populations of *Adineta* and the distantly related species *Macrotrachela quadricornifera* might not be explained easily by asyngamous recombination alone. These include **allele sharing** trees (Box 2) and other patterns of incongruence inferred from phased sequence blocks [37,38], leading to explanations involving facultative sex and hybridisation in the recent history of these lineages. How can we reconcile these findings with the continued absence of males? We explore three possible resolutions of this apparent paradox.

There is cryptic sex but males or hermaphrodites have gone undetected

It remains possible that bdelloid rotifers do produce males that are either exceedingly rare, produced only under specific conditions, or have been taxonomically mis-assigned. Alternatively, male function in a putative bdelloid hermaphrodite could be highly reduced, anatomically unusual, or expressed only transiently. By contrast with many taxa, where outcrossing is inferred from genomic patterns but not observed directly (e.g., placozoa [52] or many protists [53]), bdelloids are cosmopolitan and easy to access, as evidenced by centuries of close observation and taxonomic descriptions of wild-caught specimens from a wide range of habitats [9,54]. Monogonont rotifers are facultative parthenogens that live in habitats overlapping those of bdelloids. Their

Trends in Genetics

CellPress
OPEN ACCESS

Box 2. What constitutes a robust genomic signature of genetic exchange?

DNA sequences record their own histories, and different histories of recombination and genetic exchange ought to leave distinct signatures [82,84]. Simple predictions regarding allele tree topologies have been used to test for asexual evolution in bdelloid rotifers (Figure I).

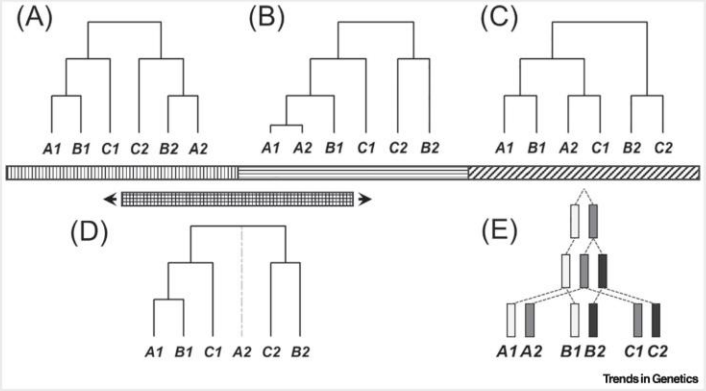


Figure I. Examples of allele tree topologies under different scenarios as explained in the main box text.

(A) If bdelloids arose from a diploid sexual ancestor but have since reproduced without any forms of recombination or genetic exchange, then homologous regions should show independent divergence over time (the 'Meselson effect') [30,43,84]. The tree for a locus (vertically hatched box) would consist of two sub-trees (for copies *1* and *2*), each recapitulating the same genealogy of individuals *A*, *B*, and *C*. With strict linkage, allele tree topologies should be the same (i.e., congruent) across all loci.

(B) If bdelloids reproduce asexually but with mechanisms for asyngamous recombination, then genealogies are not necessarily congruent across loci. For example, a gene conversion event in individual *A* leaves alleles *A1* and *A2* grouping together and an apparent sister relationship between alleles *B2* and *C2* (though with some divergence).

(C) Not all patterns of incongruence can be explained easily by asyngamous recombination alone. A class of patterns referred to as 'allele sharing' are expected with mechanisms for genetic exchange in the population. A simple case at a single locus is when alleles from one individual are reciprocal closest relatives of alleles from two other individuals [37]: for example, in a cyclical pattern, as shown (i.e., for individual *A*, allele *1* is shared with individual *B*, but allele *2* is shared with individual *C*; similarly for individuals *B* and *C*). The term is used more broadly to refer to any case where individuals share highly similar alleles at one copy, but more divergent alleles at the other diploid copy [38].

For example, the finding of incongruent allele topologies in a sample of eight *Adineta* individuals, including >12% of trees with at least one case of reciprocal allele sharing (as inferred in stringently filtered phased blocks) has been interpreted as evidence of genetic exchange [37]. Similarly, two *Macrotrachela quadricornifera* individuals shared identity across 315 out of 622 surveyed genome regions (mean length ~20 kb), whereas the remaining regions were more divergent, which was attributed to a very recent bout of sex [38].

Questions remain, however, regarding the effects of inference methods and other processes. First, asyngamous recombination can generate complex patterns of topological incongruence if trees are reconstructed from genomic windows containing a mixture of recombination histories. For instance, a gene conversion event in part of a window used for tree inference can 'pull' one copy towards an intermediate position between the two sub-trees (e.g., a region that spanned trees shown in (A) and (B) could generate the tree shown in (D), with allele *A2* in an intermediate position shown as the grey dashed branch). This could give the appearance of divergent alleles for individuals that have shared alleles at other copies/loci.

(E) Finally, other asexual processes might occur to enable a wider range of possible tree topologies. For instance, a recent autopolyploidisation event followed by independent reversals to diploidy through loss of different haplomes could generate genome-wide patterns of allele sharing.

males are reduced in size but bear a morphological similarity to females of their species, and they have been comprehensively described over the same period [8,54,55]. The single account of a possible sighting of a bdelloid male was in a mixed wild sample also containing monogonont rotifers, and framed very cautiously ('With great hesitation I venture to remark…'): two animals

CellPress
OPEN ACCESS

Trends in Genetics

resembling monogonont males were seen swimming among a dense population of bdelloids [54], but were not isolated or drawn, leaving open the possibility that they were, in fact, monogonont males. This contrasts with other putatively ancient asexual animals, where ongoing production of males has been documented for some time [12–14], and genomic evidence of their involvement in cryptic sex has recently emerged [56,57]. While negative evidence is not conclusive, the extensive history of rotifer sampling across aquatic and semiterrestrial habitats makes it difficult to suggest new ways to test the cryptic male hypothesis directly (but see [38]). One approach might involve leveraging new data and techniques [58,59] to revisit early attempts at inferring 'sperm-specific' proteins in other rotifers [58–60] and examining their fate in bdelloids.

There are neither males nor sex, but genetic exchange occurs by alternative mechanisms

Another hypothesis is that bdelloid rotifers might exchange or transfer genes within populations in alternative ways that are distinct from outcrossing. For example, perhaps horizontal transfer between homologous loci occurs by uptake of exogenous DNA (for example, during DNA repair after desiccation [40]) or via vectors such as mobile elements (analogous to transformation and transduction, respectively, in bacteria [61]). This hypothesis was initially prompted by the discovery of high levels of distant HGT from non-metazoan sources [40], though whether near HGT within populations would occur by similar means is unknown. Evidence to assess this possibility directly is currently lacking (Box 1), and we know of no successful transformation experiments with bdelloids to date. Frequent HGT might be expected to generate a patchwork of allele-sharing patterns at restricted sets of loci rather than the genome-wide shuffling or sharing expected through outcrossing [38]. Other alternative mechanisms might include parasexual exchange, as in fungi, which can involve the transfer of large genome regions or chromosomes [62], but requires a haploid life stage which is thus far unknown in bdelloids. All these hypotheses are speculative at present, and it is unclear to what extent they might recapitulate theoretical benefits of sex. Nonetheless, even heterodox ideas should be considered, given the puzzle of the missing males.

There are neither males, sex, nor any other kinds of exchange

The final possibility is that both outcrossing and genetic exchange are absent in bdelloid rotifer populations, and signatures interpreted in this light have other explanations. For example, these might include gene duplication and loss, rare recombination between divergent paralogous copies within gene families, uncertainties in haplotype or ancestral recombination reconstruction, and unrepresentative subsampling or filtering from the full set of genomic loci (Box 1). Both studies reporting allele sharing patterns analysed only a fraction of the genome (<10%), so that biases in assembly, variant calling, filtering, and tree inference stages could influence some results. Trees inferred within arbitrary genomic windows are likely to encompass mixed signal from sequence blocks with different histories due to asyngamous recombination (Box 2). This could lead to topological incongruence and apparent allele sharing as an artefact (e.g., Figure S4 in [63]), potentially even without sex. Unexpected patterns of allelic divergence could also arise from broader genome-scale mechanisms, such as further tiers of historic polyploidy, disparities in ploidy between germline and somatic nuclei, or asymmetries of evolutionary rates between haplomes. Genome data from an expanding range of metazoans is revealing diverse genetic systems that could affect signatures in ways that are difficult to anticipate [64].

So far, many studies have adopted a qualitative approach (Box 2), in which allele trees or sharing patterns incompatible with verbal predictions of strict asexuality are taken as evidence of outcrossing or alternative forms of genetic exchange. Further resolution will come partly from chromosome-scale genomic data for more populations and species, but also from applying population genetic models and simulations to generate quantitative predictions about the effects of different genetic systems on the frequency of certain genomic signatures [37,65]. Comparisons

CellPress
OPEN ACCESS

of tree topologies among loci could use ancestral recombination graph (ARG) approaches that infer how genealogical relationships change along the genome due to recombination breakpoints [66–68]. Modelling would enable alternative assumptions, scenarios, and interactions to be defined and quantified, and then establish whether the parameters underpinning these scenarios are compatible with, for example, strict asexuality or rare sex. Philosophically, the Bayesian prior for such tests ought to be uniform: evaluating evidence across a range of scenarios rather than directing the burden of proof towards a particular claim. Whichever way the paradox of males is finally resolved, its investigation is bringing a deeper understanding of the effects of sex, recombination, and genetic exchange in animal genomes.

Why is there so much HGT in bdelloid genomes?

A remarkably high proportion of bdelloid genes apparently have been acquired via HGT from non-metazoan sources. Over 8% of genes share closer sequence identity with non-metazoans than with metazoans, or encode proteins not found in other animals, indicating an unusually high level of non-homologous, inter-kingdom horizontal transfer (denoted 'distant HGT') compared with other animals (Figure 2A). The pattern is consistent across a range of data types (fosmid [40], transcriptomic [32], and genomic [31,34,36]), and among all bdelloid species investigated thus far, while absent from their nearest phylogenetic relatives [32] (but see [59]).

Contamination is ruled out by the unambiguous placement of HGT candidate genes (**HGTcs**) within assembled bdelloid chromosomes [36] (Figure 2C). Alternative evolutionary explanations – such as loss of ancient gene families from all other metazoa except bdelloids, gain of many genes in a single event (e.g., from a parasite or endosymbiont), or convergent evolution of bdelloid genes towards non-metazoan sequence motifs – are difficult to reconcile given the diversity of putative donors from multiple bacterial phyla, plants, fungi, and single-celled eukaryotes (Figure 2B). Most work has focused on non-metazoan sources to date because of the ease of detection against a metazoan background, but the same mechanisms could presumably work for metazoan DNA. The increasing number and diversity of high-quality animal genomes will allow robust phylogenetic estimation of the level of animal DNA that has been acquired.

Unlike cases in prokaryotes, most HGTcs in bdelloids are too highly modified from their closest non-metazoan matches (including acquiring introns and metazoan promoters [40]) to establish a precise origin, and likely descend from ancient acquisitions. Given the challenges and modifications involved in domesticating transferred genes, most retained HGTcs probably benefit the animal. The precise functions of HGTcs are mostly unknown, however, because of the current lack of tools for gene knockdown or modification in bdelloids. Functional annotations and expression patterns nonetheless support roles in processes such as DNA repair [69,70], resistance to fungal pathogens [71], TE silencing [35] and/or gene regulation via epigenetic DNA modification [72], and long-chain fatty acid biosynthesis [73]. Functional annotations include biochemical pathways that are greatly expanded compared with those of other animals, such as carbohydrate metabolism and toxin degradation [32]. Those HGTcs that show degenerate tetraploidy in *A. vaga* (and hence are assumed to be present in the most recent common ancestor of extant bdelloids) are enriched for DNA recombination and ligation functions, which could have contributed to bdelloids' ability to repair **DNA double-stranded breaks (DSBs)** (next section). Future methods for genetic manipulation will be required to test these functions directly.

How HGTcs are acquired is currently unknown. An early hypothesis was that they could be incorporated rarely and accidentally during repair of DSBs after desiccation, perhaps by non-homologous end joining [10,39,40]. This has not been observed directly, however, and bdelloid species that live in fully aquatic habitats and lack measurable survival upon desiccation still have

CellPress OPEN ACCESS

Trends in Genetics

unique HGTcs acquired after their divergence [36,39], together with a higher density of TEs [35]. Perhaps exogenous DNA is picked up during dynamic rearrangements in bdelloid telomeres and then shuffled to other genomic locations via TE movements or transposon-mediated ectopic recombination. Recently discovered giant retroelements called *Terminons* (exceeding 40 kb in length) may play a role in transfer [74], although their dynamics and effect on HGT remain to be investigated.

Why do bdelloids have so many HGTcs? They might have mechanisms that promote higher rates of arrival of exogenous DNA into their germlines. Alternatively, perhaps the rate of exposure to potential transfers is similar to that in other animals, but bdelloids are more able or under stronger selection to retain them. It is tempting to relate HGT to the other unusual features of bdelloids, namely anhydrobiosis and the lack of males, but comparisons across bdelloid species do not support a strong causal role for desiccation in promoting HGT [34], nor do other anhydrobiotic animals (e.g., tardigrades [75]) show equivalent levels of HGT (though their mechanisms of desiccation tolerance may also differ). Similarly, there is no clear tendency for high levels of HGT in other asexual animals [41], though such cases are often interspersed with close sexual relatives and retain the ability to produce males. Even though the level of HGT from non-metazoan sources is high, the rate of gain appears to be low, estimated as 12.8 gains per million years [39]. This rate is too low to act as a direct replacement for outcrossing, but could be viewed as a slow but steady source of new functions. It is also too low to facilitate direct observation and experimentation into causes of HGT, meaning that future resolution will depend upon phylogenetic and genomic inferences, such as identifying putative cases of recent transfer from a known donor. Sampling of genomes from across the eukaryote tree of life will allow a robust assessment of the 'uniqueness' of high HGT in bdelloids and may reveal cases in other taxa that would shed light on its correlates. For now, bdelloids are an important system to understand the transfer of metabolic and biochemical functions across domains of life.

How does stress tolerance both influence and depend upon genome dynamics?

Bdelloid rotifers have long been recognised as extraordinarily resistant to multiple stressors, including cold, heat, vacuum, and ultraviolet radiation [76]. However, many of these extremophilic capabilities appear to be directly or indirectly related to their tolerance of desiccation, which is an ecologically crucial trait in their temporary water habitats. Among numerous adverse effects, desiccation disrupts cell membranes, produces reactive oxygen species (ROS), and denatures proteins [77]. Particularly relevant to genome dynamics, however, is the potential to cause DSBs. The discovery that bdelloids are extraordinarily resistant to ionising radiation (IR) – a stressor that is not as ecologically salient, but also results in DSBs [19] – led to the development of the DSB-repair hypothesis [10]. This proposes that the ability to repair DSBs caused by desiccation is a key attribute explaining bdelloid stress tolerance that might unite various features of bdelloid genome dynamics (summarised in Figure 3A). For instance, maintenance of homologous chromosomes as templates for DNA repair could explain their collinearity and low divergence [48], while breaks and their repair have been speculated to facilitate HGT via incorporation of exogenous DNA.

Recent imaging and molecular experiments have supported several core elements of this synthesis (Table 1), including short-term repair dynamics, the timing of which appears to differ between somatic and germline cells (Figure 3B,C). A report of chromosome pairing during oogenesis provides a potential mechanism for germline DNA repair [27]. Other parts of the hypothesis, however, especially in relation to evolutionary and genomic consequences of repair (such as for HGT) remain hypothetical or partly contradicted by current evidence (Table 1). One area for future work is to distinguish the effects of IR from those of desiccation. Experiments have focused on IR as much

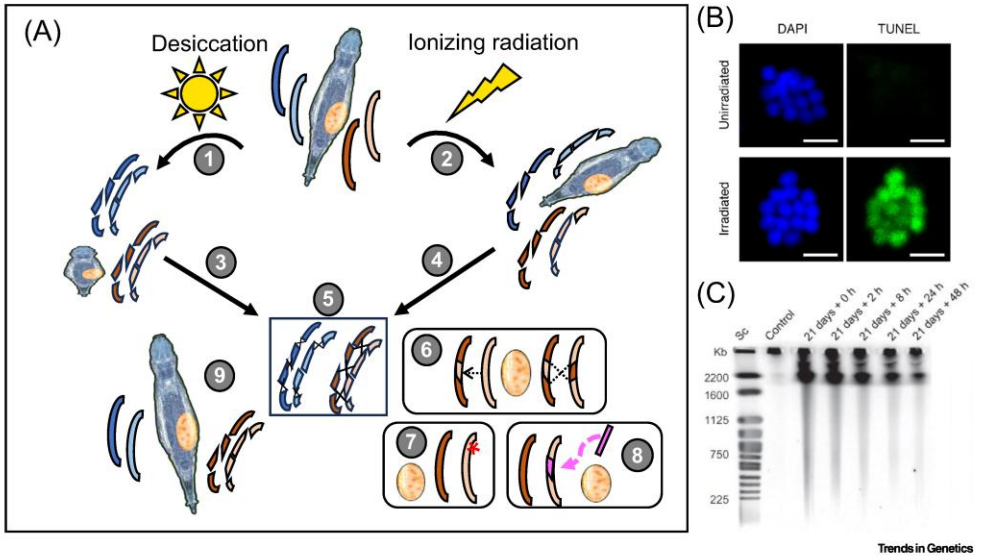


Figure 3. Evidence for key links in the DNA double-strand break (DSB) repair hypothesis and its extensions. (A) The core steps 1–5 propose that repair of DSBs is a key part of bdelloid tolerance of desiccation and ionising radiation; later steps 6–9 associate this process with other phenomena, such as loss of heterozygosity (LoH). The two stressors are shown separately to distinguish evidence in each case, where numbers link to Table 1. Different hypotheses have been proposed for somatic (blue) and germline (orange) cells, with one pair of homologous chromosomes depicted for each. (B) Imaging of primary oocytes in *Adineta vaga* showing DNA (in blue), with DSBs revealed in proton-irradiated animals by terminal deoxynucleotidyl transferase dUTP nick end labelling (TUNEL). Unirradiated animals were desiccated for 72 h, but show no TUNEL signal that would indicate germline DSBs (from [27], scale bar 10 μm). (C) Pulsed-field gel electrophoresis (PFGE) showing repair of fragmented DNA following 21 days of desiccation at different time points post-rehydration (from [26], with permission), together with intact DNA remaining in wells. Abbreviation: DAPI, 4′,6-diamidino-2-phenylindole.

as on desiccation, because it is tractable, recapitulates some of the effects of desiccation, and is interesting for astrobiology, genome stability, and synthetic biology [21,78]. Yet current evidence indicates that the two stressors may not be directly interchangeable (Table 1). A recent study found that only 7% of genes significantly upregulated in response to 14 days of desiccation were also upregulated in response to IR without desiccation [79]. The response to UV radiation seems to differ again in ways that would be worth investigating [26]. Tracking the dynamics of repair and recombination over generational timeframes will also be important, with early work in this area indicating that DSBs may be induced even without external stressors, although desiccation and IR increase their frequency [51].

Evaluation of the importance of DNA repair as a key trait behind desiccation tolerance will require revisiting other aspects of the bdelloid stress response, such as protection against ROS and protein denaturing, compared with other animals. Desiccation tolerance mechanisms might not explain resilience to other stresses; for instance, chemical toxins [32], starvation [80], anoxia, pathogens, and freezing probably require additional pathways [76]. A major question is to what extent non-metazoan genes (whether or not their acquisition results from DSB repair) help to underpin stress tolerance. There is evidence that certain acquired genes play a key role in recovery from desiccation [69], in DNA repair [36,70], and potentially in degradation of chemical toxins [32]. Many horizontally acquired genes are upregulated in response to ionising radiation, though these

CellPress OPEN ACCESS

Trends in Genetics

Table 1. Evaluation of evidence for the different steps of the DSB-repair hypothesis for tolerance of desiccation and ionising radiation as numbered in Figure 3A

#	Hypothesis or link	Status of evidence
1	Desiccation induces DSBs	Good evidence in other systems [77] and bdelloids. Pulsed-field gel electrophoresis (PFGE) reveals modest DNA degradation, increasing after 21–42 days (*A. vaga*), albeit with limited resolution for larger fragments [26]. Replicated across multiple genera: *Habrotrocha*, *Philodina* [20]. PFGE reflects somatic rather than germline DNA outcomes; no evidence of DSBs in germline after 72 h desiccation (Figure 3C).
2	IR induces DSBs	Well-established radiobiology, strong evidence in many organisms [77], including bdelloids [26]. PFGE reveals massive fragmentation in soma at even modest doses. DSBs also apparent in germline cells (primary oocytes) [27] (Figure 3C).
3	Desiccation-induced DSBs are repaired in somatic and germline cells	Direct evidence for DSB repair in one PFGE (Figure 3B), 0–48 h after rehydration. Modest differences between pre- and post-repair DNA, mostly somatic DNA [26]. Intact high-molecular-weight DNA is also present throughout. Nuclear staining indicates no DNA synthesis in somatic cells or developing eggs after 24 h desiccation, but PFGE suggests that damage is not extensive. Germline DNA damage from longer desiccations in nature must be successfully repaired. DNA repair pathways strongly upregulated after desiccation, at least in somatic cells [69]
4	IR-induced DSBs are repaired in somatic and germ cells	Strong PFGE evidence for somatic cell DNA repair in response to various IR sources [20,21,26]. Recovery of DNA sequence (not just size) shown by restriction profiling [27]. Staining reveals rapid DNA synthesis during somatic cell repair, but not in primary oocytes; germline repair is delayed until oocyte maturation and perhaps beyond [51]. DNA repair genes strongly upregulated after irradiation and expressed in somatic nuclei [70], but only a minority of IR-upregulated genes (7–18%) overlap with the desiccation response [79]
5	DSB repair involves pairing of homologous chromosomes	Chromosomes are homologous [36], and bivalents form during normal oogenesis [27], but pairing is not observed immediately after DSB damage occurs, nor in somatic cells. Repair genes upregulated in response to desiccation belong primarily to the non-homologous end-joining and break excision pathways [69,79], rather than homologous recombination as in other systems [77]. Germline damage must be repaired because an original restriction profile is restored in F1 [27], and this may involve different pathways from somatic cells [51]
6	DSB repair causes LoH and/or recombination	Modified meiosis with pairing might be linked to LoH irrespective of external stressors, as seen in hydrated lines [36,51]. Desiccation- or IR-induced DSBs may accelerate LoH, but are not required. Other observations also are inconsistent with a requirement for desiccation (e.g., non-desiccating rotifers have higher LoH [34]; other non-desiccating asexuals show meiotic pairing and LoH)
7	DSB repair aids selection against deleterious mutations	Unknown, despite the intuition that, if DNA repair were associated with recombination, it could alleviate some of the predicted costs of asexuality [31,85]. Unclear whether desiccation facilitates selection in the longer term or is mutagenic (mutation accumulation experiments are needed). Older studies suggest slightly higher or equal deleterious substitution rates in bdelloids versus monogononts [86]
8	Desiccation and DSB repair promote HGT	No evidence at present for either near or distant HGT. Other desiccating animals lack HGT, or elevated incorporation of non-nuclear (e.g., mitochondrial) DNA [87]. Non-desiccating bdelloids still have HGT gains [39]. No direct observations of HGT via desiccation in experiments (may be too rare)
9	DSBs and their repair underpin bdelloid stress tolerance	Repair of DSB is necessary but probably not sufficient. Desiccation duration correlates with survival and so does DNA damage [26], but survival is more robust after proton irradiation despite far more DNA breaks than 42 days of desiccation. UV radiation, despite not causing DNA damage as severe as proton radiation, strongly decreases survival, presumably in other ways (e.g., ROS, mutations, protein damage). Different types of IR cause the same DSB patterns at the same doses [21], but show differently shaped survival and fecundity curves. Desiccation-intolerant *Rotaria* spp. survive radiation as well as desiccating bdelloids (although their fertility is more impacted) and have similar capacity for repairing the DSBs as desiccating bdelloids [20]. Mitigating other harms of desiccation may be at least as important in survival as DSBs [28], such as protection of proteins from ROS [77]

Trends in Genetics

CellPress
OPEN ACCESS

are not overrepresented relative to the genomic baseline, as is seen following exposure to desiccation [79] and pathogens [71]. There is scope to measure the contribution of HGT to stress-induced expression more generally. Further transcriptomic experiments (ideally combined with genetic manipulation) and comparisons with non-desiccating rotifers, as well as other stress-tolerant animals such as tardigrades and nematodes, will help to clarify the importance of HGT for bdelloid resilience. Do acquired genes replace or supplement other pathways, and are they more strongly associated with some stressors than others? Valuable insights will also arise from investigating how shared animal genes, which still greatly outnumber HGTcs, have adapted to provide ecological resilience in a group far removed from well-studied metazoan models.

Key figure

Diagram of potential interactions between four elements of bdelloid biology, and their potential influence on genome dynamics

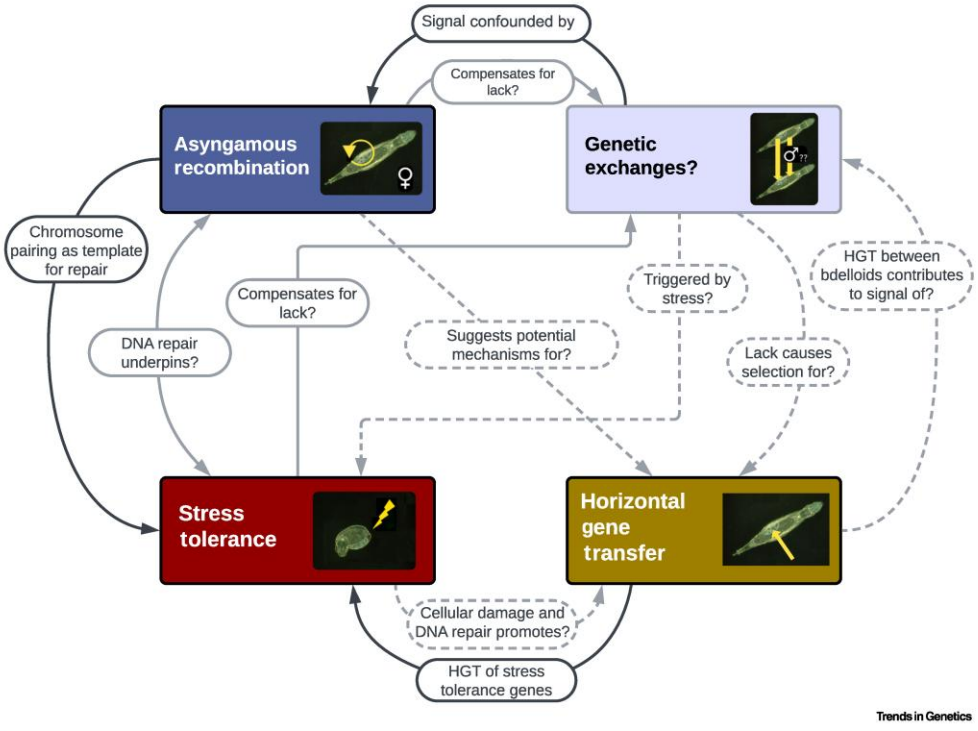


Figure 4. Some hypothetical links from this review and the broader literature are shown, but this is not exhaustive. Arrows and boxes in black indicate links with clearer evidence, grey indicates emerging but partially incomplete evidence, and dashed grey indicates connections or phenomena we view as more ambiguous or hypothetical at the time of writing. Abbreviation: HGT, horizontal gene transfer.

CellPress OPEN ACCESS

Trends in Genetics

Concluding remarks

The combination of more and better genomes with improved cytological imaging has led to a recent step change in knowledge of the genetic processes at work in bdelloid rotifers. Our view of the diversity of reproductive modes has also moved beyond a binary classification into sexual or asexual [64] towards an understanding of how mechanisms of genetic transmission and recombination interact to produce long- and short-term genomic consequences. Whatever resolution is eventually reached, efforts to interpret the genetic system of bdelloids have already contributed to a greater understanding of animal genome evolution. Some notes of caution and caveats exist for the remaining puzzles. Most experimental and genomic work has focused on one lab-cultivated species, *A. vaga*, and we should not assume that all bdelloids are the same: they have varied lifestyles and habitats, and have diverged over tens of millions of years. Other species show hints of departure from strictly diploid organisation of karyotypes [44]. Finally, because bdelloids are unusual, it is tempting to expect or accept unusual conclusions about their biology. Care is needed to provide evidence for each process and the hypothesised links between various 'strange' features (Figure 4, Key figure). Key future advances (see Outstanding questions) will come from methods of genetic manipulation to establish the basis of bdelloid phenotypes; from multispecies population genomics based on single-individual long-read sequencing; from structural, transcriptional, and phylogenetic comparisons; and from interpreting genomic patterns using a quantitative, simulation-based framework.

Outstanding questions

How frequently does recombination bring together DNA from different parental genomes, relative to recombination within a parthenogenetic line of descent?

Without direct observations, what constitute robust signatures of outcrossing against a background of asyngamous recombination and reconstruction artefacts?

Over what genomic scale does asyngamous recombination occur during parthenogenesis? If it typically leads to loss of heterozygosity, how is heterozygosity restored or maintained?

If genetic exchange does occur, is this by cryptic males, or some other mechanism? If outcrossing is implied by genomic data, what do the males or hermaphrodites look like and how were they missed?

Is metazoan DNA captured by HGT and, if so, more or less than from other sources? Do similar or different mechanisms transfer homologous DNA within or between bdelloid populations compared with heterologous sequences?

How is exogenous DNA first acquired into the germline? Does it involve DNA repair, telomeric rearrangements, or TEs? What source pool of environmental DNA are bdelloids exposed to? How do they domesticate and retain DNA from non-metazoan sources into functioning, expressed genes?

What are HGTcs used for? Have they led to major shifts in the biochemical and functional capabilities of bdelloids, such as stress tolerance?

Does desiccation shape genome structure and content through its effects on DSBs and associated repair mechanisms? How important are DNA repair mechanisms and HGTcs for desiccation and other stresses in bdelloids, relative to other protection mechanisms? How is mitochondrial DNA repaired or protected from DSBs?

Does desiccation tolerance promote HGT and asyngamous recombination, or are these processes largely independent?

Acknowledgments

We thank our colleagues for insightful discussions that informed ideas in this review, especially Irina Arkhipova, Chiara Boschetti, Isobel Eyres, Diego Fontaneto, David Mark Welch, Giulio Melone, Matthew Meselson, Cuong Tang, Alan Tunnacliffe, and Karine Van Doninck. We thank Jerome Kelleher, Karine Van Doninck, Matthew Meselson, and an anonymous reviewer for comments on the manuscript, and Michael Plewka for rotifer images. We dedicate our review to the memory of Claudia Ricci for her pioneering work on bdelloids and for carrying the torch for bdelloid research into the present millennium. The authors were funded by UKRI Natural Environment Research Council grants NE/M01651X/1 and NE/S010866/2, and Early Career Researchers pilot project NEOF1446. T.P. is supported by the UKRI Natural Environment Research Council and Clarendon Fund Scholarships.

Declaration of interests

The authors have no conflicts of interest to declare.

References

1. Darwin Tree of Life Project Consortium (2022) Sequence locally, think globally: the Darwin tree of life project. *Proc. Natl. Acad. Sci.* 119, e2115642118
2. Ricci, C.N. (1987) Ecology of bdelloids: how to be successful. In *Rotifer Symposium IV: Proceedings of the Fourth Rotifer Symposium, held in Edinburgh, Scotland, August 18–25, 1985*, pp. 117–127, Springer
3. van Leeuwenhoek, A. (1676) *Letter to H. Oldenburg, Secretary of the Royal Society, dated 9th October 1676*, Digitale Bibliotheek voor de Nederlandse Letteren https://www.dbnl.org/tekst/leeu027alle02_01/leeu027alle02_01_0006.php#b0026
4. Ford, B.J. (1982) The rotifera of Antony van Leeuwenhoek. *Microscopy* 34, 362–373
5. Vasilikopoulos, A. *et al.* (2024) Whole-genome analyses converge to support the Hemirotifera hypothesis within Syndermata (Gnathifera). *Hydrobiologia*, Published online January 18, 2024. http://doi.org/10.1007/s10750-023-05451-9
6. Segers, H. (2007) Annotated checklist of the rotifers (Phylum Rotifera), with notes on nomenclature, taxonomy and distribution. *Zootaxa* 1564, 1–104
7. Tang, C.Q. *et al.* (2014) Sexual species are separated by larger genetic gaps than asexual species in rotifers. *Evolution* 68, 2901–2916
8. Hudson, C.T. and Gosse, P.H. (1886) *The Rotifera or Wheel-Animalcules*, Longmans, Green & Co
9. Donner, J. (1965) *Ordnung Bdelloidea (Rotatoria, Radertiere)*, Akademie-Verlag
10. Mark Welch, D.B. *et al.* (2009) Bdelloid rotifers: progress in understanding the success of an evolutionary scandal. In *Lost Sex: The Evolutionary Biology of Parthenogenesis* (Schön, I. *et al.*, eds), pp. 259–279, Springer
11. Birky Jr., C.W. (2010) Positively negative evidence for asexuality. *J. Hered.* 101, S42–S45
12. Schwander, T. *et al.* (2013) Neutral and selection-driven decay of sexual traits in asexual stick insects. *Proc. R. Soc. B Biol. Sci.* 280, 20130823
13. Smith, R.J. *et al.* (2006) Living males of the 'ancient asexual' Darwinulidae (Ostracoda: Crustacea). *Proc. R. Soc. B Biol. Sci.* 273, 1569–1578
14. Taberly, G. (1968) Researches on the thelytokous parthenogenesis of two species of Oribatid mites –*Trhypochthonius tectorum* (Berlese) and *Platynothrus peltifer* (Koch). 4. Observations on atavic males. *Acarologia* 29, 95–107
15. Maynard Smith, J. (1986) Evolution: contemplating life without sex. *Nature* 324, 300–301
16. Judson, O.P. and Normark, B.B. (1996) Ancient asexual scandals. *Trends Ecol. Evol.* 11, 41–46
17. Normark, B.B. *et al.* (2003) Genomic signatures of ancient asexual lineages. *Biol. J. Linn. Soc.* 79, 69–84

18. Otto, S.P. and Lenormand, T. (2002) Resolving the paradox of sex and recombination. *Nat. Rev. Genet.* 3, 252–261
19. Gladyshev, E. and Meselson, M. (2008) Extreme resistance of bdelloid rotifers to ionizing radiation. *Proc. Natl. Acad. Sci.* 105, 5139–5144
20. Hespeels, B. *et al.* (2023) Back to the roots, desiccation and radiation resistances are ancestral characters in bdelloid rotifers. *BMC Biol.* 21, 72
21. Hespeels, B. *et al.* (2020) Iron ladies – how desiccated asexual rotifer *Adineta vaga* deal with X-rays and heavy ions? *Front. Microbiol.* 11, 1792
22. Ricci, C. (1998) Anhydrobiotic capabilities of bdelloid rotifers. *Hydrobiologia* 387, 321–326
23. van Leeuwenhoek, A. (1702) *Letter to Hendrik van Bleyswijk, dated 9th February 1702*, Digitale Bibliotheek voor de Nederlandse Letteren https://www.dbnl.org/tekst/leeu027alle14_01/leeu027alle14_01_0010.php#fb0233
24. Ricci, C. and Caprioli, M. (2005) Anhydrobiosis in bdelloid species, populations and individuals. *Integr. Comp. Biol.* 45, 759–763
25. Hellweg, C.E. *et al.* (2023) Space radiobiology. In *Radiobiology Textbook*, pp. 503–569, Springer
26. Hespeels, B. *et al.* (2014) Gateway to genetic exchange? DNA double-strand breaks in the bdelloid rotifer *Adineta vaga* submitted to desiccation. *J. Evol. Biol.* 27, 1334–1345
27. Terwagne, M. *et al.* (2022) DNA repair during nonreductional meiosis in the asexual rotifer *Adineta vaga*. *Sci. Adv.* 8, eadc8829
28. Krisko, A. *et al.* (2012) Extreme anti-oxidant protection against ionizing radiation in bdelloid rotifers. *Proc. Natl. Acad. Sci.* 109, 2354–2357
29. Arkhipova, I. and Meselson, M. (2000) Transposable elements in sexual and ancient asexual taxa. *Proc. Natl. Acad. Sci.* 97, 14473–14477
30. Mark Welch, D.B. and Meselson, M. (2000) Evidence for the evolution of bdelloid rotifers without sexual reproduction or genetic exchange. *Science* 288, 1211–1215
31. Flot, J.-F. *et al.* (2013) Genomic evidence for ameiotic evolution in the bdelloid rotifer *Adineta vaga*. *Nature* 500, 453–457
32. Boschetti, C. *et al.* (2012) Biochemical diversification through foreign gene expression in bdelloid rotifers. *PLoS Genet.* 8, e1003035
33. Boschetti, C. *et al.* (2011) Foreign genes and novel hydrophilic protein genes participate in the desiccation response of the bdelloid rotifer *Adineta ricciae*. *J. Exp. Biol.* 214, 59–68
34. Nowell, R.W. *et al.* (2018) Comparative genomics of bdelloid rotifers: insights from desiccating and nondesiccating species. *PLoS Biol.* 16, e2004830
35. Nowell, R.W. *et al.* (2021) Evolutionary dynamics of transposable elements in bdelloid rotifers. *eLife* 10, e63194
36. Simion, P. *et al.* (2021) Chromosome-level genome assembly reveals homologous chromosomes and recombination in asexual rotifer *Adineta vaga*. *Sci. Adv.* 7, eabg4216
37. Vakhrusheva, O.A. *et al.* (2020) Genomic signatures of recombination in a natural population of the bdelloid rotifer *Adineta vaga*. *Nat. Commun.* 11, 6421
38. Laine, V.N. *et al.* (2022) Genomic signature of sexual reproduction in the bdelloid rotifer *Macrotrachella quadricornifera*. *Genetics* 220, iyab221
39. Eyres, I. *et al.* (2015) Horizontal gene transfer in bdelloid rotifers is ancient, ongoing and more frequent in species from desiccating habitats. *BMC Biol.* 13, 1–17
40. Gladyshev, E.A. *et al.* (2008) Massive horizontal gene transfer in bdelloid rotifers. *Science* 320, 1210–1213
41. Jaron, K.S. *et al.* (2021) Genomic features of parthenogenetic animals. *J. Hered.* 112, 19–33
42. Hespeels, B. *et al.* (2015) Against all odds: trehalose-6-phosphate synthase and trehalase genes in the bdelloid rotifer *Adineta vaga* were acquired by horizontal gene transfer and are upregulated during desiccation. *PLoS One* 10, e0131313
43. White, M.J.D. (1973) *Animal Cytology & Evolution*, Cambridge University Press
44. Mark Welch, J.L. and Meselson, M. (1998) Karyotypes of bdelloid rotifers from three families. In *Rotifera VIII: A Comparative Approach: Proceedings of the VIIIth International Rotifer Symposium, held in Collegeville, MN, USA, 22–27 June 1997*, pp. 403–407, Springer
45. Gladyshev, E.A. and Arkhipova, I.R. (2007) Telomere-associated endonuclease-deficient Penelope-like retroelements in diverse eukaryotes. *Proc. Natl. Acad. Sci.* 104, 9352–9357
46. Gladyshev, E.A. and Arkhipova, I.R. (2010) Genome structure of bdelloid rotifers: shaped by asexuality or desiccation? *J. Hered.* 101, S85–S93
47. Gladyshev, E.A. *et al.* (2007) A deep-branching clade of retrovirus-like retrotransposons in bdelloid rotifers. *Gene* 390, 136–145
48. Mark Welch, D.B. *et al.* (2008) Evidence for degenerate tetraploidy in bdelloid rotifers. *Proc. Natl. Acad. Sci.* 105, 5145–5149
49. Hur, J.H. *et al.* (2009) Degenerate tetraploidy was established before bdelloid rotifer families diverged. *Mol. Biol. Evol.* 26, 375–383
50. Ricci, C. (2017) Bdelloid rotifers: 'sleeping beauties' and 'evolutionary scandals', but not only. *Hydrobiologia* 796, 277–285
51. Houtain, A. *et al.* (2024) Transgenerational chromosome repair in the asexual bdelloid rotifer *Adineta vaga*. *bioRxiv*, Published online January 29, 2024. http://doi.org/10.1101/2024.01.25.577190
52. Schierwater, B. *et al.* (2021) The enigmatic Placozoa part 1: exploring evolutionary controversies and poor ecological knowledge. *BioEssays* 43, 2100080
53. Speijer, D. *et al.* (2015) Sex is a ubiquitous, ancient, and inherent attribute of eukaryotic life. *Proc. Natl. Acad. Sci.* 112, 8827–8834
54. Wesenberg-Lund, C. (1923) *Contributions to the Biology of the Rotifera*, A.F. Høst og Søn
55. Ricci, C. and Melone, G. (1998) Dwarf males in monogonont rotifers. *Aquat. Ecol.* 32, 361–365
56. Freitas, S. *et al.* (2023) Evidence for cryptic sex in parthenogenetic stick insects of the genus *Timema*. *Proc. R. Soc. B* 290, 20230404
57. Boyer, L. *et al.* (2021) Not so clonal asexuals: unraveling the secret sex life of *Artemia parthenogenetica*. *Evol. Lett.* 5, 164–174
58. Feng, H. *et al.* (2023) Highly efficient CRISPR-mediated gene editing in a rotifer. *PLoS Biol.* 21, e3001888
59. Mauer, K. *et al.* (2020) The genome, transcriptome, and proteome of the fish parasite *Pomphorhynchus laevis* (Acanthocephala). *PLoS ONE* 15, e0232973
60. Hanson, S.J. *et al.* (2013) Inventory and phylogenetic analysis of meiotic genes in monogonont rotifers. *J. Hered.* 104, 357–370
61. Arnold, B.J. *et al.* (2022) Horizontal gene transfer and adaptive evolution in bacteria. *Nat. Rev. Microbiol.* 20, 206–218
62. Mishra, A. *et al.* (2021) Parasexuality of *Candida* species. *Front. Cell. Infect. Microbiol.* 11, 796929
63. Wilson, C.G. *et al.* (2018) Cross-contamination explains 'inter and intraspecific horizontal genetic transfers' between asexual bdelloid rotifers. *Curr. Biol.* 28, 2436–2444. e2414
64. Ross, L. *et al.* (2022) Asymmetric inheritance: the diversity and evolution of non-Mendelian reproductive strategies. *Annu. Rev. Ecol. Evol. Syst.* 53, 1–23
65. Hartfield, M. *et al.* (2018) Coalescence and linkage disequilibrium in facultatively sexual diploids. *Genetics* 210, 683–701
66. Kelleher, J. *et al.* (2019) Inferring whole-genome histories in large population datasets. *Nat. Genet.* 51, 1330–1338
67. Speidel, L. *et al.* (2019) A method for genome-wide genealogy estimation for thousands of samples. *Nat. Genet.* 51, 1321–1329
68. Rasmussen, M.D. *et al.* (2014) Genome-wide inference of ancestral recombination graphs. *PLoS genetics* 10, e1004342
69. Hecox-Lea, B.J. and Mark Welch, D.B. (2018) Evolutionary diversity and novelty of DNA repair genes in asexual bdelloid rotifers. *BMC Evol. Biol.* 18, 1–25
70. Nicolas, E. *et al.* (2023) Horizontal acquisition of a DNA ligase improves DNA damage tolerance in eukaryotes. *Nat. Commun.* 14, 7638
71. Nowell, R.W. *et al.* (2021) Bdelloid rotifers use hundreds of horizontally acquired genes against fungal pathogens. *bioRxiv*, Published online September 6, 2021. http://doi.org/10.1101/2021.09.04.458992
72. Rodriguez, F. *et al.* (2022) Bacterial N4-methylcytosine as an epigenetic mark in eukaryotic DNA. *Nat. Commun.* 13, 1072
73. Ribes-Navarro, A. *et al.* (2023) Examination of gammarid transcriptomes reveals a widespread occurrence of key metabolic genes from epibiont bdelloid rotifers in freshwater species. *Open Biol.* 13, 230196

Taken together, how do the aforementioned mechanisms interact to generate and preserve genomic variation within and between bdelloid populations, and promote adaptation and diversification? Specifically, how would these processes influence the presumed costs and benefits of life without males, such as removing deleterious mutations, maintaining beneficial gene combinations, and responding to changing selection?

CellPress
OPEN ACCESS

Trends in Genetics

74. Arkhipova, I.R. *et al.* (2017) Giant reverse transcriptase-encoding transposable elements at telomeres. *Mol. Biol. Evol.* 34, 2245–2257
75. Koutsovoulos, G. *et al.* (2016) No evidence for extensive horizontal gene transfer in the genome of the tardigrade *Hypsibius dujardini*. *Proc. Natl. Acad. Sci.* 113, 5053–5058
76. Tunnacliffe, A. and Lapinski, J. (2003) Resurrecting Van Leeuwenhoek's rotifers: a reappraisal of the role of disaccharides in anhydrobiosis. *Philos. Trans. R. Soc. Lond. Ser. B. Biol. Sci.* 358, 1755–1771
77. Lim, S. *et al.* (2019) Conservation and diversity of radiation and oxidative stress resistance mechanisms in *Deinococcus* species. *FEMS Microbiol. Rev.* 43, 19–52
78. Hashimoto, T. *et al.* (2016) Extremotolerant tardigrade genome and improved radiotolerance of human cultured cells by tardigrade-unique protein. *Nat. Commun.* 7, 12808
79. Moris, V.C. *et al.* (2024) Ionizing radiation responses appear incidental to desiccation responses in the bdelloid rotifer *Adineta vaga*. *BMC Biol.* 22, 1–27
80. Marotta, R. *et al.* (2012) Surviving starvation: changes accompanying starvation tolerance in a bdelloid rotifer. *J. Morphol.* 273, 1–7
81. Chen, P. and Zhang, J. (2021) Asexual experimental evolution of yeast does not curtail transposable elements. *Mol. Biol. Evol.* 38, 2831–2842
82. Signorovitch, A. *et al.* (2015) Allele sharing and evidence for sexuality in a mitochondrial clade of bdelloid rotifers. *Genetics* 200, 581–590
83. Debortoli, N. *et al.* (2016) Genetic exchange among bdelloid rotifers is more likely due to horizontal gene transfer than to meiotic sex. *Curr. Biol.* 26, 723–732
84. Birky Jr., C.W. (1996) Heterozygosity, heteromorphy, and phylogenetic trees in asexual eukaryotes. *Genetics* 144, 427–437
85. Engelstadter, J. (2017) Asexual but not clonal: evolutionary processes in automictic populations. *Genetics* 206, 993–1009
86. Mark Welch, D.B. and Meselson, M.S. (2001) Rates of nucleotide substitution in sexual and anciently asexual rotifers. *Proc. Natl. Acad. Sci.* 98, 6720–6724
87. Li, X. *et al.* (2020) Desiccation does not drastically increase the accessibility of exogenous DNA to nuclear genomes: evidence from the frequency of endosymbiotic DNA transfer. *BMC Genomics* 21, 1–12

Chapter 1: Detecting and quantifying rare sex in natural populations



——————————— O ———————————

Tymoteusz Pieszko, Jerome Kelleher, Christopher G. Wilson, Timothy G. Barraclough

——————————— O ———————————

Contributions

- ➔ I designed and performed the research. I wrote an initial draft of the manuscript, which was then edited by all co-authors. A previous version of this work was posted as a preprint:
  - Pieszko, T., Kelleher, J., Wilson, C.G. and Barraclough, T.G. (2025). Detecting and quantifying rare sex in natural populations. *bioRxiv*, DOI: https://doi.org/10.1101/2025.06.03.657731.
- ➔ I rewrote and expanded the preprint for inclusion in the thesis. The chapter is formatted for journal submission and follows an 'Introduction → Results → Discussion → Methods' order of sections.

Abstract

The distinction between sexual and asexual reproduction is fundamental to eukaryotic evolution. Testing theories about the evolution of reproductive modes first requires knowing whether sex is present or absent in a population. While this seems straightforward, the literature on asexuality reflects a history of shifting claims and uncertainty regarding reproductive mode, especially where sex is potentially rare or cryptic. Here, we develop a new framework to address the challenges in detecting and quantifying sexual reproduction from population genomic data, based on genetic simulations. We first show that commonly calculated population genetic statistics do not reliably distinguish sexual and obligate asexual scenarios if asexuality is accompanied by sex-independent homologous recombination, as emerging evidence suggests is often the case. We then present a new method to quantify the relationship between evolutionary trees and mode of reproduction by exhaustively classifying local trees for pairs of diploid individuals using ancestral recombination graphs (ARGs). This approach accurately distinguishes signatures of genetic exchange and homologous recombination, although uncertainty remains due to unavoidable biases in the steps needed to reconstruct trees from genome data. We introduce new statistics and simulation models to account for common reconstruction biases. Our approach offers the potential for improved quantitative inference of reproductive modes that is extendable and applicable to a broad range of eukaryotes.

Introduction

Sex is a defining feature of eukaryotic life, and fundamental questions about its benefits, costs and prevalence remain of considerable interest in evolutionary biology (Hartfield & Keightley, 2012; Maynard Smith, 1978; Otto, 2021; Kondrashov, 2018). Testing hypotheses about the evolution of reproductive mode depends critically on the ability to detect the presence or absence of sex reliably and, if sexual and asexual reproduction co-occur, to estimate the frequency of sex accurately. Because direct observations in the wild are often infeasible (but see Neiman et al., 2018), a more common approach has been to use DNA sequence data to infer the rates of different modes of reproduction (Schurko et al., 2009; Tibayrenc et al., 1991), first from genetic markers (e.g., Burt et al., 1996; Kuhn et al., 2021) and now chiefly with whole genome data (Brandt et al., 2021; Freitas et al., 2023; Vakhrusheva et al., 2020).

Sexual reproduction has important consequences for genetic variation (Otto, 2003) and therefore patterns of sequence evolution were long predicted to provide clear evidence of reproductive modes (Maynard Smith, 1999; Normark et al., 2003; Schurko et al., 2009; Tibayrenc et al., 1991). In some taxa, this approach yielded insights that were later validated (Eitel et al., 2011; Signorovitch et al., 2005). However, numerous other cases remain ambiguous, including some of agricultural (Lee et al., 2024; Yildirir et al., 2020) and medical (Carpenter et al., 2012; Cooper et al., 2007; Poxleitner et al., 2008; Bradic & Carlton, 2018) importance. The literature on asexual animals alone demonstrates the complexities in applying these methods, with numerous revised claims and uncertainty that spans decades of study (Boyer et al., 2021; Freitas et al., 2023; Mark Welch et al., 2008; Molinier et al., 2025; Schwander et al., 2011; Vakhrusheva et

al., 2020). Classically-predicted features of obligate asexuality (Normark et al. 2003) have failed to materialise in genomic surveys (Jaron et al., 2021; Nowell et al., 2018), while sequence-based evidence for the presence of cryptic sex sometimes contradicts the described natural history (Wilson et al., 2024). Before we can confidently assess which reproductive modes are present, we need to understand why this remains such a difficult task.

One fundamental problem is that many tests do not formally separate the two main components of sexual reproduction – crossover recombination, and genetic exchange mediated by chromosome segregation and the syngamy of haploid gametes (Fig. 1A). It is now clear, however, that homologous recombination between diploid chromosomes also occurs during asexual reproduction via a range of mechanisms, such as gene conversion, crossing-over, and break-induced replication associated with either mitotic or meiotic pathways (Jinks-Robertson & Petes, 2021; Engelstädter, 2017). We group such sex-independent mechanisms of recombination using the term ‘asyngamous recombination’ (Wilson et al., 2024). The main evidence for asyngamous recombination comes from the loss of heterozygosity (LOH) (Fig. 1B and C), observed even in lab-reared populations where the contribution of sex can be excluded. LOH is widespread across a range of asexual eukaryotes, including plants such as pineapple (Chen et al., 2019), fungi such as *Saccharomyces cerevisiae* (Sui et al., 2020), *Candida albicans* (Forche et al., 2011) and *Aspergillus nidulans* (Cardoso et al., 2010), diatoms (Bulankova et al., 2021), and parthenogenetic animals (Flynn et al., 2017; Houtain et al., 2024; Simion et al., 2021). Some forms of asyngamous recombination additionally result in reciprocal exchanges between the homologs (Fig. 1D) (Jinks-Robertson & Petes,

2021; Mateus et al., 2022). Yet, most genetic tests for sex in wild populations still assume that asyngamous recombination is negligible (e.g., Ali et al., 2016; Nicoll et al., 2024; Stoeckel et al., 2021; Tsai et al., 2008; Vakhrusheva et al., 2020), whereas others consider the evolutionary consequences of asyngamous recombination but assume obligate asexuality in the study system (e.g., Jaron et al., 2021; Jaron et al., 2022; Kershenbaum et al., 2023; Flot et al., 2013). There is hence an apparent mismatch between the bulk of theory, which assumes asexually-produced offspring only differ by new mutations, and growing evidence that asexual reproduction involves homologous recombination.

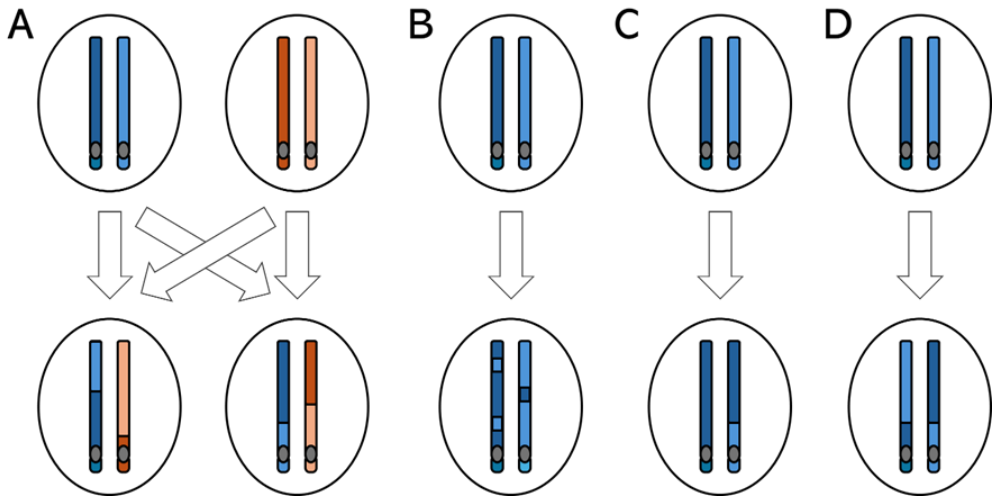


Fig. 1. Immediate effects of sexual and asexual reproduction on sequence diversity across a diploid chromosome arm. (A) Sexual reproduction with crossover recombination. (B) Mitotic parthenogenesis with gene conversion. Gene conversion during mitotic parthenogenesis results in localised loss of heterozygosity (LOH). (C) Meiotic parthenogenesis (central fusion automixis) with crossover recombination. Crossovers during central fusion automixis may result in long-range LOH or reciprocal recombination with a change of linkage (D).

Another key issue is the limited consideration given to stochasticity and inference error. For instance, it has long been recognised that different regimes of DNA transmission are expected to result in distinct genealogical relationships (Birky Jr., 1996; Koufopanou et al., 1997). In diploids, clonal transmission should group homologs from different individuals as two symmetric sub-trees corresponding to allelic copies 1 and 2 (Birky Jr., 1996; Lam et al., 2011; Mark Welch & Meselson, 2000). However, past applications of these approaches have not always accounted for the various reasons why trees might deviate from patterns compatible with strict asexuality. Many studies treated the discovery of any such deviations as strong evidence of genetic exchange (Debortoli et al., 2016; Laine et al., 2022; Signorovitch et al., 2015; Vakhrusheva et al., 2020; Chen et al., 2018), but inferred trees will vary for additional biological and technical reasons, including non-neutral evolution, biases in the mutation process, gene and genome duplications and loss, and reconstruction artefacts (Auxier & Bazzicalupo, 2019; Steenwyk et al., 2023; Wilson et al., 2018; Wilson et al., 2024) – alongside asyngamous recombination as outlined above.

Here, we investigate the detection and quantification of sex in eukaryotic diploids by developing new individual-based models. Our models incorporate recognized mechanisms of asexual reproduction and asyngamous recombination (Neiman et al., 2014), enabled by efficient and flexible forward-time simulations in SLiM4 (Haller et al., 2019; Haller & Messer, 2023). We first show that common population genetic statistics do not distinguish between sexual and obligate asexual scenarios under a realistic range of asyngamous recombination rates. We then develop a new tree-based approach that captures genome-wide heterogeneity using ancestral recombination graphs (ARGs).

Increasingly recognised as a natural framework to disentangle reticulate evolution (Nielsen et al., 2025; Lewanski et al., 2024; Brandt et al., 2024), ARGs describe evolutionary histories of genome regions delimited by recombination breakpoints (Wong et al., 2024) which can be represented as local trees (Fig. 2). Specifically, we decompose the problem by exhaustively classifying local trees for pairs of diploid individuals according to reproductive mode, and introduce novel tree-based statistics that capture different signals of reproductive histories. Our results highlight, however, that even the most powerful current approaches are affected by unavoidable technical biases. Taken together, our work establishes a simulation-based framework for inferring the presence and rate of sexual reproduction from population genomic data and quantifies the inherent uncertainty in tests of reproductive modes.

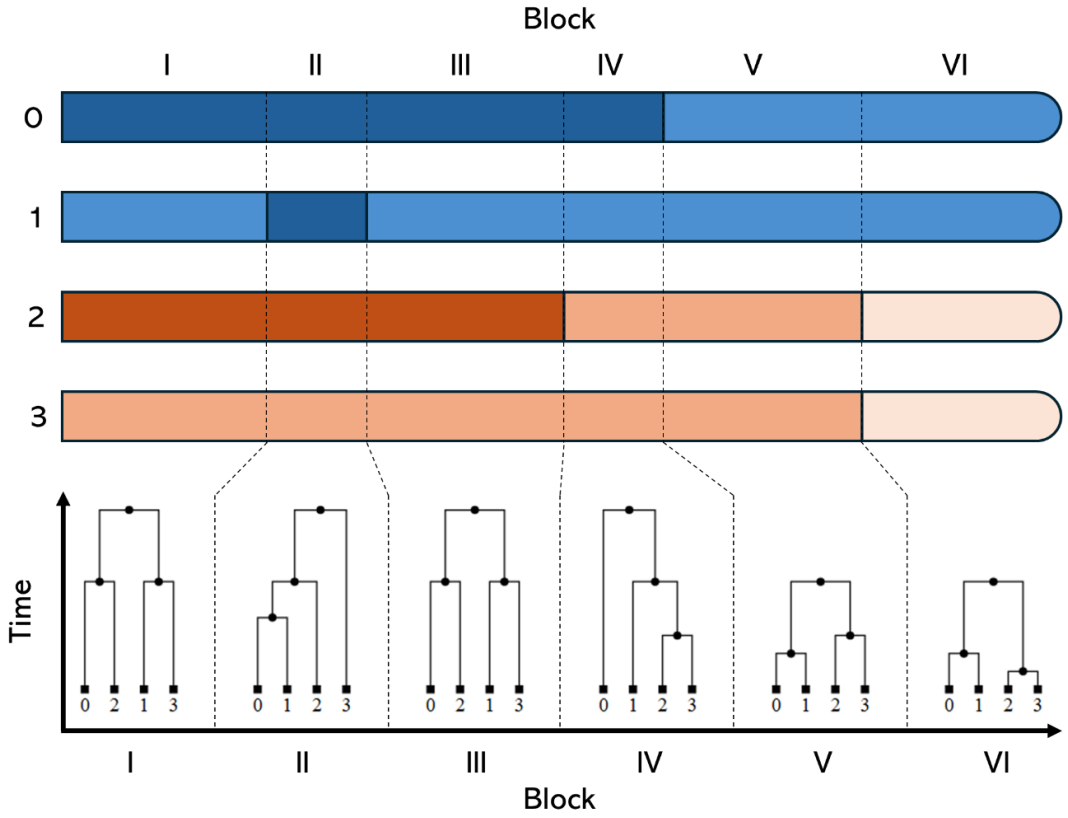


Fig. 2. Changes in sequence diversity along a heterogenous genealogy. In this example, the genealogy of two diploid individuals (blue and orange, with chromosomes 0, 1 and 2, 3, respectively) changes due to asyngamous recombination. The resulting patterns of diversity, with loss of heterozygosity (LOH) in one (blocks II and IV) or both (blocks V and VI) individuals, occurring more anciently (e.g., block II) or recently (e.g., block VI), are best represented as the underlying ancestral recombination graph (ARG) with local trees that describe non-recombining histories.

Results

Simulated scenarios of mixed reproduction

We constructed models of two kinds of asexual reproduction: mitotic parthenogenesis (referred to as 'MP') and automixis via central fusion ('CF') (Stenberg & Saura, 2009). The models further incorporate two kinds of asyngamous recombination: gene

conversion (in the MP model) and crossover recombination (in the CF model). Our simulations can be adapted for any mode of asexual reproduction and recombination, but we choose these as two illustrative examples. In the MP model, all breakpoints initiate gene conversion tracts, each with only a local effect, that always result in LOH. In the CF model, all breakpoints initiate crossovers affecting all the downstream positions of the chromosome; here, only 50% of recombinant regions result in LOH, with a further 25% resulting in a change of linkage. Hence, while 'central fusion' *sensu stricto* describes a specific cytological pathway (Stenberg & Saura, 2009; Blanc et al., 2025), our model applies to any form of abortive meiosis where ploidy is maintained via co-segregation of non-sister chromatids (Beukeboom & Pijnacker, 2000; Eisman & Kaufman, 2007; Hiruta et al., 2010; Terwagne et al., 2022). Full model descriptions and validation with analytical results (Engelstädter, 2017) can be found in Methods and Supplementary Text 1.

We ran simulations using a Snakemake pipeline (Mölder et al., 2021) described in Methods and Supplementary Text 2. We simulated scenarios where a 1 Mb chromosome arm evolves neutrally in populations of N = 1,000 individuals reproducing sexually with probability σ and asexually with probability 1 - σ under both modes in turn. To capture the uncertainty in empirical tests for the presence and rate of sex, we explored scenarios ranging from obligate asexuality (σ = 0) to rare sex ($0 < \sigma \leq 10^{-3}$) and frequent sex ($10^{-3} < \sigma \leq 10^{-0.5}$, where $10^{-0.5} \approx 0.316$), with $\frac{1}{N}$ (where N is the population size) as a boundary rate based on previous studies (Bengtsson, 2003; Hartfield et al., 2018). With the rate of sexual crossovers fixed at a high value ($r = 10^{-6}$, or a single crossover per gamete on average), we varied the per-site per-generation rate of

asyngamous recombination from 0 to 10^{-6} under both models, spanning clonality to sex-like rates of recombination. The rate of asyngamous recombination can alternatively be expressed in terms of the per-site per-generation rate of loss of heterozygosity (LOH) γ (Kopčak & Hartfield, 2024) and we follow this convention hereafter, with γ ranging from 0 to 0.005 under MP (eq. 7 in Supplementary Text 1) and from 0 to 0.16 under CF (eq. 6). Unless stated otherwise, we present results based on the MP model; we discuss differences between the models in Supplementary Text 3.

Commonly calculated statistics are often uninformative about reproductive mode

As expected from previous theory (Tibayrenc et al., 1990; Hartfield et al., 2016, 2018), the statistics of H_I (individual-level heterozygosity), F_{IS} (inbreeding coefficient) and r^2 (a measure of linkage disequilibrium decay; here calculated as an average for SNP pairs < 1,000 bp apart) tended towards values predicted for a fully sexual, randomly mating population as sexual reproduction became more frequent (Fig. 3: H_I tended towards $4N_e\mu = 0.002$; F_{IS} tended to 0 for an outbred population; r^2 tended to low values). In the absence of asyngamous recombination (bottom rows of the heatmaps in Fig. 3), the transitions between asexuality and sex-driven values were sharpest at $\sigma \approx 0.001$ (i.e., $\frac{1}{N}$). In the absence of asyngamous recombination and sex (bottom left), the statistics tended towards values expected under clonal reproduction (high H_I and r^2, $F_{IS} \ll 0$) (Tibayrenc et al., 1990; Birky Jr., 1996).

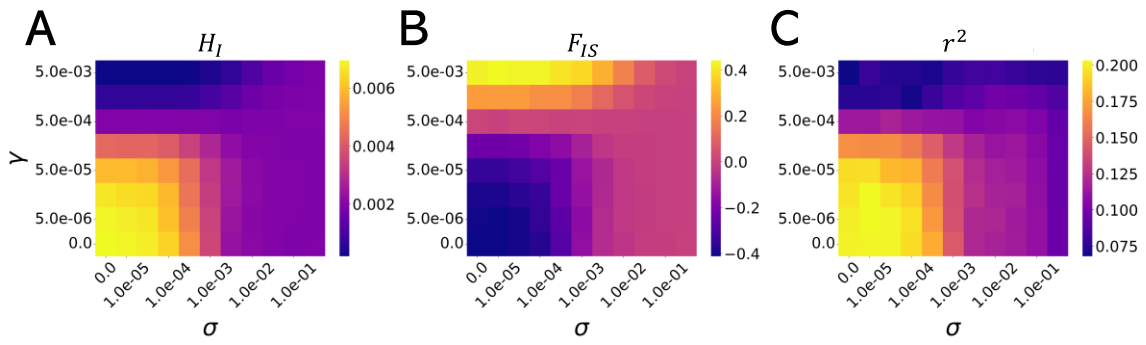


Fig. 3. Simulation results for population genetic statistics. Average H_I, F_{IS} and r^2 for SNP pairs < 1,000 bp apart across the space of the sex rate σ, increasing from the left to the right of each heatmap, and the LOH rate γ, increasing from the bottom to the top; MP model. For each scenario, mean statistic values were obtained for samples of 100 random individuals and averaged across 100 replicates.

Introducing increasing rates of asyngamous recombination, however, led to a wide range of H_I, F_{IS} and r^2 values under both obligate asexuality and rare sex (Fig 3). For instance, under obligate asexuality, H_I varied between < 0.001 and 0.007 (Fig. 3A) – values that are within the range of estimates from sexual (e.g., Mackintosh et al., 2019; Romiguier et al., 2014) and predominantly asexual groups (Jaron et al., 2021; Nowell et al., 2018). F_{IS} varied between strongly negative values at the lower end of the simulated γ range (≈ -0.4) to strongly positive values at its higher end (≈ 0.4; Fig. 3B), which would normally be interpreted as evidence of inbreeding. Finally, there was considerable LD decay (SNPs < 1,000 bp apart) with r^2 ≤ 0.11 for γ ≥ 5 × 10^{-4} (Fig. 3C). Under CF, the patterns were qualitatively similar but reflected the higher overall rates of LOH (Fig. S1). Very high rates (γ > 2.4 × 10^{-2}) led to less LD decay (Fig. S1C), as there was little diversity left.

An appealing approach to test for sex is to compare population genetic metrics in a target population with either a theoretical sexual expectation (e.g., Vakhrusheva et al., 2020) or patterns in related populations known to reproduce sexually (e.g., Freitas et al., 2023; Phan Thi et al., 2025), with the assumption that overlapping values are sufficient to reject obligate asexuality. However, our results indicate that for each of the statistics, there exists a range of γ where these metrics are comparable in value between populations with frequent sex and their obligate asexual counterparts (Fig. 3; Fig. S1). This range appears very narrow for H_I and F_{IS} ($\gamma \approx 5 \times 10^{-4}$; Fig. 3; Fig. S1); as previously noted by Vakhrusheva et al. (2020), whose analytical model predicts $F_{IS} \approx 0$ only if γ is almost precisely $\frac{1}{2N}$, a scenario they consider unlikely. Using a likelihood analysis based on our numerical approach, we explored whether sampling stochasticity could broaden the range of γ scenarios explaining an observed $F_{IS} \approx 0$ under obligate asexuality. As expected from the analytical model, a scenario of $\gamma = \frac{1}{2N}$ was always best supported under both modes of asexuality and given realistic sample sizes (n = 5, 10, or 15). Nonetheless, while Akaike weights computed for scenarios with other values of γ were low under MP (w = 36%, 9%, and 4%, respectively; Fig. S2), they were considerably higher under CF (w = 60%, 45%, and 41%, respectively; Fig. S3), suggesting that scenarios of γ varying more than 10-fold around $\frac{1}{2N}$ are still quite likely to generate $F_{IS} \approx 0$. We hence conclude that, with small sample sizes and especially in the presence of automictic crossing-over, observing $F_{IS} \approx 0$ is compatible with obligate asexuality without unrealistically stringent assumptions on the rate of asyngamous recombination.

The γ range where σ had little effect on calculated values was wider for LD decay, spanning scenarios of $\gamma \geq 5 \times 10^{-4}$ (Fig. 3C; Fig. S1C). While recognizing that asyngamous recombination creates LD decay, some authors have interpreted certain characteristics of the decay curves as specifically indicating sex, such as the steepness of decay (Freitas et al., 2023; Vakhrusheva et al., 2020) or a specifically 'logarithmic-exponential' shape (Phan Thi et al., 2025) if r^2 is plotted as a function of inter-site distance. To evaluate these verbal arguments, we plotted r^2 curves (n = 10, a maximum of 500 SNPs sampled per simulation) across the MP and CF scenarios (Fig. S4; Fig. S5). Especially under MP, the shape of the curves was remarkably similar under frequent sex and a range of obligate asexual scenarios (γ between 5×10^{-5} and 1.6×10^{-3}), with LD falling to $r^2 \approx 0.16$ even within the first 20 kb (for $\gamma = 5 \times 10^{-4}$), rendering these properties uninformative. Taken together, we conclude that judgment based on classical population genetic statistics is not a reliable method of detecting cryptic or rare sex when the cytological basis of asexuality is incompletely understood and asyngamous recombination has not been quantified.

Tree composition analysis

We present a new method for quantitative tree-based analysis of reproductive history. This approach divides the 18 possible two-individual, four-tip coalescent trees (Wakeley, 2008) into the following categories:

(1) Category CL: compatible with clonality (4 trees; blue in Fig. 4A). Trees whose topologies are compatible with asexual descent without recombination (clonality), but can be also generated by other processes. In CL trees, homologs from different individuals cluster together (Birky Jr., 1996).

(2) Category AR: compatible with asyngamous recombination (6 trees; green in Fig. 4A). Trees whose topologies are compatible with asyngamous recombination in an asexual background. Asyngamous recombination can only result in a subset of topological changes that bring homologs together within asexual lineages (Birky Jr., 1996).

(3) Category SX: specific to sex (8 trees; orange in Fig. 4A). Trees whose topology is sex-specific, i.e., can only be generated through sexual reproduction or other forms of genetic exchange. When trees for more than 2 individuals are considered, these include 'allele sharing' patterns used by earlier studies (Laine et al., 2022; Signorovitch et al., 2015; Vakhrusheva et al., 2020; Vastrade et al., 2022).

We propose that the contributions of asexual and sexual reproduction to a genealogy can be quantified as the relative genomic proportions of local CL, AR and SX trees – a summary metric we refer to as the 'tree composition'. Given a genealogy for n individuals ($2n$ tips), our approach enables exhaustive classification of signatures by aggregating them across all the possible $\binom{n}{2}$ relationships (Fig. S6). This pairwise decomposition moves beyond the use of trees as a categorical signature (where patterns such as 'allele sharing' are used as a 0-1 indicator of sex) while avoiding the combinatorial impracticality of attempting to classify all possible trees for more than two individuals.

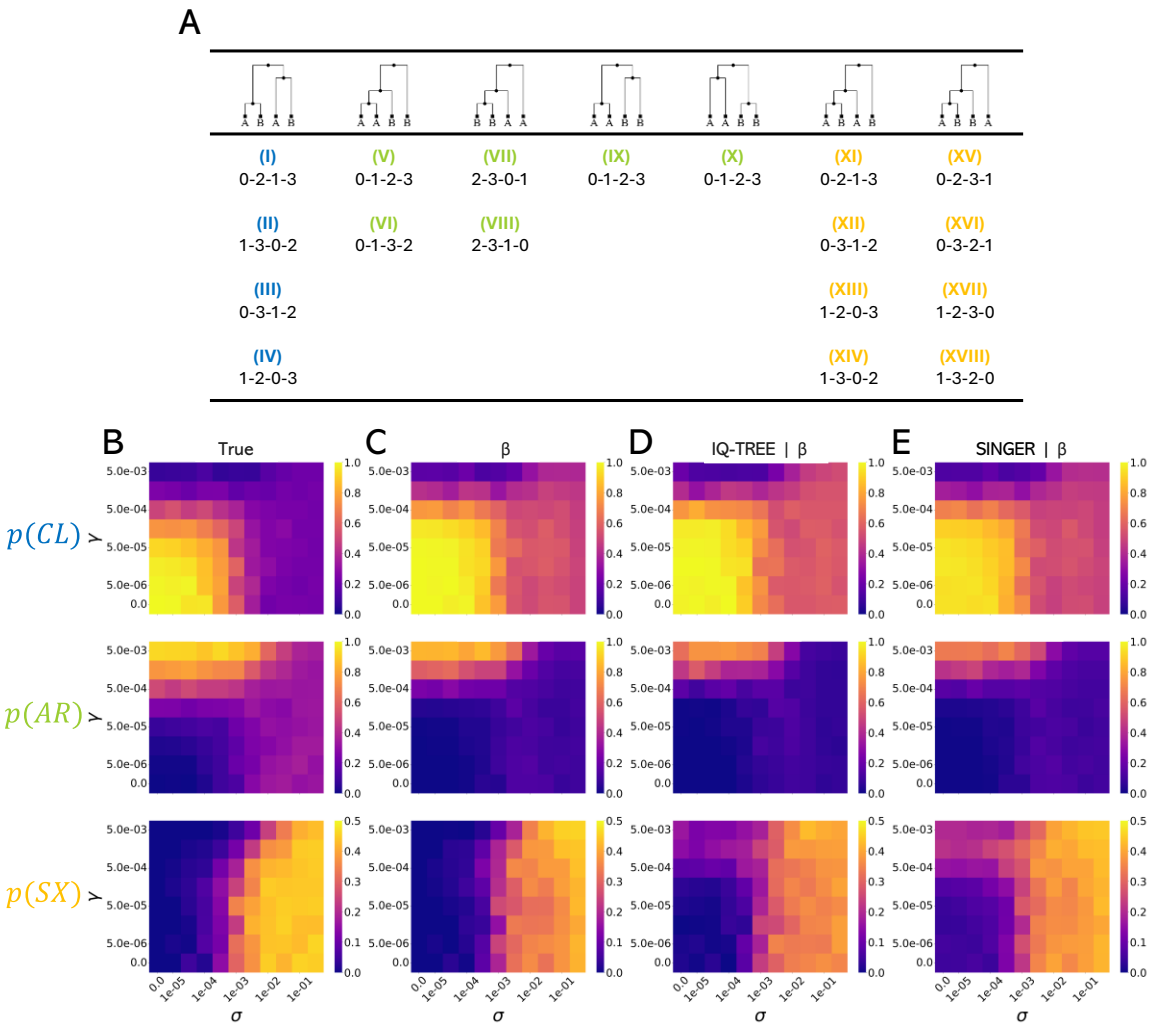


Fig. 4. Systematic analysis of tree composition. (A) The 18 two-individual, four-tip coalescent trees can be classified into three categories: clonality-compatible (CL; blue), asyngamous recombination-compatible (AR; green) and sex-specific (SX; orange). Here, the trees are drawn for individuals A (homologs 0 and 1) and B (homologs 2 and 3), with the possible tip labelling displayed below. (B)-(E) Tree proportions p falling into the CL, AR and SX categories across the space of the sex rate σ, increasing from the left to the right of each heatmap, and the LOH rate γ, increasing from the bottom to the top; MP model. $p(CL)$, $p(AR)$ and $p(SX)$ reflect the rates of sex and asyngamous recombination (B), a relationship that is biased towards CL trees through sampling heterozygous genome regions (C), and broken down when SX trees are generated through inference error (D – IQ-TREE, E – SINGER). Note that the colour scale is capped at 1.0 in the $p(CL)$ and $p(AR)$ heatmaps and at 0.5 in the $p(SX)$ heatmaps.

In contrast to past studies that used arbitrarily delimited genome regions (e.g., entire scaffolds) to reconstruct trees (e.g., Laine et al., 2022; Öztoprak et al., 2025), an ARG framework explicitly accounts for the varying genomic span of local non-recombining trees. Below, by sampling two-individual ARGs from simulation output (see Methods), we explore the variation in the expected tree composition across the simulated space of σ and γ.

Tree composition discriminates asexual and sexual scenarios in true ARGs

Across the parameter space examined, the tree composition of true ARGs (i.e., without reconstruction error) reflected the rates of the underlying generative processes (Fig. 4B; see Fig. S7A for the CF results). As σ increased, the proportion of SX trees $p(SX)$ tended towards the value expected under outcrossing ($\frac{4}{9} \approx 0.44$) (Wakeley, 2008), with a steep transition at the $\sigma = \frac{1}{N}$ boundary between rare and frequent sex. At the higher end of γ, the value of σ required to achieve outcrossing-like $p(SX)$ was higher. Under obligate asexuality without recombination (bottom left of the heatmaps in Fig. 4B), only category CL trees were represented, whereas $p(CL)$ decreased, and $p(AR)$ increased with increasing γ (left-most columns). We conclude that tree composition expectations distinguish scenarios of obligate asexuality, rare sex and frequent sex, assuming that local trees can be accurately estimated.

Heterozygosity bias in phased data increases the proportion of CL trees

Implementing our method (or any analysis of diploid copies) requires phasing of haplotypes within individuals, but with short-read data, this is only possible for relatively heterozygous regions of the genome (Martin et al., 2016). This introduces a potential

'heterozygosity bias', i.e., that regions with high H_I are more likely to be included. For instance, among published genomic studies on asexual animals, the proportion of the reference assembly recovered in phased segments is < 10% (Brandt et al., 2021; Laine et al., 2022; Vakhrusheva et al., 2020) and only occasionally higher (21%; Öztoprak et al., 2025). To evaluate this issue, we added a 'heterozygosity bias' to our pipeline, which we denote by β, representing the proportion of genomic regions with the highest mean H_I that are sampled. Based on estimates from real datasets, we modelled the effect of a bias of β = 0.1 across parameter space.

Adding the heterozygosity bias increased $p(CL)$ at the expense of $p(AR)$ across the simulated scenarios (Fig. 4C; Fig. S7B). Under frequent sex (e.g., $\sigma = 10^{-0.5}$), $p(CL)$ is expected to approach $\frac{2}{9}$ (≈ 0.22), but the bias increased this approximately two-fold ($p(CL) \approx 0.45$), as would be consistent with a rate of sex two orders of magnitude lower ($\sigma = 10^{-3}$), or even with obligate asexuality (when $\gamma = 5 \times 10^{-4}$). The impact on $p(SX)$ was more subtle. In regions of parameter space with high H_I (approx. $H_I \geq 4N\mu$), $p(SX)$ decreased; on the other hand, $p(SX)$ increased in the regions with low H_I (Fig. S8). Taken together, a realistic bias can drastically change the expected relative proportions of CL and AR trees, which could lead to overestimates of the contribution of clonality to the reproductive history.

Reconstruction artefacts increase the proportion of SX trees

True genealogies are unknown for natural populations and must be inferred from sequence data. To investigate how reconstruction errors might impact or bias estimates of the tree composition, we inferred trees from simulated datasets using two

approaches: a phylogenetic approach using equally sized genomic windows for the maximum likelihood inference of local trees (IQ-TREE v2; Fig. 4D; Supplement, Fig. 7C) (Minh et al., 2020) and an ARG reconstruction method SINGER (Deng et al., 2024) that identifies recombination breakpoints and infers local trees under the sequentially Markovian coalescent model (Fig. 4E; Fig. 7D) (Deng et al., 2024). We chose these methods as contrasting approaches with different strengths and weaknesses (Supplementary Text 4), and applied them in combination with a heterozygosity bias (β = 0.1) to reflect the typical data currently available.

Under obligate asexuality, both methods erroneously inferred SX trees, with maximum $p(SX)$ of 0.17 and 0.21 for IQ-TREE and SINGER, respectively (Fig. 4D and E). Since $p(SX)$ increased with γ, the mis-inference of SX trees may be attributed to asyngamous recombination, acting via mixed signal from CL and AR trees, mutational stochasticity in AR regions, or both. While IQ-TREE over- or under-estimated $p(SX)$ across the simulations (Fig. S9), SINGER inference consistently resulted in overestimates, but less so with increasing σ (Fig. S10), consistent with an increasing match to SINGER's assumption of a sexual population model (Deng et al., 2024). Taken together, we conclude that the two inference methods interact with asyngamous recombination to introduce different biases to tree composition. In both cases, however, the recovery of SX trees from phased genomic data, even at proportions otherwise consistent with sex as frequent as one in 1000 reproductive events (Fig. 4B), cannot be taken as strong evidence against obligate asexuality.

Tree-based statistics to quantify genome-wide signal of reproductive mode

To further quantify the signal of reproductive mode, we devised additional statistics stemming from the tree-based framework. First, we note that the external branches of CL trees should have equal lengths under obligate asexuality, reflecting the number of generations to the most recent common ancestral individual. In contrast, SX and CL trees generated through sexual exchange should display different lengths of external branches, either through differently timed internal nodes (CL) or the topology itself (SX). Accordingly, our first statistic measures the degree of asymmetry in external branch lengths. We define Δ as:

$$\Delta = \frac{\bar{\delta}_{between} - \bar{\delta}_{within}}{\bar{\tau}}$$

Where $\bar{\delta}_{between}$ is the mean absolute difference in branch lengths τ between the two external subtrees, $\bar{\delta}_{within}$ is the mean absolute difference in τ within subtrees, and $\bar{\tau}$ is the overall mean. An example of calculating $\bar{\delta}_{between}$ and $\bar{\delta}_{within}$ is shown in Fig. 5A (see Methods for further details). We calculate Δ for contiguous runs of CL and / or SX trees with the same unrooted topology (see Fig. S11 for examples); its expected value is 0 under obligate asexuality and > 0 if sexual reproduction contributed to the genealogy (Fig. 5A). The degree of the deviation from 0 should be proportional to the degree of variation in the coalescence times of internal nodes and, indirectly, the rate of sex

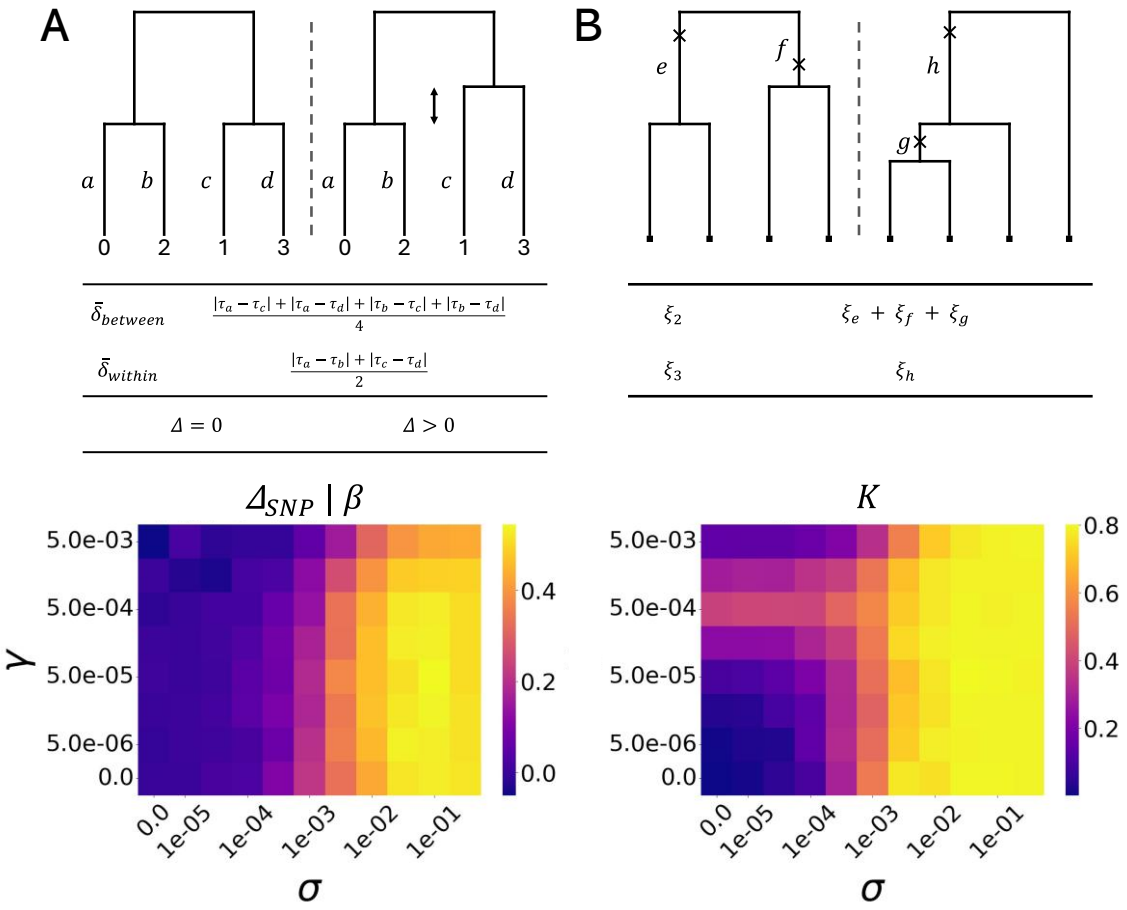


Fig. 5. Tree-based statistics to distinguish between asexual and sexual scenarios. (A) Δ: a statistic calculable for haplotype-resolved segments. Top: example CL trees with equal (left) and unequal (right) timing of internal nodes. The lengths τ of branches a, b, c and d are used to calculate $\bar{\delta}_{between}$ and $\bar{\delta}_{within}$; see Results. The values of Δ reflect the asymmetry in the timing of internal nodes in CL and SX trees. Bottom: variation in Δ is driven by the rate of sex σ. (B) K: a statistic calculable for genome-wide SNPs. Top: Mutations ('×') arising on different branches of balanced (left; CL or AR) and unbalanced (right; AR or SX) trees contribute to the pool of doubletons (ξ_2) and tripletons (ξ_3). ξ_2 and ξ_3 can be used to summarise the genome-wide signal of reproductive mode; see Results. Bottom: K values vary with the rate of LOH γ but are predominantly driven by the rate of sex σ.

As previously, two important considerations are whether (1) Δ unambiguously distinguishes asexual and sexual scenarios and (2) it is robust to the artefacts identified

above. To assess these conditions, we calculated Δ across the simulated parameter space using the true intervals of local trees (Δ_{tree}), SINGER-reconstructed trees ($\Delta_{SING.}$), and a SNP-based procedure independent of tree reconstruction (Δ_{SNP}; see Methods and Fig. S12). In agreement with the expectation, Δ_{tree} was ≈ 0 under obligate asexuality and increased with σ, reaching ≈ 0.41 (no bias) or ≈ 0.55 under β = 0.1 (Fig. S13). $\Delta_{SING.}$ was inflated at the higher end of γ (up to 0.14; Fig. S13), an effect that was nonetheless more modest than the impact of reconstruction error on $p(SX)$ (25% vs 48% of the respective cross-scenario maxima). Finally, Δ_{SNP} faithfully reflected the statistic's expected behaviour, despite being computed under the heterozygosity bias (Fig. 5A). These results indicate that Δ distinguishes between asexual and sexual scenarios under realistic assumptions of data quality and sampling error.

We also devised a statistic that incorporates polarised SNPs within unphased regions to summarise the signal of reproductive mode. We observe that, under the infinite sites model (Kimura, 1969), doubleton SNPs (i.e., two ancestral and two derived alleles per locus) and tripleton SNPs (i.e., three ancestral and one derived allele per locus) arise on defined branches of balanced and unbalanced four-tip trees (Fig. 5B). We therefore define K (kappa) as:

$$K = 1 - \frac{\xi_2 - \xi_3}{\xi_2 + \xi_3}$$

Where ξ_2 and ξ_3 are counts of doubleton and tripleton SNPs, respectively. When sex is frequent, the expected value of K is ≈ 0.79; under obligate asexuality, values of K depend on the asyngamous recombination rate but do not exceed ≈ 0.39 (Fig. 5B, see

Supplementary Text 5 for a complementary numerical exploration of K under obligate asexuality). Expected values that do not overlap between the opposite ends of the asexuality-sex spectrum set K apart from the standard summaries of unphased sequence variation (cf. Fig. 3).

We assessed the performance of the tree-based statistics using approximate Bayesian computation (ABC) through a rejection algorithm (R package 'abc', tolerance of 0.01, log-transformed parameter values) (Csilléry et al., 2012). For each simulated scenario (MP model), we designated 10 replicates as 'observed' and the remaining 90 as draws from the prior distribution. As a performance criterion, we used the coefficient of determination (R^2) between the prior and posterior values of σ, providing a measure of how well each statistic, or summary vectors composed of multiple statistics, predicted the rate of sex (Fig. 6). Overall, the true tree composition, tree composition together with tree-based statistics computed for biased regions (β = 0.1; except the K statistic based on unphased SNPs), and the tree-based statistics alone, performed best (R^2 = 0.841, 0.840 and 0.836, respectively). Classical summaries H_I, F_{IS} and r^2 (R^2 = 0.739) compared favourably to tree composition computed under heterozygosity bias (R^2 = 0.522). Taken together, while technical artefacts compromise the predictive power of reconstructed tree composition, our novel tree-based statistics mitigate this challenge and provide the best indicator of reproductive mode to date.

	H_I	F_{IS}	r^2	$p(CL)$	$p(AR)$	$p(SX)$	Δ_{SNP}	K
I	-	-	-	β	β	β	-	-
II	+	+	+	-	-	-	-	-
III	-	-	-	-	-	-	β	+
IV	-	-	-	β	β	β	β	+
V	-	-	-	+	+	+	-	-

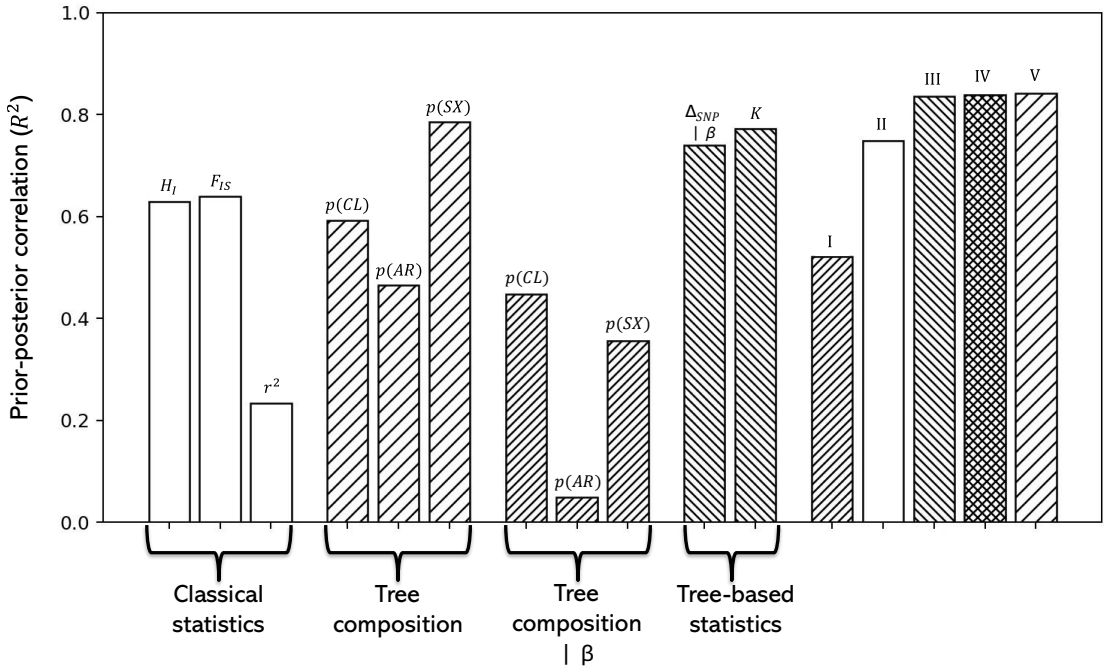


Fig. 6. Predictability of the sex rate σ from different summary statistics: the coefficient of determination (R^2) between the prior (simulated; MP model) and posterior values obtained through rejection-based approximate Bayesian computation (ABC) (Csilléry et al., 2012). The predictive power of statistics was tested individually and in combinations I-V (see the legend at the top; '+' – included, '-' – excluded, 'β' – calculated under heterozygosity bias). The per-simulation vectors of summaries were obtained using samples of 8 individuals.

Discussion

Estimating the rates of sexual and asexual reproduction is a prerequisite for answering a range of fundamental evolutionary questions. Interpreting the genomic landscape as an outcome of an inferred reproductive history could shed light on deep links between reproductive mode and microevolutionary patterns (Feretzaki & Heitman, 2013; Morran

et al., 2011), macroevolutionary trends (Barraclough, 2019), and a range of ecological, genetic, and life history peculiarities (Jeffries et al., 2025; Wilson et al., 2024). However, while jointly modelling multiple forces that shape genome-wide variation has become a gold standard in many branches of evolutionary research (e.g., Laetsch et al., 2023), the same is not true for reproductive history analysis. As a step towards addressing this issue, we focus on homologous recombination that operates independently of the sexual pathway, which remains largely overlooked in current approaches to quantifying sex from sequence data (e.g., Ali et al., 2016; Nicoll et al., 2024; Stoeckel et al., 2021; Tsai et al., 2008; Vakhrusheva et al., 2020).

Using simulation models of asexuality, we found that 'asyngamous' recombination confounds sequence-based statistics commonly used to support the presence of sex (e.g., Freitas et al., 2023; Phan Thi et al., 2025; Vakhrusheva et al., 2020). Specifically, under intermediate rates of asyngamous recombination, these statistics take values characteristic of outcrossing populations even when sex is rare or absent. Estimates of the per-site rate of LOH across asexual systems are consistently on the order of 10^{-5} to 10^{-4} (Table S2), broadly aligning with the values required to mimic sex-like patterns of variation. For example, a recent laboratory evolution study (Houtain et al., 2024) estimated a per-site per-generation LOH rate of 3.24×10^{-4} in the bdelloid rotifer *Adineta vaga*, a representative of a widespread and abundant group where no sexual reproduction, males or hermaphrodites have ever been observed (Birky Jr, 2010; Wilson et al., 2024). We find that this value is consistent with $F_{IS} \approx 0$ in our simulated scenarios (Fig. 3; Fig. S2 and Fig. S3), potentially explaining close compatibility with the Hardy-Weinberg expectation observed in a wild *A. vaga* population (Vakhrusheva et al., 2020).

Although it might seem improbable that asyngamous recombination would take exactly those values required to confound tests of sex, there are biological reasons why this might be expected. The generation of LOH has two contrasting consequences for fitness. On the one hand, exposure of recessive deleterious mutations leads to loss of fitness and inbreeding depression (Charlesworth & Willis, 2009). On the other, LOH can help fix beneficial mutations and counteract Muller's ratchet by overwriting deleterious mutations (Flot et al., 2013; Kopčak & Hartfield, 2024; Mandegar & Otto, 2007). To maximise fitness benefits, the spontaneous rate of asyngamous recombination and LOH might be expected to be selected in a similar way to recombination rate in sexual organisms (Dapper & Payseur, 2017), or via programmed distortion of chromatid segregation (Blanc et al., 2023; Lacy et al., 2024). Concurrently, observed levels of LOH might be biased towards intermediate values through selection against excess homozygosity (Flynn et al., 2017).

The majority of ARG inference methods are rooted in a simple model of a sexual population with crossover recombination (Li & Stephens, 2003; McVean & Cardin, 2005). Here, we show that ARG-based methods can be extended to systems with non-canonical reproductive biology. Specifically, we present tools to simulate ARGs for populations with mixed sexual and realistically modelled asexual reproduction, and to interrogate such reproductive histories. Our results confirm that the tree composition of a true ARG is the best predictor of the rate of sex and most clearly distinguishes scenarios across the studied range of σ. In addition, our simulation models provide a powerful basis to develop ARG-based methods for evolutionary inference in asexual diploids,

including processes such as demography (Fan et al., 2025; Osmond & Coop, 2024; Wohns et al., 2022) and selection (Hejase et al., 2022; Stern et al., 2019).

Nevertheless, we caution that the accuracy of inference from haplotype-resolved segments is still limited by technical artefacts, which cause inferred genealogies to be unrepresentative of the true ARG. We find that a bias towards heterozygous regions of the genome, inherent to read-based haplotype phasing, on the one hand, and asyngamous recombination, on the other, result in overrepresentation of tree-level signatures of clonality and sex, respectively. These results have implications for tree-based inferences of reproductive mode, whether reporting evidence of long-term asexuality (Brandt et al., 2021; Öztoprak et al., 2025) or cryptic sex (Laine et al., 2022; Vakhrusheva et al., 2020), and such datasets would be interesting to revisit with our quantitative approach to tree composition analysis. Importantly, other biases associated with the sequencing, assembly and phasing procedures, as well as limitations to inference itself (Lin et al., 2024), will need to be considered beyond the simple biases simulated here. We anticipate that further advances in obtaining long-range phased blocks (Lin et al., 2022; Porubsky et al., 2021) and the development of nonparametric ARG reconstruction methods (Kelleher et al., 2019; Rasmussen & Guo, 2023; Speidel et al., 2019; Schaefer et al., 2021) will be critical to fully benefit from an ARG-based approach. Bearing these limitations in mind, we introduce two new statistics Δ and K that capture the genealogical signal of reproductive mode and yet appear more robust to biases. Interestingly, our Δ statistic bears a conceptual similarity to the recently proposed A_m statistic for measuring gene flow under an isolation with migration model (Mackintosh

& Setter, 2024), highlighting the potential for methodological cross-talk between speciation and reproductive mode research.

Simulating genome-wide genealogies offers a powerful tool for the exploration and inference of evolutionary scenarios (Lauterbur et al., 2023). Integrating our approach with statistical frameworks in an empirical setting could help address several outstanding problems. For instance, the status of putative ‘ancient asexuals’ (Judson & Normark, 1996) remains contentious, with claims of cryptic sex in the well-documented absence of males (Laine et al., 2022; Vakhrusheva et al., 2020; Wilson et al., 2024; Birky Jr, 2010), and conversely, claims of long-term asexuality in their presence (Öztoprak et al., 2025; Taberly, 1988). Apart from Approximate Bayesian Computation (Johri et al., 2022), ARG-based inference could be performed even more directly through supervised machine learning (Schrider & Kern, 2018) or convolutional neural networks (Whitehouse et al., 2024; Korfmann et al., 2023). Our results provide a guide for future studies to (1) explicitly account for asyngamous recombination, (2) address technical and methodological limitations and (3) quantitatively and exhaustively classify signatures that can be explicitly linked to asexual and sexual reproduction in turn. To this aim, we provide the building blocks that will help disentangle the idiosyncrasies of different systems of reproduction and recombination.

Methods

We used tskit v0.5.8 (Kelleher et al., 2016; Wong et al., 2024) to process simulated ARGs, scikit-allel v1.3.13 (Miles et al., 2024) to work with SNP data, and matplotlib v3.9.2 (Hunter, 2007) and seaborn v0.13.2 (Waskom, 2021) for visualisation in Python.

The simulation pipeline and post-simulation code are available at https://github.com/TymekPieszko/SexSigns_2025.

Simulation models of asexuality

We implemented both the MP and CF models in scenarios where a single diploid chromosome of length L evolved in populations conforming to Wright-Fisher assumptions (discrete, non-overlapping generations, constant population size), in which offspring are produced sexually by hermaphroditic parents with probability σ and asexually with probability 1 - σ (see Table S1 for definitions of all simulation parameters). Parthenogenesis is accompanied by asyngamous recombination: gene conversion with an initiation rate r_{GC} in the MP model and crossover recombination at rate r_{CO} in the CF model (see Supplementary Text 1 for descriptions of the recombination routines). The length of gene conversion tracts is geometrically distributed with mean λ and can be set independently of the tract initiation rate. Sexual reproduction is accompanied by crossover recombination at rate r using the standard machinery of SLiM4.

To validate the CF model, we followed Engelstädter (2017) in assuming that crossovers occur between all four chromatids without interference (Fig. S14) and used the equilibrium individual-level heterozygosity $\hat{H}_I$ as an indicator of concordance with the analytical model (Engelstädter, 2017) (see Supplementary Text 1 for a summary). To validate the MP model, we used Engelstädter's (2017) suggestion for deriving the expected $\hat{H}_I$ (Supplementary Text 1). In both cases, we obtained close concordance between analytical and simulated values after 200,000 simulated generations (each recombination scenario in 30 replicates, other parameters as in Table S1), except at low

recombination rates ($\gamma \leq 5 \times 10^{-6}$; Fig. S15; Fig. S16), where this duration was still insufficient for attaining mutation-LOH equilibria. Although finite run times constrain how closely individual-based simulations can match analytical expectations at edge cases (including in our main pipeline; see below), equilibria are unlikely to be encountered in nature for the same reason.

Simulation pipeline

We ran our simulations in a pipeline written using the workflow management system Snakemake v8.13.0 (Mölder et al., 2021). In summary, the pipeline consisted of three major steps. First, we used the MP and CF models to run simulations with tree-sequence recording of output (Haller et al., 2019) across the space of sex rates σ and LOH rates γ (see Table S1 for all parameter values used). Each scenario was run for 5,000 generations and replicated 100 times. Second, after ensuring complete coalescence of simulated ARGs using pyslim v1.0.4 (Haller et al., 2019), we subsampled each ARG to two random individuals and generated files for downstream processing of these target samples. Using msprime v1.3.2 (Baumdicker et al., 2022), we added neutral mutations at a per-site per-generation rate $\mu = 5 \times 10^{-7}$ chosen to avoid the computational burden of simulating larger populations (see Supplementary Text 2). Finally, for each two-individual ARG, we re-inferred genealogies using IQ-TREE v2.2.2.6 (Minh et al., 2020) and SINGER v0.1.8-beta (Deng et al., 2024). Details of the pipeline are described in Supplementary Text 2.

Calculating population genetic statistics

We calculated population genetic statistics using sub-ARGs of 100 random individuals processed as above. We calculated H_I using the TreeSequence.diversity method

(mode='site') (Ralph et al., 2020), and r^2 and F_{IS} using scikit-allel. For each 100-individual ARG, we calculated mean H_I, F_{IS} and average r^2 for SNP pairs < 1,000 bp apart. We finally calculated mean values across the replicates and plotted heatmaps for the simulated space of σ and γ (Fig. 3; Fig. S1). To visualise LD decay curves (Fig. S4 and Fig. S5), we calculated mean r^2 values for SNPs binned by distance in windows of 1 kb.

F_{IS} likelihood analysis

Under the obligate asexual scenarios, we additionally calculated F_{IS} for smaller sub-ARGs (n = 5, 10 or 15). Assuming normally distributed replicated F_{IS} values, we computed the likelihood of observing F_{IS} = 0 for each scenario and value of n, which we transformed to Akaike information criterion (AIC) values (with one parameter). Finally, for each value of n and set of MP and CF scenarios, we computed Akaike weights of evidence (w) for different values of γ (Fig. S2 and Fig. S3).

Tree composition analysis

We implemented our approach to classifying two-individual trees (Fig. 4A) to be applicable to tree sequences (simulated or output by SINGER) and Newick-format trees (output by IQ-TREE). For each two-individual ARG sampled within the pipeline, we summed the spans of trees falling into the CL, AR and SX categories, which we expressed as proportions of the total: $p(CL)$, $p(AR)$ and $p(SX)$, respectively. We repeated this calculation after applying the heterozygosity bias of β = 0.1 and re-inferring genealogies with IQ-TREE and SINGER in turn. To obtain tree proportions for SINGER genealogies, we summed tree spans across the samples of each MCMC chain.

Approaches to calculating Δ

We used two approaches to delineate intervals for calculating Δ. Both exploit the correlation between neighbouring local trees in an ARG (Wong et al., 2024), allowing Δ values to be obtained for contiguous runs of CL and / or SX trees that share the same unrooted topology (see Fig. S11 for examples). In the first approach (Δ_{tree}, $\Delta_{SING.}$), Δ is calculated for intervals defined by tree boundaries: simulated (Δ_{tree}) or inferred ($\Delta_{SING.}$). For each such interval, the counts of the four different classes of singleton SNPs (i.e., sites with a single derived and three ancestral alleles) are used as proxies for the cumulative length of the external branches on which they arise. The second approach, visualised in Fig. S12 (Δ_{SNP}) differs in that locations of the target unrooted topologies are identified from the configurations of doubleton SNPs. For each tree sequence, we computed mean Δ across runs; to obtain $\Delta_{SING.}$, we performed additional averaging across samples of the MCMC chains.

Acknowledgments

We thank Dmitri Filatov, Aziz Aboobaker, Alan Grafen, Antoine Houtain and Reuben Nowell for comments on earlier versions of the work and manuscript drafts. Simulations were run on the University of Oxford Advanced Research Computing (ARC) facility (http://dx.doi.org/10.5281/zenodo.22558). T.P. was supported by the UKRI Natural Environment Research Council and Clarendon Fund Scholarships. J.K. was funded by the Robertson Foundation. T.G.B. and C.G.W. were funded by UKRI Natural Environment Research Council grants NE/M01651X/1 and NE/S010866/2.

References

Ali, S., Soubeyrand, S., Gladieux, P., Giraud, T., Leconte, M., Gautier, A., Mboup, M., Chen, W., de Vallavieille-Pope, C., & Enjalbert, J. (2016). CLONCASE: estimation of sex frequency and effective population size by clonemate resampling in partially clonal organisms. *Molecular ecology resources*, *16*(4), 845–861.

Auxier, B., & Bazzicalupo, A. (2019). Comment on'Single nucleus sequencing reveals evidence of inter-nucleus recombination in arbuscular mycorrhizal fungi'. *eLife*, *8*, e47301.

Barraclough, T. G. (2019). *The evolutionary biology of species*. Oxford University Press.

Baumdicker, F., Bisschop, G., Goldstein, D., Gower, G., Ragsdale, A. P., Tsambos, G., Zhu, S., Eldon, B., Ellerman, E. C., & Galloway, J. G. (2022). Efficient ancestry and mutation simulation with msprime 1.0. *Genetics*, *220*(3), iyab229.

Bengtsson, B. O. (2003). Genetic variation in organisms with sexual and asexual reproduction. *Journal of Evolutionary Biology*, *16*(2), 189–199.

Beukeboom, L. W., & Pijnacker, L. P. (2000). Automictic parthenogenesis in the parasitoid Venturia canescens (Hymenoptera: Ichneumonidae) revisited. *Genome*, *43*(6), 939–944.

Birky Jr, C. W. (2010). Positively negative evidence for asexuality. *Journal of Heredity*, *101*(suppl_1), S42–S45.

Birky Jr., C. W. (1996). Heterozygosity, heteromorphy, and phylogenetic trees in asexual eukaryotes. *Genetics*, *144*(1), 427–437.

Blanc, C., Saclier, N., Le Faou, E., Marie-Orleach, L., Wenger, E., Diblasi, C., Glemin, S., Galtier, N., & Delattre, M. (2023). Co-segregation of recombinant chromatids maintains genome-wide heterozygosity in an asexual nematode. *bioRxiv*, 2023.2003. 2017.533182.

Blanc, C. S., Delattre, M., & Van Doninck, K. (2025). Cracking the meiotic secrets behind animals asexuality When cytology seduces genomics to decode asexual meiosis. *Journal of Evolutionary Biology*, voaf045.

Boyer, L., Jabbour-Zahab, R., Mosna, M., Haag, C. R., & Lenormand, T. (2021). Not so clonal asexuals: Unraveling the secret sex life of Artemia parthenogenetica. *Evolution Letters*, *5*(2), 164–174.

Bradic, M., & Carlton, J. M. (2018). Does the common sexually transmitted parasite Trichomonas vaginalis have sex? *PLoS pathogens*, *14*(3), e1006831.

Brandt, A., Tran Van, P., Bluhm, C., Anselmetti, Y., Dumas, Z., Figuet, E., François, C. M., Galtier, N., Heimburger, B., & Jaron, K. S. (2021). Haplotype divergence supports long-term asexuality in the oribatid mite Oppiella nova. *Proceedings of the National Academy of Sciences*, *118*(38), e2101485118.

Brandt, D. Y., Huber, C. D., Chiang, C. W., & Ortega-Del Vecchyo, D. (2024). The promise of inferring the past using the ancestral recombination graph. *Genome Biology and Evolution*, *16*(2), evae005.

Bulankova, P., Sekulić, M., Jallet, D., Nef, C., Van Oosterhout, C., Delmont, T. O., Vercauteren, I., Osuna-Cruz, C. M., Vancaester, E., & Mock, T. (2021). Mitotic recombination between homologous chromosomes drives genomic diversity in diatoms. *Current Biology*, *31*(15), 3221–3232. e3229.

Burt, A., Carter, D. A., Koenig, G. L., White, T. J., & Taylor, J. W. (1996). Molecular markers reveal cryptic sex in the human pathogen Coccidioides immitis. *Proceedings of the National Academy of Sciences*, *93*(2), 770–773.

Cardoso, R., Pires, L., Zucchi, T., Zucchi, F. D., & Zucchi, T. (2010). Mitotic crossing-over induced by two commercial herbicides in diploid strains of the fungus Aspergillus nidulans. *Gen Mol Res*, *9*, 231–238.

Carpenter, M. L., Assaf, Z. J., Gourguechon, S., & Cande, W. Z. (2012). Nuclear inheritance and genetic exchange without meiosis in the binucleate parasite Giardia intestinalis. *Journal of cell science*, *125*(10), 2523–2532.

Charlesworth, D., & Willis, J. H. (2009). The genetics of inbreeding depression. *Nature Reviews Genetics*, *10*(11), 783–796.

Chen, E. C., Mathieu, S., Hoffrichter, A., Sedzielewska-Toro, K., Peart, M., Pelin, A., Ndikumana, S., Ropars, J., Dreissig, S., & Fuchs, J. (2018). Single nucleus sequencing reveals evidence of inter-nucleus recombination in arbuscular mycorrhizal fungi. *eLife*, *7*, e39813.

Chen, L.-Y., VanBuren, R., Paris, M., Zhou, H., Zhang, X., Wai, C. M., Yan, H., Chen, S., Alonge, M., & Ramakrishnan, S. (2019). The bracteatus pineapple genome and domestication of clonally propagated crops. *Nature genetics*, *51*(10), 1549–1558.

Cooper, M. A., Adam, R. D., Worobey, M., & Sterling, C. R. (2007). Population genetics provides evidence for recombination in Giardia. *Current Biology*, *17*(22), 1984–1988.

Csilléry, K., François, O., & Blum, M. G. (2012). abc: an R package for approximate Bayesian computation (ABC). *Methods in ecology and evolution*, *3*(3), 475–479.

Dapper, A. L., & Payseur, B. A. (2017). Connecting theory and data to understand recombination rate evolution. *Philosophical Transactions of the Royal Society B: Biological Sciences*, *372*(1736), 20160469.

Debortoli, N., Li, X., Eyres, I., Fontaneto, D., Hespeels, B., Tang, C. Q., Flot, J.-F., & Van Doninck, K. (2016). Genetic exchange among bdelloid rotifers is more likely due to horizontal gene transfer than to meiotic sex. *Current Biology*, *26*(6), 723–732.

Deng, Y., Nielsen, R., & Song, Y. S. (2024). Robust and accurate Bayesian inference of genome-wide genealogies for large samples. *bioRxiv*, 2024.2003. 2016.585351.

Eisman, R. C., & Kaufman, T. C. (2007). Cytological investigation of the mechanism of parthenogenesis in Drosophila mercatorum. *Fly*, *1*(6), 317–329.

Eitel, M., Guidi, L., Hadrys, H., Balsamo, M., & Schierwater, B. (2011). New insights into placozoan sexual reproduction and development. *PLoS One*, *6*(5), e19639.

Engelstädter, J. (2017). Asexual but Not Clonal: Evolutionary Processes in Automictic Populations. *Genetics*, *206*(2), 993–1009. https://doi.org/10.1534/genetics.116.196873

Fan, C., Cahoon, J. L., Dinh, B. L., Ortega-Del Vecchyo, D., Huber, C. D., Edge, M. D., Mancuso, N., & Chiang, C. W. (2025). A likelihood-based framework for demographic inference from genealogical trees. *Nature genetics*, 1–10.

Feretzaki, M., & Heitman, J. (2013). Unisexual reproduction drives evolution of eukaryotic microbial pathogens. *PLoS pathogens*, *9*(10), e1003674.

Flot, J.-F., Hespeels, B., Li, X., Noel, B., Arkhipova, I., Danchin, E. G., Hejnol, A., Henrissat, B., Koszul, R., & Aury, J.-M. (2013). Genomic evidence for ameiotic evolution in the bdelloid rotifer Adineta vaga. *Nature*, *500*(7463), 453–457.

Flynn, J. M., Chain, F. J., Schoen, D. J., & Cristescu, M. E. (2017). Spontaneous mutation accumulation in Daphnia pulex in selection-free vs. competitive environments. *Molecular Biology and Evolution*, *34*(1), 160–173.

Forche, A., Abbey, D., Pisithkul, T., Weinzierl, M., Ringstrom, T., Bruck, D., Petersen, K., & Berman, J. (2011). Stress alters rates and types of loss of heterozygosity in Candida albicans. *MBio*, *2*(4), 10.1128/mbio. 00129–00111.

Freitas, S., Parker, D. J., Labédan, M., Dumas, Z., & Schwander, T. (2023). Evidence for cryptic sex in parthenogenetic stick insects of the genus Timema. *Proceedings of the Royal Society B*, *290*(2007), 20230404.

Haller, B. C., Galloway, J., Kelleher, J., Messer, P. W., & Ralph, P. L. (2019). Tree-sequence recording in SLiM opens new horizons for forward-time simulation of whole genomes. *Molecular ecology resources*, *19*(2), 552–566.

Haller, B. C., & Messer, P. W. (2023). SLiM 4: Multispecies Eco-Evolutionary Modeling. *The American Naturalist*, *201*(5), E127–E139. https://doi.org/10.1086/723601

Hartfield, M., & Keightley, P. D. (2012). Current hypotheses for the evolution of sex and recombination. *Integrative zoology*, *7*(2), 192–209.

Hartfield, M., Wright, S. I., & Agrawal, A. F. (2016). Coalescent times and patterns of genetic diversity in species with facultative sex: effects of gene conversion, population structure, and heterogeneity. *Genetics*, *202*(1), 297–312.

Hartfield, M., Wright, S. I., & Agrawal, A. F. (2018). Coalescence and linkage disequilibrium in facultatively sexual diploids. *Genetics*, *210*(2), 683–701.

Hejase, H. A., Mo, Z., Campagna, L., & Siepel, A. (2022). A deep-learning approach for inference of selective sweeps from the ancestral recombination graph. *Molecular Biology and Evolution*, *39*(1), msab332.

Hiruta, C., Nishida, C., & Tochinai, S. (2010). Abortive meiosis in the oogenesis of parthenogenetic Daphnia pulex. *Chromosome Research*, *18*, 833–840.

Houtain, A., Derzelle, A., Llirós, M., Hespeels, B., Nicolas, É., Simion, P., Virgo, J., Lenormand, T., Hallet, B., & Van Doninck, K. (2024). Transgenerational chromosome repair in the asexual bdelloid rotifer *Adineta vaga*. *bioRxiv*, 2024.2001.2025.577190. https://doi.org/10.1101/2024.01.25.577190

Hunter, J. D. (2007). Matplotlib: A 2D graphics environment. *Computing in science & engineering*, *9*(03), 90–95.

Jaron, K. S., Bast, J., Nowell, R. W., Ranallo-Benavidez, T. R., Robinson-Rechavi, M., & Schwander, T. (2021). Genomic features of parthenogenetic animals. *Journal of Heredity*, *112*(1), 19–33.

Jaron, K. S., Parker, D. J., Anselmetti, Y., Tran Van, P., Bast, J., Dumas, Z., Figuet, E., François, C. M., Hayward, K., & Rossier, V. (2022). Convergent consequences of parthenogenesis on stick insect genomes. *Science Advances*, *8*(8), eabg3842.

Jeffries, D., Benvenuto, C., Böhne, A., Fraisse, C., Garcia, S., Jay, P., Kratochvíl, L., McDonough-Goldstein, C. E., Ruiz-Herrera, A., & Sotero-Caio, C. G. (2025). The Tree of Sex consortium: A global initiative for studying the evolution of reproduction in eukaryotes. *Journal of Evolutionary Biology*, voaf053.

Jinks-Robertson, S., & Petes, T. D. (2021). Mitotic recombination in yeast: what we know and what we don't know. *Current opinion in genetics & development*, *71*, 78–85.

Johri, P., Aquadro, C. F., Beaumont, M., Charlesworth, B., Excoffier, L., Eyre-Walker, A., Keightley, P. D., Lynch, M., McVean, G., & Payseur, B. A. (2022).

Recommendations for improving statistical inference in population genomics. *PLoS biology*, *20*(5), e3001669.
Judson, O. P., & Normark, B. B. (1996). Ancient asexual scandals. *Trends in ecology & evolution*, *11*(2), 41–46.
Kelleher, J., Etheridge, A. M., & McVean, G. (2016). Efficient coalescent simulation and genealogical analysis for large sample sizes. *PLOS Computational Biology*, *12*(5), e1004842.
Kelleher, J., Wong, Y., Wohns, A. W., Fadil, C., Albers, P. K., & McVean, G. (2019). Inferring whole-genome histories in large population datasets. *Nature genetics*, *51*(9), 1330–1338.
Kershenbaum, S., Jara-Espejo, M., Griffin, A., & Aboobaker, A. (2023). Gene conversion limits the cost of asexuality in immortal worms. *bioRxiv*, 2023.2003. 2020.533553.
Kimura, M. (1969). The number of heterozygous nucleotide sites maintained in a finite population due to steady flux of mutations. *Genetics*, *61*(4), 893.
Kondrashov, A. S. (2018). Through sex, nature is telling us something important. *Trends in Genetics*, *34*(5), 352–361.
Kopčak, D., & Hartfield, M. (2024). How do self-fertilising and facultative sexual populations differ in mutation accumulation? *bioRxiv*, 2024.2008. 2030.610445.
Korfmann, K., Gaggiotti, O. E., & Fumagalli, M. (2023). Deep learning in population genetics. *Genome Biology and Evolution*, *15*(2), evad008.
Koufopanou, V., Burt, A., & Taylor, J. W. (1997). Concordance of gene genealogies reveals reproductive isolation in the pathogenic fungus Coccidioides immitis. *Proceedings of the National Academy of Sciences*, *94*(10), 5478–5482.
Kuhn, A., Aron, S., & Hardy, O. J. (2021). Detection of Cryptic Sex in Automictic Populations: Theoretical Expectations and a Case Study in Cataglyphis Desert Ants. *Frontiers in Ecology and Evolution*, *9*, 741959.
Lacy, K. D., Hart, T., & Kronauer, D. J. (2024). Co-inheritance of recombined chromatids maintains heterozygosity in a parthenogenetic ant. *Nature Ecology & Evolution*, *8*(8), 1522–1533.
Laetsch, D. R., Bisschop, G., Martin, S. H., Aeschbacher, S., Setter, D., & Lohse, K. (2023). Demographically explicit scans for barriers to gene flow using gIMble. *PLoS Genetics*, *19*(10), e1010999.
Laine, V. N., Sackton, T. B., & Meselson, M. (2022). Genomic signature of sexual reproduction in the bdelloid rotifer Macrotrachella quadricornifera. *Genetics*, *220*(2), iyab221.
Lam, F., Langley, C. H., & Song, Y. S. (2011). On the genealogy of asexual diploids. *Journal of Computational Biology*, *18*(3), 415–428.
Lauterbur, M. E., Cavassim, M. I. A., Gladstein, A. L., Gower, G., Pope, N. S., Tsambos, G., Adrion, J., Belsare, S., Biddanda, A., & Caudill, V. (2023). Expanding the stdpopsim species catalog, and lessons learned for realistic genome simulations. *eLife*, *12*, RP84874.
Lee, S.-J., Risse, E., Mateus, I. D., & Sanders, I. R. (2024). Evolution of unexpected diversity in a putative mating type locus and its correlation with genome variability reveals likely asexuality in the model mycorrhizal fungus Rhizophagus irregularis. *BMC genomics*, *25*(1), 888.

Lewanski, A. L., Grundler, M. C., & Bradburd, G. S. (2024). The era of the ARG: An introduction to ancestral recombination graphs and their significance in empirical evolutionary genomics. *PLoS Genetics*, *20*(1), e1011110.

Li, N., & Stephens, M. (2003). Modeling linkage disequilibrium and identifying recombination hotspots using single-nucleotide polymorphism data. *Genetics*, *165*(4), 2213–2233.

Lin, J.-H., Chen, L.-C., Yu, S.-C., & Huang, Y.-T. (2022). LongPhase: an ultra-fast chromosome-scale phasing algorithm for small and large variants. *Bioinformatics*, *38*(7), 1816–1822.

Lin, Q., Goldberg, E. E., Leitner, T., Molina-París, C., King, A. A., & Romero-Severson, E. O. (2024). The Number and Pattern of Viral Genomic Reassortments are not Necessarily Identifiable from Segment Trees. *Molecular Biology & Evolution*, *41*(6), msae078. https://doi.org/https://doi.org/10.1093/molbev/msae078

Mackintosh, A., Laetsch, D. R., Hayward, A., Charlesworth, B., Waterfall, M., Vila, R., & Lohse, K. (2019). The determinants of genetic diversity in butterflies. *Nature Communications*, *10*(1), 3466.

Mackintosh, A., & Setter, D. (2024). Genealogical asymmetry under the isolation with migration model and a two-taxon test for gene flow. *Genetics*, *228*(4), iyae157.

Mandegar, M. A., & Otto, S. P. (2007). Mitotic recombination counteracts the benefits of genetic segregation. *Proceedings of the Royal Society B: Biological Sciences*, *274*(1615), 1301–1307.

Mark Welch, D. B., Mark Welch, J. L., & Meselson, M. (2008). Evidence for degenerate tetraploidy in bdelloid rotifers. *Proceedings of the National Academy of Sciences*, *105*(13), 5145–5149.

Mark Welch, D. B., & Meselson, M. (2000). Evidence for the evolution of bdelloid rotifers without sexual reproduction or genetic exchange. *Science*, *288*(5469), 1211–1215.

Martin, M., Patterson, M., Garg, S., O Fischer, S., Pisanti, N., Klau, G. W., Schöenhuth, A., & Marschall, T. (2016). WhatsHap: fast and accurate read-based phasing. *bioRxiv*, 085050.

Mateus, I. D., Auxier, B., Ndiaye, M. M., Cruz, J., Lee, S.-J., & Sanders, I. R. (2022). Reciprocal recombination genomic signatures in the symbiotic arbuscular mycorrhizal fungi Rhizophagus irregularis. *PLoS One*, *17*(7), e0270481.

Maynard Smith, J. (1978). *The evolution of sex*. Cambridge University Press.

Maynard Smith, J. (1999). The detection and measurement of recombination from sequence data. *Genetics*, *153*(2), 1021–1027.

McVean, G. A., & Cardin, N. J. (2005). Approximating the coalescent with recombination. *Philosophical Transactions of the Royal Society B: Biological Sciences*, *360*(1459), 1387–1393.

Miles, A., Rodrigues, M. F., Ralph, P., Kelleher, J., Schelker, M., Pisupati, R., Rae, S., & Millar, T. (2024). cggh/scikit-allel (v1.3.13). In. Zenodo.

Minh, B. Q., Schmidt, H. A., Chernomor, O., Schrempf, D., Woodhams, M. D., Von Haeseler, A., & Lanfear, R. (2020). IQ-TREE 2: new models and efficient methods for phylogenetic inference in the genomic era. *Molecular Biology and Evolution*, *37*(5), 1530–1534.

Mölder, F., Jablonski, K. P., Letcher, B., Hall, M. B., Tomkins-Tinch, C. H., Sochat, V., Forster, J., Lee, S., Twardziok, S. O., & Kanitz, A. (2021). Sustainable data analysis with Snakemake. *F1000Research*, *10*.

Molinier, C., Clément, C., Calzan, H., Lenormand, T., & Haag, C. R. (2025). Rare sexual reproduction by females of “obligate parthenogenetic” lineages of Daphnia cf. pulex. *Journal of Evolutionary Biology*, voaf044.

Morran, L. T., Schmidt, O. G., Gelarden, I. A., Parrish, R. C., & Lively, C. M. (2011). Running with the Red Queen: host-parasite coevolution selects for biparental sex. *Science*, *333*(6039), 216–218.

Neiman, M., Meirmans, P. G., Schwander, T., & Meirmans, S. (2018). Sex in the wild: How and why field-based studies contribute to solving the problem of sex. *Evolution*, *72*(6), 1194–1203.

Neiman, M., Sharbel, T., & Schwander, T. (2014). Genetic causes of transitions from sexual reproduction to asexuality in plants and animals. *Journal of Evolutionary Biology*, *27*(7), 1346–1359.

Nicoll, A. G., Kilford, H., Grace, C. A., Reis-Cunha, J. L., Jeffares, D. C., & Constable, G. W. (2024). Estimating the rate of sexual reproduction and the inbreeding rate in Leishmania. *bioRxiv*, 2024.2010. 2015.618469.

Nielsen, R., Vaughn, A. H., & Deng, Y. (2025). Inference and applications of ancestral recombination graphs. *Nature Reviews Genetics*, *26*(1), 47–58.

Normark, B. B., Judson, O. P., & Moran, N. A. (2003). Genomic signatures of ancient asexual lineages. *Biological Journal of the Linnean Society*, *79*(1), 69–84.

Nowell, R. W., Almeida, P., Wilson, C. G., Smith, T. P., Fontaneto, D., Crisp, A., Micklem, G., Tunnacliffe, A., Boschetti, C., & Barraclough, T. G. (2018). Comparative genomics of bdelloid rotifers: Insights from desiccating and nondesiccating species. *PLoS biology*, *16*(4), e2004830.

Osmond, M., & Coop, G. (2024). Estimating dispersal rates and locating genetic ancestors with genome-wide genealogies. *eLife*, *13*, e72177.

Otto, S. P. (2003). The advantages of segregation and the evolution of sex. *Genetics*, *164*(3), 1099–1118.

Otto, S. P. (2021). Selective interference and the evolution of sex. *Journal of Heredity*, *112*(1), 9–18.

Öztoprak, H., Gao, S., Guiglielmoni, N., Brandt, A., Zheng, Y., Errbii, M., Bednarski, V., Becker, C., Becker, K., & Borgschulte, L. (2025). Chromosome-scale genome dynamics reveal signatures of independent haplotype evolution in the ancient asexual mite Platynothrus peltifer. *Science Advances*, *11*(4), eadn0817.

Phan Thi, N., Danchin, E. G., Koutsovoulos, G. D., Rancurel, C., Vermeire, M.-l., Besnard, G., & Bellafiore, S. (2025). Genomic rearrangements promote diversification of a facultative meiotic parthenogenetic nematode pest (Meloidogyne graminicola). *bioRxiv*, 2025.2003. 2020.644268.

Porubsky, D., Ebert, P., Audano, P. A., Vollger, M. R., Harvey, W. T., Marijon, P., Ebler, J., Munson, K. M., Sorensen, M., & Sulovari, A. (2021). Fully phased human genome assembly without parental data using single-cell strand sequencing and long reads. *Nature biotechnology*, *39*(3), 302–308.

Poxleitner, M. K., Carpenter, M. L., Mancuso, J. J., Wang, C.-J. R., Dawson, S. C., & Cande, W. Z. (2008). Evidence for karyogamy and exchange of genetic material

in the binucleate intestinal parasite Giardia intestinalis. *Science*, *319*(5869), 1530–1533.
Ralph, P., Thornton, K., & Kelleher, J. (2020). Efficiently summarizing relationships in large samples: a general duality between statistics of genealogies and genomes. *Genetics*, *215*(3), 779–797.
Rasmussen, D. A., & Guo, F. (2023). Espalier: efficient tree reconciliation and ancestral recombination graphs reconstruction using maximum agreement forests. *Systematic Biology*, *72*(5), 1154–1170.
Romiguier, J., Gayral, P., Ballenghien, M., Bernard, A., Cahais, V., Chenuil, A., Chiari, Y., Dernat, R., Duret, L., & Faivre, N. (2014). Comparative population genomics in animals uncovers the determinants of genetic diversity. *Nature*, *515*(7526), 261–263.
Schaefer, N. K., Shapiro, B., & Green, R. E. (2021). An ancestral recombination graph of human, Neanderthal, and Denisovan genomes. *Science Advances*, *7*(29), eabc0776.
Schrider, D. R., & Kern, A. D. (2018). Supervised machine learning for population genetics: a new paradigm. *Trends in Genetics*, *34*(4), 301–312.
Schurko, A. M., Neiman, M., & Logsdon, J. M. (2009). Signs of sex: what we know and how we know it. *Trends in ecology & evolution*, *24*(4), 208–217.
Schwander, T., Henry, L., & Crespi, B. J. (2011). Molecular evidence for ancient asexuality in Timema stick insects. *Current Biology*, *21*(13), 1129–1134.
Signorovitch, A., Hur, J., Gladyshev, E., & Meselson, M. (2015). Allele sharing and evidence for sexuality in a mitochondrial clade of bdelloid rotifers. *Genetics*, *200*(2), 581–590.
Signorovitch, A. Y., Dellaporta, S. L., & Buss, L. W. (2005). Molecular signatures for sex in the Placozoa. *Proceedings of the National Academy of Sciences*, *102*(43), 15518–15522.
Simion, P., Narayan, J., Houtain, A., Derzelle, A., Baudry, L., Nicolas, E., Arora, R., Cariou, M., Cruaud, C., & Gaudray, F. R. (2021). Chromosome-level genome assembly reveals homologous chromosomes and recombination in asexual rotifer Adineta vaga. *Science Advances*, *7*(41), eabg4216.
Speidel, L., Forest, M., Shi, S., & Myers, S. R. (2019). A method for genome-wide genealogy estimation for thousands of samples. *Nature genetics*, *51*(9), 1321–1329.
Steenwyk, J. L., Li, Y., Zhou, X., Shen, X.-X., & Rokas, A. (2023). Incongruence in the phylogenomics era. *Nature Reviews Genetics*, *24*(12), 834–850.
Stenberg, P., & Saura, A. (2009). Cytology of Asexual Animals. In (pp. 63–74). Springer Netherlands. https://doi.org/10.1007/978-90-481-2770-2_4
Stern, A. J., Wilton, P. R., & Nielsen, R. (2019). An approximate full-likelihood method for inferring selection and allele frequency trajectories from DNA sequence data. *PLoS Genetics*, *15*(9), e1008384.
Stoeckel, S., Porro, B., & Arnaud-Haond, S. (2021). The discernible and hidden effects of clonality on the genotypic and genetic states of populations: Improving our estimation of clonal rates. *Molecular ecology resources*, *21*(4), 1068–1084.
Sui, Y., Qi, L., Wu, J.-K., Wen, X.-P., Tang, X.-X., Ma, Z.-J., Wu, X.-C., Zhang, K., Kokoska, R. J., & Zheng, D.-Q. (2020). Genome-wide mapping of spontaneous

genetic alterations in diploid yeast cells. *Proceedings of the National Academy of Sciences*, *117*(45), 28191–28200.

Taberly, G. (1988). Researchs on the thelytokous parthenogenesis of two species of Oribatid mites-Trhypochthonius tectorum (Berlese) and Platynothrus peltifer (Koch). 4. Observations on atavic males. *Acarologia*, *29*(1), 95–107.

Terwagne, M., Nicolas, E., Hespeels, B., Herter, L., Virgo, J., Demazy, C., Heuskin, A.-C., Hallet, B., & Van Doninck, K. (2022). DNA repair during nonreductional meiosis in the asexual rotifer Adineta vaga. *Science Advances*, *8*(48), eadc8829.

Tibayrenc, M., Kjellberg, F., Arnaud, J., Oury, B., Brenière, S. F., Dardé, M.-L., & Ayala, F. J. (1991). Are eukaryotic microorganisms clonal or sexual? A population genetics vantage. *Proceedings of the National Academy of Sciences*, *88*(12), 5129–5133.

Tibayrenc, M., Kjellberg, F., & Ayala, F. J. (1990). A clonal theory of parasitic protozoa: the population structures of Entamoeba, Giardia, Leishmania, Naegleria, Plasmodium, Trichomonas, and Trypanosoma and their medical and taxonomical consequences. *Proceedings of the National Academy of Sciences*, *87*(7), 2414–2418.

Tsai, I. J., Bensasson, D., Burt, A., & Koufopanou, V. (2008). Population genomics of the wild yeast Saccharomyces paradoxus: quantifying the life cycle. *Proceedings of the National Academy of Sciences*, *105*(12), 4957–4962.

Vakhrusheva, O. A., Mnatsakanova, E. A., Galimov, Y. R., Neretina, T. V., Gerasimov, E. S., Naumenko, S. A., Ozerova, S. G., Zalevsky, A. O., Yushenova, I. A., Rodriguez, F., Arkhipova, I. R., Penin, A. A., Logacheva, M. D., Bazykin, G. A., & Kondrashov, A. S. (2020). Genomic signatures of recombination in a natural population of the bdelloid rotifer Adineta vaga. *Nature Communications*, *11:6421*. https://doi.org/10.1038/s41467-020-19614-y

Vastrade, M., Etoundi, E., Bournonville, T., Colinet, M., Debortoli, N., Hedtke, S. M., Nicolas, E., Pigneur, L.-M., Virgo, J., & Flot, J.-F. (2022). Substantial genetic mixing among sexual and androgenetic lineages within the clam genus Corbicula. *Peer Community Journal*, *2*.

Wakeley, J. (2008). *Coalescent Theory: An Introduction*. Roberts & Company Publishers.

Waskom, M. L. (2021). Seaborn: statistical data visualization. *Journal of Open Source Software*, *6*(60), 3021.

Whitehouse, L. S., Ray, D. D., & Schrider, D. R. (2024). Tree sequences as a general-purpose tool for population genetic inference. *Molecular Biology and Evolution*, *41*(11), msae223.

Wilson, C. G., Nowell, R. W., & Barraclough, T. G. (2018). Cross-contamination explains “inter and intraspecific horizontal genetic transfers” between asexual bdelloid rotifers. *Current Biology*, *28*(15), 2436–2444. e2414.

Wilson, C. G., Pieszko, T., Nowell, R. W., & Barraclough, T. G. (2024). Recombination in bdelloid rotifer genomes: asexuality, transfer and stress. *Trends in Genetics*.

Wohns, A. W., Wong, Y., Jeffery, B., Akbari, A., Mallick, S., Pinhasi, R., Patterson, N., Reich, D., Kelleher, J., & McVean, G. (2022). A unified genealogy of modern and ancient genomes. *Science*, *375*(6583), eabi8264.

Wong, Y., Ignatieva, A., Koskela, J., Gorjanc, G., Wohns, A. W., & Kelleher, J. (2024). A general and efficient representation of ancestral recombination graphs. *Genetics*, *228*(1), iyae100.

Yildirir, G., Kokkoris, V., & Corradi, N. (2020). Parasexual and sexual reproduction in arbuscular mycorrhizal fungi: room for both. *Trends in microbiology*, *28*(7), 517–519.

Supplement to Chapter 1



——————————— O ———————————

Tymoteusz Pieszko

——————————— O ———————————

Supplementary Text 1: Models of asexuality with asyngamous recombination

To validate the design of our model of automixis via central fusion (CF), we compared it to analytical models. Engelstädter (2017) derived expressions for the equilibrium individual-level heterozygosity $\widehat{H_I}$, along with several other diversity metrics, under obligate automixis via central fusion. The analytical model assumes that crossover recombination occurs with equal probability between all four possible pairs of non-sister chromatids, consistent with the absence of chromatid interference (Sarens et al., 2021). Previous simulation work investigated the alternative assumption of full negative chromatid interference (Blanc et al., 2023). Below, we first use an analytical approach to demonstrate that allowing for recombination between only one pair of chromatids yields distinct predictions for $\widehat{H_I}$. Second, we describe how our CF model uses the machinery of SLiM4 (Haller & Messer, 2023) to accurately translate Engelstädter's (2017) model into an individual-based framework.

Analytical derivations and justification of approach

During asexual reproduction, heterozygous genotypes are either passed intact to offspring or transition to a homozygous state through asyngamous recombination. Engelstädter (2017) provides a general formula for $\widehat{H_I}$ under obligate asexual reproduction:

$$\widehat{H_I} \approx \frac{2\mu}{2\mu + \gamma} \qquad (1)$$

Where μ is the per-site per-generation mutation rate and γ is the probability of a transition from the heterozygous state in the parent to a homozygous state in the offspring (i.e., the rate of loss of heterozygosity specific to a site), with the approximation valid for small μ. Previous simulation work on central fusion (Blanc et al., 2023) implemented a recombination routine where all crossovers consistently occur between only one pair of chromatids, herein called the 'CI' (chromatid interference) model. Under the CI assumption, crossovers between the centromere and a focal locus induce switches between 2 configurations: recombinant (for odd crossover numbers) and non-recombinant (for even crossover numbers). Given n crossovers between the centromere and a focal locus, the probability of arriving at the recombinant state $r(n)$ is:

$$r(n) \mid CI = \sum_{i=1}^{n} (-1)^{i-1}$$
$$= \frac{1}{2}(1 - (-1)^n) \quad (2)$$

If the number of crossovers is Poisson-distributed with mean $\bar{n}$, Eq. (2) can be modified to obtain the expected fraction of recombinant configurations at a locus using Taylor series expansion:

$$\bar{r}(\bar{n}) \mid CI = \sum_{k=0}^{\infty} \frac{\bar{n}^k \, e^{-\bar{n}}}{k!} r(k)$$
$$= \frac{1}{2} \sum_{k=1}^{\infty} \frac{\bar{n}^k \, e^{-\bar{n}}}{k!} (1 - (-1)^n)$$
$$= \frac{1}{2} \left(1 - e^{-\bar{n}} - \sum_{k=1}^{\infty} \frac{\bar{n}^k \, e^{-\bar{n}}}{k!} \right)$$

$$= \frac{1}{2}\left(1 - e^{-\bar{n}} - e^{-\bar{n}}(e^{-\bar{n}} - 1)\right)$$
$$= \frac{1}{2}(1 - e^{-2\bar{n}})$$

(3)

Finally, by incorporating the regime of chromatid segregation specific to central fusion (where, for a given crossover, a recombinant and a non-recombinant chromatid have a 50% chance of segregating together; see Fig. 1 in Engelstädter, 2017), we obtain γ_{CF}, the probability of a transition from the heterozygous state in the parent to a homozygous state in the offspring produced through central fusion:

$$\gamma_{CF} \left| CI \right. = \frac{1}{2}\, \bar{r}(\bar{n}) \left| CI \right.$$
$$= \frac{1}{4}(1 - e^{-2\bar{n}})$$

(4)

This can be contrasted with the expression obtained by Engelstädter (2017) under the assumption of no chromatid interference ('NCI'):

$$\gamma_{CF} \mid NCI = \frac{1}{3}\left(1 - e^{-\frac{3\bar{n}}{2}}\right)$$

(5)

In Fig. S17, we compare the values of $\widehat{H}_I$ obtained by combining Eq. (1) with Eq. (4) or Eq. (5) across a range of expected crossover numbers $\bar{n}$. As expected, the match is close when $\bar{n} \leq 0.01$, but decays with higher values of $\bar{n}$. We conclude that, while the CI recombination model can capture the properties of Engelstädter's (2017) analytical

model at low $\bar{n}$, implementing the NCI routine in simulations is required to extend Engelstädter's results in a fully compatible way.

Finally, the mean chromosome-wide rate of loss of heterozygosity (LOH) $\bar{\gamma}_{CF}$ can be obtained as:

$$\bar{\gamma}_{CF} = \frac{1}{L-1}\sum_{i=1}^{L-1}\gamma_i \qquad (6)$$

Where L is the chromosome length in number of sites. Under mitotic parthenogenesis with gene conversion, an analogous result can be obtained simply, following Engelstädter (2017):

$$\bar{\gamma}_{MP} = r_{GC} \times \lambda \qquad (7)$$

Where r_{GC} is the rate of gene conversion tract initiation and λ is the mean gene conversion tract length. Eq. (7) can be combined with Eq. (1) to obtain $\widehat{H_I}$ under mitotic parthenogenesis (Engelstädter, 2017).

Simulation model description

SLiM4 (Haller & Messer, 2023) is a scriptable framework for constructing individual-based, genetically explicit simulations. While SLiM4 supports both sex and clonality, it does not natively support asyngamous recombination. A workaround is to draw breakpoint positions using custom code in SLiM's Eidos scripting language and generate offspring 'genomes' (SLiM's term for single DNA molecules) using the genomes of a

single parent as templates. Below, we outline the steps for drawing recombination breakpoints under the mitotic parthenogenesis (MP) and CF models, as well as for incorporating sexual and asexual reproduction in simulated scenarios.

Gene conversion in MP. The generation of offspring genomes is accompanied by a Poisson-distributed number of gene conversion tracts with mean $\bar{n}_{GC}$. Each tract, with mean length λ, is modelled as two breakpoints marking its start and end. The Poisson distribution of tract number is achieved by following a Poisson process with interarrival times (here, distances between the end of one tract and the start point of the next) geometrically distributed with parameter r_{GC}; hence, $\bar{n}_{GC} = r_{GC} \times L$, assuming $\lambda \ll L$. Implementation of the Poisson process specific to the MP model is outlined in Algorithm A; note that the algorithm does not avoid edge effects.

Algorithm A. Legend: i – current position, i_{max} – maximum position, D – distance to next breakpoint, i_{start} – track start position, i_{end} – tract end position, Z – length of a tract (see also Table S1).

1 Set i = 0, i_{max} = L and BREAKS = []

2 **while** $i < i_{max}$ **do**

3 Draw D = rand(Geom(r_{GC}))

4 Set $i_{start} = i + D$

5 **if** $i_{start} > i_{max}$ **then**

6 **exit**

7 Draw Z = rand(Geom($\frac{1}{\lambda}$))

8 Set $i_{end} = i_{start} + Z$

9 **if** $i_{end} > i_{max}$ **then**

10 **exit**

12 BREAKS.append([i_{start}, i_{end}])

13 Set $i = i_{end}$

Return BREAKS

Conversion tracts drawn via Algorithm A are randomly assigned to the four possible pairs of non-sister chromatids. Finally, parent genomes are randomly assigned to each of the two 'slots' of the offspring individual (i.e., passed in random order to the addRecombinant() method), and offspring genomes incorporating the conversion tracts are generated.

Crossover recombination in CF. The generation of offspring genomes is accompanied by a Poisson-distributed number of crossovers with mean $\bar{n}_{CO}$. Each crossover is modelled as a breakpoint that simultaneously affects two chromatids, resulting in a

switch in the parental copying template. The Poisson distribution of crossover number is achieved by following a Poisson process with interarrival times (here, distances between breakpoints) geometrically distributed with parameter r_{CO}; hence, $\bar{n}_{CO} = r_{CO} \times L$ (Table S1). Implementation of the Poisson process specific to the CF model is outlined in Algorithm B; note that the algorithm does not avoid edge effects.

Algorithm B. Legend: i – current position, i_{max} – maximum position, D – distance to next breakpoint, i_{CO} – position of a crossover (see also Table S1).

```
Set i = 0, i_max = L and BREAKS = []
while i < i_max do
    Draw D = rand(Geom(r_CO))
    Set i_CO = i + D
    if i_CO > i_max then
        exit
    BREAKS.append(i_CO)
    Set i = i_CO
Return BREAKS
```

Crossovers drawn via Algorithm B are first randomly assigned to the four possible pairs of non-sister chromatids. These assignments are then modified to reflect how the physical cutting and rejoining of DNA molecules affects the outcomes at linked loci, a process of ‘crossover resolution’ illustrated in Fig. S14. Finally, parent genomes are randomly assigned to each of the two ‘slots’ of the offspring individual (i.e., passed in random order to the addRecombinant() method), and offspring genomes are generated according to the resolved crossovers.

Mixed reproductive scenarios. We followed section 15.13 of the SLiM manual (Haller & Messer, 2024) to achieve Wright-Fisher-like dynamics using the non-Wright-Fisher machinery of SLiM. Briefly, generation t + 1 is produced by sampling generation t with replacement, with sampling probabilities proportional to fitness (equal for all individuals under neutral scenarios). In our mixed reproductive scenarios, two pools of parents are sampled. If an offspring is to be produced asexually, a parent from pool 1 is used; if an offspring is to be produced sexually, a parent from pool 1 is paired with a parent from pool 2.

Supplementary Text 2: Simulation pipeline

Below, we provide details on the processing of simulated ARGs and the re-inference of genealogies implemented in the Snakemake pipeline (Mölder et al., 2021) used to run our simulations.

Processing of simulated ARGs

We performed several in-memory operations on the simulated tree sequences. First, to ensure complete coalescence of the genealogies, we performed recapitation using pyslim v1.0.4 (Haller et al., 2019). 'Recapitation' is a post-hoc procedure of adding a sexual burn-in for a hypothetical sexual progenitor of the asexual lineage using a coalescent simulator msprime (Baumdicker et al., 2022), for which we used an ancestral N_a = 1000 and crossover rate r_a = 10^{-6}. Second, we randomly subsampled each simulated ARG twice: first, to obtain an ARG for two random target individuals, second, to obtain an ARG for 100 individuals that included the targets. We then used msprime v1.3.2 (Baumdicker et al., 2022) to overlay neutral mutations under the Jukes-Cantor model at a per-site per-generation rate μ = 5 × 10^{-7} on top of the subsampled ARGs.

This value of μ is two orders of magnitude higher than is typically reported in invertebrates (Wang and Obbard, 2023); paired with N = 1,000, it was chosen to avoid the computational burden of simulating very large populations. Under the traditional scaling approach (Uricchio and Hernandez, 2014), these parameter values would approximate the evolutionary processes in a population of 100,000 individuals. We nonetheless note that our non-canonical models are unlikely to conform to the scaling trick and, accordingly, we report the simulated rates of γ. Per simulation, we output the two-individual ARG, a corresponding VCF file, and FASTA files for non-overlapping 5-kb windows corresponding to the 100-individual ARG (a total of 200 files per simulation).

Re-inference of genealogies

Using both IQ-TREE and SINGER, we re-inferred genealogies for the target two-individual ARGs in windows of 5 kb. The two-individual ARGs contained 448 to 5,823 non-recombining blocks (Table S3) and 3,177 to 8,125 SNPs on average (Table S4) in MP scenarios, allowing us to test the inference algorithms' performance in the presence of mixed genealogical signal. For IQ-TREE re-inference, we inferred window-wise trees using the FASTA files as input. We ran IQ-TREE with default parameters, except we set the substitution model to Jukes-Cantor (-m JC69). We rooted the trees using the function 'midpoint' from the R package phangorn v2.11.1 (Schliep, 2011). For analyses, from each tree we extracted sub-trees corresponding to target individuals represented in the two-individual ARGs. For SINGER re-inference, we used the two-individual VCF files as input. As scaling parameters, we used the simulated values of N and μ. We kept the recombination **:** mutation rate ratio of 1 across the simulated scenarios and assumed random polarity of variants. For efficiency, we only inferred ARGs for the 0.1 of windows with highest average H_I (β = 0.1), as calculated using the statistics interface of tskit

(Ralph et al., 2020). Per run of the MCMC chain, we output 10 samples, evenly distributed between steps 1,000 and 2,000 of the chain. The SINGER algorithm terminates if there is excessive mismatch between input diversity and the expectation of $4N_e\mu$; we did not repeat failed runs, and under most scenarios the success rate (MCMC samples generated / expected total per scenario) was higher than 80% (Table S5).

Supplementary Text 3: Comparison of MP and CF models

Our MP and CF models simulate distinct cytological pathways of reproduction that capture two respective forms of asyngamous recombination: gene conversion and crossover recombination, often considered separately in theoretical studies (e.g., Kopčak & Hartfield, 2024; Engelstädter, 2017). Specifically, we based the CF model on the analytical approach of Engelstädter (2017), as described in Supplementary Text 1. The MP model is based on mitotic recombination insights from *Saccharomyces cerevisiae*, where LOH tracts attributed to gene conversion are usually < 15 kb (Sui et al., 2020), informing our choice of λ = 5,000 bp (Table S1).

Given the different outcomes of recombination, our choice to simulate the same ranges of r_{GC} and r_{CO} values resulted in different overall levels of LOH (γ) between the MP and CF scenarios. Comparing MP scenarios of $\gamma = 5 \times 10^{-4}$ with CF scenarios of $\gamma = 2.5 \times 10^{-4}$ and $\gamma = 7.9 \times 10^{-4}$ (all for $\sigma = 0$), confirmed that average statistic values were similar given equivalent LOH levels. Interestingly, statistic values under the MP scenario of $\gamma = 5 \times 10^{-4}$ (e.g., F_{IS} = 0.01, $p(CL)$ = 0.49 and, after applying the heterozygosity bias, 0.76) were generally closer to the CF scenario of $\gamma = 7.9 \times 10^{-4}$ (0.03, 0.44 and 0.88, respectively) than $\gamma = 2.5 \times 10^{-4}$ (-0.16, 0.72 and 0.96, respectively). Our analyses of F_{IS} stochasticity and LD patterns additionally demonstrated that CF showed a broader range

of γ values compatible with F_{IS} = 0 (Fig. S2 and S3) and a less 'sex-like' shape of R^2 curves (Fig. S4 and S5). We attribute these results to differences between the recombination routines that go beyond average γ. Under CF, the chance of recombining increases with distance from position 0 (i.e., the 'centromere'), whereas this chance is equal for all sites under MP. Individual LOH events are also on average longer under CF. Together, these features explain greater variation between replicated CF simulations and a more linear pattern of LD decay (given longer span of local trees).

In nature, mechanisms and patterns of asyngamous recombination are likely to be more complex and less easily categorised. For instance, mitotic asexuality might be accompanied by long-range recombination (due to, e.g., mitotic crossing-over or break-induced replication) and different types of crossover and non-crossover gene conversion (Jinks-Robertson & Petes, 2021). Similarly, gene conversion is expected to co-occur with crossover recombination in meiotic asexuality (Chen et al., 2007). While our models represent 'pure' scenarios, studying the combined effects of different asyngamous recombination regimes may be of future interest.

Supplementary Text 4: Comparison of genealogical inference with IQ-TREE and SINGER

IQ-TREE and SINGER represent two distinct approaches to estimating genome-wide genealogies, with differences that are relevant to the present study.

Reticulate evolution can be interrogated through the inference of independent local trees along a genome (e.g., Martin & Van Belleghem, 2017). In this widely-used approach, the genome is divided into windows, which contain enough informative sites for tree reconstruction but are presumably short enough to limit the mixing of phylogenetic

signal. We used IQ-TREE v2 (Minh et al., 2020) to reconstruct local trees for phased diploid sequences via maximum likelihood, under the assumption of a clock-like mutation process. Thus-obtained estimate of a genealogy is a sequence of independent trees, one per window, with uncertainty on branching patterns that could be quantified via bootstrapping.

Recently, there has been considerable progress in the development of methods that jointly reconstruct the positions of recombination breakpoints and local trees along phased genome segments (Nielsen et al., 2025). Here, we used SINGER (Deng et al., 2024), a Bayesian method that explores the posterior distribution of possible ancestral recombination graphs (ARGs) using a Markov chain Monte Carlo algorithm. Given SINGER outputs a user-specified number of ARG samples, it enables to explicitly account for reconstruction uncertainty, a feature that appears particularly useful when summarising the contributions of distinct trees to the genealogy.

We did not compare the fine-scale performance of the two methods (e.g., topological distance from the true ARG or the accuracy of recombination breakpoints reconstructed by SINGER). ARG reconstruction with SINGER in particular, requires specifying scaling parameters (such as the recombination **:** mutation ratio or effective population size) grounded in a model formulated for an outcrossing population with crossover recombination and hence not directly applicable to our simulated scenarios of asexuality with asyngamous recombination. While developing an ARG reconstruction method explicitly tailored to non-model reproductive modes seems a promising avenue of future research, we note that tree composition reconstructions with IQ-TREE and SINGER did

not differ substantially, with a slight advantage of IQ-TREE as measured by the proportion of mis-inferred SX trees under obligate asexuality.

Supplementary Text 5: K, a statistic to measure the signal of reproductive mode from unphased, genome-wide SNPs.

The site frequency spectrum (SFS) is routinely used to summarise evolutionary histories (Wakeley, 2008). An unfolded SFS for four haplotypes comprises three categories of SNPs: singletons (sites with one derived allele), doubletons (two derived alleles) and tripletons (three derived alleles). Below, we explain how the relative counts of doubletons (ξ_2) and tripletons (ξ_3) reflect the rate of asyngamous recombination under obligate asexuality, as captured by our new statistic K.

Under obligate asexuality, CL trees (Fig. A; note that alternative tip labelling 0-3-1-2 is equally likely) are generated through clonal descent, whereas AR trees are generated through asyngamous recombination that results in loss of heterozygosity (LOH). Three types of AR trees can be distinguished by whether one (AR_1) or both (AR_{2A} and AR_{2B}) asexual lineages experienced LOH, and by the directionality of the second LOH event (AR_{2A}: 3 → 2; AR_{2B}: 2 → 3).

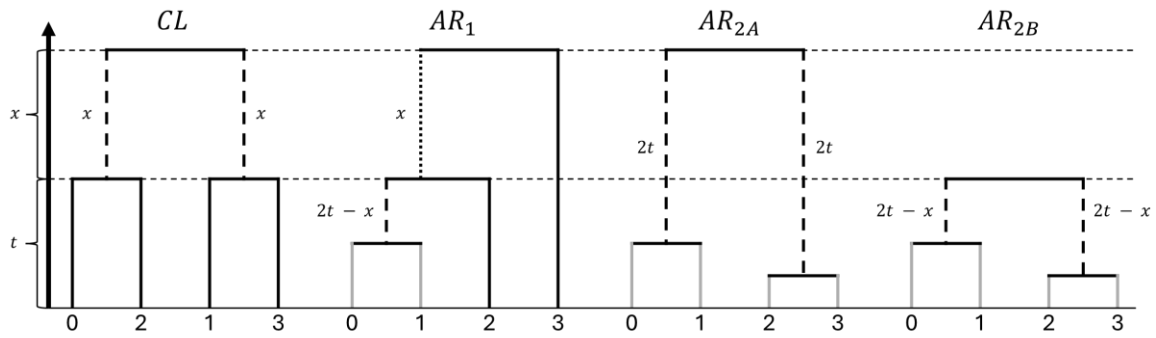


Fig. A. Two-individual, four-tip local trees under obligate asexuality with asyngamous recombination. Epoch t precedes the divergence of asexual lineages; epoch x precedes coalescence due to LOH. Branches that terminate in LOH within epoch t (with expected length x – t) are marked in grey. The expected lengths of branches on which doubletons (dashed) and tripletons (dotted) arise are displayed alongside them.

Assuming LOH events in an asexual lineage follow a Poisson process, the probability of a LOH event occurring within t generations is $1 - e^{-\gamma t}$, where γ is the per-locus, per-generation LOH rate. For two lineages, the probabilities of arriving with no LOH, with LOH in a single lineage, or with LOH in both lineages are, respectively:

$$P(CL) = e^{-2\gamma t}$$

$$P(AR_1) = e^{-\gamma t}(1 - e^{-\gamma t})$$

$$P(AR_2) = (1 - e^{-\gamma t})^2 \qquad (8)$$

To obtain the expected genomic proportions of CL, AR_1 and AR_2 trees (i.e., $p(CL)$, $p(AR_1)$ and $p(AR_2)$), we drew 10^5 times t from the distribution of divergence times between asexual lineages in a population of size N = 1000 ($T \sim \mathrm{Exp}\left(\frac{1}{N}\right)$) and calculated average values using Eq. (9). In Fig. B, we show that thus-obtained tree proportions match those simulated using the individual-based MP model.

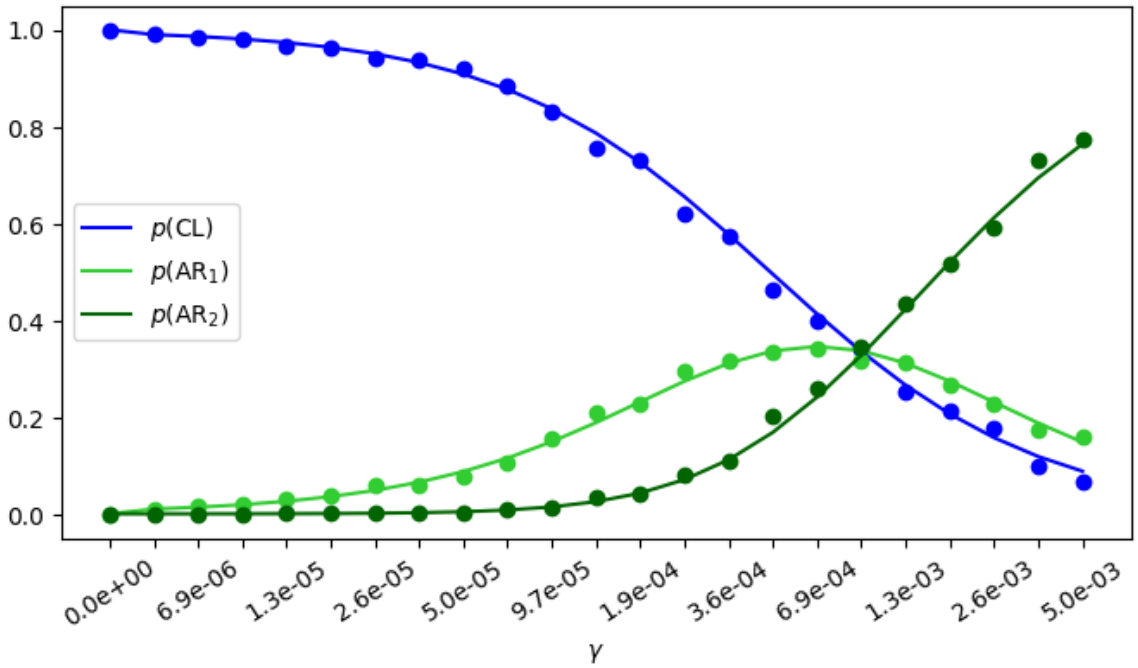


Fig. B. Tree proportions $p(CL)$, $p(AR_1)$ and $p(AR_2)$ under obligate asexuality and a range of per-locus, per-generation LOH rates γ (N = 1000): comparison of expressions obtained here (lines) and the values obtained using the MP model (points; each scenario in 100 replicates).

In a pair of obligate asexual genomes, tripleton SNPs only arise on the stem branch of AR_1 trees (Fig A). We find that $p(AR_1)$ is maximised when $\gamma \times t = \ln 2$ (≈ 0.693), which, for N = 1000, corresponds to $\gamma \approx 6.93 \times 10^{-4}$. To obtain the maximum value of K under obligate asexuality, one must further consider the length of the branches on which doubletons and tripletons arise. For this purpose, we define x as the expected stem branch length in CL trees (with $x = \frac{1}{\gamma}$), and $x - t$ as the expected time until LOH in AR trees (as LOH needs to occur before the divergence time t; Fig. A). Accordingly, the relative contributions of SNPs arising at different trees to the total pool of doubletons and tripletons can be expressed as shown in Fig. A and summarised in Table B.

Table A. Relative cumulative lengths of branches in different trees (see Fig. A) contributing to the total pool of doubletons (outer subscript 2) and tripletons (outer subscript 3) under obligate asexuality. The factor of 0.5 in the $(AR_{2A})_2$ and $(AR_{2B})_2$ expressions reflects equal proportions of the contributing trees.

$(CL)_2$	$(AR_1)_2$	$(AR_{2A})_2$	$(AR_{2B})_2$	$(AR_1)_3$
$2x$	$2t - x$	$0.5 \times 4t$	$0.5 \times (4t - 2x)$	x

Using the values that maximise $p(AR_1)$ (γ = 6.93 × 10^{-4}, t = 1000) in the expressions from Table A, we find that the ratio of ξ_3 to ξ_2 has a maximum expected value of approx. 0.24 under obligate asexuality. Finally, the corresponding formula for K can be expressed as:

$$K = 1 - \frac{p(CL)(CL)_2 + p(AR_1)(AR_1)_2 + p(AR_2)((AR_{2A})_2 + (AR_{2B})_2) - p(AR_1)(AR_1)_3}{p(CL)(CL)_2 + p(AR_1)(AR_1)_2 + p(AR_2)((AR_{2A})_2 + (AR_{2B})_2) + p(AR_1)(AR_1)_3} \quad (9)$$

Using the values that maximise $p(AR_1)$, we obtain K_{max} ≈ 0.396. In Fig C, we show that this result agrees with a value obtained using the individual-based MP model. We conclude that, at least with regards to its expected value, the new K statistic can leverage information in unphased SNPs to provide insight into the mode of reproduction.

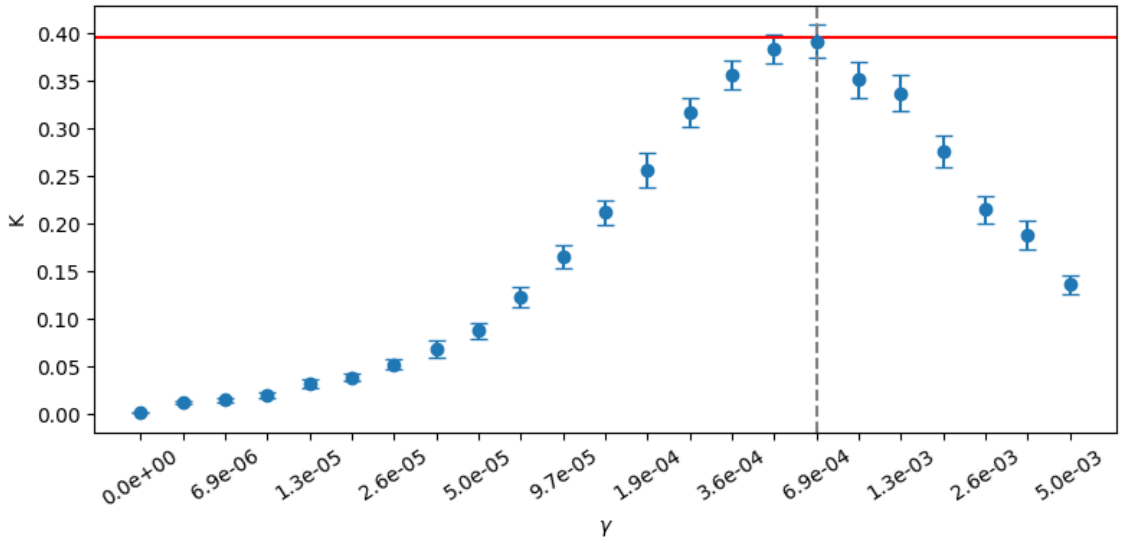


Fig. C. K under obligate asexuality and a range of per-locus, per-generation LOH rates γ (N = 1000): comparison of the maximum value obtained here (red line) and the values obtained using the MP model (points; bars show standard error among 100 replicates).

Supplementary Figures

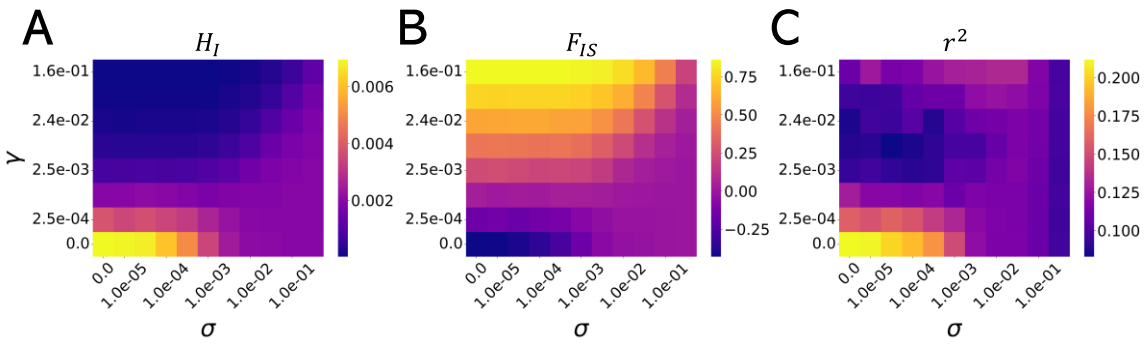


Fig. S1. H_I, F_{IS} and r^2 for SNPs < 1,000 bp apart across the space of the sex rate σ, increasing from the left to the right of each heatmap, and the LOH rate γ, increasing from the bottom to the top; CF model. For each scenario, mean statistic values were obtained for samples of 100 random individuals and averaged across 100 replicates.

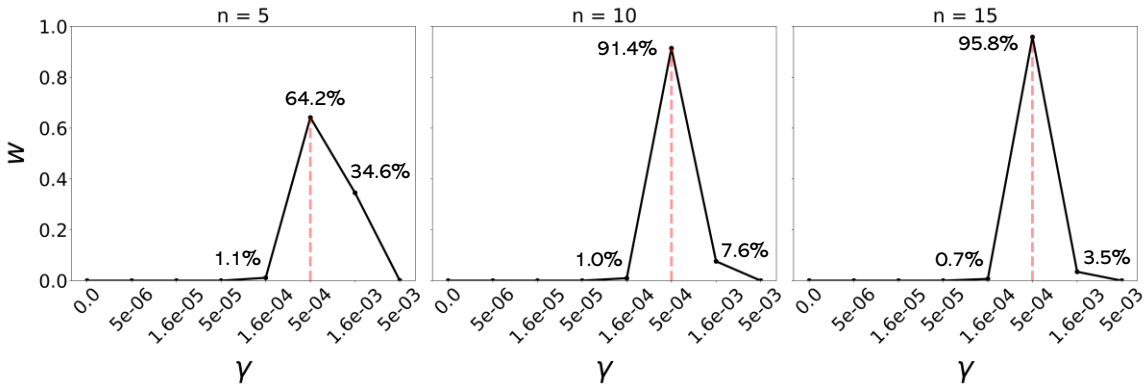


Fig. S2. Akaike weights of evidence (w) for different LOH rates γ given an observed F_{IS} = 0 and distributions of values obtained via sampling n = 5, 10 or 15 individuals from obligate MP populations replicated 100 times. Dashed vertical lines indicate γ = $\frac{1}{2N}$.

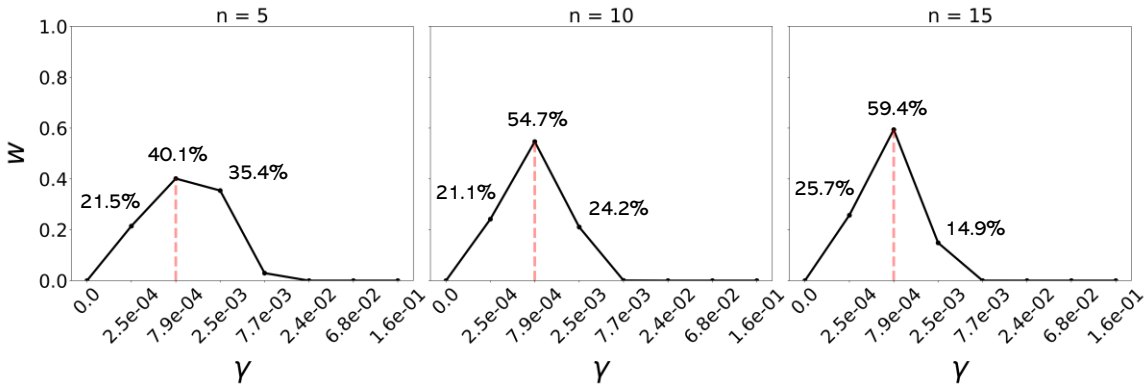


Fig. S3. Akaike weights of evidence (w) for different LOH rates γ given an observed F_{IS} = 0 and distributions of values obtained via sampling n = 5, 10 or 15 individuals from obligate CF populations replicated 100 times. Dashed vertical lines indicate γ closest to $\frac{1}{2N}$.

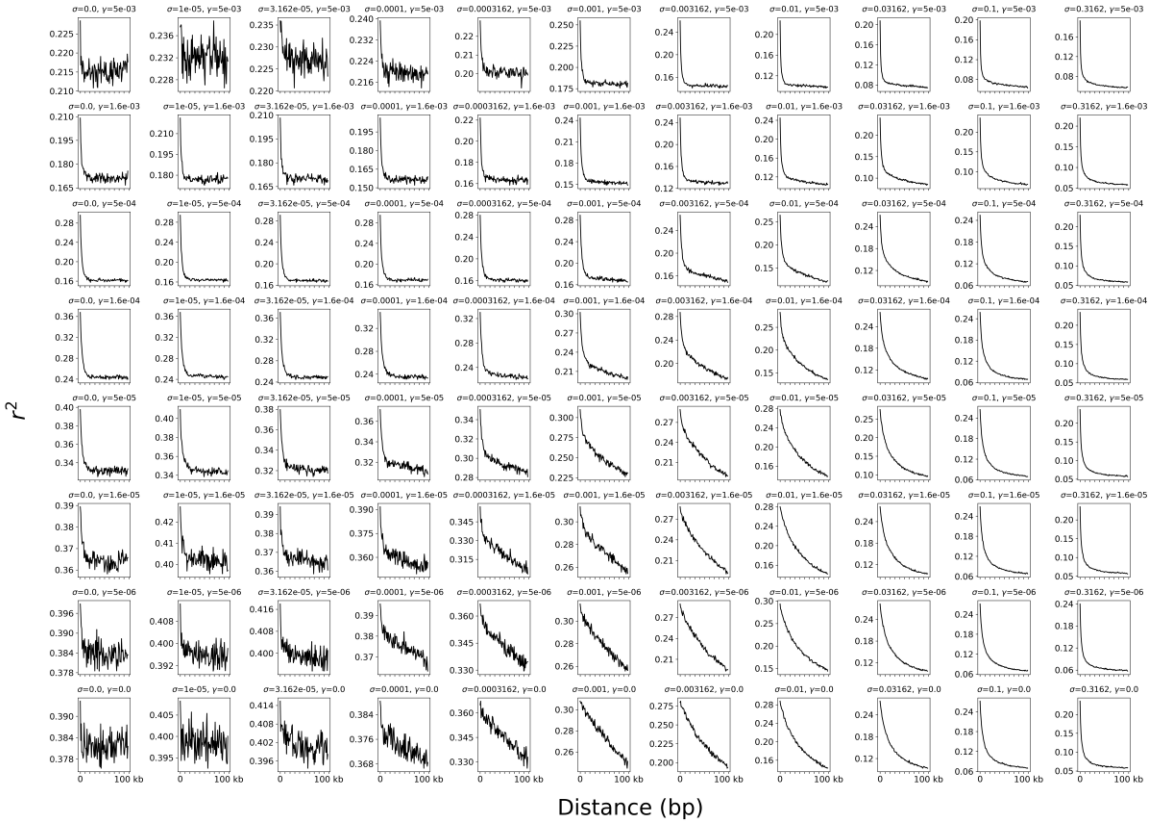


Fig. S4. r^2 as a function of inter-site distance across the space of sex rates σ and LOH rates γ; MP model. r^2 was calculated using samples of 10 individuals and a maximum of 500 SNPs. Variability in some curves is due to a limiting number of SNPs.

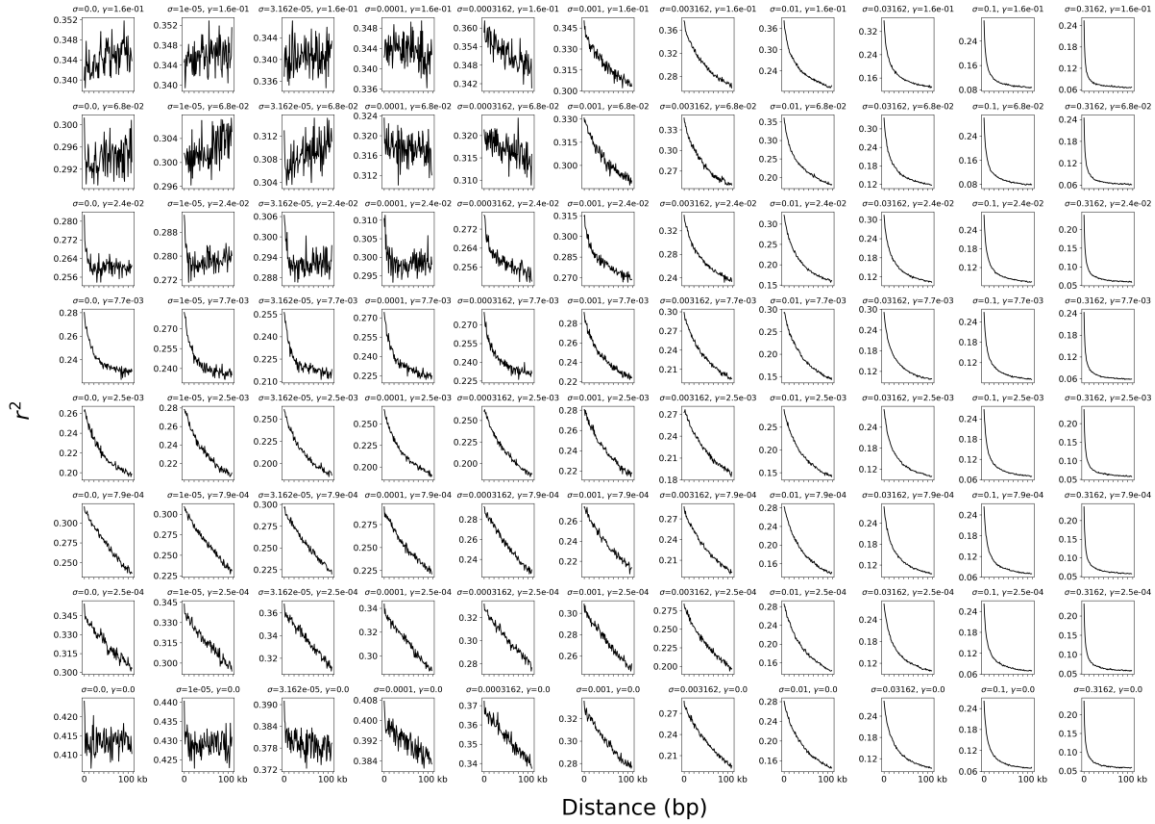


Fig. S5. r^2 as a function of inter-site distance across the space of sex rates σ and LOH rates γ; CF model. r^2 was calculated using samples of 10 individuals and a maximum of 500 SNPs. Variability in some curves is due to a limiting number of SNPs.

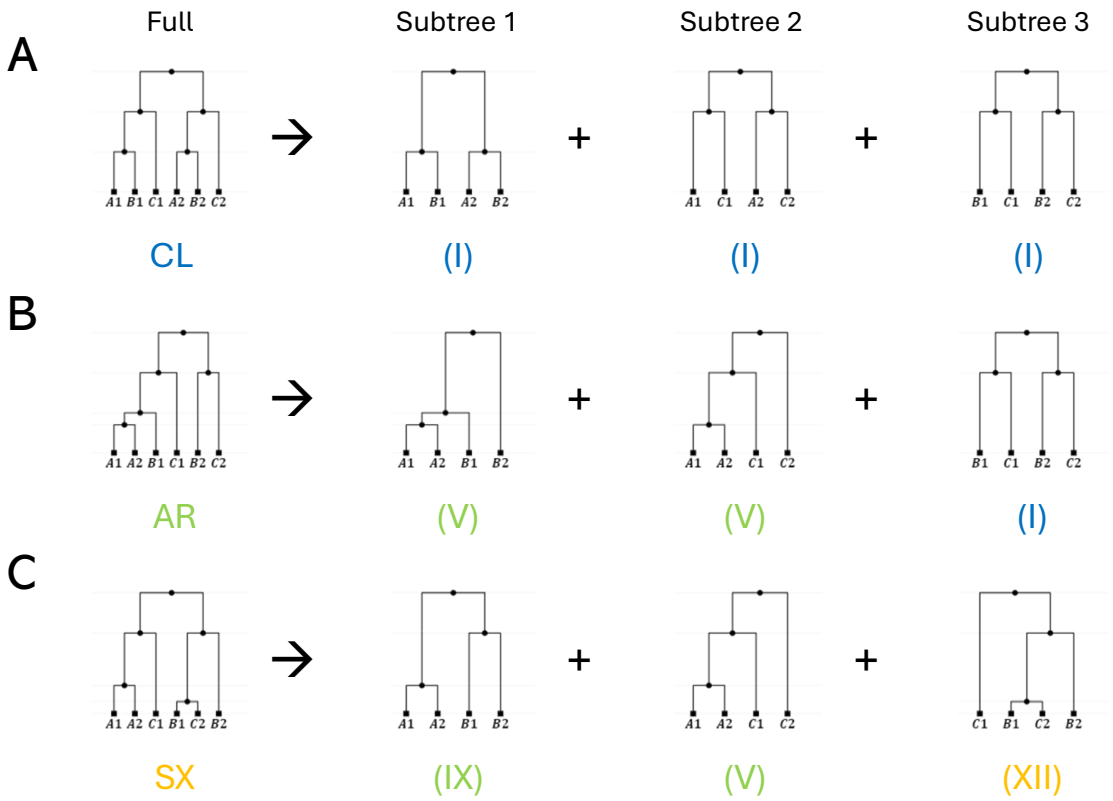


Fig. S6. Exhaustive tree classification: example of 3 individuals. To disentangle the reproductive history, trees for individuals $\boldsymbol{A}$, $\boldsymbol{B}$ and $\boldsymbol{C}$ (each with alleles 1 and 2) can be decomposed into subtrees for the $\binom{3}{2}$ possible pairs of individuals. Roman numerals and colours correspond to Fig. 4A. (A) A clonal tree is decomposed into CL subtrees (note the equal timing of internal nodes that is not recovered by many inference algorithms and hence ignored in Fig. 4A). (B) The signature of asyngamous recombination is reflected in subtrees 1 and 2. (C) The signature of sex is reflected in subtree 3.

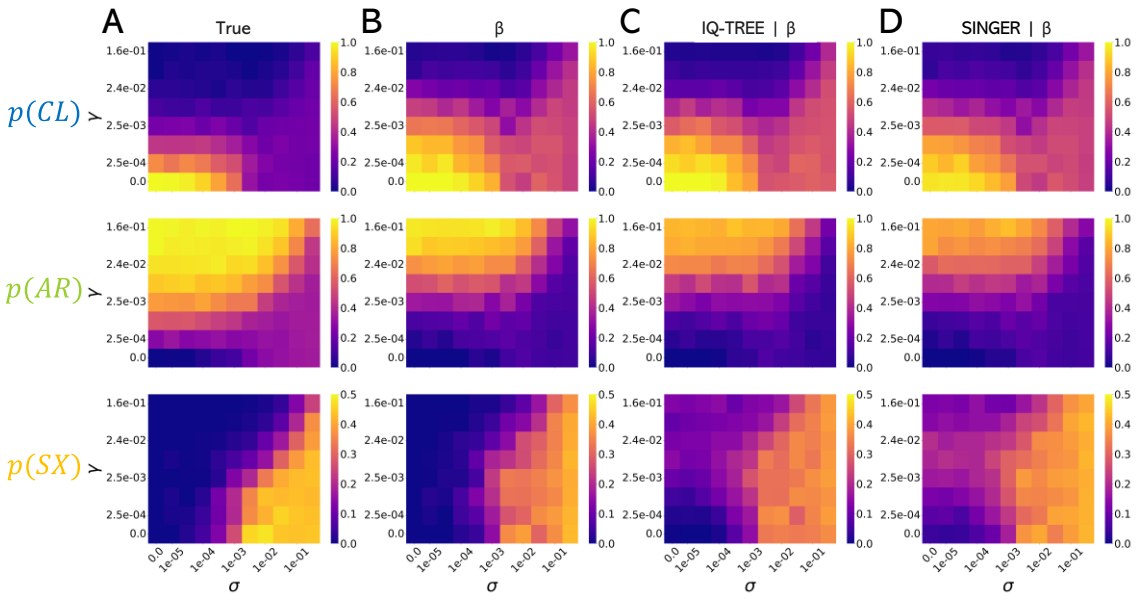


Fig. S7. Tree proportions p falling into the CL, AR and SX categories across the space of the sex rate σ, increasing from the left to the right of each heatmap, and the LOH rate γ, increasing from the bottom to the top; CF model. Note that the colour scale is capped at 1 in the $p(CL)$ and $p(AR)$ heatmaps, and at 0.5 in the $p(SX)$ heatmaps. (A) True values. (B) Heterozygosity bias of β = 0.1. (C) IQ-TREE inference, (D) SINGER inference.

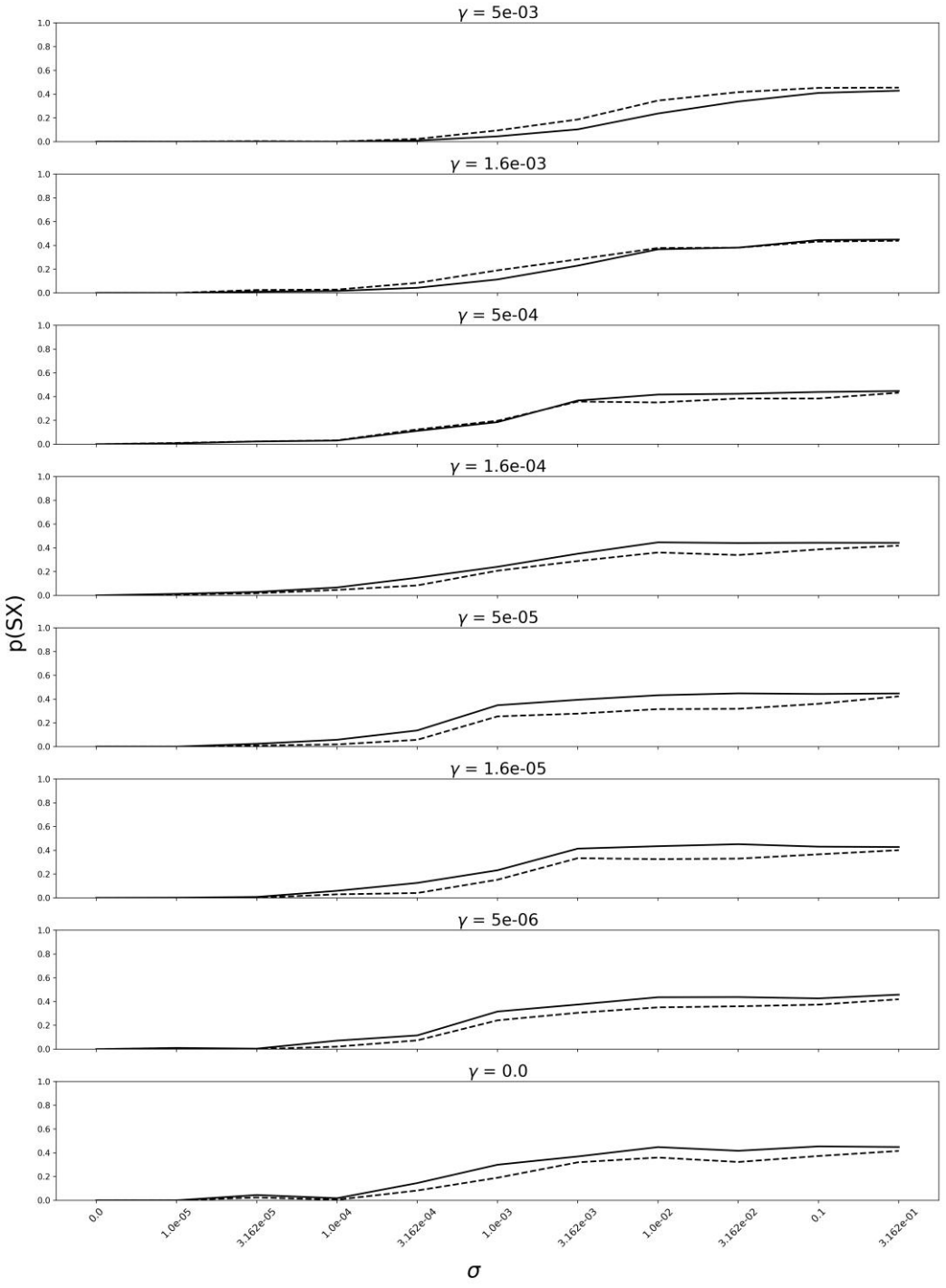


Fig. S8. True $p(SX)$ (solid lines) and $p(SX)$ in heterozygous genome regions (β = 0.1; dashed lines) as a function of σ under different scenarios of γ; MP model.

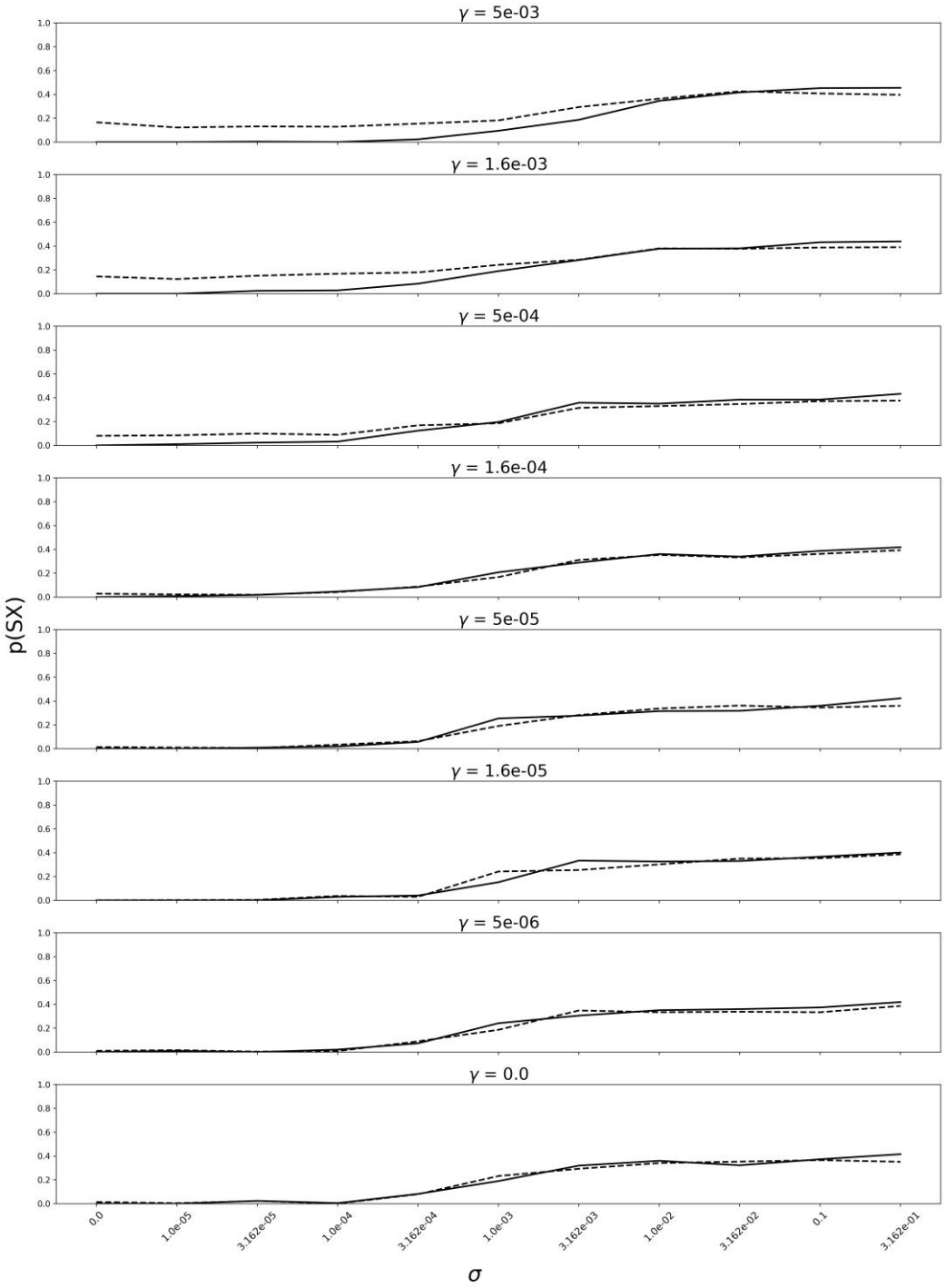


Fig. S9. $p(SX)$ in heterozygous genome regions (β = 0.1; solid lines) and $p(SX)$ after additional genealogical inference with IQ-TREE (dashed lines) as a function of σ under different scenarios of γ; MP model.

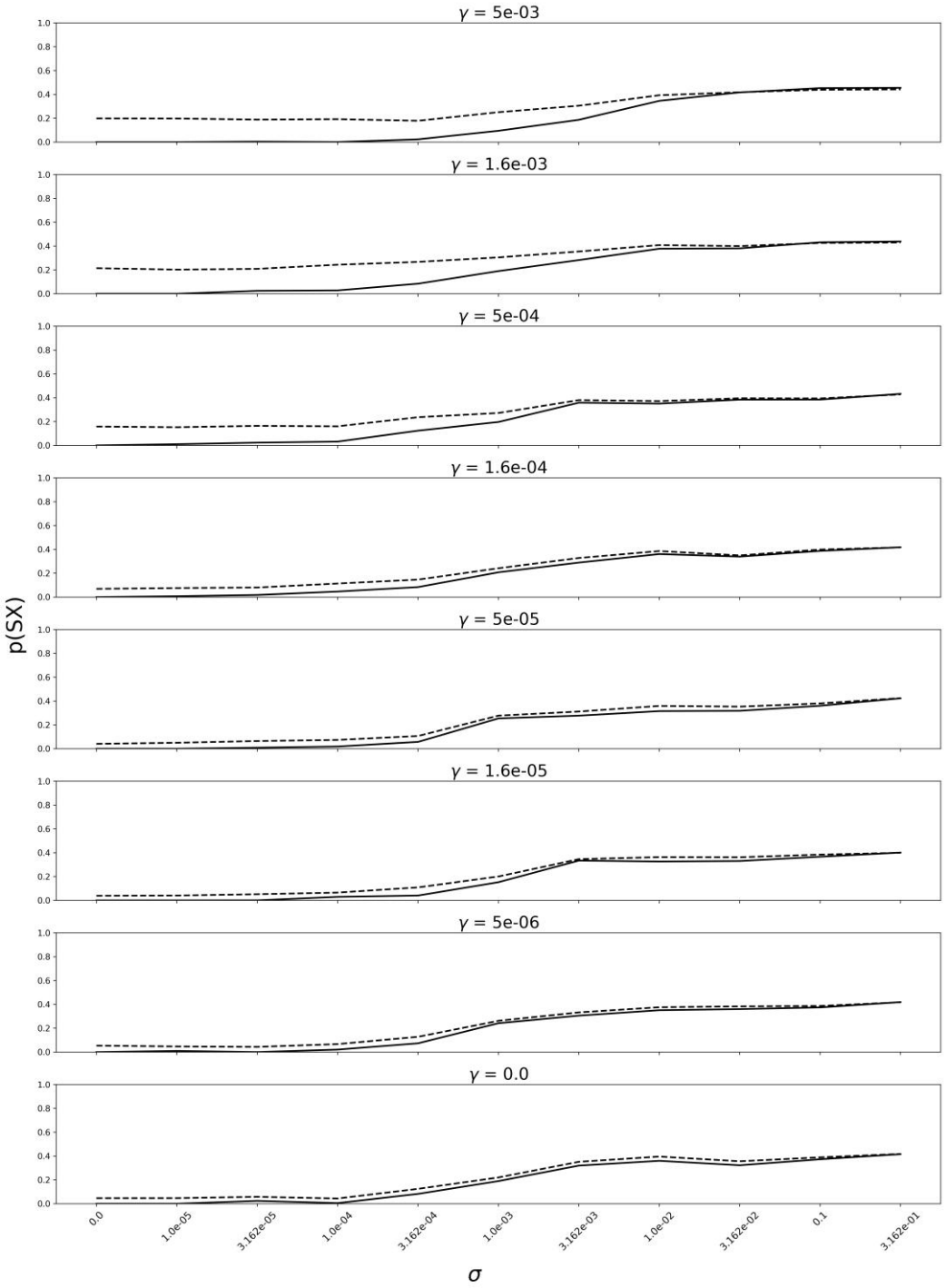


Fig. S10. $p(SX)$ in heterozygous genome regions (β = 0.1; solid lines) and $p(SX)$ after additional genealogical inference with SINGER (dashed lines) as a function of σ under different scenarios of γ; MP model.

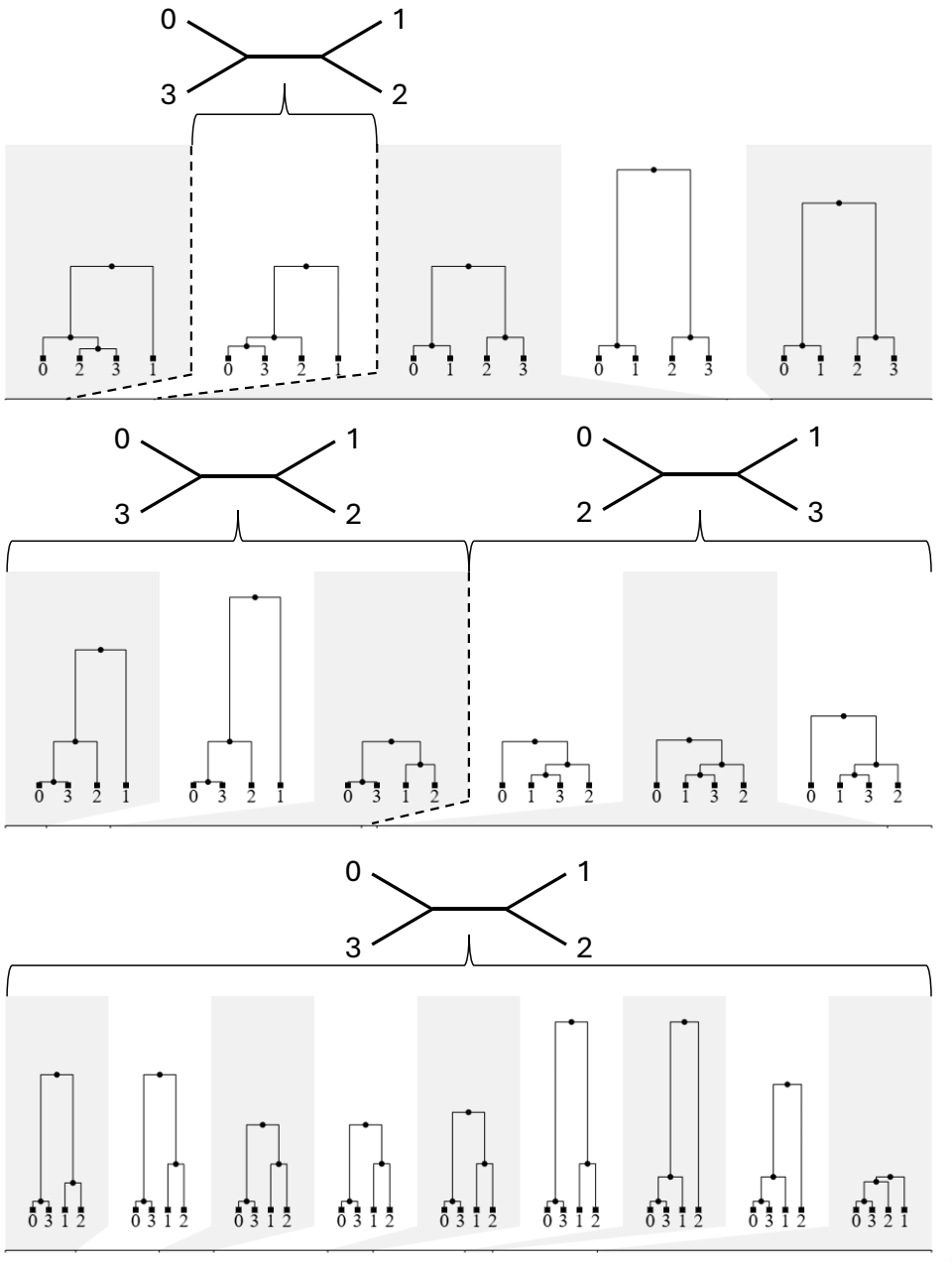
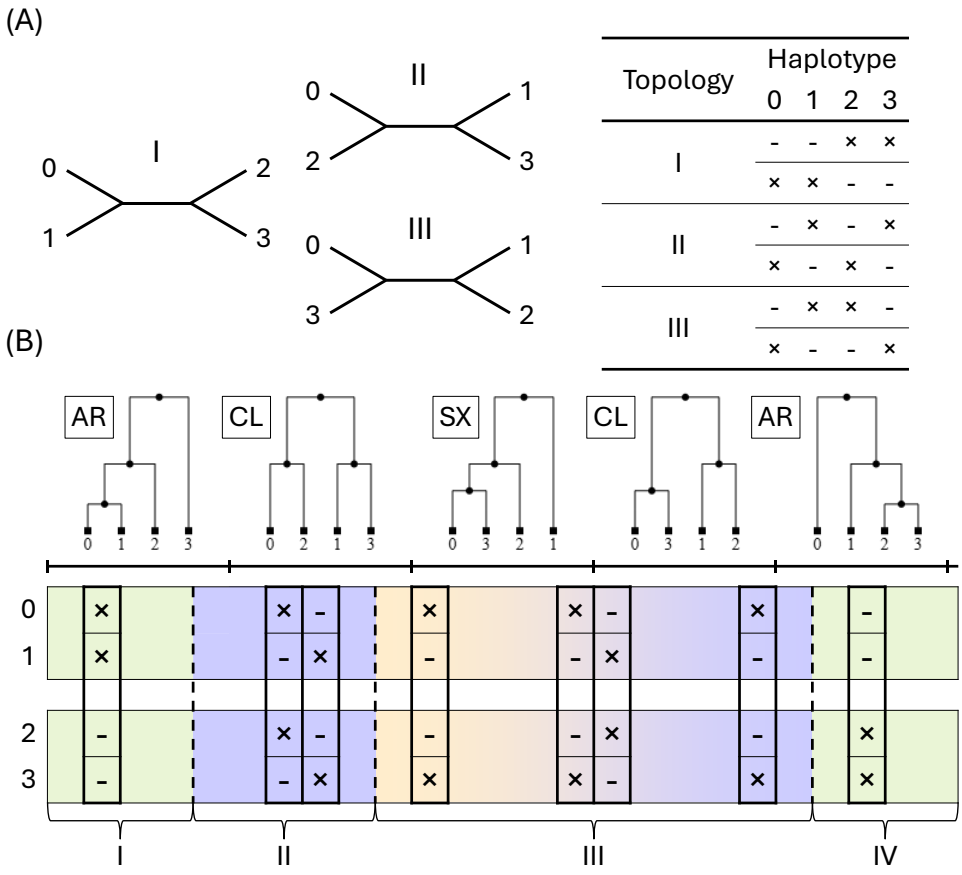


Fig. S11. Runs of CL and / or SX trees used for calculating Δ must share the same unrooted topology: examples simulated using msprime v1.3.2 (Baumdicker et al., 2022). The target regions (curly brackets) might contain a single tree or multiple correlated trees. See Methods for further details on tree run delineation; a SNP-based procedure is illustrated in Fig. S12.



Topology	Haplotype 0	1	2	3
I	-	-	×	×
	×	×	-	-
II	-	×	-	×
	×	-	×	-
III	-	×	×	-
	×	-	-	×

Fig. S12. A SNP-based procedure for calculating Δ. (A) The three topologies of unrooted trees with four tips (left). Assuming no double mutation, pairs of doubleton SNP classes (right; derived alleles denoted with '×') correspond uniquely to one of the unrooted topologies. Topologies II and III are the targets for computing Δ. (B) Local four-tip trees (top) are reflected in runs of doubleton SNPs (bottom) determined by the unrooted topology (e.g., I for all AR trees). Runs are delimited by mid-points between terminal doubletons, a proxy for local tree boundaries. A Δ value is computed using the counts of singleton SNPs (not shown) as a measure of external branch length; here, Δ would be computed separately for runs II and III.

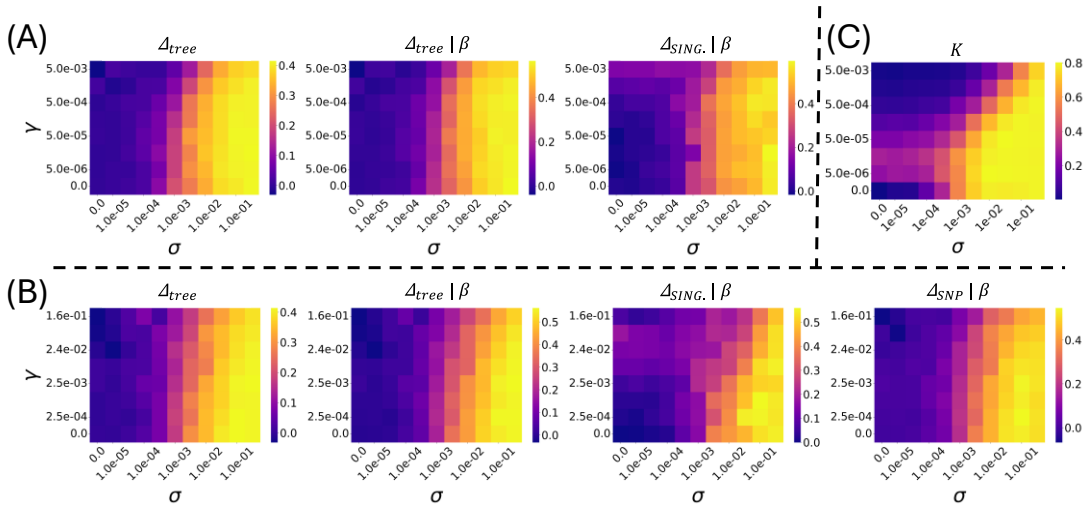


Fig. S13. Tree-based statistics across the space of the sex rate σ, increasing from the left to the right of each heatmap, and the LOH rate γ, increasing from the bottom to the top; supplementary results. (A) Δ calculated based on true trees (Δ_{tree}) or reconstructed trees ($\Delta_{SING.}$); MP model. β = 0.1. (B) Δ calculated based on true (Δ_{tree}), reconstructed trees ($\Delta_{SING.}$) or SNP-based intervals ($\Delta_{SNP.}$); CF model. β = 0.1. (C) K under the CF model.

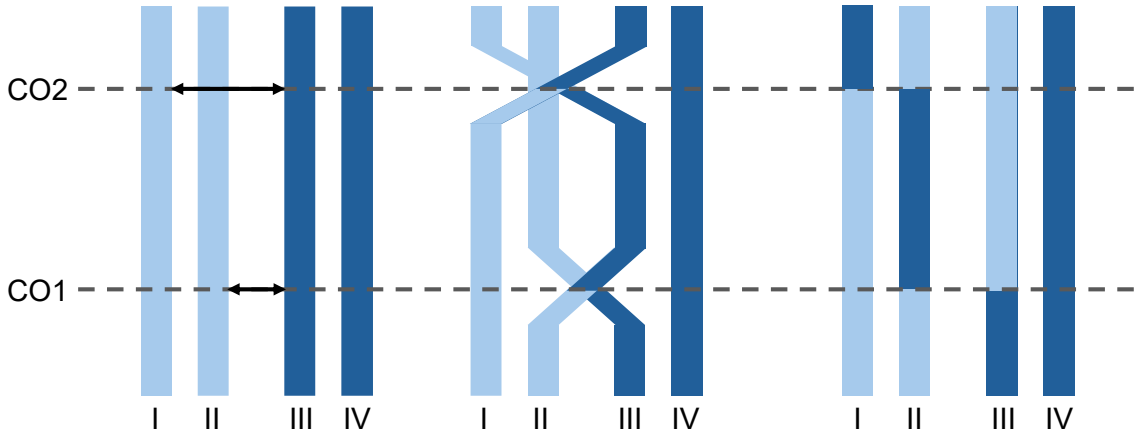


Fig. S14. Resolution of crossovers. Two crossovers occur: between chromatids II and III (CO1) and between chromatids I and III (CO2). Although chromatid II was not involved in CO2, the reconnecting of broken DNA molecules results in a double crossover on this chromatid.

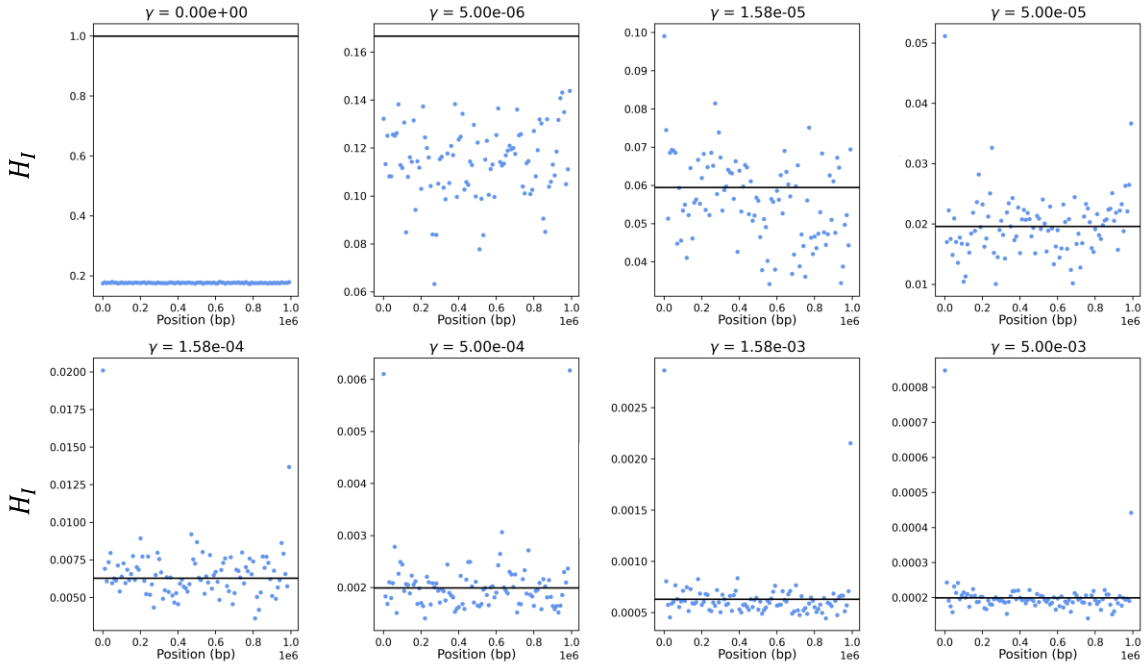


Fig. S15. H_I after 200,000 simulated generations of obligate mitotic parthenogenesis (MP) (blue dots) compared to the analytical predictions (black lines; section A, Eq. 7) under a range of LOH rates γ.

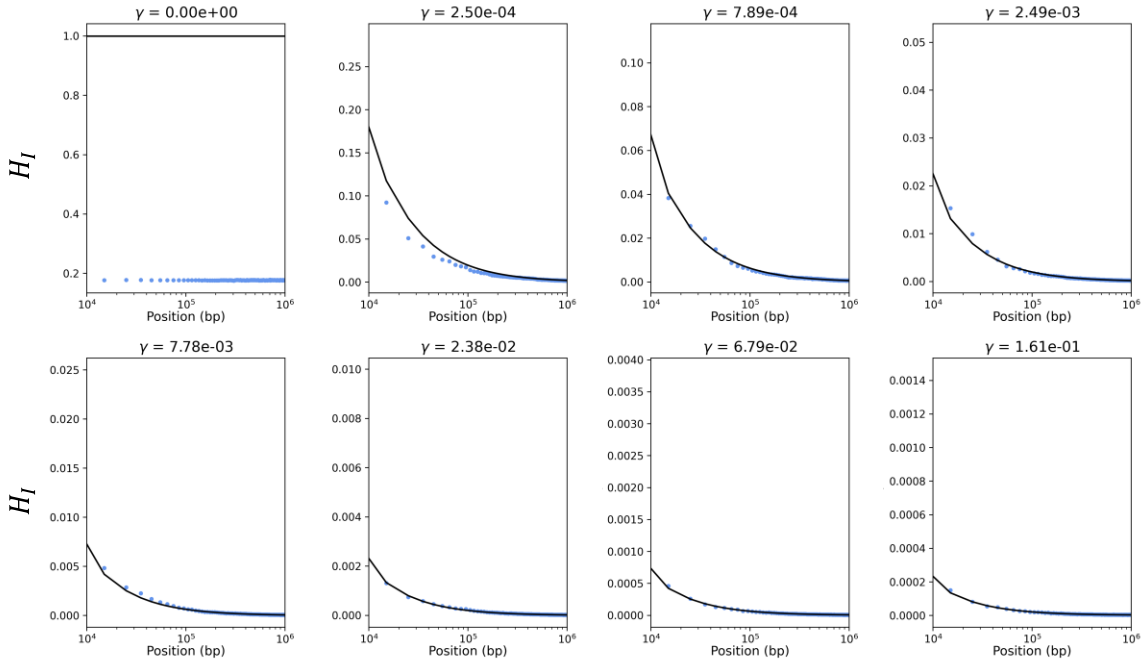


Fig. S16. H_I after 200,000 simulated generations of obligate central fusion (CF) (blue dots) compared to the analytical predictions of Engelstädter (2017) (black lines; section A, Eq. 5) under a range of LOH rates γ. Chromosome positions 0-10^4 (i.e., with very high H_I values) are not shown for clarity.

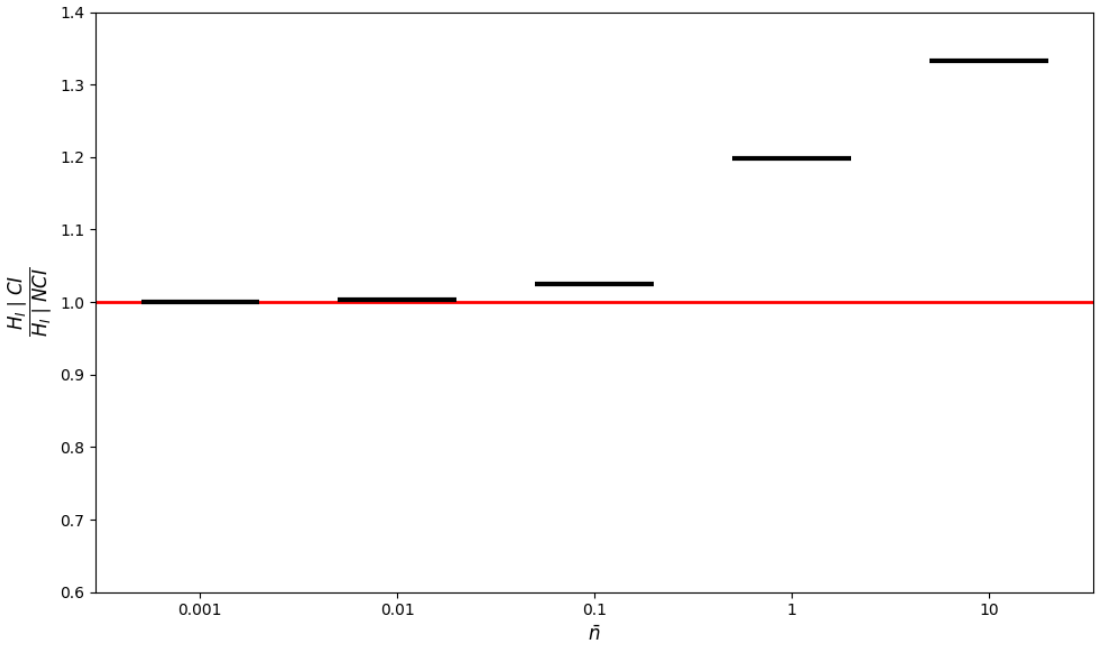


Fig. S17. Comparison of the CI and NCI models of crossover recombination during central fusion. A ratio of the equilibrium individual-level heterozygosity $\widehat{H}_I$ under the CI model to that expected under the NCI model as a function of the expected number of crossovers between the centromere and the focal locus $\bar{n}$.

Supplement to Chapter 1

Supplementary Tables

Table S1. Simulation parameters and their values used in the simulation pipeline.

Parameter	Definition	Values
L	Chromosome length in bp	10^6
N	Diploid population size	10^3
σ	Probability of offspring produced sexually by hermaphroditic parents	[0, 10^{-5}, 3.162×10^{-5}, 10^{-4}, 3.162×10^{-4}, 10^{-3}, 3.162×10^{-3}, 0.01, 0.03162, 0.1, 0.3162]
r_{GC}	Per-site per-generation rate of gene conversion tract initiation during MP	[0, 10^{-9}, 3.162×10^{-9}, 10^{-8}, 3.162×10^{-8}, 10^{-7}, 3.162×10^{-7}, 10^{-6}]
λ	Mean gene conversion tract length in bp; tract length is geometrically distributed where $\frac{1}{\lambda}$ is the probability of tract termination	5×10^3
r_{CO}	Per-site per-generation rate of crossing-over during CF	[0, 10^{-9}, 3.162×10^{-9}, 10^{-8}, 3.162×10^{-8}, 10^{-7}, 3.162×10^{-7}, 10^{-6}]
γ	Per-site per-generation rate of loss of heterozygosity (LOH)	Section A: Eq. 7 (MP) and Eq. 6 (CF)
r	Per-site per-generation rate of crossing-over during sexual reproduction	10^{-6}
μ	Per-site per-generation mutation rate	5×10^{-7}

Table S2. Estimates of the rate of LOH per site (γ) from mutation accumulation (MA) experiments. We report the total estimates of γ which include contributions from short-range (e.g., gene conversion) and long-range (e.g., crossing-over, break-induced replication) forms of asyngamous recombination.

Organism	Reference	Detection method	Mechanism of asexuality	Estimate of γ (LOH site^{-1})
Daphnia pulex	Omilian et al. (2006)	Microsatellite analysis	meiotic	2.1×10^{-4}
	Xu et al. (2011)			3.9×10^{-5}
	Keith et al. (2016)	WGS		1.18×10^{-5}
	Flynn et al. (2017)			4.8×10^{-5}
Adineta vaga	Houtain et al. (2024)	WGS	meiotic	3.24×10^{-4}
Saccharomyces cerevisiae	Sui et al. (2020)	WGS	mitotic	2.6×10^{-5}
	Dutta et al. (2021)			7.1×10^{-5}

Table S3. The average number of non-recombining blocks in two-individual ARGs across the space of sex rates σ and LOH rates γ.

(A) MP.

σ / γ	0	10^{-5}	3.2×10^{-5}	10^{-4}	3.2×10^{-4}	10^{-3}	3.2×10^{-3}	10^{-2}	3.2×10^{-2}	0.1	0.32
5×10^{-3}	1432	1435	1432	1382	1550	1763	2312	3467	4717	5492	5862
1.6×10^{-3}	1222	1227	1255	1193	1225	1420	1548	1894	2119	2465	3348
5×10^{-4}	1316	1258	1385	1272	1190	1080	961	933	1060	1410	2534
1.6×10^{-4}	1926	1863	1860	1828	1447	986	732	576	697	1043	2269
5×10^{-5}	2430	2379	2309	2096	1619	1059	567	523	621	968	2179
1.6×10^{-5}	2563	2493	2562	2249	1757	975	601	448	572	943	2130
5×10^{-6}	2663	2588	2526	2289	1659	1007	582	471	548	908	2121
0.0	2621	2644	2597	2301	1798	1030	546	450	523	916	2121

(B) CF.

σ / γ	0	10^{-5}	3.2×10^{-5}	10^{-4}	3.2×10^{-4}	10^{-3}	3.2×10^{-3}	10^{-2}	3.2×10^{-2}	0.1	0.32
0.16	47	50	59	60	70	92	122	187	411	978	2411
6.8×10^{-2}	45	53	39	87	90	87	108	174	325	799	2129
2.4×10^{-2}	71	45	67	137	50	94	113	172	347	806	2087
7.7×10^{-3}	131	94	98	105	87	132	119	204	424	857	2125
2.5×10^{-3}	220	215	192	170	199	245	226	295	479	913	2121
7.9×10^{-4}	618	532	635	514	450	308	373	366	495	887	2119
2.5×10^{-4}	1419	1253	1345	1103	1003	661	487	391	532	905	2113
0.0	2672	2631	2528	2291	1831	1025	526	431	530	885	2131

Table S4. The average number of SNPs in two-individual ARGs across the space of sex rates σ and LOH rates γ.

(A) MP.

σ / γ	0	10^{-5}	3.2×10^{-5}	10^{-4}	3.2×10^{-4}	10^{-3}	3.2×10^{-3}	10^{-2}	3.2×10^{-2}	0.1	0.32
5×10^{-3}	3250	3224	3254	3177	3300	3452	3700	4030	4354	4586	4676
1.6×10^{-3}	3641	3717	3761	3633	3644	3963	4124	4482	4620	4660	4706
5×10^{-4}	4755	4613	4887	4703	4716	4682	4682	4649	4673	4695	4709
1.6×10^{-4}	6433	6439	6298	6335	5936	5312	4870	4713	4698	4661	4706
5×10^{-5}	7270	7388	7453	7051	6472	5792	5271	4891	4763	4706	4710
1.6×10^{-5}	7667	7602	7784	7241	6730	5758	5166	4851	4768	4761	4675
5×10^{-6}	8125	7826	7733	7476	6688	5933	5046	4871	4809	4719	4685
0.0	8049	7986	7830	7428	6930	6125	5069	4928	4722	4723	4690

(B) CF.

σ / γ	0	10^{-5}	3.2×10^{-5}	10^{-4}	3.2×10^{-4}	10^{-3}	3.2×10^{-3}	10^{-2}	3.2×10^{-2}	0.1	0.32
0.16	2934	2983	3022	2958	3071	3068	3092	3103	3285	3601	4099
6.8×10^{-2}	3099	3031	3077	3053	3167	3090	3130	3260	3457	3872	4396
2.4×10^{-2}	3055	3212	3122	3183	3069	3223	3399	3496	3840	4239	4559
7.7×10^{-3}	3340	3283	3456	3332	3343	3452	3587	3836	4267	4510	4668
2.5×10^{-3}	3695	3820	3858	3794	3782	3863	4051	4425	4515	4677	4691
7.9×10^{-4}	4809	4595	4765	4599	4533	4457	4752	4699	4657	4693	4702
2.5×10^{-4}	6100	5811	5758	5863	5708	5180	4960	4731	4719	4731	4676
0.0	8038	7908	7803	7474	6814	5654	5133	4827	4791	4686	4695

Table S5. The proportion of MCMC samples successfully output by SINGER across the space of sex rates σ and LOH rates γ.

(A) MP.

σ \ γ	0	10^{-5}	3.2×10^{-5}	10^{-4}	3.2×10^{-4}	10^{-3}	3.2×10^{-3}	10^{-2}	3.2×10^{-2}	0.1	0.32
5×10^{-3}	0.81	0.80	0.83	0.83	0.84	0.93	0.98	1.00	1.00	1.00	1.00
1.6×10^{-3}	1.00	1.00	1.00	0.99	1.00	1.00	0.99	1.00	1.00	1.00	1.00
5×10^{-4}	1.00	1.00	1.00	1.00	1.00	1.00	1.00	1.00	1.00	1.00	1.00
1.6×10^{-4}	1.00	1.00	1.00	1.00	1.00	1.00	1.00	1.00	1.00	1.00	1.00
5×10^{-5}	1.00	1.00	1.00	1.00	1.00	1.00	1.00	1.00	1.00	1.00	1.00
1.6×10^{-5}	1.00	1.00	1.00	1.00	1.00	1.00	1.00	1.00	1.00	1.00	1.00
5×10^{-6}	1.00	1.00	1.00	1.00	1.00	1.00	0.99	1.00	1.00	1.00	1.00
0.0	1.00	1.00	1.00	1.00	1.00	1.00	1.00	1.00	1.00	1.00	1.00

(B) CF.

σ \ γ	0	10^{-5}	3.2×10^{-5}	10^{-4}	3.2×10^{-4}	10^{-3}	3.2×10^{-3}	10^{-2}	3.2×10^{-2}	0.1	0.32
0.16	0.74	0.74	0.77	0.73	0.79	0.83	0.85	0.86	0.96	0.99	1.00
6.8×10^{-2}	0.85	0.78	0.81	0.76	0.82	0.82	0.86	0.93	0.98	0.99	1.00
2.4×10^{-2}	0.83	0.85	0.81	0.86	0.83	0.86	0.93	0.96	1.00	1.00	1.00
7.7×10^{-3}	0.91	0.91	0.94	0.94	0.94	0.93	0.96	0.98	0.99	1.00	1.00
2.5×10^{-3}	0.98	0.97	0.99	0.98	0.98	0.97	0.98	1.00	1.00	1.00	1.00
7.9×10^{-4}	1.00	1.00	1.00	0.99	1.00	0.99	1.00	1.00	1.00	1.00	1.00
2.5×10^{-4}	1.00	1.00	1.00	1.00	1.00	1.00	1.00	1.00	1.00	1.00	1.00
0.0	1.00	1.00	1.00	1.00	1.00	1.00	1.00	1.00	1.00	1.00	1.00

References

Baumdicker, F., Bisschop, G., Goldstein, D., Gower, G., Ragsdale, A. P., Tsambos, G., Zhu, S., Eldon, B., Ellerman, E. C., & Galloway, J. G. (2022). Efficient ancestry and mutation simulation with msprime 1.0. *Genetics*, *220*(3), iyab229.

Blanc, C., Saclier, N., Le Faou, E., Marie-Orleach, L., Wenger, E., Diblasi, C., Glemin, S., Galtier, N., & Delattre, M. (2023). Co-segregation of recombinant chromatids maintains genome-wide heterozygosity in an asexual nematode. *bioRxiv*, 2023.2003. 2017.533182.

Chen, J.-M., Cooper, D. N., Chuzhanova, N., Férec, C., & Patrinos, G. P. (2007). Gene conversion: mechanisms, evolution and human disease. *Nature Reviews Genetics*, *8*(10), 762–775.

Deng, Y., Nielsen, R., & Song, Y. S. (2024). Robust and accurate Bayesian inference of genome-wide genealogies for large samples. *bioRxiv*, 2024.2003. 2016.585351.

Dutta, A., Dutreux, F., & Schacherer, J. (2021). Loss of heterozygosity results in rapid but variable genome homogenization across yeast genetic backgrounds. *eLife*, *10*, e70339.

Engelstädter, J. (2017). Asexual but Not Clonal: Evolutionary Processes in Automictic Populations. *Genetics*, *206*(2), 993–1009. https://doi.org/10.1534/genetics.116.196873

Flynn, J. M., Chain, F. J., Schoen, D. J., & Cristescu, M. E. (2017). Spontaneous mutation accumulation in Daphnia pulex in selection-free vs. competitive environments. *Molecular Biology and Evolution*, *34*(1), 160–173.

Haller, B. C., & Messer, P. W. (2023). SLiM 4: Multispecies Eco-Evolutionary Modeling. *The American Naturalist*, *201*(5), E127–E139. https://doi.org/10.1086/723601

Haller, B. C., & Messer, P. W. (2024). SLiM: An Evolutionary Simulation Framework. In.

Houtain, A., Derzelle, A., Lliros, M., Hespeels, B., Nicolas, E., Simion, P., Virgo, J., Heuskin, A.-C., Lenormand, T., Hallet, B., & Van Doninck, K. (2024). *Transgenerational chromosome repair in the asexual bdelloid rotifer Adineta vaga*. Cold Spring Harbor Laboratory. https://dx.doi.org/10.1101/2024.01.25.577190

Jinks-Robertson, S., & Petes, T. D. (2021). Mitotic recombination in yeast: what we know and what we don't know. *Current opinion in genetics & development*, *71*, 78–85.

Keith, N., Tucker, A. E., Jackson, C. E., Sung, W., Lledó, J. I. L., Schrider, D. R., Schaack, S., Dudycha, J. L., Ackerman, M., & Younge, A. J. (2016). High mutational rates of large-scale duplication and deletion in Daphnia pulex. *Genome research*, *26*(1), 60–69.

Kopčak, D., & Hartfield, M. (2024). How do self-fertilising and facultative sexual populations differ in mutation accumulation? *bioRxiv*, 2024.2008. 2030.610445.

Martin, S. H., & Van Belleghem, S. M. (2017). Exploring evolutionary relationships across the genome using topology weighting. *Genetics*, *206*(1), 429–438.

Minh, B. Q., Schmidt, H. A., Chernomor, O., Schrempf, D., Woodhams, M. D., Von Haeseler, A., & Lanfear, R. (2020). IQ-TREE 2: new models and efficient methods for phylogenetic inference in the genomic era. *Molecular Biology and Evolution*, *37*(5), 1530–1534.

Mölder, F., Jablonski, K. P., Letcher, B., Hall, M. B., Tomkins-Tinch, C. H., Sochat, V., Forster, J., Lee, S., Twardziok, S. O., & Kanitz, A. (2021). Sustainable data analysis with Snakemake. *F1000Research*, *10*.

Nielsen, R., Vaughn, A. H., & Deng, Y. (2025). Inference and applications of ancestral recombination graphs. *Nature Reviews Genetics*, *26*(1), 47–58.

Omilian, A. R., Cristescu, M. E., Dudycha, J. L., & Lynch, M. (2006). Ameiotic recombination in asexual lineages of Daphnia. *Proceedings of the National Academy of Sciences*, *103*(49), 18638–18643.

Ralph, P., Thornton, K., & Kelleher, J. (2020). Efficiently summarizing relationships in large samples: a general duality between statistics of genealogies and genomes. *Genetics*, *215*(3), 779–797.

Sarens, M., Copenhaver, G. P., & De Storme, N. (2021). The role of chromatid interference in determining meiotic crossover patterns. *Frontiers in Plant Science*, *12*, 656691.

Schliep, K. (2011). phangorn: phylogenetic analysis in R. Bioinformatics 27, 592e593. In.

Sui, Y., Qi, L., Wu, J.-K., Wen, X.-P., Tang, X.-X., Ma, Z.-J., Wu, X.-C., Zhang, K., Kokoska, R. J., & Zheng, D.-Q. (2020). Genome-wide mapping of spontaneous genetic alterations in diploid yeast cells. *Proceedings of the National Academy of Sciences*, *117*(45), 28191–28200.

Wakeley, J. (2008). *Coalescent Theory: An Introduction*. Roberts & Company Publishers.

Xu, S., Omilian, A. R., & Cristescu, M. E. (2011). High rate of large-scale hemizygous deletions in asexually propagating Daphnia: implications for the evolution of sex. *Molecular Biology and Evolution*, *28*(1), 335–342.

Chapter 2: A parsimony-based approach to genealogical analysis of reproductive mode



——————————— O ———————————

Tymoteusz Pieszko

——————————— O ———————————

Contributions

➔ A classical chapter of which I am the sole author. In contrast to Chapter 1, this chapter describes work that has not yet been prepared for publication and follows an ‘Introduction → Methods → Results → Discussion’ order of sections.

Introduction

Inferring the patterns of recombination is a fundamental problem in evolutionary genetics. On a population scale, genome-wide variation in recombination rate is of interest because of its interrelationship with the effectiveness of natural selection (e.g., Samuk et al., 2020; Wang et al., 2016), with low-recombination regions subject to stronger Hill-Robertson interference (General Introduction). In phylogenomic inference, on the other hand, recombination in the ancestral population is often viewed as a nuisance source of conflict between local histories and the overarching species tree of interest (Rannala, 2025; Steenwyk et al., 2023). One of the goals of this thesis is to demonstrate that reconstructing past reproduction cannot be separated from reconstructing recombination (whether sexual or asyngamous) and is best conceptualised as an ancestral recombination graph (ARG) inference problem.

In Chapter 1, I developed a suite of metrics to quantify the genealogical signal of reproductive mode. These metrics varied in how they handled signal heterogeneity: from a fixed-window approach that 'bets' on neighbouring sites sharing the same history (coupled with maximum-likelihood tree inference), through delimiting regions expected to share a signal (for calculating the Δ statistic), to breakpoint inference with a parametric model that approximates the coalescent with recombination (using SINGER). In a simulation-based framework, artefacts associated with unaccounted-for genealogical heterogeneity could be implicitly controlled for by benchmarking against simulated data, an approach I take in Chapter 3. In the present chapter, however, I revisit the specific problem of localising recombination breakpoints that delimit local asexuality-compatible and sex-specific histories, situating it within the broader literature on recombination-aware genealogical analyses.

For certain evolutionary questions, inference of local histories in windows of short, fixed length (physical or in terms of SNPs), many of which can be reasonably treated as non-recombining, may indeed provide an approximation of the genealogy at the required resolution. For example, the method *Twisst* (Martin & Van Belleghem, 2017) has been designed to explore genome-wide relationships between taxa by 'weighting' local tree

topologies. In a typical *Twisst* analysis, a fixed-window approach is pragmatic, given a focus on population-level processes of divergence and gene flow (e.g., Martin et al., 2019; de Jong et al., 2023).

By contrast, algorithms for recombination detection originated from the interest in fine-scale analyses, for example, of viral and bacterial sequences (e.g., Maynard Smith, 1992; Zhou et al., 1997). These algorithms can be divided into three major classes (Cen & Rasmussen, 2024). First, *parsimony approaches* (e.g., Maynard Smith & Smith, 1998; Bruen et al., 2006) stem from the classic work of Hudson and Kaplan (1985). Hudson and Kaplan's four-gamete test posits that, for a given pair of biallelic loci, the four possible haplotypes (e.g., 00, 01, 10 and 11) can coexist only through reciprocal recombination under the infinite sites model (Kimura, 1969). Statistics based on this idea, such as Φ (Bruen et al., 2006), can be computed window-wise to locate putative regions of increased recombination but not individual breakpoints per se. Incidentally, the four-gamete test was recommended as a test for cryptic sex (Martin et al., 2011) and used as such (e.g., Lasek-Nesselquist et al., 2009; Weedall et al., 2012; Phan Thi et al., 2025). The second, larger class of *similarity approaches* (e.g., Posada & Crandall, 2001; Martin & Rybicki, 2000; Maynard Smith, 1992; Sawyer, 1989; Boni et al., 2007) exploits the distribution of SNPs within and across an alignment. A basic example is the MaxChi approach (Maynard Smith, 1992), which iteratively cuts a pair of sequences at arbitrary positions and constructs 2 × 2 contingency tables of SNPs on both sides of each cut. The position that maximises the χ^2 statistic is considered a candidate recombination breakpoint. 3SEQ (Boni et al., 2007), in turn, performs more explicit tests for recombination by considering all the possible sequence triplets. For each variable site, 3SEQ matches mutations in a focal sequence against those in candidate parent sequences, and uses a hypergeometric random-walk model to test for their non-random distribution (indicative of recombination). The final class of *phylogenetic approaches* (e.g., Salminen et al., 1995; Maynard Smith & Smith, 1998; Kosakovsky Pond et al., 2006) formulates the breakpoint inference problem as tests for conflicting topologies of

local trees. GARD (Kosakovsky Pond et al., 2006), for example, uses the Akaike information criterion (AIC) to test whether a given alignment is better explained by a single tree or by two trees flanking a candidate breakpoint. Methods from all three classes are expected to perform best given a large number of true informative sites within linkage blocks – as occurs when the mutation rate is high relative to the recombination rate – and be particularly sensitive to large differences between local histories (e.g., in topology) (Cen & Rasmussen, 2024).

These and related ideas have been incorporated in approaches to heuristic ARG reconstruction. The first step of the Espalier workflow (Rasmussen & Guo, 2023), for instance, is the localization of recombination breakpoints through an external algorithm, with the authors recommending 3SEQ. Thus-identified intervals are used for phylogenetic inference, and local trees are subsequently processed by a 'reconciliation' algorithm to minimise phylogenetic noise and introduce additional breakpoints, if necessary (Rasmussen & Guo, 2023). Methods such as SARGE (Schaefer et al., 2021) and Relate (Speidel et al., 2019), though very different conceptually, both identify breakpoints as changes in tree topology. SARGE is entirely parsimony-guided, with clades defined by shared derived mutations and breakpoints inferred whenever conflicting clades are implied. To limit the propagation of error (e.g., from recurrent mutation), SARGE assigns a fixed genomic span to each new node, which is extended when identical clades overlap. Relate, in contrast, infers per-SNP trees from pairwise distance matrices computed under the Li and Stephens (LS) model (Li & Stephens, 2003). In a frequentist setting, the LS model finds a 'copying path' across a sample of haplotypes by assuming that the kth haplotype can be represented as a mosaic of the k – 1 previously observed haplotypes. Accordingly, the Relate algorithm iterates over SNPs starting at the 5' end of the sequence and only infers a new tree, and thus an additional recombination breakpoint, if a conflicting SNP is encountered. Finally, tsinfer (Kelleher et al., 2019) also employs the LS model but is conceptually a similarity method, with breakpoints defined as switches in the copying path between the extant and

inferred ancestral haplotypes. By design, methods such as SARGE, Relate and tsinfer are expected to miss a substantial number of breakpoints, since they heuristically identify only those recombination events that are explicitly supported by mutational evidence.

A distinct class of algorithms adopts a model-based approach to recombination inference, grounded in the coalescent with recombination (CoR; Griffiths & Marjoram, 1997; Hudson, 1983). CoR-derived methods, such as the likelihood-based LDhat (McVean et al., 2002) and Bayesian LDhelmet (Chan et al., 2012), estimate the population-scaled recombination ($\rho = 4N_e r$) at fine genomic resolution. Among the CoR-based ARG reconstruction methods, SINGER (Deng et al., 2025) represents the current state of the art, having superseded the earlier ARGweaver (Rasmussen et al., 2014). SINGER performs full probabilistic Bayesian inference of the ARG under the sequentially Markov coalescent (SMC) approximation of the CoR (McVean & Cardin, 2005). The method's core ARG-building algorithm proceeds by iterative 'threading' of haplotypes into a partially built ARG: for each local tree, new branches are sampled from a Hidden Markov Model based on the LS model. To explore the posterior space of possible ARGs, SINGER performs prune-and-regraft operations following a Markov Chain Monte Carlo (MCMC) algorithm. On data simulated under the CoR (Baumdicker et al., 2022), SINGER outperforms other methods across all aspects of ARG inference, including the accuracy of local tree topologies and breakpoint estimation. In Chapter 1, I applied SINGER to sequence data simulated across the space of asexuality-sex scenarios. To run the algorithm, I provided scaling parameters – N_e, μ and r – as if the simulated scenarios were all obligate sexual. Indeed, SINGER uses the population-scaled recombination rate ρ to determine the probability that subsequent trees differ through ancestral recombination. While I did not investigate the accuracy of breakpoint inference, I found that the recovered tree composition was increasingly accurate with increasing rate of sex, without an obvious advantage under obligate asexuality compared to a fixed-window approach (Chapter 1, Fig. 4 and Fig. S10). It hence appears questionable whether SINGER can be of comparable

value in non-standard reproductive systems as it promises in human-focused applications – as expected from first principles due to its formulation around a sexual (panmictic) model.

I propose a ‘parsimony block delimitation’ (PBD) approach for reconstructing local tree topologies and recombination breakpoints in four-haplotype alignments. Rather than a general method for genealogical reconstruction, the new approach specifically answers the challenge of detecting rare sex signatures in a predominantly asexual background. I preliminarily explore the PBD approach using the asexuality-sex simulations from Chapter 1, followed by an application to datasets for two bdelloid rotifer species in Chapter 3. I argue that grounding a genealogical analysis in transparent and well-defined assumptions may ultimately be the most fruitful approach to investigating controversial signatures of cryptic sex.

Methods

The PBD approach establishes a correspondence between the 10 parsimony-informative SNP classes and four-tip trees under the infinite sites model. In Chapter 2, I used parsimony to delimit the boundaries of unrooted four-tip trees by assuming that doubleton SNPs (i.e., sites with two alleles represented in two copies each) uniquely reflect the three possible groupings of four tips (Chapter 1, Fig. S12). Here, I further note that tripleton SNPs (i.e. sites with three derived and one ancestral allele) can only arise on unbalanced four-tip trees. Crucially, local combinations of doubleton and tripleton SNPs can be classified as conflicting or compatible, according to simple rules. Each tripleton is, in principle, compatible with three different doubletons: for instance, 1110 is compatible with 1100, 1010 and 0110. At the same time, however, defining a tripleton-doubleton combination (e.g., 1110-1100) narrows down compatibility to only those SNP classes. The same principle applies to doubleton-doubleton combinations (e.g., 1100-0011). If the genome can be partitioned into blocks of compatible SNPs only, blocks with tripleton-doubleton combinations are specific to unbalanced trees (Table 1A) and blocks with doubleton-doubleton combinations are specific to balanced trees (Table 1B).

Table 1. Compatible SNP combinations in a four-haplotype alignment and the corresponding trees. Ancestral and derived alleles are denoted as 0s and 1s, respectively. Roman numerals refer back to the tree classification presented in Chapter 1, Fig. 4A.

(A) Doubleton-tripleton combinations are specific to unbalanced trees. A lone tripleton (i.e., flanked by incompatible sites) is equally compatible with three different unbalanced trees.

Doubleton	Tripleton	Tree
1100	1110	AR (V)
	1101	AR (VI)
0011	1011	AR (VII)
	0111	AR (VIII)
1010	1110	SX (XI)
	1011	SX (XV)
0101	1101	SX (XIV)
	0111	SX (XVIII)
1001	1101	SX (XII)
	1011	SX (XVI)
0110	1110	SX (XIII)
	0111	SX (XVII)

(B) Doubleton-doubleton combinations are specific to balanced trees. The order of internal coalescences (distinguishing, e.g., trees IX and X) can be determined from the relative counts of doubleton 1 and doubleton 2.

Doubleton 1	Doubleton 2	Tree
1100	0011	AR (IX or X)
1010	0101	CL (I or II)
1001	0110	CL (III or IV)

Implementation of the approach consists of two main steps. The first step runs an algorithm that identifies sequence blocks consistent with unbalanced (SX or AR) trees (Algorithm S1). The blocks are built greedily around tripleton SNPs, incorporating sites until an incompatibility, or an existing block, is encountered. Block extension is strictly parsimony-driven: for example, if a tripleton site is flanked by two distinct compatible doubletons (e.g., 1100–1110–1010), the extension proceeds only towards the nearer doubleton (Algorithm S1). The second step partitions regions outside the SX / AR blocks, which contain doubletons only, as shown in Chapter 1, Fig. S12. Some of the doubleton-only blocks will contain a single doubleton class – given the assumption of predominant asexuality, these can be parsimoniously explained through AR / CL trees (Table 1B). Taken together, the 'run_pbd()' function takes a four-haplotype genotype array G, a corresponding position array P and sequence length L as inputs, and outputs a list of non-overlapping intervals that define

distinct trees. The PBD approach therefore capitalises on the small SNP-tree space at four-haplotype level to jointly delimit and infer local histories.

I applied the PBD approach to data simulated across the asexuality-sex parameter space (MP model, parameters as in Chapter 1, Table S1; L = 1 Mb, N = 1,000, $\mu = 5 \times 10^{-7}$, 100 replicates, 16 individuals sampled per simulation). For comparison with a standard genealogical analysis, I inferred local trees in fixed windows of k = 100 SNPs (per two diploid genomes), with window boundaries defined as the midpoints between terminal SNPs (the 'fixed-window' or 'FW' approach). For each window, a distance matrix was computed using the 'cityblock' method implemented in scikit-allel v1.3.13 (Miles et al., 2024), and the matrices were used to reconstruct trees using the Farthest Point Algorithm implemented in scipy v1.14.1 (Virtanen et al., 2020) ('scipy.hierarchy.linkage' with 'method = "complete"'). I compared estimates of tree composition (Chapter 1) obtained through the PBD and FW methods. To test the accuracy of breakpoint inference, I focused on the inferred SX blocks, the candidate localities of SX trees, which I compared against the ground truth using the Jaccard similarity index (J) computed with scipy 1.16.2 (Virtanen et al., 2020). Following the convention implemented in BEDTools (Quinlan & Hall, 2010), J = 0.0 translates to no overlap between true and inferred SX blocks, whereas J = 1.0 translates to full overlap between true and inferred SX blocks (no false negatives, no false positives).

Results

Tree composition

Tree composition obtained through the PBD approach across the space of sex rates σ and LOH rates γ tracked the true values remarkably closely (Fig. 1A; cf. Chapter 1, Fig. 4B). I compared the PBD and FW estimates of $p(SX)$ computed for whole simulated chromosomes (Fig. 1B). Both methods led to similar maximum estimates of $p(SX)$ under obligate asexuality (PBD: 0.103, FW: 0.088). While the FW approach overestimated $p(SX)$ under rare sex and underestimated $p(SX)$ at the higher end of σ, the PBD approach consistently overestimated

$p(SX)$ (though with only a slight deviation of ≈ 0.02 under frequent sex). This behaviour is consistent with the greediness of the PBD algorithm for block-building around tripleton sites. Finally, I compared the absolute difference in deviations from true $p(SX)$ between the two methods (Fig. 1C), finding that, given $\sigma < 10^{-3}$, PBD performed better when $\gamma < 5 \times 10^{-4}$ and FW performed better when $\gamma \geq 5 \times 10^{-4}$.

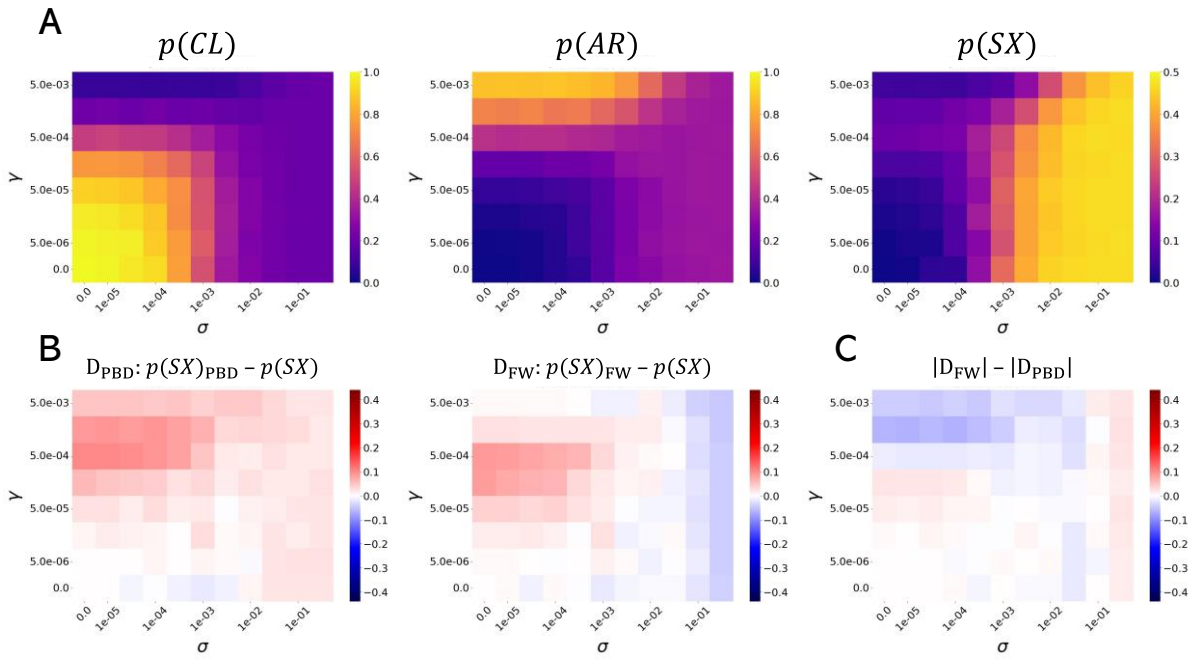


Fig. 1. Tree composition estimated through the PBD approach; comparison with FW inference through clustering (k = 100 SNPs). (A) PBD-based $p(CL)$, $p(AR)$ and $p(SX)$ estimates across the simulated space of sex rates σ and LOH rates γ (note the color scale is capped at 0.5 in the $p(SX)$ heatmap). (B) Deviations D from true $p(SX)$ associated with the PBD and FW approaches. (C) Absolute difference in deviations from true $p(SX)$ between the two approaches: red indicates PBD is closer to truth, blue indicates FW is closer to truth.

The performance of a greedy, parsimony-based algorithm may be influenced by technical artefacts that disrupt block extension, such as sequence fragmentation inherent in read-based phasing procedures. Fig. S1 illustrates this effect using coalescent simulations of obligate sex, with a bias towards balanced trees for short simulated sequence (< 5 kb when $r = \mu$) and vice versa, as sequence length increases. I therefore recomputed PBD and FW-based tree composition estimates across the asexuality-sex parameter space, but using sequence fragmented into 5-kb segments (Fig. S2). I found that the PBD-based proportion of

(always unbalanced) SX trees was now underestimated under frequent sex, but not under rare sex or, for obvious reasons, obligate asexuality (Fig. S2B). Interestingly, this modification of input data rendered PBD advantageous over the FW approach across the obligate asexual and rare sex scenarios (Fig. S2C), as could be explained by < 100 SNPs being on average available for tree building.

Recombination breakpoints

Fig. 2 visualizes the general challenge of identifying local histories with FW-type approaches (see also Cen & Rasmussen, 2024) and how the PBD approach addresses it. If inference is performed in fixed-length windows, the strength of phylogenetic signal is positively correlated with window size. However, with larger windows more likely to span multiple non-recombining histories, the optimal window size is likely intermediate but unknown a priori. In contrast, the PBD approach avoids this trade-off by jointly identifying breakpoints and local histories, eliminating the need for user-defined parameters.

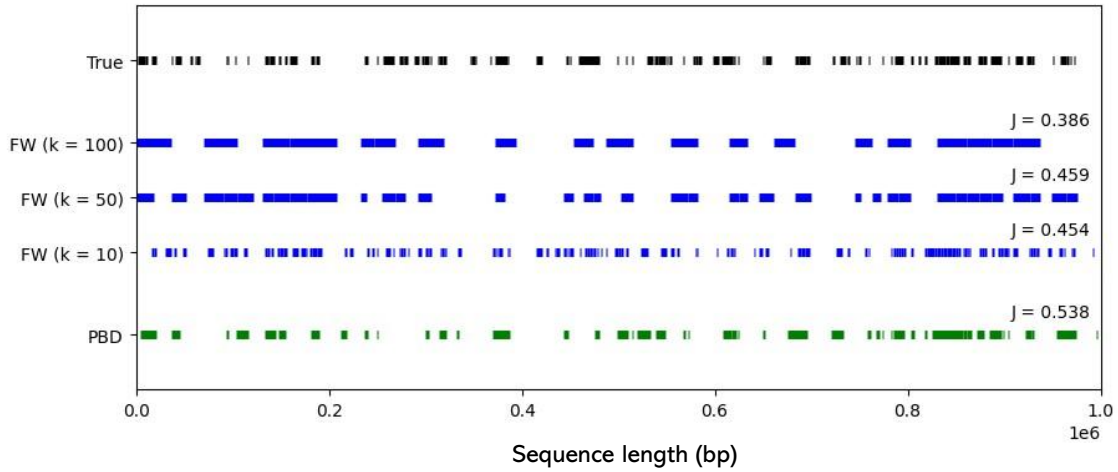


Fig. 2. Breakpoint delimitation through the PBD (green) and FW (blue) approaches: SX blocks in an example ARG (σ = 0.001, $\gamma = 5 \times 10^{-4}$). The accuracy of SX blocks recovered by the FW approach depends on window size k. For the given example ARG, the PBD approach performs best (Jaccard similarity index values J on the right).

I compared the accuracy of SX block delimitation between the PBD and FW (k = 100 SNPs) approaches across the asexuality-sex space of scenarios. Both methods performed the worst under intermediate γ values when $\sigma < 10^{-4}$ (as indicated by near-zero values of J; Fig.

3A). Similarly, both methods performed well for $\sigma \approx 10^{-3}$-10^{-2} ($J \approx 0.90$ and 0.80 for PBD and FW, respectively), but FW was exceptionally accurate under very low and, conversely, very high γ at the lower end of σ ($J > 0.90$). Across the parameter space, a general pattern emerged with FW being advantageous under rare sex and PBD under frequent sex (Fig. 3B). Given the PBD approach anchors SX blocks at tripleton SNPs and extends them depending on the context of neighbouring sites, these results suggest that the sex-specific SNP combinations arise artefactually even in simulated obligate asexual scenarios.

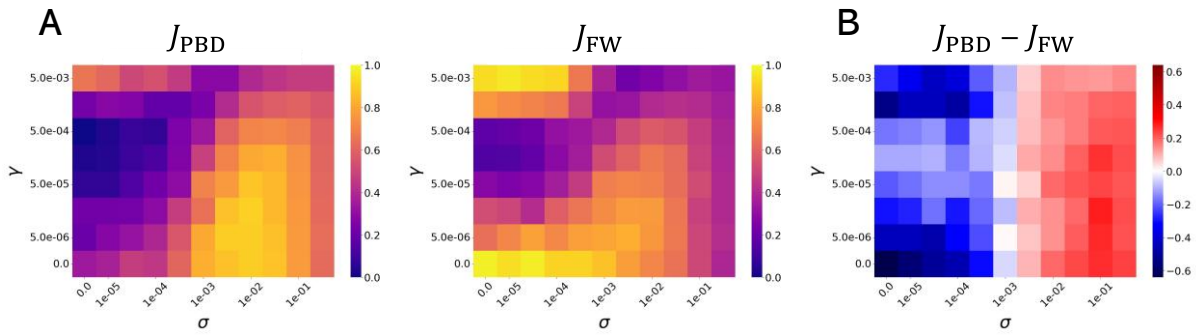


Fig. 3. Accuracy of SX block delimitation through the PBD and FW (k = 100 SNPs) approaches. (A) Comparisons against the simulated ground truth as measured with the Jaccard similarity index J. (B) Difference in J between the two approaches. Blue regions correspond to higher accuracy of FW; red regions correspond to higher accuracy of PBD.

Spurious sex signals

Despite the absence of SX trees in simulated ARGs, both approaches identified SX blocks under obligate asexuality. Table 2 summarises their features with respect to (1) the presence of tripletons and (2) the trees on which the tripletons arose. As expected, PBD inference resulted in SX blocks that all contained tripletons, whereas under FW inference, the proportion of tripleton-containing blocks depended on γ. In PBW inference, the 'offending' tripletons were associated with CL or unbalanced AR trees; in FW inference, the tripletons were associated exclusively with unbalanced AR trees.

Table 2. The presence and origin of tripleton SNPs in SX blocks mis-inferred under obligate asexual scenarios (two individuals sampled per simulation to a total of 100 Mb of sequence per scenario). In very rare cases (typically << 1%), blocks contained tripletons associated with both CL and AR trees or with polytomies, which are omitted for clarity.

(A) PBD approach.

γ	Tripleton(s) present? (% blocks, total count)	CL	AR_U*
0.0	100.0% (134)	100.0%	0.0%
5×10^{-6}	100.0% (214)	65.4%	34.6%
5×10^{-5}	100.0% (616)	15.0%	85.0%
5×10^{-4}	100.0% (1558)	2.0%	98.0%
5×10^{-3}	100.0% (159)	0.0%	100.0%

(B) FW approach.

γ	Tripleton(s) present? (% blocks, total count)	CL	AR_U*
0.0	0.0% (0)	-	-
5×10^{-6}	66.7% (44)	0.0%	100.0%
5×10^{-5}	99.2% (279)	0.0%	100.0%
5×10^{-4}	100.0% (344)	0.0%	100.0%
5×10^{-3}	85.7% (6)	0.0%	100.0%

*Unbalanced AR trees.

In contrast to the FW approach where SX blocks are mis-inferred even in the absence of tripletons, two concrete sources of error affect the PBD approach (Fig. 4). First, tripleton SNPs may arise due to recurrent mutation (homoplasy) of doubleton sites on external branches of CL trees and form compatible blocks with surrounding doubletons (Fig. 4A). Second, true informative tripletons may arise in isolation (or at terminal positions) on unbalanced AR trees and form compatible blocks with doubletons from neighbouring CL trees (Fig. 4B). A clear understanding of the mechanisms underlying spurious sex signals paves the way for further investigation (see Discussion).

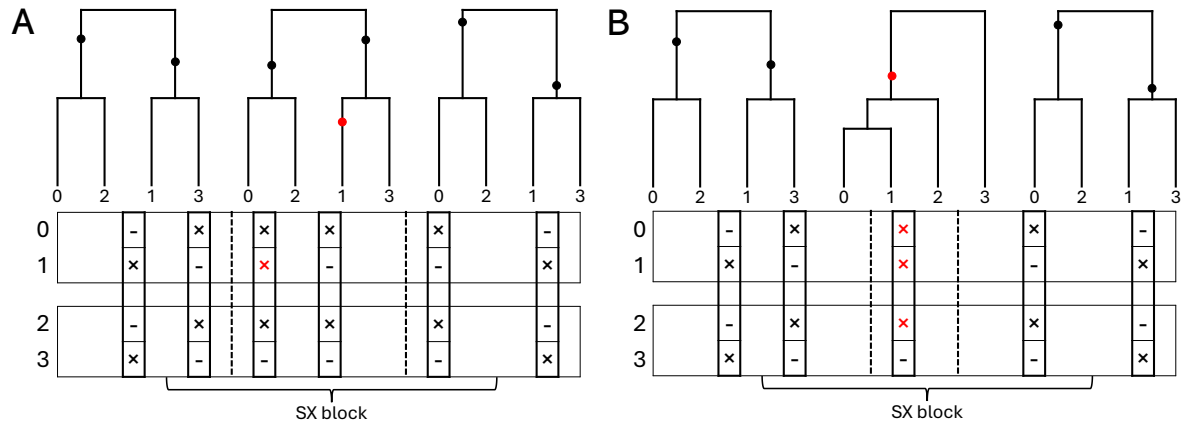


Fig. 4. Spurious sex signals identified by the PBD approach. (A) An SX block anchored at a tripleton that arose through recurrent mutation (homoplasy). (B) An SX block anchored at a tripleton that arose on an unbalanced AR tree.

Discussion

In this chapter, I introduced the 'parsimony block delimitation' (PBD) approach for genealogical analysis of four-haplotype alignments. On a conceptual level, the new approach draws on the principles of parsimony and equity between recombination breakpoints and inferred topological changes, paralleling established general methods. Although not intended to estimate local trees in an unbiased manner, the method performs competitively with, and under certain conditions exceeds (Fig. S2C), standard inference based on fixed-length windows. Limitations of the PBD approach, such as its focus on topology-changing breakpoints, are not qualitatively different from those of more complex heuristic algorithms; however, unlike the latter, they are fully transparent.

In the context of rare sex detection, I argue that the main advantage of the new method lies in the explicit definition of local SNP combinations that, in an idealized scenario, are indicative of sex. Standard approaches do not provide such definition: both the boundaries of local trees and their topologies can change depending on the parametrisation of an algorithm and other assumptions, such as the mutation model. Philosophically speaking, the use of parsimony narrows down the genomic landscape to regions that require explanation

in the light of the reproductive hypothesis proposed for a system (e.g., obligate asexuality), even if this explanation involves unforeseen biological or technical factors.

The use of maximum parsimony in molecular phylogenetics is generally discouraged due to its demonstrated shortcomings (e.g., homoplasy-driven long-branch attraction) that are better addressed by models of sequence evolution (Felsenstein, 1978, 1983). On the other hand, parsimony solutions have been recently applied in the ARG field, with maximum parsimony-based methods such as SARGE (Schaefer et al., 2021) or KwARG (Ignatieva et al., 2021). While, in principle, one could imagine a parametric ARG inference method based on a facultative asexual coalescent model (Hartfield et al., 2016, 2018), it is not obvious that such a method would fundamentally solve the challenge of distinguishing between obligate asexuality and rare sex, not to mention accounting for the idiosyncrasies of different asexual systems. Instead, it appears that explicitly considering sources of inference error in well-defined target regions could be more productive. The probability of sex-informative recurrent mutation, for example, depends on the length of external CL branches which, in neutral scenarios, is determined by the population size (and meta-population mixing, sampling scheme, etc.). One way to estimate the probability of such events could be through local singleton densities as a proxy for external branch lengths. Similarly, mixed AR-CL signal would be particularly likely for sex-informative tripletons that co-occur with AR-specific doubletons. Finally, one could test correlation between SX blocks and a range of biological and technical metrics, such as transposable element mapping, read mapping and variant quality, position in phased blocks or signatures of sample cross-contamination (Wilson et al., 2018).

The work presented here constitutes a preliminary investigation of an approach that opens several avenues for future research. For example, cross-validation of standard genealogical inference with the PBD approach could help identify putative sex-specific regions that arose artefactually, thereby revising downward an estimated rate of sex. Irrespective of the means, it appears that the flipping of perspective from *Can we detect signature of sex?* to *Can we*

explain the inevitable signatures of sex in other ways? might be key for better understanding of predominantly asexual systems. Future work will focus on a Python library that will incorporate these ideas.

References

Baumdicker, F., Bisschop, G., Goldstein, D., Gower, G., Ragsdale, A. P., Tsambos, G., Zhu, S., Eldon, B., Ellerman, E. C., & Galloway, J. G. (2022). Efficient ancestry and mutation simulation with msprime 1.0. *Genetics*, *220*(3), iyab229.

Boni, M. F., Posada, D., & Feldman, M. W. (2007). An exact nonparametric method for inferring mosaic structure in sequence triplets. *Genetics*, *176*(2), 1035–1047.

Bruen, T. C., Philippe, H., & Bryant, D. (2006). A simple and robust statistical test for detecting the presence of recombination. *Genetics*, *172*(4), 2665–2681.

Cen, S., & Rasmussen, D. A. (2024). Exploring the accuracy and limits of algorithms for localizing recombination breakpoints. *Molecular Biology and Evolution*, *41*(7), msae133.

Chan, A. H., Jenkins, P. A., & Song, Y. S. (2012). Genome-wide fine-scale recombination rate variation in Drosophila melanogaster. *PLoS Genetics*, *8*(12), e1003090.

de Jong, M. J., Niamir, A., Wolf, M., Kitchener, A. C., Lecomte, N., Seryodkin, I. V., Fain, S. R., Hagen, S. B., Saarma, U., & Janke, A. (2023). Range-wide whole-genome resequencing of the brown bear reveals drivers of intraspecies divergence. *Communications Biology*, *6*(1), 153.

Deng, Y., Nielsen, R., & Song, Y. S. (2025). Robust and accurate Bayesian inference of genome-wide genealogies for hundreds of genomes. *Nature genetics*, 1–12.

Felsenstein, J. (1978). Cases in which parsimony or compatibility methods will be positively misleading. *Systematic zoology*, *27*(4), 401–410.

Felsenstein, J. (1983). Statistical inference of phylogenies. *Journal of the Royal Statistical Society Series A: Statistics in Society*, *146*(3), 246–262.

Griffiths, R. C., & Marjoram, P. (1997). An ancestral recombination graph. *Institute for Mathematics and its Applications*, *87*, 257.

Hartfield, M., Wright, S. I., & Agrawal, A. F. (2016). Coalescent times and patterns of genetic diversity in species with facultative sex: effects of gene conversion, population structure, and heterogeneity. *Genetics*, *202*(1), 297–312.

Hartfield, M., Wright, S. I., & Agrawal, A. F. (2018). Coalescence and linkage disequilibrium in facultatively sexual diploids. *Genetics*, *210*(2), 683–701.

Hudson, R. R. (1983). Properties of a neutral allele model with intragenic recombination. *Theoretical population biology*, *23*(2), 183–201.

Hudson, R. R., & Kaplan, N. L. (1985). Statistical properties of the number of recombination events in the history of a sample of DNA sequences. *Genetics*, *111*(1), 147.

Ignatieva, A., Lyngsø, R. B., Jenkins, P. A., & Hein, J. (2021). KwARG: parsimonious reconstruction of ancestral recombination graphs with recurrent mutation. *Bioinformatics*, *37*(19), 3277–3284.

Kelleher, J., Wong, Y., Wohns, A. W., Fadil, C., Albers, P. K., & McVean, G. (2019). Inferring whole-genome histories in large population datasets. *Nature genetics*, *51*(9), 1330–1338.

Kimura, M. (1969). The number of heterozygous nucleotide sites maintained in a finite population due to steady flux of mutations. *Genetics*, *61*(4), 893.

Kosakovsky Pond, S. L., Posada, D., Gravenor, M. B., Woelk, C. H., & Frost, S. D. (2006). Automated phylogenetic detection of recombination using a genetic algorithm. *Molecular Biology and Evolution*, *23*(10), 1891–1901.

Lasek-Nesselquist, E., Welch, D. M., Thompson, R. C. A., Steuart, R. F., & Sogin, M. L. (2009). Genetic exchange within and between assemblages of Giardia duodenalis. *Journal of Eukaryotic Microbiology*, *56*(6), 504–518.

Li, N., & Stephens, M. (2003). Modeling linkage disequilibrium and identifying recombination hotspots using single-nucleotide polymorphism data. *Genetics*, *165*(4), 2213–2233.

Martin, D., & Rybicki, E. (2000). RDP: detection of recombination amongst aligned sequences. *Bioinformatics*, *16*(6), 562–563.

Martin, D. P., Lemey, P., & Posada, D. (2011). Analysing recombination in nucleotide sequences. *Molecular ecology resources*, *11*(6), 943–955.

Martin, S. H., Davey, J. W., Salazar, C., & Jiggins, C. D. (2019). Recombination rate variation shapes barriers to introgression across butterfly genomes. *PLoS biology*, *17*(2), e2006288.

Martin, S. H., & Van Belleghem, S. M. (2017). Exploring evolutionary relationships across the genome using topology weighting. *Genetics*, *206*(1), 429–438.

Maynard Smith, J. (1992). Analyzing the mosaic structure of genes. *Journal of molecular evolution*, *34*(2), 126–129.

Maynard Smith, J., & Smith, N. H. (1998). Detecting recombination from gene trees. *Molecular Biology and Evolution*, *15*(5), 590–599.

McVean, G., Awadalla, P., & Fearnhead, P. (2002). A coalescent-based method for detecting and estimating recombination from gene sequences. *Genetics*, *160*(3), 1231–1241.

McVean, G. A., & Cardin, N. J. (2005). Approximating the coalescent with recombination. *Philosophical Transactions of the Royal Society B: Biological Sciences*, *360*(1459), 1387–1393.

Phan Thi, N., Danchin, E. G., Koutsovoulos, G. D., Rancurel, C., Vermeire, M.-l., Besnard, G., & Bellafiore, S. (2025). Genomic rearrangements promote diversification of a facultative meiotic parthenogenetic nematode pest (Meloidogyne graminicola). *bioRxiv*, 2025.2003. 2020.644268.

Posada, D., & Crandall, K. A. (2001). Evaluation of methods for detecting recombination from DNA sequences: computer simulations. *Proceedings of the National Academy of Sciences*, *98*(24), 13757–13762.

Quinlan, A. R., & Hall, I. M. (2010). BEDTools: a flexible suite of utilities for comparing genomic features. *Bioinformatics*, *26*(6), 841–842.

Rannala, B. (2025). Recombination and phylogenetic inference. *Evolutionary Journal of the Linnean Society*, *4*(1), kzaf016.

Rasmussen, D. A., & Guo, F. (2023). Espalier: efficient tree reconciliation and ancestral recombination graphs reconstruction using maximum agreement forests. *Systematic Biology*, *72*(5), 1154–1170.

Rasmussen, M. D., Hubisz, M. J., Gronau, I., & Siepel, A. (2014). Genome-wide inference of ancestral recombination graphs. *PLoS Genetics*, *10*(5), e1004342.

Salminen, M. O., Carr, J. K., Burke, D. S., & McCUTCHAN, F. E. (1995). Identification of breakpoints in intergenotypic recombinants of HIV type 1 by bootscanning. *AIDS research and human retroviruses*, *11*(11), 1423–1425.

Samuk, K., Manzano-Winkler, B., Ritz, K. R., & Noor, M. A. (2020). Natural selection shapes variation in genome-wide recombination rate in Drosophila pseudoobscura. *Current Biology*, *30*(8), 1517–1528. e1516.

Sawyer, S. (1989). Statistical tests for detecting gene conversion. *Molecular Biology and Evolution*, *6*(5), 526–538.

Schaefer, N. K., Shapiro, B., & Green, R. E. (2021). An ancestral recombination graph of human, Neanderthal, and Denisovan genomes. *Science Advances*, *7*(29), eabc0776.

Speidel, L., Forest, M., Shi, S., & Myers, S. R. (2019). A method for genome-wide genealogy estimation for thousands of samples. *Nature genetics*, *51*(9), 1321–1329.

Steenwyk, J. L., Li, Y., Zhou, X., Shen, X.-X., & Rokas, A. (2023). Incongruence in the phylogenomics era. *Nature Reviews Genetics*, *24*(12), 834–850.

Virtanen, P., Gommers, R., Oliphant, T. E., Haberland, M., Reddy, T., Cournapeau, D., Burovski, E., Peterson, P., Weckesser, W., & Bright, J. (2020). SciPy 1.0: fundamental algorithms for scientific computing in Python. *Nature Methods*, *17*(3), 261–272.

Wang, J., Street, N. R., Scofield, D. G., & Ingvarsson, P. K. (2016). Natural selection and recombination rate variation shape nucleotide polymorphism across the genomes of three related Populus species. *Genetics*, *202*(3), 1185–1200.

Weedall, G. D., Clark, C. G., Koldkjaer, P., Kay, S., Bruchhaus, I., Tannich, E., Paterson, S., & Hall, N. (2012). Genomic diversity of the human intestinal parasite Entamoeba histolytica. *Genome biology*, *13*(5), R38.

Wilson, C. G., Nowell, R. W., & Barraclough, T. G. (2018). Cross-contamination explains "inter and intraspecific horizontal genetic transfers" between asexual bdelloid rotifers. *Current Biology*, *28*(15), 2436–2444. e2414.

Zhou, X., Liu, Y., Calvert, L., Munoz, C., Otim-Nape, G. W., Robinson, D. J., & Harrison, B. D. (1997). Evidence that DNA-A of a geminivirus associated with severe cassava mosaic disease in Uganda has arisen by interspecific recombination. *Journal of General Virology*, *78*(8), 2101–2111.

Supplement to Chapter 2



———————— O ————————

Tymoteusz Pieszko

———————— O ————————

Supplementary Figures

Algorithm S1. A high-level overview of the procedure for identifying blocks with compatible tripleton-doubleton combinations in a four-haplotype alignment.

Input Genotype array G with n sites;
array P of genotype positions;
sequence length L

1 Set M = [0, midpoints between P, L]
2 Initialise BLOCKS = [ ] `# to store half-open intervals [START, END)`
3 **for** i = 1 to n **do**
4 $g = G[i]$; $p = P[i]$
5 **if** g not a tripleton **then**
6 **continue**
7 **if** length(BLOCKS) > 0 and p < BLOCKS[LAST][END] **then** `# p already covered`
8 **continue**
10 Initialise $j = i - 1$ and $k = i + 1$
11 **while** $j \geq 0$ and isCompatible($G[j]$, g) **do** `# extend greedily to the left`
12 $j = j - 1$
13 **while** $k < n$ and isCompatible($G[k]$, g) **do** `# extend greedily to the right`
14 $k = k + 1$
Set START = $M[j+1]$; END = $M[k]$;
15 G_1 = unique($G[j$ to $i-1]$); `# unique genotypes in the left segment`
G_2 = unique($G[i+1$ to $k]$); `# unique genotypes in the right segment`
16 **if** isCompatible(G_1, G_2) **then**
17 BLOCKS.append((START, END))
18 **else if** not isCompatible(G_1, G_2) **then**
19 $d_1 = p - P[i-1]$; $d_2 = P[i+1] - p$;
20 **if** $d_1 \leq d_2$ **then**
21 BLOCKS.append((START, $M[i+1]$))
22 **if** $d_1 > d_2$ **then**
23 BLOCKS.append(($M[i]$, END))

Return BLOCKS

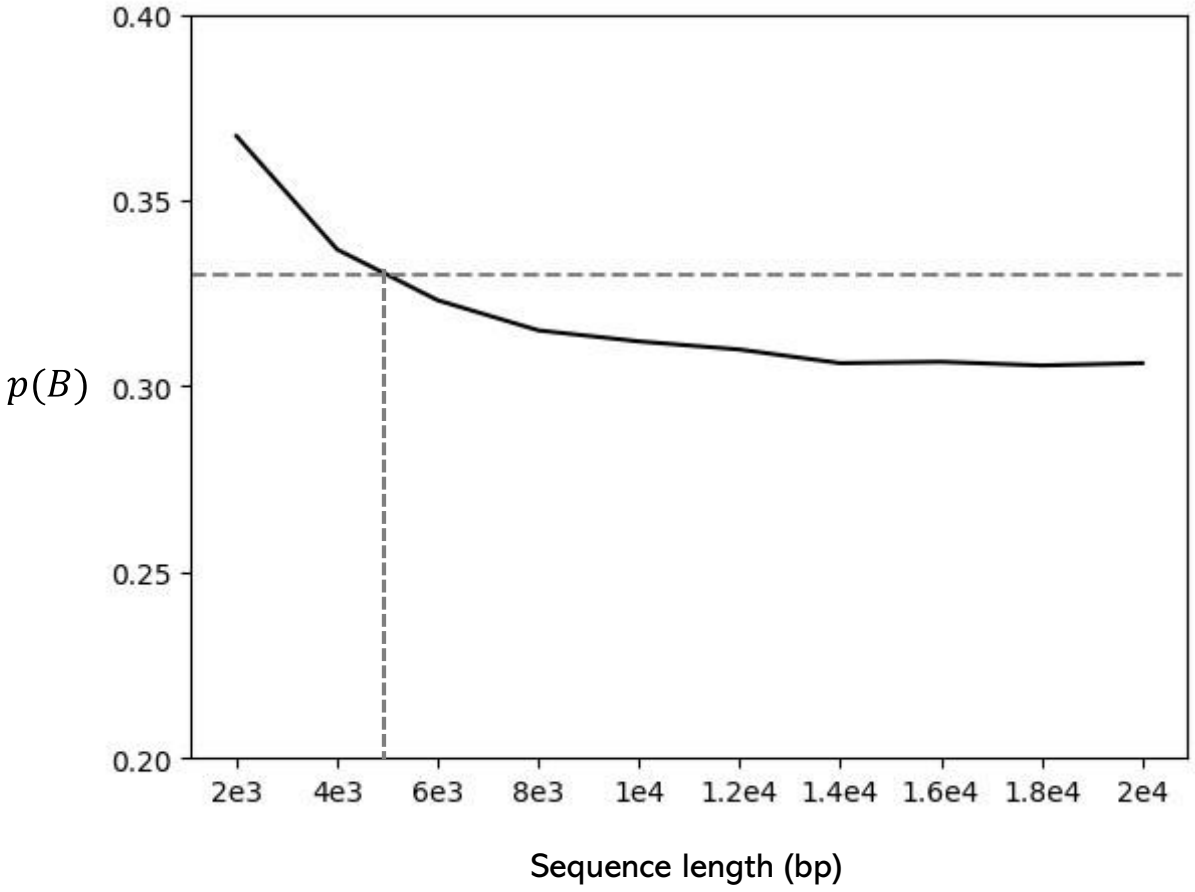


Fig. S1. Proportion of balanced trees $p(B)$ obtained through the PBD approach as a function of sequence length: obligate sexual scenarios simulated using msprime v1.3.2 (r = μ = 10^{-6}, N = 1,000) (Baumdicker et al., 2022). Dashed horizontal line represents the expected value of $p(B)$ under obligate sex.

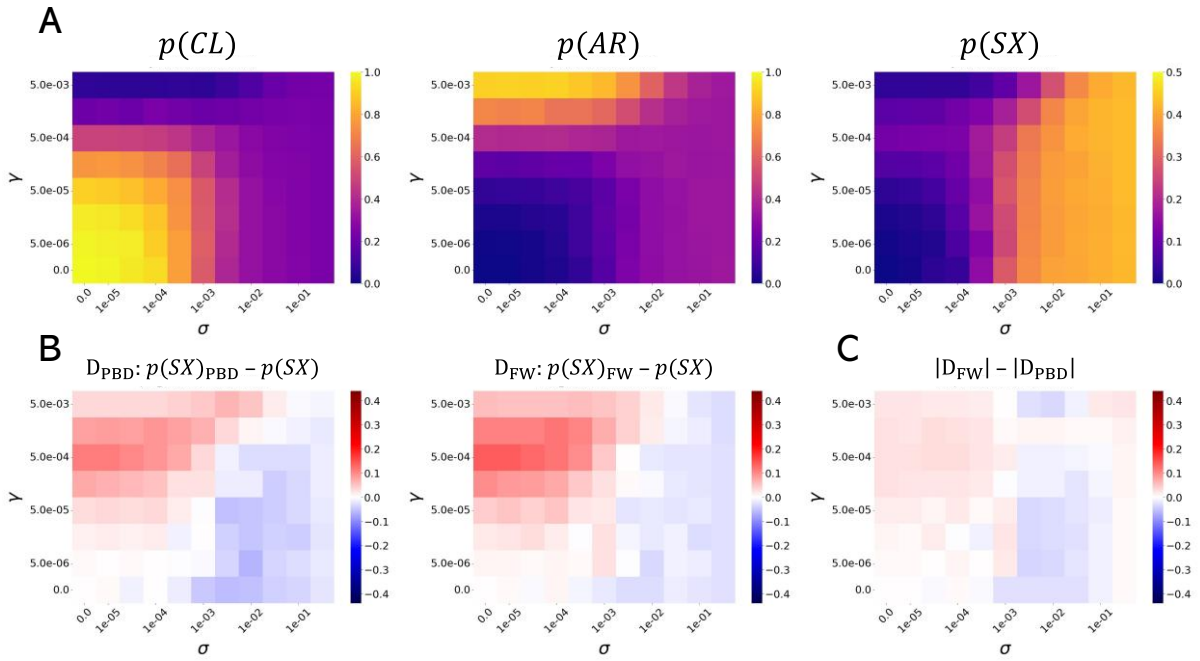


Fig. S2. Tree composition estimated through the PBD approach; comparison with FW inference through clustering (k = 100 SNPs) given fragmented input sequence (5-kb segments). (A) $p(CL)$, $p(AR)$ and $p(SX)$ across the simulated space of sex rates σ and LOH rates γ (note the color scale is capped at 0.5 in the $p(SX)$ heatmap). (B) Deviations D from true $p(SX)$ associated with the PBD and FW approaches. (C) Absolute difference in deviations from true $p(SX)$ between the two approaches: red indicates PBD is closer to truth, blue indicates FW is closer to truth.

References

Baumdicker, F., Bisschop, G., Goldstein, D., Gower, G., Ragsdale, A. P., Tsambos, G., Zhu, S., Eldon, B., Ellerman, E. C., & Galloway, J. G. (2022). Efficient ancestry and mutation simulation with msprime 1.0. *Genetics*, *220*(3), iyab229.

Chapter 3: Asexual divergence in epibiotic bdelloid rotifers of the genus *Rotaria*



——————————— O ———————————

Tymoteusz Pieszko, Reuben W. Nowell, Christopher G. Wilson, Jerome Kelleher, Timothy G. Barraclough

——————————— O ———————————

Contributions

- ➔ The genomic dataset was generated by R.W.N., C.G.W. and T.G.B.; genome assembly, variant calling and read-based phasing were performed by R.W.N.; all subsequent population genetic analyses were performed by me.
- ➔ A chapter modified from an in-preparation manuscript where R.W.N. and I are joint first authors. The chapter follows an 'Introduction → Results → Discussion → Materials and Methods' order of sections.

Abstract

Species and speciation are traditionally thought of as properties of sexual organisms. Interbreeding maintains genetic cohesion within species, whereas reproductive isolation permits divergence between them. The importance of sex for diversification has been challenged, however, by comparisons between sexual and asexual lineages. Bdelloid rotifers comprise a class of animals in which no males have been described, but which have diversified into genetically and morphologically distinct species, potentially without any contribution of sex. Yet, the possibility remains that cryptic sex or genetic exchange by some other mechanism has shaped patterns of divergence between bdelloid species. Here, we test whether two bdelloid species that co-exist as epibionts of the water louse (*Asellus aquaticus*) diverged in the absence of genetic exchange. By integrating multiple metrics explicitly linked to reproductive mode, we find that – despite some signal to the contrary – sequence diversity patterns in both species are overall consistent with obligate asexuality. Our results suggest that sex might not be essential for diversification in eukaryotes, while also highlighting the technical challenges and uncertainties inherent in inferring reproductive mode from sequence data.

Introduction

According to the biological species concept, species are interbreeding groups of organisms that are reproductively isolated from other such groups (Dobzhansky, 1937; Mayr, 1963). Guided by this definition, speciation research focused on finding isolating mechanisms that prevent interbreeding between co-occurring species (Coyne & Orr, 2004). Later theory emphasized that strong selection can drive ecological divergence even in the face of gene flow, without strict reproductive barriers (Gavrilets, 2004; Feder et al., 2012). The field's primary focus, however, remains on how divergence occurs against a backdrop of genetic mixing by sexual recombination, and on understanding the relative interplay between selection and isolation (Schluter & Rieseberg, 2022). Genome sequencing is now widely used to investigate alternative mechanisms based on genome-wide patterns of differentiation, selection and recombination (Chase et al., 2021; Ravinet et al., 2017; Sendell-Price et al., 2020; Stankowski et al., 2019).

Classic accounts suggested that quantifying diversity patterns in asexual clades could provide deep insights as to why clades diversify into species (Maynard Smith & Szathmary, 1995; Barraclough et al., 2003; Coyne & Orr, 2004). An asexual population faced with geographical isolation, or with divergent selection between two niches, is expected to diverge in a qualitatively similar way to the sexual case (Cohan, 2001; Barraclough et al., 2003; Barraclough, 2019). The speed and magnitude of differentiation should vary, however, depending on the relative importance of different processes. If reproductive isolation is a limiting step for divergence in sexuals, then asexuals should diversify more readily, because no special barriers are needed (Barraclough et al., 2003). Alternatively, if the rate of adaptation to new ecological opportunities is a limiting step, asexuals might diversify less than sexuals, because they adapt more slowly to new

conditions (Burt, 2000; Colegrave, 2002; Becks & Agrawal, 2012; Goddard et al., 2005). In general, equivalent diversity patterns in asexuals and sexuals would show that sex and reproductive isolation are less important for speciation than widely thought. Testing these hypotheses is difficult, however, because most asexual lineages are evolutionarily young, indicative of high extinction rates (Judson & Normark, 1996; Burt, 2000; Moreira et al., 2021). The lack of gene flow may indeed be a barrier to speciation, but perhaps asexual lineages rarely persist long enough to have the chance to diversify.

One group proposed as a test case for these ideas is the class Bdelloidea (phylum Syndermata; Vasilikopoulos et al., 2024). Bdelloid rotifers are microscopic animals that live in habitats with temporary or permanent freshwater (Ricci, 1987). Unusually for animals, no males have been described in over two centuries of observation (Birky Jr, 2010; Wilson et al., 2024). Contrary to the expected fate of asexual lineages, the clade has diversified into hundreds of described species (Segers, 2007) and persisted for many tens of millions of years (Tang et al., 2014). Previous work indicated the presence of discrete genetic clusters within bdelloid clades, consistent with independently evolving species (Birky et al., 2005; Fontaneto et al., 2007). For example, species of the bdelloid genus *Rotaria* live in a range of habitats from terrestrial to fully aquatic and have experienced divergent selection on their feeding morphology (Fontaneto et al., 2007). Indeed, bdelloids appear to have diversified at a faster rate than a related facultative sexual group (monogonont rotifers), which was interpreted as evidence that reproductive isolation is a limiting step for speciation in sexual groups (Tang et al., 2014).

An open question remains whether bdelloids have diverged into ecologically divergent clusters strictly through asexual descent, or whether sex or some other form of genetic

exchange played a role. Several studies have sought to test the hypothesis that bdelloid rotifers are ‘ancient asexuals' (Judson & Normark, 1996) and obligate parthenogens. Initial evidence that seemed to rule out sexual reproduction, based on patterns of allelic divergence (Mark Welch & Meselson, 2000) or extensive chromosomal rearrangements (Flot et al., 2013), was later shown to have alternative explanations that neither confirmed nor refuted obligate asexuality (Mark Welch et al., 2008; Simion et al., 2021). Two recent studies reported evidence of ‘allele sharing’ – where alleles in the same individual share a close relationship with copies from two different individuals in the population – seemingly inconsistent with strictly asexual descent (Vakhrusheva et al., 2020; Laine et al., 2022). It nonetheless remains possible that these patterns, too, have other explanations, in the absence of direct evidence for males, syngamy or canonical meiosis (Wilson et al., 2024).

In contrast, two other forms of genetic recombination have been more extensively documented in bdelloids. The first, termed asyngamous recombination (Wilson et al., 2024), encompasses homologous recombination that occurs within a parthenogenetic line of descent without syngamy. This includes gene conversion-like processes, resulting in localised loss of heterozygosity (LOH), as well as crossover recombination, leading to long-range LOH or altered physical linkage between alleles. In the bdelloid *Adineta vaga*, eggs are produced through a non-reductive meiotic pathway accompanied by both short and long-range recombination (Simion et al., 2021; Terwagne et al., 2022; Houtain et al., 2024). Recent work has used individual-based models to demonstrate that standard sequence diversity metrics – such as the inbreeding coefficient F_{IS} and linkage disequilibrium (LD) decay – can be driven to ‘sex-like’ values solely by asyngamous processes (Pieszko et al., 2025). Building on these results, alternative approaches have

become available that explicitly distinguish between signatures of recombination and those of the reproductive mode itself (Pieszko et al., 2025).

A second form of recombination found repeatedly across bdelloid species is uptake of non-metazoan genes through horizontal transfer (Gladyshev et al., 2008). Up to 10% of genes match more closely with bacterial, fungal, protist or plant genes than with their closest metazoan counterparts (Boschetti et al., 2012; Nowell et al., 2018; Simion et al., 2021). Moreover, some of these genes bring novel biochemical functions that are typically absent from other animals (Boschetti et al., 2012; Nowell et al., 2024). The observation of ‘distant’ HGT led to the hypothesis that similar mechanisms might transfer DNA between bdelloid individuals within populations (i.e. ‘near’ HGT) (Wilson et al., 2024), by analogy to homologous recombination in bacteria (Gladyshev et al., 2008). If so, HGT might affect speciation in two ways: by bringing genetic novelty and new functions to aid adaptation to new niches (Eyres et al., 2015); and perhaps by shuffling genotypes within populations so regularly that sustained divergence between populations would require isolating mechanisms or strong divergent selection. Previous work found that closely related species of *Rotaria* did differ partly in their complement of horizontally transferred genes (Eyres et al., 2015), consistent with the genetic novelty hypothesis. The more speculative hypothesis of regular horizontal DNA transfer among bdelloids remains to be tested(Wilson et al., 2018).

Here, we investigate the potential role of genetic exchange during the divergence of two bdelloid rotifer species: *R. magnacalcarata* and *R. socialis*, both epibionts of the water louse (*Asellus aquaticus*) with distinct ecological niches. By sequencing multiple genomes, we test two hypotheses for speciation in the genus *Rotaria*. First, the ‘asexual’

hypothesis posits that divergence occurred in the absence of sex, potentially supplemented by horizontal uptake of distant, non-metazoan genes from the environment. Second, the 'cryptic exchange' hypothesis posits that existing mechanisms of inter-individual genetic exchange – such as sexual outcrossing or near HGT[1] – became progressively restricted to operate within, rather than between, species. The two hypotheses raise different predictions for genome-wide patterns of genealogy, which we investigate using a recently developed framework (Pieszko et al., 2025). Our findings complement genomic insights on speciation from conventionally sexual animals (Feder et al., 2012; Tigano & Friesen, 2016; Wolfsberger et al., 2022) and highlight that sex might not be a necessary driver of the formation and maintenance of species barriers.

Results

Population genomic dataset for epibiotic *Rotaria*

We sampled ten individuals each of *R. magnacalcarata* and *R. socialis* (Fig. 1A). Both species are filter feeders that occur on the ventral surface of the water louse (Fontaneto & Ambrosini, 2010). *R. magnacalcarata* is larger (~ 400 µm) and occurs mostly on the middle part of the ventral thorax, whereas *R. socialis* is smaller (~ 200 µm) and occurs mainly along the sides of the posterior body, near the bases of the legs (Fig. 1B). Consistent with their permanently aquatic habitat, both are desiccation-intolerant and there is no known recovery from desiccation in laboratory assays, unlike many other bdelloids (Eyres et al., 2015). A single louse often harbours dozens of individuals of both species, presenting an excellent case study for coexistence and opportunities for genetic exchange. An individual rotifer could easily cross the whole body of the louse in minutes

[1] Findings of the HGT analysis, performed by my co-authors, are summarised in the Discussion.

and thus there is no geographical barrier. The two species are phylogenetically close, having either diverged sympatrically after a single colonisation or originated from independent colonisations by closely related free-living ancestors. Divergence time has been estimated at approximately 6–7 Mya (Fontaneto et al., 2008; Eyres et al., 2015). Our sampling focused on the Silwood Park campus of Imperial College London (eight individuals per species). Anticipating low diversity in the single locality, we included additional individuals from another UK and an Italian locality (Table S1). We report results for populations denoted as RM_{SIL}, RM_{total}, RS_{SIL} and RS_{total}, where 'RM' stands for *R. magnacalcarata*, 'RS' for *R. socialis*, 'SIL' for Silwood Park and 'total' for all sampled individuals.

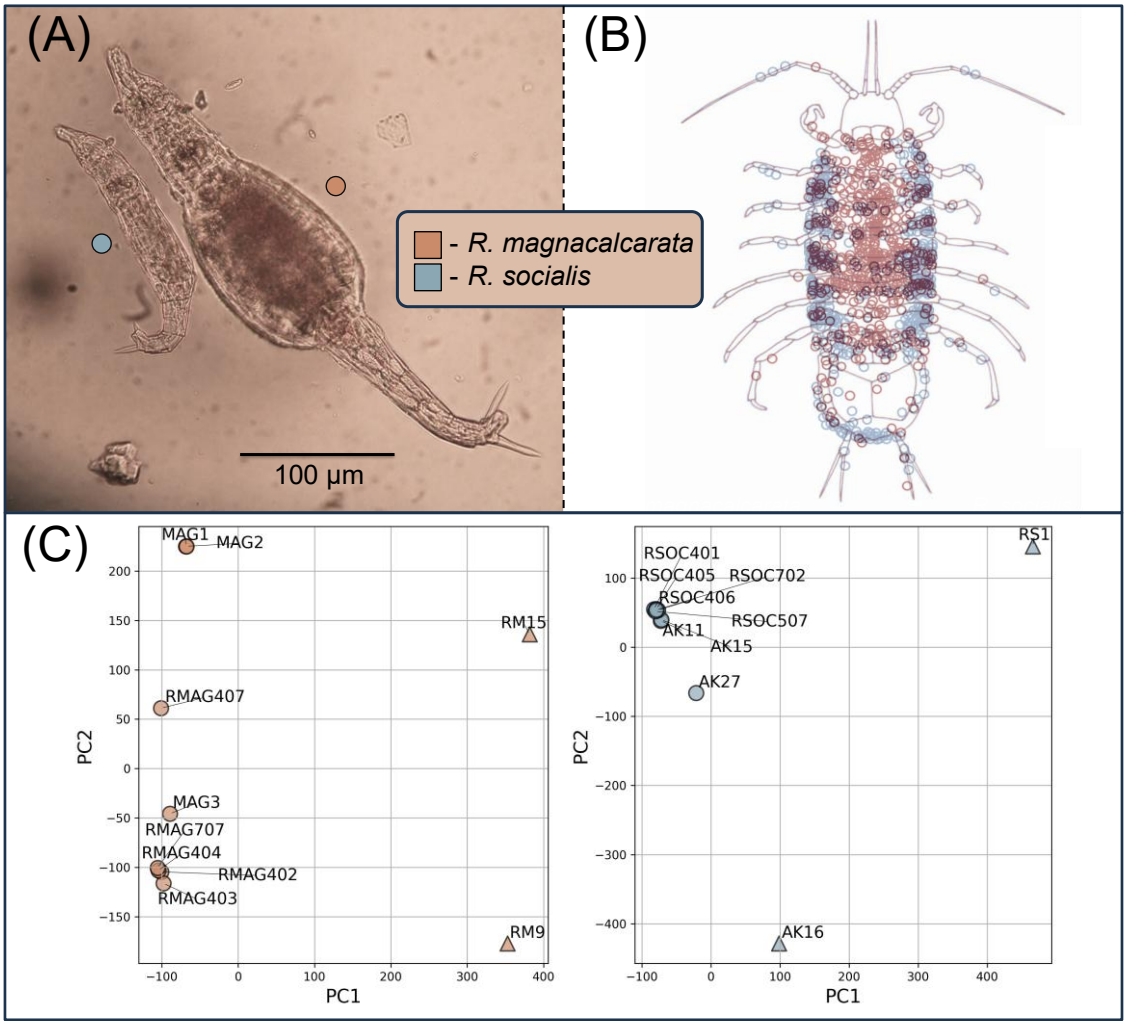


Fig. 1. A dataset for epibiotic *Rotaria*. (A) Representatives of both species isolated from a single water louse, *Asellus aquaticus*. (B) The body regions occupied by the two species; redrawn with permission from Fontaneto & Ambrosini (2010). (C) Principal components analysis (PCA) of high-quality biallelic SNPs (see Materials and Methods). PCA was performed on linkage pruned SNPs (r^2_{max} = 0.2) using scikit-allel v1.3.13 (Miles et al., 2024). Silwood individuals are denoted with circles; non-Silwood with triangles (see Table S1 for all sampling localities).

We generated de novo assemblies from whole-genome amplified Illumina libraries as described in Nowell et al. (2021) and the Materials and Methods (see Table S1 for assembly sizes and N50 values). Longer read methods could not be used, because these species could not be cultured in the laboratory to yield sufficient input DNA. Ten of the genomes were reported previously (Nowell et al., 2021), ten are newly reported here.

The *Rotaria* genomes show a signature of ancient tetraploidisation typical of bdelloid genomes (Mark Welch et al., 2008; Simion et al., 2021). Diploid chromosome pairs are largely collapsed in the assembly due to low homologous divergence (RM_{total}: 0.25%, RS_{total}: 0.27% average genome-wide), but clearly distinguishable from their tetraploid homoeologs (RMtotal: 37.8%, RStotal: 39.5% average pairwise divergence). Consistent with population sub-division in both species, the eight Silwood samples formed distinct clusters, as evident from mitochondrial trees (Fig. S1A) and patterns of genome-wide variation (Fig. 1C).

Classical statistics suggest predominant asexuality

We first tested predictions of the 'asexual' vs 'cryptic exchange' hypotheses with respect to within-species variation, using high-quality unphased SNPs called against an Italian reference assembly for both species (Fig. 2; see Materials and Methods). Positive values of Tajima's D (RM_{total}: 0.711; RS_{total}: 0.264), especially high in the Silwood populations (RM_{SIL}: 1.369; RS_{SIL}: 1.196), indicated a deficit of rare variants relative to the neutral panmictic expectation, as is characteristic of deep-branching genealogies (Tajima, 1989). Specifically, the site frequency spectra (SFS) of Silwood populations (Fig. 2A) displayed a marked excess of intermediate-frequency variants, with modes at 50% frequency, consistent with a symmetric pattern of deep coalescences within diploid genotypes known as the 'Meselson effect' (Birky Jr., 1996; Mark Welch & Meselson, 2000; Hartfield et al., 2016). Similarly aligning with the clonal expectation, average within-genome divergence ('heterozygosity') was substantially elevated (RM_{SIL}: 0.28%; RS_{SIL}: 0.28%) compared with the average divergence between genomes, calculated as the mean allelic difference (RM_{SIL}: 0.192%; RS_{SIL}: 0.180%; Fig. 2B). To further explore

these initial results, we calculated additional statistics commonly used to support hypotheses of reproductive mode (e.g., Van den Broeck et al., 2020; Vakhrusheva et al., 2020; Blanc et al., 2023) and interpreted their values in the context of simulated obligate and facultative asexual scenarios (Pieszko et al., 2025; see Materials and Methods for details).

We obtained markedly negative values of the inbreeding coefficient F_{IS} (RM_{SIL}: -0.33, RS_{SIL}: -0.45; Fig. 2C), again consistent with clonal reproduction. Concurrently, we observed rapid decay of LD with distance between SNPs (RM_{SIL}: r^2 from ~ 0.60 to 0.40, RS_{SIL}: r^2 from ~ 0.50 to 0.20), stabilising at around 2 kb (Fig. 2D). While LD decay points to homologous recombination, a cursory assessment of its magnitude or steepness is insufficient to discriminate between sexual and asyngamous mechanisms. In simulated scenarios, realistic rates of asyngamous recombination (short- or long-range) led to steep LD decay even under obligate asexuality (Pieszko et al., 2025). Assuming obligate asexuality, however, an upper bound of $\frac{1}{2N}$ (where N is the population size) can be inferred for the asyngamous recombination rate, as higher rates eliminate the intermediate-frequency peak in the SFS (compare Fig. 2A with Fig. S2). On the other hand, negative F_{IS} constrains the per-generation rate of sex to < $\frac{1}{N}$, where N is the population size (Pieszko et al., 2025), but does not demonstrate its absence. Inclusion of the non-Silwood individuals led to higher values of both r^2 and F_{IS} (Fig. 2C and D), consistent with geographical isolation (i.e., the ‘Wahlund effect’ classically described for obligate sexual populations; Garnier-Géré & Chikhi, 2013). Overall, these results alone cannot substantiate strong claims about the *Rotaria* reproductive system or distinguish between the two hypotheses for divergence.

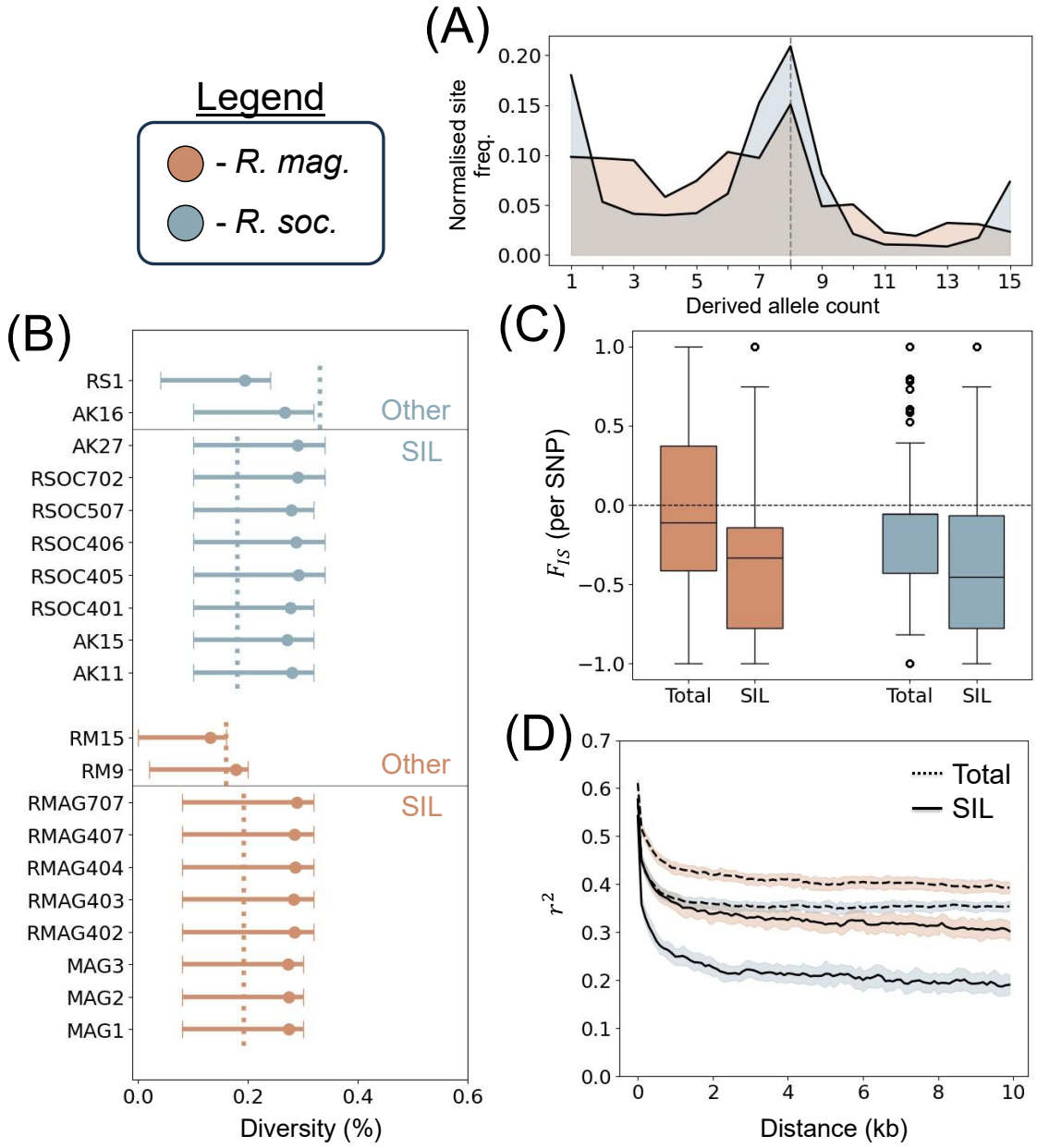


Fig 2. Population genetics of epibiotic *Rotaria* (*R. magnacalcarata* – orange, *R. socialis* – blue). (A) Unfolded site frequency spectra for the Silwood populations. SNPs were polarised against an Italian sample for each species (see Materials and Methods); fixed derived alleles are not shown. The dashed vertical line indicates the 50% frequency class. (B) Mean sequence divergence within (point per individual; bars represent the central 50% of values calculated in 5-kb windows) and between (dashed lines) genomes. (C) Distribution of per-SNP inbreeding coefficient F_{IS}. (D) Linkage disequilibrium (LD) decay with distance. r^2 between unphased genotypes (Rogers & Huff, 2009) was computed relative to 10,000 random SNPs, and means were obtained for 100-bp windows. Shaded areas represent 95% confidence intervals obtained via bootstrapping (100 replicates). All calculations were performed using scikit-allel v1.3.13 (Miles et al., 2024).

Genealogical analyses suggest that sex likely absent

To distinguish between the two hypotheses while explicitly accounting for asyngamous recombination, we applied the framework developed by Pieszko et al. (2025). Grounded in the concept of ancestral recombination graphs (ARGs), Pieszko et al. proposed to analyse local two-individual, four-tip trees along haplotype-resolved (i.e., 'phased') genomic segments (Pieszko et al., 2025). The 18 possible trees are classified into three categories – CL (clonality-compatible), AR (asyngamous recombination compatible) and SX (sex-specific) – whose relative genomic proportions p reflect the reproductive history, as summarized in Fig. 3. Under obligate asexuality, only CL and AR trees are expected, with $p(AR)$ positively correlated with the asyngamous recombination rate. $p(SX)$ increases with the rate of sex and, when sex is frequent, $p(CL)$, $p(AR)$ and $p(SX)$ are expected to conform to a ratio of 2 **:** 3 **:** 4 (Fig. 3; see Fig. S3A for tree proportions across the space of simulated scenarios). The 'tree composition' of a sample of n diploids is therefore defined as the relative genomic proportions of CL, AR and SX trees computed for all $\binom{n}{2}$ pairings (Pieszko et al., 2025).

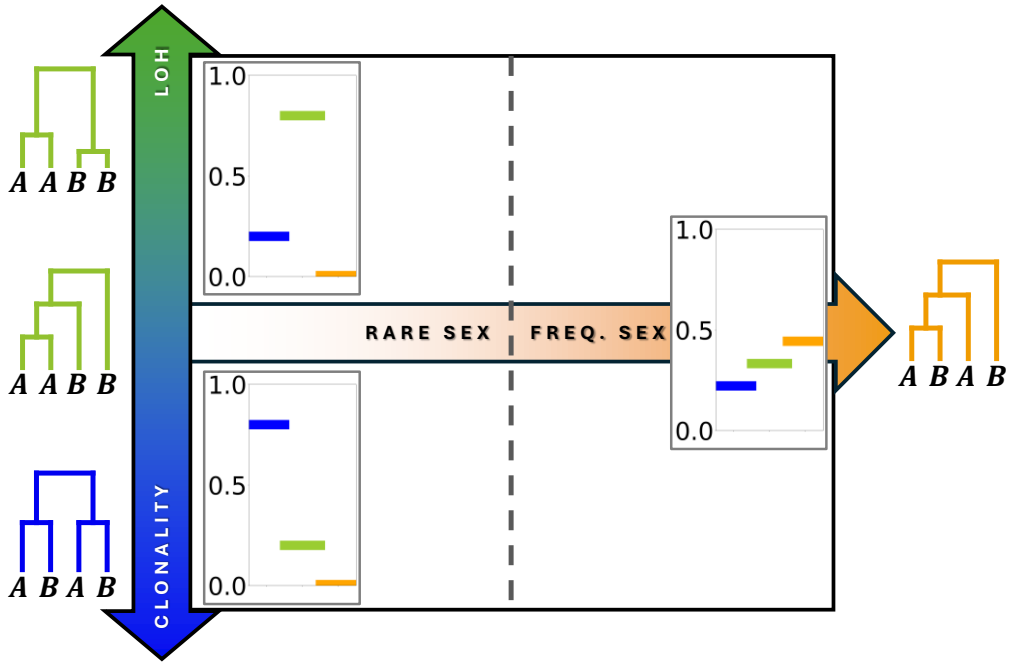


Fig. 3. Genealogical signatures of reproductive mode. Relative proportions p of CL (blue), AR (green) and SX (orange) classes of four-tip trees ('tree composition'; bar plots) distinguish asexual and sexual scenarios (axes). Trees are shown for diploid individuals $\boldsymbol{A}$ and $\boldsymbol{B}$. Total $p(AR)$, and the proportion of balanced AR trees (top left), increase with the rate of asyngamous recombination; $p(SX)$ increases with the rate of sex. See Pieszko et al. (2025) for more details.

To test tree composition signatures for the 45 possible pairs of individuals per *Rotaria* species, we extracted phased segments where all four haplotypes could be resolved simultaneously (Materials and Methods; Table S2 and S3). After filtering out segments with < 100 variants (likely to display weak genealogical signal), we retained 1,361–2,709 such segments for *R. magnacalcarata* pairs (average length 4.6–5.5 kb; total 10.6 Mb; Table S3) and 1,119–1,876 for *R. socialis* pairs (average length 4.7–5.6 kb; total 8.1 Mb; Table S3). We then reconstructed local trees using a simple clustering approach[2] validated by simulation (Materials and Methods; see Fig S3B for tree composition

[2] The same approach as in Chapter 2.

reconstructed across the space of simulated scenarios). In the Silwood populations of both species (Fig. 4A; see Table S4 for per-pair proportions of trees), $p(CL)$ was highest (RM_{SIL}: 0.875; RS_{SIL}: 0.901), $p(AR)$ was lowest (RM_{SIL}: 0.013; RS_{SIL}: 0.08), and $p(SX)$ was intermediate (RM_{SIL}: 0.111; RS_{SIL}: 0.091).

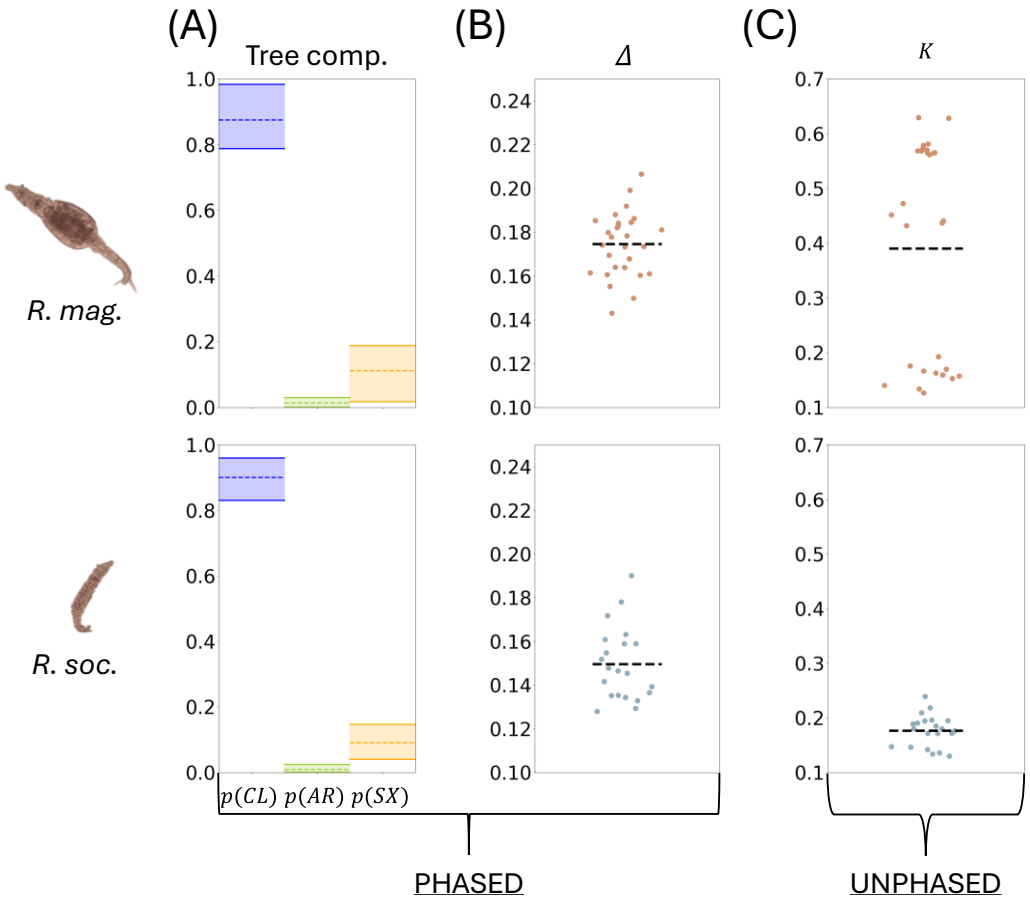


Fig. 4. Results of genealogical analysis in *Rotaria*: metrics calculated for phased segments (A - tree composition, B - Δ) and unphased, genome-wide SNPs (C - K). Each plot is based on values obtained for the 28 pairs of individuals from the Silwood populations. Dashed horizontal lines denote means; the tree composition plots additionally show the spread (minimum-maximum) within each tree category.

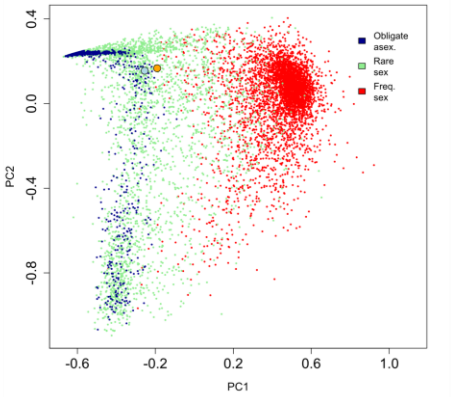
One challenge in interpreting an empirical tree composition is that phased segments may represent a biased sample of the genome. Indeed, *Rotaria* phased segments covered only 6.1% and 5.4% of the *R. magnacalcarata* and *R. socialis* reference assemblies, respectively. Strikingly, heterozygosity was approx. 10-fold higher in phased segments (an average of 2.76% across both species) than overall, consistent with an overrepresentation of CL trees (Pieszko et al., 2025). We therefore introduced a 'heterozygosity bias' (β) of a similar magnitude into our simulations by (1) only sampling the most heterozygous 5% of simulated sequence (β = 0.05) and (2) optimising mutation rates to ensure heterozygosity in these regions matched that of *Rotaria* phased segments (see Materials and Methods and Fig S3C for tree composition recomputed across the space of simulated scenarios). In both species, the observed tree composition was most similar (Euclidean distance) to that observed under a range of scenarios where the rate of sex was ≤ $\frac{1}{N}$ (Fig. S4) – that is, below a boundary rate defining 'rare sex' (Hartfield et al., 2018; Pieszko et al., 2025).

To capture additional sources of genealogical signal, we calculated two statistics derived from the tree-based framework: Δ (delta) and K (kappa) (Pieszko et al., 2025). The Δ statistic, calculated for polarised SNPs within phased segments, captures variation in internal coalescence times not accounted for by the tree classification scheme. Namely, Δ quantifies asymmetry in the lengths of external branches of local CL and, if present, SX trees, with larger average asymmetry linked to genetic exchange. In turn, the K statistic uses unphased, polarised SNPs to quantify the genome-wide signal of reproductive mode, thereby avoiding the bias associated with phasing. Both statistics take low values under obligate asexuality ($\Delta \approx 0$, $K \leq 0.39$), which increase with the rate

of sex (see Fig. S5 for values across the space of simulated scenarios after *Rotaria*-specific processing described above). In both *Rotaria* species, the average values of K (RM_{SIL}: 0.390, RS_{SIL}: 0.176; Fig. 4C) were consistent with obligate asexual histories (Fig S6). Interestingly, however, Δ was positive for all pairs of individuals (RM_{SIL}: 0.174, RS_{SIL}: 0.150 on average; Fig. 4B), similar to simulated scenarios of rare sex but not obligate asexuality (Fig S7).

To synthesise information from the various summary statistics, we performed approximate Bayesian computation (ABC) using a rejection algorithm to estimate posterior distributions of the sex rate σ and the LOH rate γ for the studied *Rotaria* (Fig. 5). We used the R package 'abc' (Csilléry et al., 2012) with a tolerance rate of 0.05. As summary statistics, we used $p(CL)$, $p(AR)$, $p(SX)$, Δ, and K, computed across the simulated parameter space of σ and γ, and compared them with the mean observed values for *R. magnacalcarata* and *R. socialis*. Within the multidimensional space of simulated statistics (Fig. 5A), the 95% credible intervals from the ABC analysis encompassed σ = 0.0 and γ = 0.0 for both species, with median estimates on the order of 10^{-2} – 10^{-1} N^{-1} for both parameters (Fig. 5B). Taken together, despite the ambiguity of individual statistics, analysis of multiple genealogical features revealed no compelling evidence for cryptic sex in *R. magnacalcarata* or *R. socialis*.

(A)



(B)

	σ_{RM}	σ_{RS}	γ_{RM}	γ_{RS}
Min.:	0.00	0.00	0.00	0.00
2.5% Perc.:	0.00	0.00	0.00	0.00
Median:	$0.316\ N^{-1}$	$0.100\ N^{-1}$	$0.158\ N^{-1}$	$0.016\ N^{-1}$
Mean:	$0.512\ N^{-1}$	$0.396\ N^{-1}$	$0.282\ N^{-1}$	$0.025\ N^{-1}$
Mode:	$0.121\ N^{-1}$	$0.036\ N^{-1}$	$0.052\ N^{-1}$	$0.005\ N^{-1}$
97.5% Perc.:	$3.16\ N^{-1}$	$0.316\ N^{-1}$	$0.158\ N^{-1}$	$0.500\ N^{-1}$
Max.:	$10.0\ N^{-1}$	$0.316\ N^{-1}$	$0.158\ N^{-1}$	$0.158\ N^{-1}$

Fig. 5. The multidimensional space of simulated $p(CL)$, $p(AR)$, $p(SX)$, Δ and K values (phased-segment statistics computed under β = 0.05). (A) The positioning of *R. magnacalcarata* (orange) and *R. socialis* (blue) from Silwood populations against the first two principal components. Scenarios of frequent sex are defined by sex rates > $\frac{1}{N}$, where N = 1,000 is the simulated population size. (B) Summaries of the posterior distributions of the rate of sex σ and rate of LOH γ obtained through rejection-based approximate Bayesian computation (ABC) (Csilléry et al., 2012). Values are expressed in terms of N (= 1,000) for general comparisons.

Independently of the analyses underlying the statistical inference of σ and γ in *Rotaria*, we applied the parsimony block delimitation (PBD) approach as an empirical test case of the novel method. Fig. 6 shows PBD estimates of tree composition obtained for *R. magnacalcarata* and *R. socialis*, alongside those presented in Fig. 4A. From the raw PBD estimates, we excluded blocks defined by lone tripleton SNPs (i.e., flanked by incompatible sites), as such sites are weakly informative – each being compatible with three different unbalanced trees – and possibly artefactual (e.g., due to mapping error). While sequence fragmentation is expected to induce a skew towards balanced trees (Chapter 2, Fig. S1), the PBD estimates for both species showed higher $p(SX)$ and lower $p(CL)$ than the clustering-based estimates ($p(CL)$: 0.875 → 0.750 in *R. mag.* and 0.901 → 0.812 in *R. soc.*; $p(SX)$: 0.111 → 0.231 in *R. mag* and 0.091 → 0.177 in *R. soc.*).

Consistently low estimates of $p(AR)$, which are affected by heterozygosity bias irrespective of reproductive mode (see Chapter 1), suggest that mixed AR-CL signal was unlikely to underlie a substantial proportion of the recovered SX blocks. Accordingly, further investigations should focus on homoplasy-driven spurious sex signals, accounting for which will likely lower the estimated $p(SX)$.

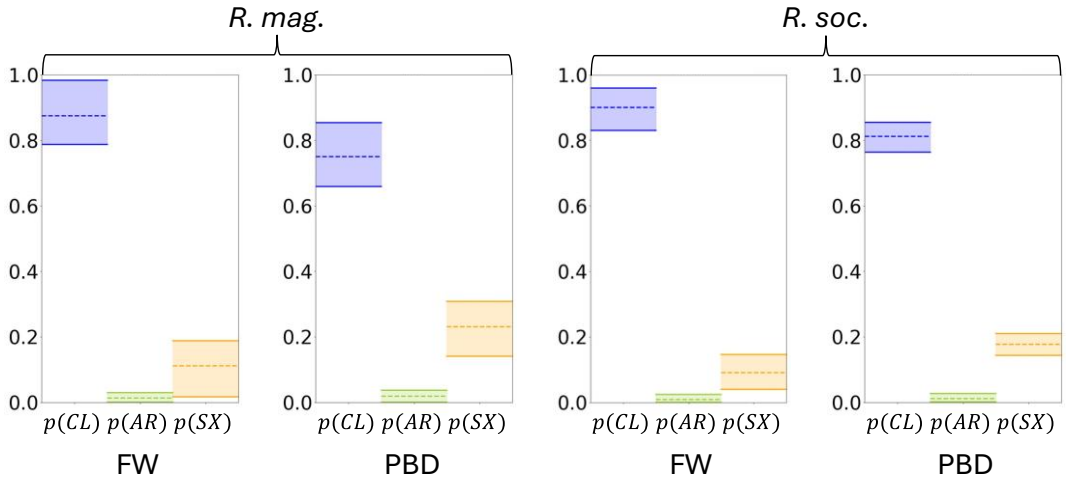


Fig. 5. PBD-based estimates of tree composition compared with those obtained using standard genealogical inference in fixed-length windows (the 'FW' approach; k = 100 SNPs). The FW estimates are reproduced from Fig. 4A. For both species, only individuals from the Silwood populations were included.

As a final, complementary analysis to check the robustness of our methodology, we analysed gene (ortholog) trees reconstructed using heterozygosity-aware substitution models. 'Lineage-level' trees inferred from concatenated orthologs were congruent with the mitochondrial trees for each species (Fig. S1). Moreover, individual gene trees showed high levels of congruence with the lineage-level trees (Fig. S1B). Besides unresolved sub-clades with minimal divergence between several individuals, gene trees displayed a consistent phylogenetic signal as opposed to an even distribution of

alternative topologies (P < 0.0001, Monte Carlo randomisation of tips across gene trees), providing independent support for the asexual divergence hypothesis and a limited extent of asyngamous recombination.

Discussion

Bdelloid rotifers present an intriguing putative case of ecological divergence and diversification into large numbers of species without direct evidence for sexual reproduction. We set out to test the role of genetic exchange for bdelloid divergence by focusing on two co-occurring species of the genus *Rotaria* that live in neighbouring micro-niches.

Overall, our results support the 'asexual hypothesis' of divergence between the two species. The limited conflict with the obligate asexual expectations (e.g., Fig. 4B) is more parsimoniously explained by deviations from assumptions of the simulation model than by cryptic sex. For example, any variation in mutation rate or patterns of selection can lead to inflated (positive) Δ values. Unlike our results, previous studies (Vakhrusheva et al., 2020; Laine et al., 2022) used population genomic data to argue for cryptic sex in other bdelloid species. While reproductive variability could be expected in a clade as ancient and diverse as the Bdelloidea (Segers, 2007; Tang et al., 2014), previous analyses did not explicitly account for the genealogical signatures of asyngamous recombination, which we do here.

Members of the genus *Rotaria* harbour the lowest levels of intragenomic divergence (< 0.5%) among the bdelloids studied to date (typically 1–5%; Nowell et al., 2018; Mark Welch et al., 2008), and the two species examined here are no exception. At first glance, relatively low heterozygosity may be taken to reflect higher rates of LOH, consistent with

high rates of asyngamous recombination or with certain modes of parthenogenetic ploidy restoration (e.g., Freitas et al., 2023). Intriguingly, we found a dominant signal of clonal descent replicated across different genome compartments: from assembly-wide SNPs (Fig. 2A-C; Fig. 4C), through coding sequence (Fig. S1), to phased sequence blocks (Fig. 4A). In this context, lower heterozygosity could be simply reflective of smaller population sizes than in other bdelloids, which appears likely for the host-confined epibionts, lower mutation rates, or both. Alternatively, LOH in *Rotaria* could occur in episodic bursts, allowing clonal signatures to accumulate in a low-diversity background.

The analyses presented here were conducted in parallel to an investigation into the possibility of near HGT between the two species (Nowell, Wilson and Barraclough, unpublished). Among 7,377 ortholog trees inferred jointly for the two species and a set of other bdelloids (see Fig. S8 for an ortholog-based species tree), the great majority (7,170; 97.2%) recovered *R. magnacalcarata* and *R. socialis* as reciprocally monophyletic sister taxa. Of the 207 trees that failed to recover monophyly, only four could not be explained by gene duplication or potential annotation or orthogroup assignment errors, consistent with the extreme rarity of near HGT events and arguing against interspecific sexual exchange. These results further imply that divergence into distinct niches can indeed occur without the usual interplay of genetic exchange (canonical or not) and diversifying selection. While the broader question of cryptic sex in bdelloid rotifers, and of the ‘ancient asexual’ status of the whole group, remains open, our analysis highlights the two *Rotaria* species as a putative case of asexual speciation in animals.

Materials and Methods

Rotifer sampling and DNA extraction

Asellus aquaticus individuals were collected from the localities in Table S1. Individual rotifers were isolated by shaking *A. aquaticus* individuals to dislodge epibionts found on the body. The two species are easily distinguishable based on size and body shape: *R. magnacalcarata* is twice as large as *R. socialis*, and rotund around the middle. After starving in distilled water for up to 10 days to reduce gut content, animals were transferred by needle to a clean tube for DNA extraction. DNA was extracted with a QIAamp DNA Micro Kit (Qiagen), whole-genome amplified (WGA) using a REPLI-g Single Cell kit (Qiagen) and sequenced on either Illumina NextSeq500 at the Department of Biochemistry, University of Cambridge (UK) or Illumina HiSeq X at Edinburgh Genomics, University of Edinburgh (UK) as in Table S1. Previous work using multiple biological replicates has supported the repeatability of sequencing, assembly and analysis steps using whole-genome amplified DNA prepared by these methods (Nowell et al. 2021).

Genome assembly, annotation and orthogroup assignment

Genomes were assembled using methods in Nowell et al. (2021). In brief, raw sequence data were filtered for low quality bases and adapter sequence, and error corrected using BBTools v37.62 (Bushnell, 2017). An initial assembly using SPAdes v3.13.0 (Bankevich et al., 2012) with default settings was refined by removal of contaminating reads from non-target organisms based on GC content, read coverage and/or taxonomic annotation using repeated rounds of BlobTools v1.1.1 (Buchfink et al., 2015; Laetsch & Blaxter, 2017). Haplotigs were collapsed using Redundans (Pryszcz & Gabaldón, 2016) before scaffolding and gap filling. We used BUSCO v3.0.2 (Simão et al., 2015) to calculate

gene-completeness scores for core eukaryotic genes (n = 303). Gene prediction was conducted using BRAKER v2.1.2 (Hoff et al., 2019; Hoff et al., 2016; Barnett et al., 2011; Stanke et al., 2008; Stanke et al., 2006) guided by trimmed and mapped RNA-seq data from Eyres et al. (2015).

Coding genes from the wider sample of bdelloid rotifer genomes including the focal genomes in the two species found on louse were assigned to orthologs using OrthoFinder v2.3.12 (Emms & Kelly, 2019). For species-level analyses, ortholog groupings were filtered to remove large gene families that might obscure inferences of relationships among individuals, and any that were poorly represented across our focal *Rotaria*. Inspection revealed two modes in number of gene copies: equal to the number of genomes (n = 46), and twice the number of genomes (n = 92). The former represent cases where divergent copies associated with tetraploidy were split into separate orthogroups, whereas the latter cases grouped tetraploid copies in a single orthogroup. Whenever two basal clades were present, both of which contained sequences from all of the represented species, we split them into arbitrary orthogroups A and B.

Variant calling

We mapped cleaned and filtered reads onto a single reference assembly for both species in turn (RM9 for *R. magnacalcarata* and RS1 for *R. socialis*) using BBMap and called variants using ‘callvariants’ from the BBTools suite (Bushnell, 2017). The geographically isolated Italian samples were chosen as reference assemblies (Table S1) to enable the calling of polarised SNPs in the target Silwood populations., Polarised SNPs arerequired for computing the Δ and K statistics (Pieszko et al., 2025). To obtain sets of high-confidence SNPs for calculating summary statistics and phasing (see

below), we excluded regions annotated de novo as repeats by RepeatModeler2 (Flynn et al., 2020) and RepeatMasker v4.1.0 (Smit et al., 2013), and retained only biallelic SNPs for downstream analysis.

Analyses of phased blocks

Using the mapped reads and filtered SNP sets, we performed within-read phasing using the 'phase' command of WhatsHap v1.4 (Martin et al. 2016), setting the flag '--distrust-genotypes' to allow optimisation of phased blocks. We used the 'stats' command with the '--block-list' flag to output phased intervals for each genome, then extracted haplotype blocks using bespoke code. Using the same intervals, we extracted VCF files corresponding to blocks simultaneously phased within all possible pairs of individuals. In total, there were 45 such pairs per species, each including 28 Silwood-only pairs individuals.

Reproductive mode inference from tree composition might be affected by reconstruction errors. For example, the mis-inference of SX trees may falsely suggest rare sex, even in its absence (Wilson et al., 2024; Pieszko et al., 2025). Here, we reconstructed local trees using a clustering approach that appears to match or even exceed the performance of more complex algorithms (Pieszko et al., 2025). We divided the input haplotypes (for two simulated or *Rotaria* individuals at a time) into windows of k SNPs (using k = 100), with midpoints between terminal SNPs as boundaries. For each window, we obtained a distance matrix computed using the 'cityblock' method implemented in scikit-allel v1.3.13 (Miles et al., 2024). We used thus-obtained matrices to reconstruct trees using the Farthest Point Algorithm implemented in scipy v1.14.1 (Virtanen et al., 2020) ('scipy.hierarchy.linkage' with 'method = "complete"'). We recorded the total span of

distinct trees for sub-samples of 8 individuals per simulation (average between $\binom{8}{2}$ individual pairs) as well as all possible pairs of *R. magnacalcarata* and *R. socialis* individuals.

To avoid the influence of error / bias in tree reconstruction, we used a SNP-based procedure of computing Δ described in Pieszko et al. (2025). In brief, we used configurations of doubleton SNPs (i.e., sites with two derived alleles) to localise target regions for computing the statistic (Pieszko et al., 2025). For these regions, we computed Δ using counts of singleton SNPs (i.e., mutations on external branches) and the formula of Pieszko et al. (2025). We obtained Δ values for sub-samples of 8 individuals per simulation (averaged between runs of target doubleton SNPs and $\binom{8}{2}$ individual pairs) as well as all possible pairs of *R. magnacalcarata* and *R. socialis* individuals.

Simulations of obligate and facultative asexuality

We used genealogies simulated using an individual-based model of mitotic parthenogenesis ('MP') with gene conversion by Pieszko et al. (2025). Since all conversion events lead to LOH in the MP model, the rate of asyngamous recombination can be conveniently expressed as the per-site per-generation rate of LOH γ. In summary, the simulated genealogies (length L = 1 Mb, population size N = 1,000, 5,000 generations) spanned a space of asexuality-sex scenarios. The per-generation rate of sex σ varied between10^{-5} and $10^{-0.5}$ (10 logarithmically-distributed rates) and the rate of LOH γ varied between 5×10^{-6} and 5×10^{-3} (7 logarithmically-distributed rates), yielding a total of 88 σ~γ combinations (including σ = 0 and γ = 0). Each scenario was replicated

100 times; sexual burn-in was added post hoc using pyslim v1.0.4 (Haller et al., 2019), See Pieszko et al. (2025) for more details.

To recapitulate the key features of *Rotaria* phased segments, we performed additional processing of the simulating genealogies. Using the coalescent simulator msprime v1.3.2 (Baumdicker et al., 2022), we overlaid neutral mutations under the Jukes-Cantor model onto the simulated genealogies. Rather than using a single mutation rate (Pieszko et al., 2025), we used rates optimised to consistently match the average heterozygosity of the phased segments (H_{obs} = 0.02755). To achieve this, we used Brent's method implemented in scipy v1.14.1 (Virtanen et al., 2020) to find rates that satisfied $H_{sim} - H_{obs} \approx 0$, where H_{sim} is the heterozygosity of the top 0.05 highly heterozygous regions of the simulated chromosomes computed in windows of 5 kb (i.e., approx. the average length of *Rotaria* phased segments). We reconstructed trees and computed Δ for both biased and total (unbiased) simulated genealogies.

References

Bankevich, A., Nurk, S., Antipov, D., Gurevich, A. A., Dvorkin, M., Kulikov, A. S., Lesin, V. M., Nikolenko, S. I., Pham, S., & Prjibelski, A. D. (2012). SPAdes: a new genome assembly algorithm and its applications to single-cell sequencing. *Journal of Computational Biology*, *19*(5), 455–477.

Barnett, D. W., Garrison, E. K., Quinlan, A. R., Strömberg, M. P., & Marth, G. T. (2011). BamTools: a C++ API and toolkit for analyzing and managing BAM files. *Bioinformatics*, *27*(12), 1691–1692.

Barraclough, T. G. (2019). Species and speciation without sex. In *Evolutionary Biology of Species*. Oxford University Press. <Go to ISI>://WOS:000482747300007

Barraclough, T. G., Birky, C. W., & Burt, A. (2003). Diversification in sexual and asexual organisms. *Evolution*, *57*(9), 2166–2172. <Go to ISI>://000185674500018

Becks, L., & Agrawal, A. F. (2012). The evolution of sex is favoured during adaptation to new environments. *PLoS biology*, *10*(5), e1001317.

Birky, C. W., Wolf, C., Maughan, H., Herbertson, L., & Henry, E. (2005). Speciation and selection without sex. *Hydrobiologia*, *546*, 29–45. <Go to ISI>://000233117900004

Birky Jr, C. W. (2010). Positively negative evidence for asexuality. *Journal of Heredity*, *101*, S42–S45. https://doi.org/10.1093/jhered/esq014

Birky Jr., C. W. (1996). Heterozygosity, heteromorphy, and phylogenetic trees in asexual eukaryotes. *Genetics*, *144*(1), 427–437.

Blanc, C., Saclier, N., Le Faou, E., Marie-Orleach, L., Wenger, E., Diblasi, C., Glemin, S., Galtier, N., & Delattre, M. (2023). Co-segregation of recombinant chromatids maintains genome-wide heterozygosity in an asexual nematode. *bioRxiv*, 2023.2003. 2017.533182.

Boschetti, C., Carr, A., Crisp, A., Eyres, I., Wang-Koh, Y., Lubzens, E., Barraclough, T. G., Micklem, G., & Tunnacliffe, A. (2012). Biochemical diversification through foreign gene expression in bdelloid rotifers. *PLoS Genetics*, *8*(11), e1003035.

Buchfink, B., Xie, C., & Huson, D. H. (2015). Fast and sensitive protein alignment using DIAMOND. *Nature Methods*, *12*(1), 59–60.

Burt, A. (2000). Perspective: Sex, recombination, and the efficacy of selection - Was Weismann right? *Evolution*, *54*(2), 337–351. <Go to ISI>://WOS:000086886500001

Bushnell, B. (2017). BBMap short read aligner, and other bioinformatic tools. https://sourceforge.net/projects/bbmap/

Chase, M. A., Ellegren, H., & Mugal, C. F. (2021). Positive selection plays a major role in shaping signatures of differentiation across the genomic landscape of two independent Ficedula flycatcher species pairs*. *Evolution*, *75*(9), 2179–2196. https://doi.org/10.1111/evo.14234

Cohan, F. M. (2001). Bacterial species and speciation. *Systematic Biology*, *50*(4), 513–524. <Go to ISI>://000171061000006

Colegrave, N. (2002). Sex releases the speed limit on evolution. *Nature*, *420*(6916), 664–666.

Coyne, J. A., & Orr, H. A. (2004). *Speciation*. Sinauer Associates.

Csilléry, K., François, O., & Blum, M. G. (2012). abc: an R package for approximate Bayesian computation (ABC). *Methods in ecology and evolution*, *3*(3), 475–479.

Dobzhansky, T. (1937). *Genetics and the origin of species*. Columbia University Press.

Emms, D. M., & Kelly, S. (2019). OrthoFinder: phylogenetic orthology inference for comparative genomics. *Genome biology*, *20*(1), 238.

Eyres, I., Boschetti, C., Crisp, A., Smith, T. P., Fontaneto, D., Tunnacliffe, A., & Barraclough, T. G. (2015). Horizontal gene transfer in bdelloid rotifers is ancient, ongoing and more frequent in species from desiccating habitats. *BMC biology*, *13*(1), 90.

Feder, J. L., Egan, S. P., & Nosil, P. (2012). The genomics of speciation-with-gene-flow. *Trends in Genetics*, *28*(7), 342–350. https://doi.org/10.1016/j.tig.2012.03.009

Flot, J.-F., Hespeels, B., Li, X., Noel, B., Arkhipova, I., Danchin, E. G., Hejnol, A., Henrissat, B., Koszul, R., & Aury, J.-M. (2013). Genomic evidence for ameiotic evolution in the bdelloid rotifer Adineta vaga. *Nature*, *500*(7463), 453–457.

Flynn, J. M., Hubley, R., Goubert, C., Rosen, J., Clark, A. G., Feschotte, C., & Smit, A. F. (2020). RepeatModeler2 for automated genomic discovery of transposable element families. *Proceedings of the National Academy of Sciences*, *117*(17), 9451–9457.

Fontaneto, D., & Ambrosini, R. (2010). Spatial niche partitioning in epibiont rotifers on the waterlouse Asellus aquaticus. *Limnology and Oceanography*, *55*(3), 1327–1337. https://doi.org/https://doi.org/10.4319/lo.2010.55.3.1327

Fontaneto, D., Barraclough, T. G., Chen, K., Ricci, C., & Herniou, E. A. (2008). Molecular evidence for broad-scale distributions in bdelloid rotifers: everything is

not everywhere but most things are very widespread. *Molecular Ecology*, *17*(13), 3136–3146.
Fontaneto, D., Herniou, E. A., Boschetti, C., Caprioli, M., Melone, G., Ricci, C., & Barraclough, T. G. (2007). Independently evolving species in asexual bdelloid rotifers. *PLoS biology*, *5*(4), 914–921. https://doi.org/ARTN e87
10.1371/journal.pbio.0050087
Freitas, S., Parker, D. J., Labédan, M., Dumas, Z., & Schwander, T. (2023). Evidence for cryptic sex in parthenogenetic stick insects of the genus Timema. *Proceedings of the Royal Society B*, *290*(2007), 20230404.
Garnier-Géré, P., & Chikhi, L. (2013). Population subdivision, Hardy–Weinberg equilibrium and the Wahlund effect. *Els*.
Gavrilets, S. (2004). *Fitness landscapes and the origin of species*. Princeton University Press.
Gladyshev, E. A., Meselson, M., & Arkhipova, I. R. (2008). Massive horizontal gene transfer in bdelloid rotifers. *Science*, *320*(5880), 1210–1213.
Goddard, M. R., Godfray, H. C. J., & Burt, A. (2005). Sex increases the efficacy of natural selection in experimental yeast populations. *Nature*, *434*(7033), 636–640.
Hartfield, M., Wright, S. I., & Agrawal, A. F. (2016). Coalescent times and patterns of genetic diversity in species with facultative sex: effects of gene conversion, population structure, and heterogeneity. *Genetics*, *202*(1), 297–312.
Hartfield, M., Wright, S. I., & Agrawal, A. F. (2018). Coalescence and linkage disequilibrium in facultatively sexual diploids. *Genetics*, *210*(2), 683–701.
Hoff, K. J., Lange, S., Lomsadze, A., Borodovsky, M., & Stanke, M. (2016). BRAKER1: unsupervised RNA-Seq-based genome annotation with GeneMark-ET and AUGUSTUS. *Bioinformatics*, *32*(5), 767–769.
Hoff, K. J., Lomsadze, A., Borodovsky, M., & Stanke, M. (2019). Whole-genome annotation with BRAKER. In *Gene prediction: methods and protocols* (pp. 65–95). Springer.
Houtain, A., Derzelle, A., Llirós, M., Hespeels, B., Nicolas, É., Simion, P., Virgo, J., Lenormand, T., Hallet, B., & Van Doninck, K. (2024). Transgenerational chromosome repair in the asexual bdelloid rotifer *Adineta vaga*. *bioRxiv*, 2024.2001.2025.577190. https://doi.org/10.1101/2024.01.25.577190
Judson, O. P., & Normark, B. B. (1996). Ancient asexual scandals. *Trends in ecology & evolution*, *11*(2), 41–46.
Laetsch, D. R., & Blaxter, M. L. (2017). BlobTools: Interrogation of genome assemblies. *F1000Research*, *6*(1287), 1287.
Laine, V. N., Sackton, T. B., & Meselson, M. (2022). Genomic signature of sexual reproduction in the bdelloid rotifer Macrotrachella quadricornifera. *Genetics*, *220*(2), iyab221.
Mark Welch, D. B., Mark Welch, J. L., & Meselson, M. (2008). Evidence for degenerate tetraploidy in bdelloid rotifers. *Proceedings of the National Academy of Sciences*, *105*(13), 5145–5149.
Mark Welch, D. B., & Meselson, M. (2000). Evidence for the evolution of bdelloid rotifers without sexual reproduction or genetic exchange. *Science*, *288*(5469), 1211–1215.
Maynard Smith, J., & Szathmary, E. (1995). *The major transitions in evolution*. W.H. Freeman.
Mayr, E. (1963). *Animal species and evolution*. Harvard University Press.

Moreira, M. O., Fonseca, C., & Rojas, D. (2021). Parthenogenesis is self-destructive for scaled reptiles. *Biology Letters*, *17*(5), 20210006.

Nowell, R. W., Almeida, P., Wilson, C. G., Smith, T. P., Fontaneto, D., Crisp, A., Micklem, G., Tunnacliffe, A., Boschetti, C., & Barraclough, T. G. (2018). Comparative genomics of bdelloid rotifers: Insights from desiccating and nondesiccating species. *PLoS biology*, *16*(4), e2004830.

Nowell, R. W., Barraclough, T. G., & Wilson, C. G. (2021). Bdelloid rotifers use hundreds of horizontally acquired genes against fungal pathogens. *bioRxiv*, 2021.2009. 2004.458992.

Nowell, R. W., Rodriguez, F., Hecox-Lea, B. J., Mark Welch, D. B., Arkhipova, I. R., Barraclough, T. G., & Wilson, C. G. (2024). Bdelloid rotifers deploy horizontally acquired biosynthetic genes against a fungal pathogen. *Nature Communications*, *15*(1), 5787.

Pieszko, T., Kelleher, J., Wilson, C. G., & Barraclough, T. G. (2025). Detecting and quantifying rare sex in natural populations. *bioRxiv*, 2025.2006. 2003.657731.

Pryszcz, L. P., & Gabaldón, T. (2016). Redundans: an assembly pipeline for highly heterozygous genomes. *Nucleic acids research*, *44*(12), e113–e113.

Ravinet, M., Faria, R., Butlin, R. K., Galindo, J., Bierne, N., Rafajlović, M., Noor, M. A. F., Mehlig, B., & Westram, A. M. (2017). Interpreting the genomic landscape of speciation: a road map for finding barriers to gene flow. *Journal of Evolutionary Biology*, *30*(8), 1450–1477. https://doi.org/https://doi.org/10.1111/jeb.13047

Ricci, C. N. (1987). Ecology of bdelloids: how to be successful. *Hydrobiologia*, *147*(1), 117–127. https://doi.org/10.1007/BF00025734

Rogers, A. R., & Huff, C. (2009). Linkage disequilibrium between loci with unknown phase. *Genetics*, *182*(3), 839–844.

Schluter, D., & Rieseberg, L. H. (2022). Three problems in the genetics of speciation by selection. *Proceedings of the National Academy of Sciences*, *119*(30), e2122153119. https://doi.org/10.1073/pnas.2122153119

Segers, H. (2007). Annotated checklist of the rotifers (Phylum Rotifera), with notes on nomenclature, taxonomy and distribution. *Biotaxa*, *1564*(1).

Sendell-Price, A. T., Ruegg, K. C., Anderson, E. C., Quilodrán, C. S., Van Doren, B. M., Underwood, V. L., Coulson, T., & Clegg, S. M. (2020). The Genomic Landscape of Divergence Across the Speciation Continuum in Island-Colonising Silvereyes (Zosterops lateralis). *G3 Genes|Genomes|Genetics*, *10*(9), 3147–3163. https://doi.org/10.1534/g3.120.401352

Simão, F. A., Waterhouse, R. M., Ioannidis, P., Kriventseva, E. V., & Zdobnov, E. M. (2015). BUSCO: assessing genome assembly and annotation completeness with single-copy orthologs. *Bioinformatics*, *31*(19), 3210–3212.

Simion, P., Narayan, J., Houtain, A., Derzelle, A., Baudry, L., Nicolas, E., Arora, R., Cariou, M., Cruaud, C., & Gaudray, F. R. (2021). Chromosome-level genome assembly reveals homologous chromosomes and recombination in asexual rotifer Adineta vaga. *Science Advances*, *7*(41), eabg4216.

Smit, A., Hubley, R., & Green, P. (2013). RepeatMasker Open-4.1.0. http://www.repeatmasker.org

Stanke, M., Diekhans, M., Baertsch, R., & Haussler, D. (2008). Using native and syntenically mapped cDNA alignments to improve de novo gene finding. *Bioinformatics*, *24*(5), 637–644.

Stanke, M., Schöffmann, O., Morgenstern, B., & Waack, S. (2006). Gene prediction in eukaryotes with a generalized hidden Markov model that uses hints from external sources. *BMC bioinformatics*, *7*(1), 62.

Stankowski, S., Chase, M. A., Fuiten, A. M., Rodrigues, M. F., Ralph, P. L., & Streisfeld, M. A. (2019). Widespread selection and gene flow shape the genomic landscape during a radiation of monkeyflowers. *PLoS biology*, *17*(7), e3000391. https://doi.org/10.1371/journal.pbio.3000391

Tajima, F. (1989). Statistical method for testing the neutral mutation hypothesis by DNA polymorphism. *Genetics*, *123*(3), 585–595.

Tang, C. Q., Obertegger, U., Fontaneto, D., & Barraclough, T. G. (2014). Sexual species are separated by larger genetic gaps than asexual species in rotifers. *Evolution*, *68*(10), 2901–2916.

Terwagne, M., Nicolas, E., Hespeels, B., Herter, L., Virgo, J., Demazy, C., Heuskin, A.-C., Hallet, B., & Van Doninck, K. (2022). DNA repair during nonreductional meiosis in the asexual rotifer Adineta vaga. *Science Advances*, *8*(48), eadc8829.

Tigano, A., & Friesen, V. L. (2016). - Genomics of local adaptation with gene flow. - *25*(-10), – 2164. - https://doi.org/10.1111/mec.13606

Vakhrusheva, O. A., Mnatsakanova, E. A., Galimov, Y. R., Neretina, T. V., Gerasimov, E. S., Naumenko, S. A., Ozerova, S. G., Zalevsky, A. O., Yushenova, I. A., Rodriguez, F., Arkhipova, I. R., Penin, A. A., Logacheva, M. D., Bazykin, G. A., & Kondrashov, A. S. (2020). Genomic signatures of recombination in a natural population of the bdelloid rotifer Adineta vaga. *Nature Communications*, *11:6421*. https://doi.org/10.1038/s41467-020-19614-y

Van den Broeck, F., Savill, N. J., Imamura, H., Sanders, M., Maes, I., Cooper, S., Mateus, D., Jara, M., Adaui, V., & Arevalo, J. (2020). Ecological divergence and hybridization of Neotropical Leishmania parasites. *Proceedings of the National Academy of Sciences*, *117*(40), 25159–25168.

Vasilikopoulos, A., Herlyn, H., Fontaneto, D., Wilson, C. G., Nowell, R. W., Flot, J.-F., Barraclough, T. G., & Van Doninck, K. (2024). Whole-genome analyses converge to support the Hemirotifera hypothesis within Syndermata (Gnathifera). *Hydrobiologia*, 1–32.

Virtanen, P., Gommers, R., Oliphant, T. E., Haberland, M., Reddy, T., Cournapeau, D., Burovski, E., Peterson, P., Weckesser, W., & Bright, J. (2020). SciPy 1.0: fundamental algorithms for scientific computing in Python. *Nature Methods*, *17*(3), 261–272.

Wilson, C. G., Nowell, R. W., & Barraclough, T. G. (2018). Cross-contamination explains “inter and intraspecific horizontal genetic transfers” between asexual bdelloid rotifers. *Current Biology*, *28*(15), 2436–2444. e2414.

Wilson, C. G., Pieszko, T., Nowell, R. W., & Barraclough, T. G. (2024). Recombination in bdelloid rotifer genomes: asexuality, transfer and stress. *Trends in Genetics*.

Wolfsberger, W. W., Battistuzzi, F. U., & Oleksyk, T. K. (2022). Genomics of Adaptation and Speciation. *Genes*, *13*(7).

Supplement to Chapter 3



———————— O ————————

Tymoteusz Pieszko, Reuben W. Nowell, Christopher G. Wilson, Jerome Kelleher, Timothy G. Barraclough

———————— O ————————

Supplementary Figures

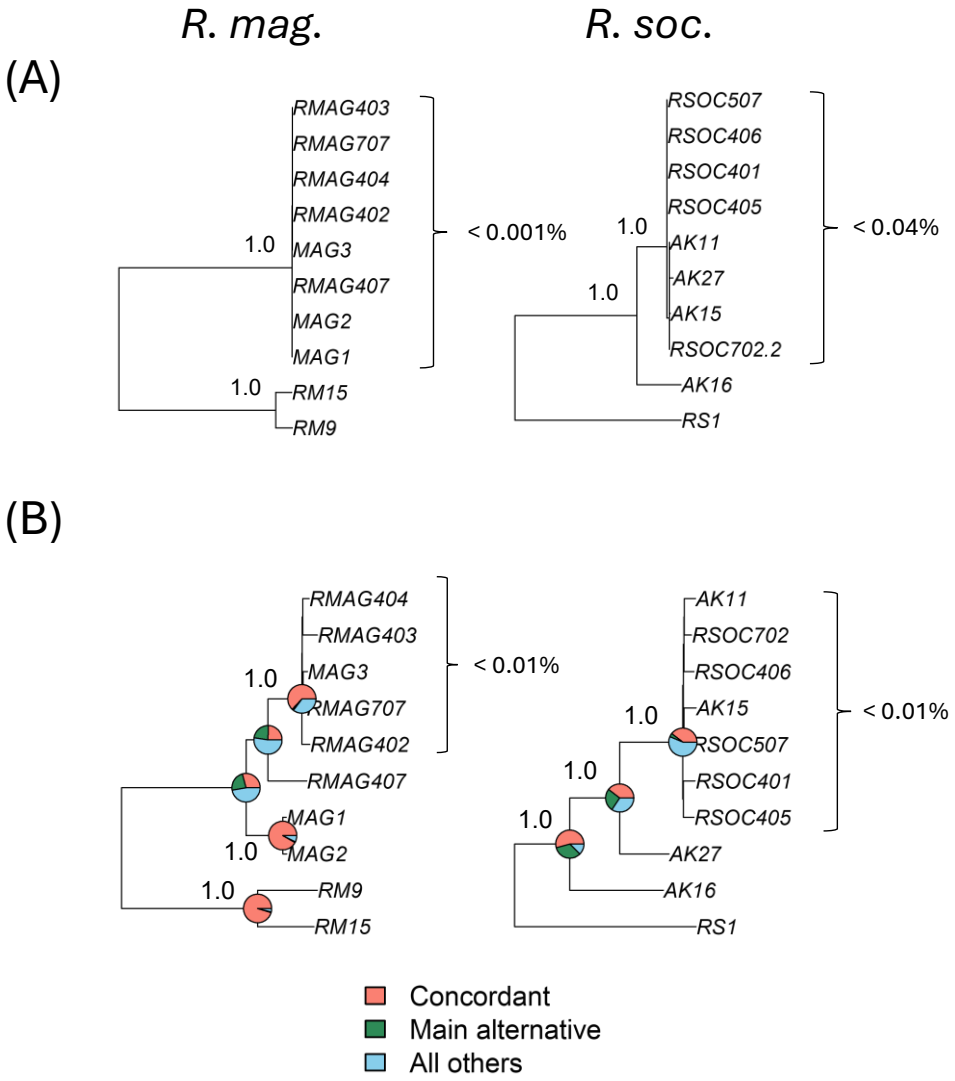


Fig. S1. Phylogenetic relationships among individuals of the two focal species in turn; trees inferred by T.G.B.. Support values show approximate likelihood-ratio test (aLRT) scores > 0.5; curly brackets denote low-divergence regions. (A) Whole mtDNA trees reconstructed using IQ-TREE v2.2.0 (Minh et al., 2020) from assemblies trimmed to exclude regions of alignment ambiguity. (B) Trees inferred from a concatenation of 5288 (*R. magnacalcarata*) and 5009 (*R. socialis*) orthologs using a heterozygosity-aware substitution model. In brief, quality-trimmed reads were mapped onto representative ortholog sequences using BBMap and variants were called using 'callvariants' from the BBTools suite (Bushnell, 2017). Heterozygous sites were represented using IUAPC ambiguity codes, and gene trees, as well as 'lineage-level' trees based on concatenated alignments, were inferred using RaXML-NG v1.2.0 (Kozlov et al., 2019) under the 'GTGTR4+G' substitution model. Pie charts show the proportions of gene trees that are concordant with the lineage-level tree (red), the main alternative topology (green) and all other contradicting topologies (blue), calculated using the R library 'phyparts'.

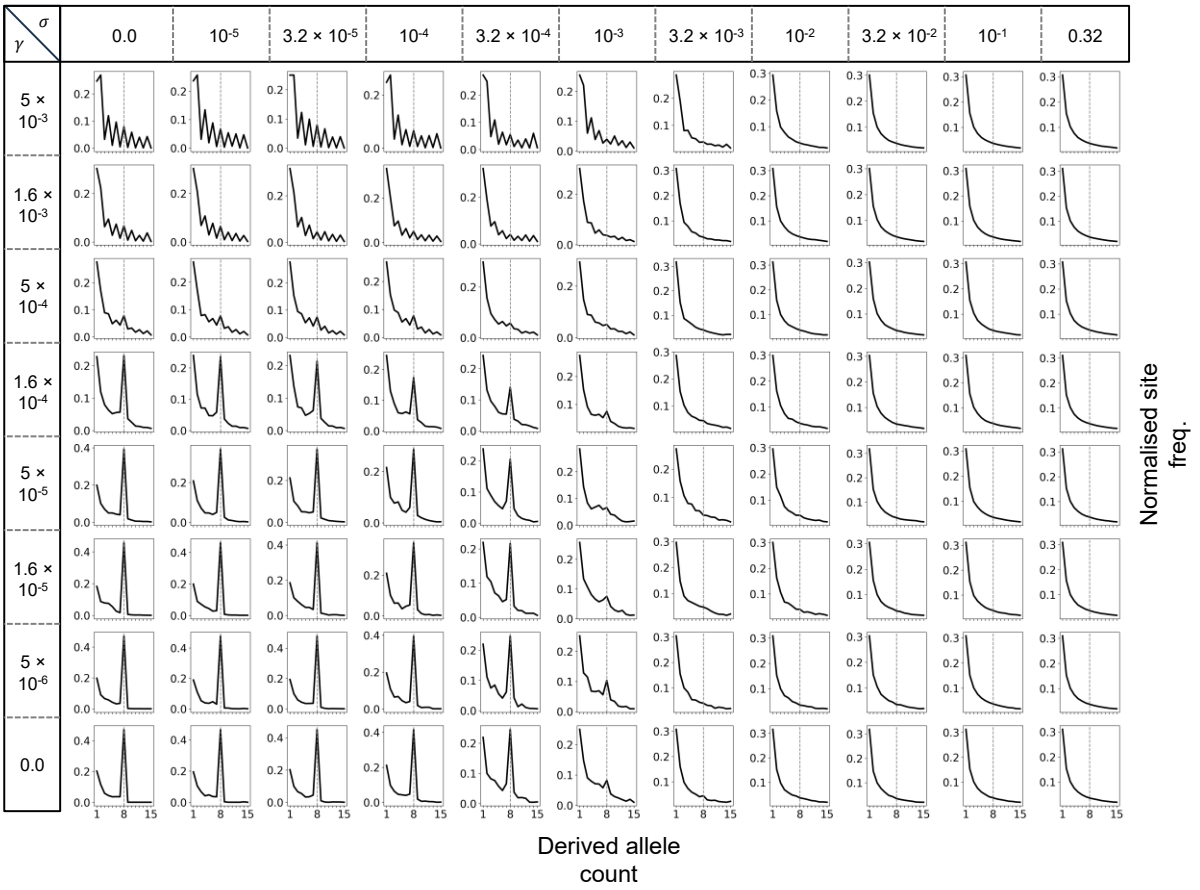


Fig. S2. Normalised site frequency spectrum (SFS; n = 8 individuals) across the simulated (Pieszko et al., 2025) space of the sex rate σ and the LOH rate γ. For each parameter combination, the SFS was obtained by summing site counts across 100 replicates and then normalising by the total number of sites; fixed derived sites are not shown. Dashed vertical lines indicate the 50% frequency class.

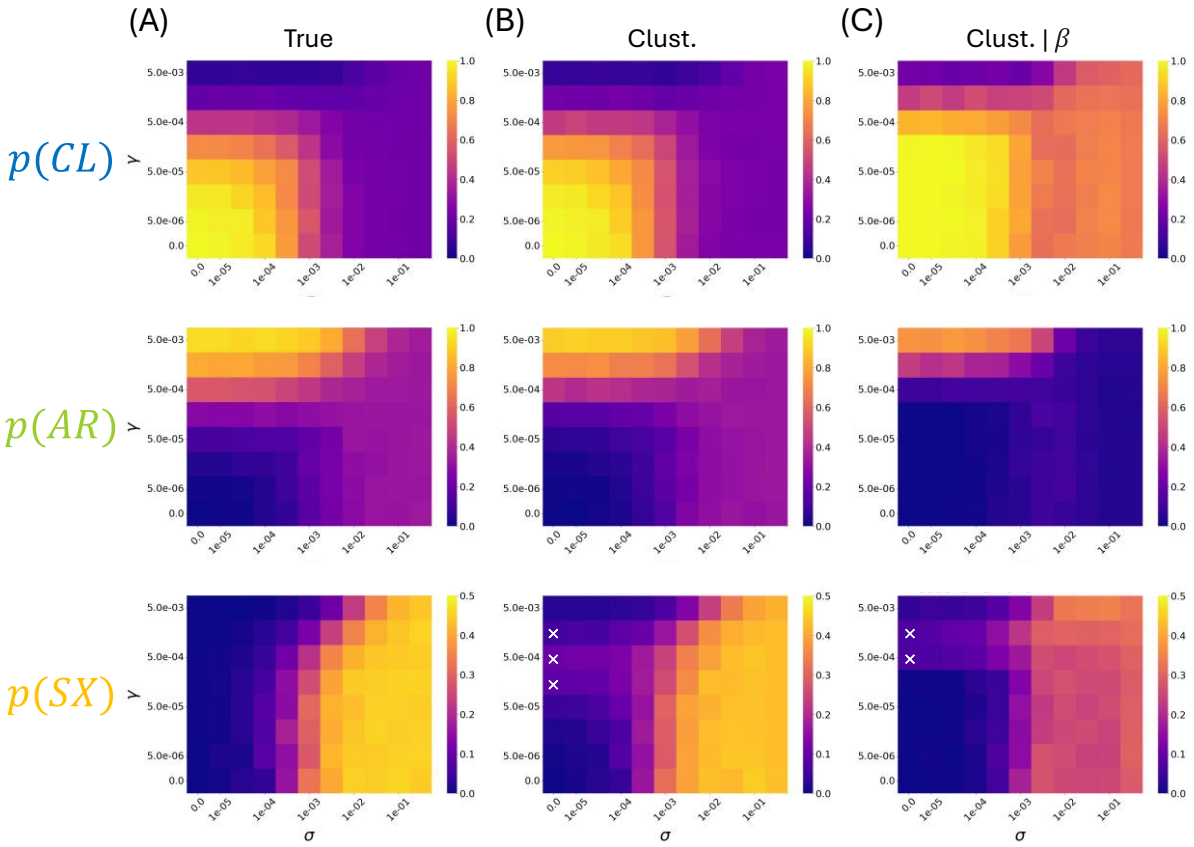


Fig S3. Proportions p of CL, AR and SX trees across the simulated (Pieszko et al., 2025) space of the sex rate σ and the LOH rate γ. Per simulation, mean values were computed for samples of 8 individuals; each scenario was replicated 100 times. White 'x' mark obligate asexual scenarios where $p(SX)$ > 0.05. (A) True proportions. (B) Proportions reconstructed using the clustering approach (k = 100). (C) Proportions reconstructed using the clustering approach (k = 100), given *Rotaria*-optimised mutation rates and when β = 0.05.

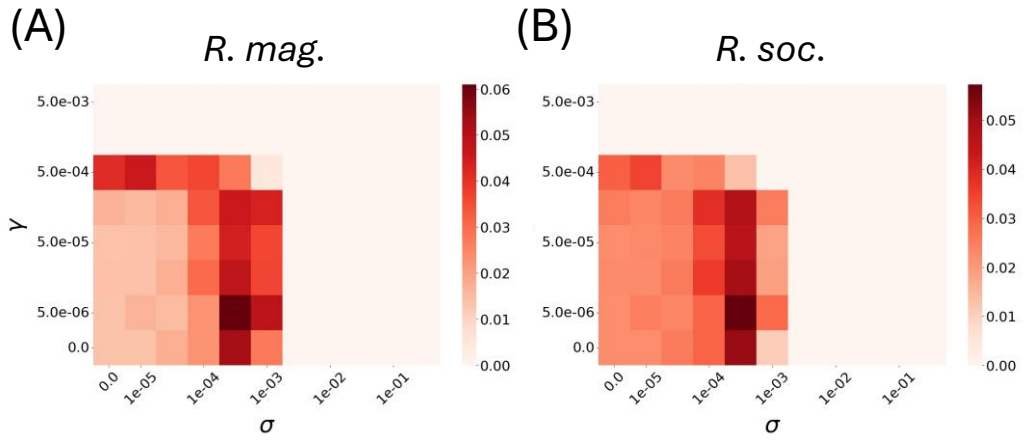


Fig. S4. Euclidean distance of observed tree composition ($p(CL)$, $p(AR)$ and $p(SX)$) from that across the simulated (Pieszko et al., 2025) space of the sex rate σ and the LOH rate γ (optimised mutation rates; β = 0.05). Distances < 0.8 were truncated, and the remaining distances were normalised. (A) *R. magnacalcarata*. (B) *R. socialis*.

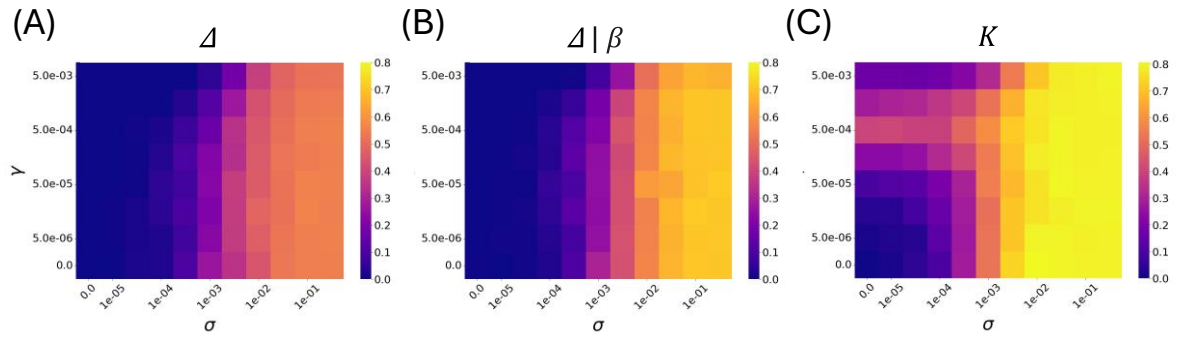


Fig. S5. Δ and K across the simulated (Pieszko et al., 2025) space of the sex rate σ and the LOH rate γ. Per simulation, mean values were computed for samples of 8 individuals; each scenario was replicated 100 times. (A) Δ computed using the SNP-based procedure (optimised mutation rates). (B) Δ (optimised mutation rates; β = 0.05). (C) K (optimised mutation rates).

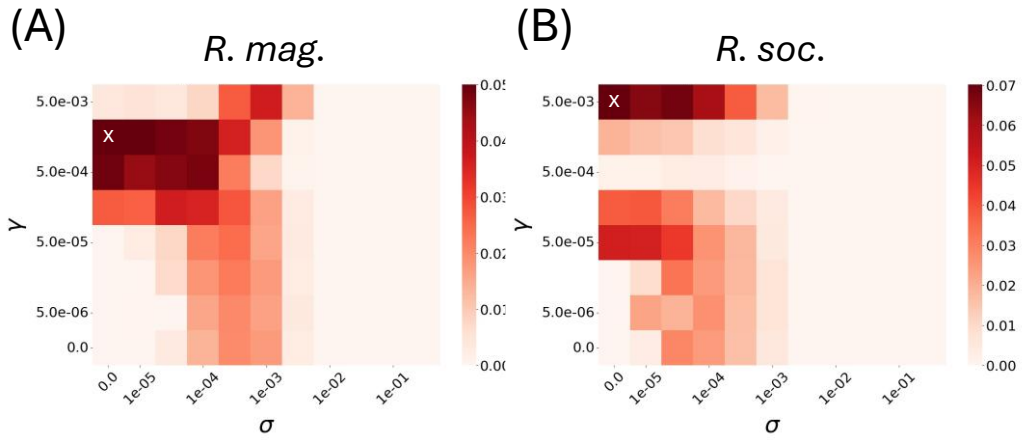


Fig. S6. Likelihood of mean K for Silwood populations across the simulated (Pieszko et al., 2025) space of the sex rate σ and the LOH rate γ (optimised mutation rates). Likelihoods were computed assuming normal distribution of simulated values per scenario (mean for 8 individuals per simulation; 100 replicates), then normalising across scenarios. White 'x' symbols mark the scenarios with highest likelihoods. (A) *R. magnacalcarata*. (B) *R. socialis*.

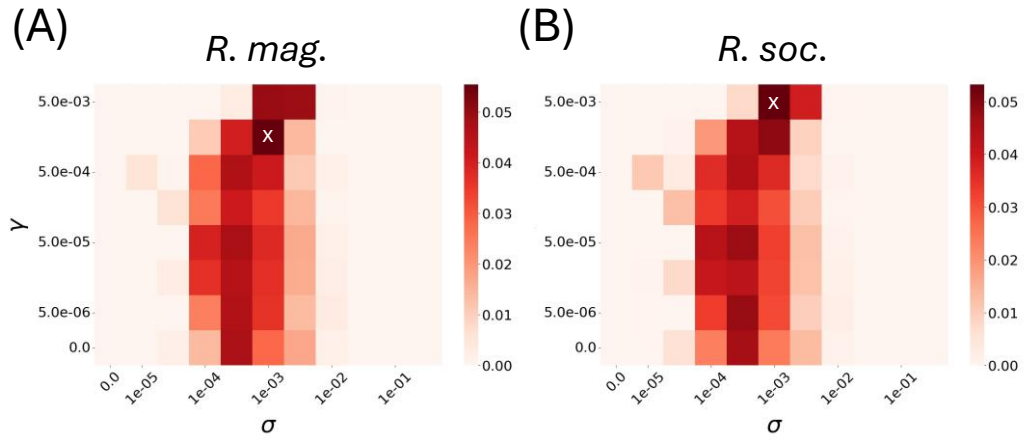


Fig. S7. Likelihood of mean Δ for Silwood populations across the simulated (Pieszko et al., 2025) space of the sex rate σ and the LOH rate γ (optimised mutation rates; β = 0.05). Likelihoods were computed assuming normal distribution of simulated values per scenario (mean for 8 individuals per simulation; 100 replicates), then normalising across scenarios. White 'x' symbols mark the scenarios with highest likelihoods. (A) *R. magnacalcarata*. (B) *R. socialis*.

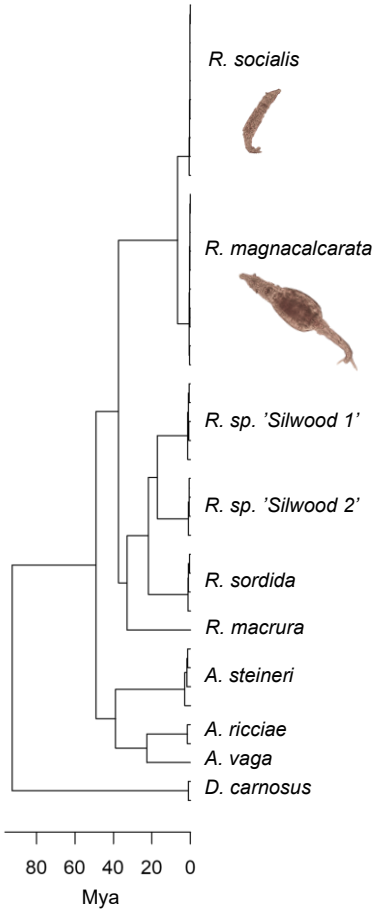


Fig S8. Phylogenomic tree of *Adineta* and *Rotaria* based on ortholog trees; tree inferred by T.G.B.. Outgroups include four additional *Rotaria* species (12 genomes), four other bdelloid species (three *Adineta* species, seven genomes; *Didymodactylos*, two genomes) and three other Syndermata (two monogonont rotifers and an acanthocephalan) from Nowell et al. (2021). Ortholog trees were reconstructed using FastTree v2.1.11 (Price et al., 2010) and a lineage-level tree was constructed using the STAG algorithm (Emms & Kelly, 2018). The tree was calibrated assuming a divergence time between *Adineta* and *Rotaria* of 49 Mya based on Tang et al. (2014). All between-species branching events have STAG support values of 1.

Supplementary Tables

Table S1. A population genomic dataset for epibiotic *Rotaria*.

Individual	Locality	Assembly (Mb)	Num. scaffolds	N50 (kb)	Coverage	Sequencing†
(A) *R. magnacalcarata*.						
MAG1‡	Pond, Silwood Park, UK	178.7	19184	42	60	NextSeq500 (Cam., 2015)
MAG2‡	Pond, Silwood Park, UK	181.1	22216	39.7	55	NextSeq500 (Cam., 2015)
MAG3‡	Pond, Silwood Park, UK	180.9	22132	40.7	51	NextSeq500 (Cam., 2015)
RM9‡	Spring, Fontaneto d'Agogna, Italy	173.8	19520	44	34	NextSeq500 (Cam., 2016)
RM15‡	Spring, Fontaneto d'Agogna, Italy	174	18391	46.5	35	NextSeq500 (Cam., 2016)
RMAG402	Pond, Silwood Park, UK	170.1	8837	67	63	HiSeq X (Edin., 2019)
RMAG403	Pond, Silwood Park, UK	170.4	10991	65.6	45	HiSeq X (Edin., 2019)
RMAG404†	Pond, Silwood Park, UK	171.3	9103	66.8	63	HiSeq X (Edin., 2019)
RMAG407	Pond, Silwood Park, UK	170.9	8847	67	76	HiSeq X (Edin., 2019)
RMAG707	Pond, Silwood Park, UK	174	12361	67	77	HiSeq X (Edin., 2019)
(B) *R. socialis*.						
AK11‡	Pond, Silwood Park, UK	149.2	6303	111.3	39	NextSeq500 (Cam., 2016)
AK15‡	Pond, Silwood Park, UK	147.4	5030	134.7	37	NextSeq500 (Cam., 2016)
AK16‡	Stream, Chobham, UK	147.4	4720	139.5	43	NextSeq500 (Cam., 2016)
AK27‡,§	Pond, Silwood Park, UK	149.9	5952	123.7	36	NextSeq500 (Cam., 2016)
RS1‡	Spring, Fontaneto d'Agogna, Italy	151.1	6254	124.9	40	NextSeq500 (Cam., 2016)
RSOC401	Pond, Silwood Park, UK	151.1	5606	155	47	HiSeq X (Edin., 2019)
RSOC405	Pond, Silwood Park, UK	149.9	4507	156.9	66	HiSeq X (Edin., 2019)
RSOC406	Pond, Silwood Park, UK	151.5	6386	148.1	76	HiSeq X (Edin., 2019)
RSOC507	Pond, Silwood Park, UK	149.4	3848	155.1	74	HiSeq X (Edin., 2019)
RSOC702	Pond, Silwood Park, UK	151.9	5618	167.9	75	HiSeq X (Edin., 2019)

† Cam. = Cambridge; Edin. = Edinburgh.
‡ Previously published in (Nowell et al., 2021).
§ Sampled from 'Lily pond' as opposed to 'Japanese pond' (remaining Silwood individuals).

Table S2. Segments phased in individual *Rotaria* genomes (> 100 SNPs).

Individual	Number of blocks	Min. length (kb)	Max. length (kb)	Mean length (kb)	Mean SNPs
(A) *R. magnacalcarata*.					
MAG2	1029	0.66	48.64	8.88	177.53
MAG3	1066	0.71	41.44	8.8	172.25
RM9	374	1.76	31.02	9.54	152.57
RM15	651	1.09	45.56	9.06	160.43
RMAG402	933	0.75	40.95	8.09	169.55
RMAG403	912	0.75	36.03	7.57	165.4
RMAG404	960	0.69	51.52	7.86	165.07
RMAG407	947	0.75	44.75	8.2	170.99
RMAG707	1007	0.75	36.45	8.04	165.7
MAG1	1029	0.7	40.9	8.77	176.8
(B) *R. socialis*.					
AK11	747	0.92	47.93	8.8	173.93
AK15	677	0.9	47.91	8.5	176.21
AK16	655	0.92	59.5	9.2	176.93
AK27	704	1.04	50.58	8.89	171.38
RS1	381	1.84	40.19	9.68	163.93
RSOC401	690	0.9	49.35	7.64	166.78
RSOC405	654	0.9	73.5	7.84	167.78
RSOC406	674	0.86	49.48	8.16	168.49
RSOC507	673	0.89	42.78	8.24	173.68
RSOC702	695	0.87	48.92	8.15	170.22

Table S3. Segments simultaneously phased in pairs of Rotaria individuals (>100 SNPs).

Pair	Number of blocks	Total length (Mb)	Prop. of reference (%)	Min. length (kb)	Max. length (kb)	Mean length (kb)	Mean number of SNPs
(A) *R. magnacalcarata*.							
MAG1_MAG2	2709	14.9	8.6	0.402	40.4	5.5	199.0
MAG1_MAG3	2452	12.9	7.4	0.497	41.4	5.3	198.6
MAG1_RMAG402	2323	11.4	6.6	0.403	35.2	4.9	194.2
MAG1_RMAG403	2274	11.0	6.3	0.403	33.8	4.8	192.0
MAG1_RMAG404	2324	11.4	6.6	0.403	39.4	4.9	194.3
MAG1_RMAG407	2312	11.7	6.7	0.403	40.2	5.1	196.8
MAG1_RMAG707	2383	11.9	6.9	0.407	34.3	5.0	195.3
MAG1_RM9	1430	6.9	4.0	0.445	24.5	4.8	188.6
MAG1_RM15	1852	9.0	5.2	0.544	34.4	4.9	191.4
MAG2_MAG3	2502	13.3	7.7	0.497	41.1	5.3	198.4
MAG2_RMAG402	2348	11.5	6.6	0.425	35.4	4.9	193.5
MAG2_RMAG403	2300	11.2	6.4	0.425	33.8	4.9	191.7
MAG2_RMAG404	2359	11.7	6.7	0.425	34.9	5.0	194.3
MAG2_RMAG407	2360	11.9	6.8	0.425	35.6	5.0	194.9
MAG2_RMAG707	2410	12.2	7.0	0.425	34.3	5.0	195.7
MAG2_RM9	1420	6.9	4.0	0.445	28.9	4.8	190.2
MAG2_RM15	1875	9.0	5.2	0.443	34.4	4.8	191.0
MAG3_RMAG402	2446	12.4	7.2	0.497	38.7	5.1	194.6
MAG3_RMAG403	2387	12.0	6.9	0.409	33.8	5.0	193.4
MAG3_RMAG404	2458	12.4	7.1	0.497	39.8	5.0	193.7
MAG3_RMAG407	2340	11.9	6.9	0.472	40.6	5.1	195.6
MAG3_RMAG707	2524	13.0	7.5	0.497	37.8	5.2	195.3
MAG3_RM9	1447	7.1	4.1	0.445	24.9	4.9	187.4
MAG3_RM15	1840	9.0	5.2	0.497	37.4	4.9	191.7
RMAG402_RMAG403	2475	12.5	7.2	0.403	33.8	5.0	192.6
RMAG402_RMAG404	2513	12.9	7.4	0.403	38.1	5.1	194.6
RMAG402_RMAG407	2381	12.2	7.0	0.403	34.7	5.1	194.6
RMAG402_RMAG707	2571	13.4	7.7	0.403	38.2	5.2	195.7
RMAG403_RMAG404	2487	12.7	7.3	0.403	34.3	5.1	193.3
RMAG403_RMAG407	2379	12.1	7.0	0.403	36.0	5.1	192.3
RMAG403_RMAG707	2563	13.1	7.6	0.403	35.5	5.1	193.2
RMAG404_RMAG407	2414	12.4	7.1	0.404	39.8	5.1	194.4
RMAG404_RMAG707	2617	13.8	7.9	0.382	37.2	5.3	195.9
RMAG407_RMAG707	2475	12.9	7.4	0.404	34.7	5.2	194.8
RM9_RMAG402	1394	6.5	3.7	0.445	27.5	4.7	185.3
RM9_RMAG403	1361	6.2	3.6	0.445	24.7	4.6	184.7
RM9_RMAG404	1400	6.5	3.7	0.445	25.4	4.6	185.2
RM9_RMAG407	1394	6.6	3.8	0.445	27.5	4.7	186.9
RM9_RMAG707	1430	6.7	3.9	0.445	27.5	4.7	185.6
RM15_RMAG402	1778	8.3	4.8	0.364	37.4	4.7	187.7
RM15_RMAG403	1759	8.0	4.6	0.364	35.7	4.6	185.0
RM15_RMAG404	1798	8.2	4.7	0.364	37.4	4.6	186.5
RM15_RMAG407	1792	8.5	4.9	0.364	34.7	4.8	189.8
RM15_RMAG707	1852	8.7	5.0	0.364	36.9	4.7	187.9
RM15_RM9	1472	7.1	4.1	0.410	28.8	4.8	187.2
(B) *R. socialis*.							
AK11_AK15	1801	10.1	6.7	0.433	47.9	5.6	205.2
AK11_RSOC401	1714	8.8	5.8	0.444	47.9	5.1	204.8
AK11_RSOC405	1698	8.7	5.8	0.456	42.1	5.1	203.6
AK11_RSOC406	1737	9.1	6.0	0.353	41.9	5.2	204.1
AK11_RSOC507	1715	9.0	6.0	0.453	42.6	5.2	205.2
AK11_RSOC702	1737	9.1	6.0	0.456	42.6	5.2	205.3

(B) *R. socialis* (continued).							
AK11_AK16	1611	8.4	5.6	0.456	39.9	5.2	203.4
AK11_AK27	1647	8.9	5.9	0.456	40.0	5.4	205.8
AK11_RS1	1166	5.8	3.8	0.456	40.0	4.9	201.1
AK15_RSOC401	1682	8.6	5.7	0.428	47.9	5.1	204.4
AK15_RSOC405	1688	8.5	5.6	0.433	42.1	5.0	203.0
AK15_RSOC406	1699	8.9	5.9	0.353	41.9	5.2	204.7
AK15_RSOC507	1703	8.8	5.8	0.433	42.6	5.2	204.0
AK15_RSOC702	1721	9.0	6.0	0.433	42.8	5.2	205.8
AK15_AK16	1558	8.1	5.3	0.433	40.5	5.2	204.4
AK15_AK27	1607	8.5	5.6	0.433	40.5	5.3	204.8
AK15_RS1	1119	5.4	3.6	0.310	40.0	4.8	200.9
RSOC401_RSOC405	1821	9.3	6.2	0.453	42.2	5.1	202.4
RSOC401_RSOC406	1830	9.4	6.2	0.394	42.1	5.1	203.3
RSOC401_RSOC507	1816	9.5	6.3	0.453	42.8	5.2	203.2
RSOC401_RSOC702	1848	9.7	6.4	0.421	42.8	5.3	203.4
RSOC405_RSOC406	1804	9.5	6.3	0.478	42.1	5.2	204.9
RSOC405_RSOC507	1843	9.6	6.3	0.478	42.2	5.2	201.2
RSOC405_RSOC702	1867	9.9	6.6	0.421	42.1	5.3	202.5
RSOC406_RSOC507	1836	9.8	6.5	0.488	42.1	5.3	204.1
RSOC406_RSOC702	1841	9.9	6.5	0.359	42.0	5.4	205.8
RSOC507_RSOC702	1876	10.2	6.7	0.493	42.6	5.4	204.7
AK16_RSOC401	1552	7.6	5.0	0.392	38.9	4.9	202.4
AK16_RSOC405	1534	7.5	5.0	0.431	38.9	4.9	202.5
AK16_RSOC406	1571	7.8	5.2	0.432	40.1	5.0	202.2
AK16_RSOC507	1561	7.7	5.1	0.432	40.1	4.9	202.4
AK16_RSOC702	1586	7.9	5.2	0.432	38.9	5.0	203.0
AK16_AK27	1586	8.3	5.5	0.444	50.6	5.2	203.2
AK16_RS1	1123	5.7	3.8	0.473	38.9	5.0	203.6
AK27_RSOC401	1585	7.7	5.1	0.453	37.2	4.9	202.4
AK27_RSOC405	1584	7.7	5.1	0.469	37.5	4.9	201.5
AK27_RSOC406	1600	8.1	5.3	0.469	40.3	5.0	203.3
AK27_RSOC507	1611	8.0	5.3	0.469	40.3	4.9	201.2
AK27_RSOC702	1599	8.1	5.3	0.469	39.8	5.0	205.1
AK27_RS1	1148	5.7	3.8	0.501	38.4	5.0	201.5
RS1_RSOC401	1128	5.3	3.5	0.453	40.2	4.7	200.1
RS1_RSOC405	1132	5.3	3.5	0.521	40.2	4.7	200.0
RS1_RSOC406	1138	5.5	3.6	0.526	40.2	4.8	201.7
RS1_RSOC507	1141	5.5	3.6	0.572	40.2	4.8	201.6
RS1_RSOC702	1142	5.6	3.7	0.518	40.0	4.9	202.2

Table S4. Statistics calculated for each pair of *Rotaria* individuals.

Pair	$p(CL)$	$p(AR)$	$p(SX)$	Δ	K
(A) *R. magnacalcarata*.					
MAG1_MAG2	0.949	0.003	0.048	0.181	0.157
MAG1_MAG3	0.825	0.019	0.156	0.199	0.565
MAG1_RMAG402	0.800	0.018	0.182	0.174	0.574
MAG1_RMAG403	0.794	0.018	0.188	0.173	0.581
MAG1_RMAG404	0.805	0.025	0.169	0.184	0.570
MAG1_RMAG407	0.807	0.019	0.174	0.161	0.629
MAG1_RMAG707	0.800	0.022	0.179	0.173	0.569
MAG1_RM9	0.461	0.218	0.321	0.056	0.319
MAG1_RM15	0.565	0.153	0.282	0.097	0.423
MAG2_MAG3	0.829	0.018	0.153	0.192	0.562
MAG2_RMAG402	0.798	0.029	0.172	0.164	0.569
MAG2_RMAG403	0.788	0.025	0.187	0.180	0.578
MAG2_RMAG404	0.809	0.024	0.166	0.164	0.565
MAG2_RMAG407	0.805	0.027	0.168	0.160	0.628
MAG2_RMAG707	0.808	0.026	0.166	0.161	0.565
MAG2_RM9	0.443	0.224	0.333	0.042	0.320
MAG2_RM15	0.548	0.157	0.295	0.093	0.421
MAG3_RMAG402	0.896	0.005	0.098	0.155	0.176
MAG3_RMAG403	0.891	0.008	0.101	0.161	0.193
MAG3_RMAG404	0.894	0.007	0.099	0.168	0.169
MAG3_RMAG407	0.831	0.017	0.152	0.143	0.472
MAG3_RMAG707	0.925	0.009	0.066	0.150	0.166
MAG3_RM9	0.447	0.233	0.320	0.047	0.316
MAG3_RM15	0.549	0.130	0.321	0.081	0.417
RMAG402_RMAG403	0.972	0.000	0.028	0.178	0.162
RMAG402_RMAG404	0.976	0.001	0.023	0.188	0.140
RMAG402_RMAG407	0.897	0.010	0.092	0.178	0.441
RMAG402_RMAG707	0.976	0.000	0.024	0.169	0.133
RMAG403_RMAG404	0.968	0.000	0.032	0.207	0.159
RMAG403_RMAG407	0.898	0.014	0.088	0.182	0.452
RMAG403_RMAG707	0.974	0.001	0.026	0.183	0.153
RMAG404_RMAG407	0.905	0.009	0.086	0.185	0.437
RMAG404_RMAG707	0.983	0.000	0.017	0.186	0.126
RMAG407_RMAG707	0.910	0.010	0.080	0.184	0.432
RM9_RMAG402	0.461	0.197	0.342	0.048	0.314
RM9_RMAG403	0.455	0.212	0.333	0.051	0.315
RM9_RMAG404	0.434	0.212	0.355	0.065	0.312
RM9_RMAG407	0.439	0.247	0.314	0.052	0.317
RM9_RMAG707	0.466	0.181	0.353	0.053	0.313
RM15_RMAG402	0.531	0.162	0.307	0.108	0.417
RM15_RMAG403	0.552	0.142	0.306	0.110	0.417
RM15_RMAG404	0.540	0.140	0.320	0.116	0.416
RM15_RMAG407	0.539	0.170	0.291	0.106	0.424
RM15_RMAG707	0.539	0.144	0.316	0.110	0.414
RM15_RM9	0.666	0.070	0.264	0.095	0.452
(B) *R. socialis*.					
AK11_AK15	0.911	0.011	0.078	0.190	0.190
AK11_RSOC401	0.888	0.012	0.100	0.161	0.172
AK11_RSOC405	0.885	0.006	0.108	0.139	0.185
AK11_RSOC406	0.848	0.008	0.143	0.148	0.218
AK11_RSOC507	0.871	0.014	0.115	0.129	0.171
AK11_RSOC702	0.867	0.008	0.125	0.128	0.171
AK11_AK16	0.651	0.052	0.297	0.129	0.731
AK11_AK27	0.744	0.031	0.225	0.229	0.672

(B) *R. socialis* (continued).					
AK11_RS1	0.429	0.236	0.335	0.038	0.508
AK15_RSOC401	0.863	0.007	0.130	0.152	0.195
AK15_RSOC405	0.862	0.017	0.121	0.155	0.209
AK15_RSOC406	0.830	0.024	0.146	0.159	0.239
AK15_RSOC507	0.850	0.011	0.139	0.133	0.194
AK15_RSOC702	0.847	0.019	0.135	0.145	0.196
AK15_AK16	0.656	0.068	0.276	0.153	0.731
AK15_AK27	0.756	0.034	0.210	0.217	0.681
AK15_RS1	0.431	0.249	0.320	0.054	0.506
RSOC401_RSOC405	0.943	0.003	0.053	0.178	0.147
RSOC401_RSOC406	0.948	0.003	0.050	0.163	0.180
RSOC401_RSOC507	0.949	0.004	0.047	0.146	0.136
RSOC401_RSOC702	0.960	0.001	0.040	0.159	0.134
RSOC405_RSOC406	0.915	0.005	0.081	0.137	0.189
RSOC405_RSOC507	0.939	0.003	0.057	0.135	0.146
RSOC405_RSOC702	0.952	0.004	0.044	0.172	0.142
RSOC406_RSOC507	0.926	0.007	0.068	0.134	0.180
RSOC406_RSOC702	0.940	0.003	0.057	0.135	0.176
RSOC507_RSOC702	0.927	0.006	0.067	0.142	0.130
AK16_RSOC401	0.679	0.050	0.271	0.153	0.729
AK16_RSOC405	0.660	0.063	0.276	0.135	0.736
AK16_RSOC406	0.639	0.063	0.297	0.136	0.733
AK16_RSOC507	0.673	0.081	0.246	0.123	0.730
AK16_RSOC702	0.633	0.063	0.305	0.116	0.732
AK16_AK27	0.639	0.060	0.301	0.146	0.758
AK16_RS1	0.433	0.224	0.342	0.067	0.561
AK27_RSOC401	0.789	0.013	0.198	0.202	0.661
AK27_RSOC405	0.750	0.025	0.226	0.187	0.669
AK27_RSOC406	0.752	0.024	0.225	0.168	0.678
AK27_RSOC507	0.758	0.015	0.226	0.184	0.665
AK27_RSOC702	0.772	0.034	0.194	0.197	0.662
AK27_RS1	0.456	0.203	0.341	0.037	0.521
RS1_RSOC401	0.420	0.213	0.367	0.059	0.499
RS1_RSOC405	0.463	0.219	0.318	0.062	0.501
RS1_RSOC406	0.435	0.212	0.353	0.068	0.501
RS1_RSOC507	0.434	0.229	0.337	0.072	0.502
RS1_RSOC702	0.480	0.197	0.323	0.060	0.502

References

Bushnell, B. (2017). BBMap short read aligner, and other bioinformatic tools. https://sourceforge.net/projects/bbmap/

Emms, D., & Kelly, S. (2018). STAG: species tree inference from all genes. *bioRxiv*, 267914.

Kozlov, A. M., Darriba, D., Flouri, T., Morel, B., & Stamatakis, A. (2019). RAxML-NG: a fast, scalable and user-friendly tool for maximum likelihood phylogenetic inference. *Bioinformatics*, *35*(21), 4453–4455.

Minh, B. Q., Schmidt, H. A., Chernomor, O., Schrempf, D., Woodhams, M. D., Von Haeseler, A., & Lanfear, R. (2020). IQ-TREE 2: new models and efficient methods for phylogenetic inference in the genomic era. *Molecular Biology and Evolution*, *37*(5), 1530–1534.

Nowell, R. W., Wilson, C. G., Almeida, P., Schiffer, P. H., Fontaneto, D., Becks, L., Rodriguez, F., Arkhipova, I. R., & Barraclough, T. G. (2021). Evolutionary dynamics of transposable elements in bdelloid rotifers. *eLife*, *10*, e63194.

Pieszko, T., Kelleher, J., Wilson, C. G., & Barraclough, T. G. (2025). Detecting and quantifying rare sex in natural populations. *bioRxiv*, 2025.2006. 2003.657731.

Price, M. N., Dehal, P. S., & Arkin, A. P. (2010). FastTree 2–approximately maximum-likelihood trees for large alignments. *PLoS One*, *5*(3), e9490.

General Discussion



——————————— O ———————————

Tymoteusz Pieszko

——————————— O ———————————

Contributions

➔ A classical chapter of which I am the sole author.

Detecting and quantifying sexual reproduction from sequence data remains a surprisingly difficult task. Despite an early optimism (Butlin, 2002; Normark et al., 2003; Schurko et al., 2009), the genomic revolution has generated many new questions on asexual systems but provided fewer definitive answers. This situation can be largely attributed to the lack of methodological developments comparable to those that have driven progress in understanding other fundamental issues, like speciation (e.g., Hey & Nielsen, 2004; Gutenkunst et al., 2009; Excoffier et al., 2021). In fact, among the literature cited in a recent paper produced by the Tree of Sex initiative (Jeffries et al., 2025), of which I am a member, primary studies on sex determination alone outnumber those on non-canonical reproductive systems by over a factor of two. One might argue that the population genomics of asexuality is a weirdly neglected frontier.

In the General Discussion, I take a broader view on the research presented in this thesis. I identify explicit consideration of natural selection as the most important omission from the implementation of the developed approaches and outline several directions for future work.

In the grip of summaries

Research on reproductive mode evolution has been so far hampered by the lack of dedicated methodology of inference. Here, again, an analogy with the speciation field comes to mind. A major goal of speciation research has been to identify barrier loci, i.e., regions of reduced gene flow between incipient species (Wu, 2001; Ravinet et al., 2017). In a widely held ‘continuum’ view of the process (Stankowski & Ravinet, 2021), the barrier effect progressively extends across the genome as speciation progresses towards an established species barrier at the endpoint. Nonetheless, the bulk of studies aiming to identify barrier loci has employed a genome scan approach, where a summary statistic, such as the differentiation index F_{ST}, is calculated genome-wide in search of outlier loci (Lewontin & Krakauer, 1973). While these outliers have been interpreted as putative barriers (Wolf & Ellegren, 2017), multiple unrelated processes drive variation in F_{ST} and other summaries,

including selective sweeps, background selection, and coalescent stochasticity (Noor & Bennett, 2009; Cruickshank & Hahn, 2014; Ravinet et al., 2017). It remains an open question just how much our view of speciation is biased by mis-interpretated summary statistics, but joint modelling of selection and gene flow (e.g., Laetsch et al., 2023) and ARG reconstruction (e.g., Pal et al., 2025) are promising ways to provide more rigorous insights.

While interest in the population genomics of mixed reproduction certainly does exist (Lynch et al., 2017), the key component – the inference of reproductive history – has not yet advanced beyond point summaries. On the other hand, model-based approaches (Lam et al., 2011; Nicoll et al., 2024) are based on the typically unrealistic assumption of non-recombining asexuality. Ideally, just like the ‘genomic landscape of speciation’ (Ravinet et al., 2017), one would like to see a ‘genomic landscape of reproduction’ investigated across diverse systems and with an explicit consideration of genome-wide heterogeneity. Even consideration of neutral scenarios paints this landscape as highly dynamic, with potentially striking variation in within and cross-locus patterns of diversity driven by asyngamous recombination and, if present, rare sex. While the present research provides the building blocks to explore such landscapes, there is one key factor I did not consider in the context of reproductive history reconstruction – selection.

Selection and the genomic landscape of reproduction

Fig. 1 shows a time-series of the mean fitness of obligate asexual populations under a simple scenario of background selection using my MP model (Kershenbaum et al., in review). A conclusion from this and another simulation model (Kopčak & Hartfield, 2024) is that LOH facilitates the purging of deleterious mutations, rescuing mean population fitness. Neither of these models, however, include the ecological costs of purging: lower absolute fitness, population decline, and higher probability of extinction. Given this observation, how could selection, asyngamous recombination and sex shape the genomic landscape of reproduction in groups where sex is at most rare?

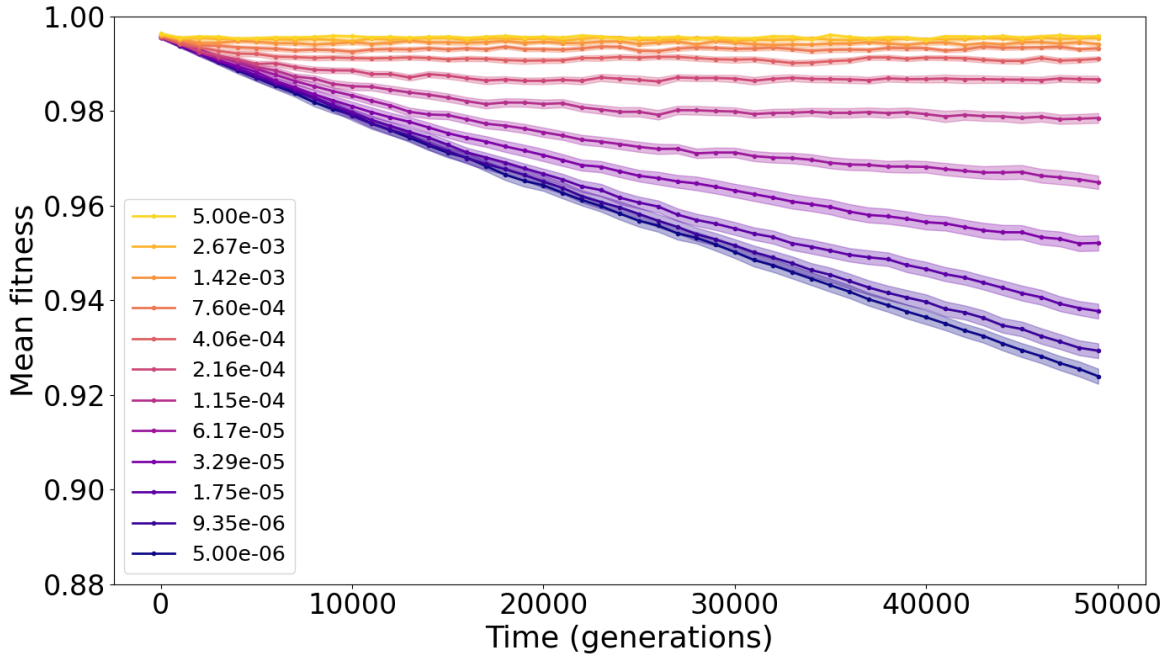


Fig. 1. Asyngamous recombination-associated LOH rescues fitness of asexual populations: a time-series. MP scenarios (chromosome length L = 1 Mb; population size N = 1,000; mean gene conversion tract length λ = 5,000 bp) were simulated with γ varying between 5 × 10^{-6} and 5 × 10^{-3}, and the per-site per-generation mutation rate μ of 5 × 10^{-9}. Each scenario was replicated 100 times. In a simple model of background selection, selection coefficients s of new mutations were drawn from a gamma distribution $s \sim Gamma(\bar{s} = -0.01,\ \alpha = 0.2$, where $\bar{s}$ is the mean and α is the shape parameter. Dominance coefficients were fixed at 0.2. Shaded areas represent 95% confidence intervals.

One broad and one specific observation can be made with relevance to spurious sex signals in asyngamous landscapes of reproduction. First, there is a strong Darwinian expectation for the rate of recombination, including that of asyngamous recombination, to be fine-tuned to maximise its benefits and minimise its costs (Lenormand & Otto, 2000). If purging is one benefit and lower absolute fitness is a cost, recombination rates could be expected to reflect these opposing forces as a trade-off. In asexual systems where the mode of ploidy restoration maintains heterozygosity (mitotic asexuality, central fusion automixis), spontaneous rates of LOH are orders of magnitude higher than typical eukaryotic rates of mutation (Chapter 1, Table S2; cf. Wang & Obbard, 2023), suggesting that ‘testing’ new mutations in the homozygous state is essential in asexuals. This point can be illustrated with a simple diploid two-locus example. Assume a recessive beneficial mutation at locus A is

fixed in the heterozygous state in a population of N = 1,000 individuals. Once converted to homozygosity, the beneficial homozygous genotype instantly sweeps to fixation. Given a per-site, per-generation mutation rate of $\mu = 10^{-9}$ and a per-individual, per-generation probability of locus A becoming homozygous for the beneficial mutation $c_A = 10^{-6}$, the probability that this occurs before a potentially interfering mutation arises at locus B is $\frac{Nc_A}{Nc_A + 2N\mu} \approx 0.998$. Combined with the fecundity advantage of uniparental reproduction (compensating for higher offspring mortality), why would variation patterns in asexual groups not appear sex-like?

Second, a more specific argument can draw on the ecology of bdelloid rotifers. Bdelloid population sizes can be enormous, reaching millions of individuals per square metre (Dartnall, 1992; Suren, 1990). In addition, meta-populations of many bdelloid species are expected to undergo extensive mixing, primarily though wind dispersal in the anhydrobiotic state (Fontaneto et al., 2008; Wilson & Sherman, 2010). With large, well-mixed populations offering clear benefits to the efficiency of selective responses, one can further imagine how such conditions might facilitate local frequency-dependent selection among asexual lineages – for example, through ecological interactions with fungal pathogens (Wilson & Sherman, 2010). If local adaptation occurs through LOH, and different lineages fix distinct homozygous genotypes across loci, bdelloid population structure could further facilitate the recovery of mixed AR-CL (‘spurious sex’) signals. Verification of this idea could come from combined spatial and temporal analyses of natural bdelloid populations.

When asexual lineages do suffer clonal erosion, rare sex could bring immediate benefits through the complementation of accumulated recessive deleterious mutations ('heterosis'; Hochholdinger & Yu, 2025). Laine et al. (2022) speculated on how such high-fitness outcrossed lineages could displace their non-outcrossed relatives across vast geographical scales in the bdelloid *Macrotrachela quadricornifera*. Such a scenario could lead to overrepresented sex signatures relative to the true frequency of sex. Nonetheless, genomic

alteration that mimic sex-like signatures, such as ploidy cycles (General Introduction, Fig. 2D), could bring similar benefits and lead to comparable population-level patterns. While polyploidy itself could bring benefits through the masking of deleterious mutations (Otto, 2007), one could also imagine a scenario in which the loss of a genome copy (e.g., a transition from triploidy to diploidy) produces a sudden fitness increase, either through a reduced dosage of deleterious mutations (from 66% to 50%) or an increased dosage of beneficial ones (from 66% to 100%). Patterns of ploidy variation and aneuploidy have been documented within asexual populations (Dujardin et al., 2014; Zhu et al., 2016), suggesting such events are not unlikely and would make an interesting subject of future simulation work.

Improved simulation-based inference

In my reconstruction of *Rotaria* reproductive histories, I interpreted the observed metrics in light of simplistic simulated scenarios in which single 1 Mb chromosomes evolved under gene conversion as the sole source of asyngamous recombination in populations of 1,000 individuals. There was a rationale behind this approach: for example, using a gene conversion-only model of asexuality (as opposed to, e.g., the CF model from Chapter 1) is justified as long as the interpreted metrics depend solely on the rate of LOH. There is nonetheless an obvious space for improved simulation-based inference. Particularly interesting opportunities are open for the ‘model bdelloid’ *Adineta vaga*, where both a chromosome-level genome assembly (Simion et al., 2021) and data on spontaneous genome-wide rates of LOH (Houtain et al., 2024) are available. Further leveraging the functionalities of SLiM, one could imagine in silico experiments where the actual *A. vaga* sequence evolves under asexual and sexual scenarios (see section 18.2 of the SLiM manual; Haller & Messer, 2024). A very recent addition to SLiM is the explicit support for simulating multiple chromosomes (Haller et al., 2025), which would allow to quantify signatures of reproductive mode against an explicit model of the focal genome, including the cross-chromosome genealogical discordance expected due to independent assortment during canonical meiosis.

One general lesson from my DPhil work is that spurious signatures of sex can be readily recovered under obligate asexuality. As a solution, I proposed an ARG-grounded quantitative framework that integrates multiple genealogical features explicitly linked to reproductive mode. One additional aspect that I touched on in Chapter 2 but did not have the chance to expand upon is the consideration of additional sources of technical error, such as sequencing or mis-mapping errors. A low-hanging fruit would be to 'sprinkle' such error on top of simulated genealogies. It would be particularly interesting to study the length distribution of the resulting SX blocks and compare it with those recovered in *Rotaria* (Chapter 3).

What's next for bdelloid rotifers?

What will constitute convincing evidence of sex in bdelloid rotifers? Datasets containing multiple chromosome-scale, fully haplotype-resolved genomes will be available very soon. In my thesis, I developed analytical tools that are precisely tailored for such datasets. One can hope that, through innovative applications of non-parametric, ARG-based approaches, far stronger evidence for, or against, bdelloid sexuality will emerge in the coming years.

So, do bdelloid rotifers have sex? There exists an enormous diversity of asexual and, more broadly, genetic systems that are not explained by classical theory on the rates of sex and clonality. The many non-canonical cases discovered in recent years (Ross et al., 2022; Jeffries et al., 2025) may represent only the tip of the iceberg. Yet, recovered patterns can only be interpreted within the limits of existing knowledge. Ultimately, until photographic documentation of male or hermaphrodite bdelloid individuals becomes available, the answer will always be – *maybe*.

References

Butlin, R. (2002). The costs and benefits of sex: new insights from old asexual lineages. *Nature Reviews Genetics*, *3*(4), 311–317.

Cruickshank, T. E., & Hahn, M. W. (2014). Reanalysis suggests that genomic islands of speciation are due to reduced diversity, not reduced gene flow. *Molecular Ecology*, *23*(13), 3133–3157.

Dartnall, H. J. (1992). The reproductive strategies of two Antarctic rotifers. *Journal of Zoology*, *227*(1), 145–162.
Dujardin, J.-C., Mannaert, A., Durrant, C., & Cotton, J. A. (2014). Mosaic aneuploidy in Leishmania: the perspective of whole genome sequencing. *Trends in parasitology*, *30*(12), 554–555.
Excoffier, L., Marchi, N., Marques, D. A., Matthey-Doret, R., Gouy, A., & Sousa, V. C. (2021). fastsimcoal2: demographic inference under complex evolutionary scenarios. *Bioinformatics*, *37*(24), 4882–4885.
Fontaneto, D., Barraclough, T. G., Chen, K., Ricci, C., & Herniou, E. A. (2008). Molecular evidence for broad-scale distributions in bdelloid rotifers: everything is not everywhere but most things are very widespread. *Molecular Ecology*, *17*(13), 3136–3146.
Gutenkunst, R. N., Hernandez, R. D., Williamson, S. H., & Bustamante, C. D. (2009). Inferring the joint demographic history of multiple populations from multidimensional SNP frequency data. *PLoS Genetics*, *5*(10), e1000695.
Haller, B. C., & Messer, P. W. (2024). SLiM: An Evolutionary Simulation Framework. In.
Haller, B. C., Ralph, P. L., & Messer, P. W. (2025). SLiM 5: Eco-evolutionary simulations across multiple chromosomes and full genomes. *bioRxiv*, 2025.2008. 2007.669155.
Hey, J., & Nielsen, R. (2004). Multilocus methods for estimating population sizes, migration rates and divergence time, with applications to the divergence of Drosophila pseudoobscura and D. persimilis. *Genetics*, *167*(2), 747–760.
Hochholdinger, F., & Yu, P. (2025). Molecular concepts to explain heterosis in crops. *Trends in Plant Science*, *30*(1), 95–104.
Houtain, A., Derzelle, A., Llirós, M., Hespeels, B., Nicolas, É., Simion, P., Virgo, J., Lenormand, T., Hallet, B., & Van Doninck, K. (2024). Transgenerational chromosome repair in the asexual bdelloid rotifer *Adineta vaga*. *bioRxiv*, 2024.2001.2025.577190. https://doi.org/10.1101/2024.01.25.577190
Jeffries, D., Benvenuto, C., Böhne, A., Fraisse, C., Garcia, S., Jay, P., Kratochvíl, L., McDonough-Goldstein, C. E., Ruiz-Herrera, A., & Sotero-Caio, C. G. (2025). The Tree of Sex consortium: A global initiative for studying the evolution of reproduction in eukaryotes. *Journal of Evolutionary Biology*, voaf053.
Kopčak, D., & Hartfield, M. (2024). How do self-fertilising and facultative sexual populations differ in mutation accumulation? *bioRxiv*, 2024.2008. 2030.610445.
Laetsch, D. R., Bisschop, G., Martin, S. H., Aeschbacher, S., Setter, D., & Lohse, K. (2023). Demographically explicit scans for barriers to gene flow using gIMble. *PLoS Genetics*, *19*(10), e1010999.
Lam, F., Langley, C. H., & Song, Y. S. (2011). On the genealogy of asexual diploids. *Journal of Computational Biology*, *18*(3), 415–428.
Lenormand, T., & Otto, S. P. (2000). The evolution of recombination in a heterogeneous environment. *Genetics*, *156*(1), 423–438.
Lewontin, R. C., & Krakauer, J. (1973). Distribution of gene frequency as a test of the theory of the selective neutrality of polymorphisms. *Genetics*, *74*(1), 175–195.
Lynch, M., Gutenkunst, R., Ackerman, M., Spitze, K., Ye, Z., Maruki, T., & Jia, Z. (2017). Population genomics of Daphnia pulex. *Genetics*, *206*(1), 315–332.
Nicoll, A. G., Kilford, H., Grace, C. A., Reis-Cunha, J. L., Jeffares, D. C., & Constable, G. W. (2024). Estimating the rate of sexual reproduction and the inbreeding rate in Leishmania. *bioRxiv*, 2024.2010. 2015.618469.
Noor, M. A., & Bennett, S. M. (2009). Islands of speciation or mirages in the desert? Examining the role of restricted recombination in maintaining species. *Heredity*, *103*(6), 439–444.
Normark, B. B., Judson, O. P., & Moran, N. A. (2003). Genomic signatures of ancient asexual lineages. *Biological Journal of the Linnean Society*, *79*(1), 69–84.
Otto, S. P. (2007). The evolutionary consequences of polyploidy. *Cell*, *131*(3), 452–462.

Pal, A., Shipilina, D., Le Moan, A., McNairn, A. J., Grenier, J. K., Kucka, M., Coop, G., Chan, Y. F., Barton, N. H., & Field, D. L. (2025). Genealogical analysis of replicate flower colour hybrid zones in Antirrhinum. *Molecular Ecology*, e70067.

Ravinet, M., Faria, R., Butlin, R. K., Galindo, J., Bierne, N., Rafajlović, M., Noor, M. A. F., Mehlig, B., & Westram, A. M. (2017). Interpreting the genomic landscape of speciation: a road map for finding barriers to gene flow. *Journal of Evolutionary Biology*, *30*(8), 1450–1477. https://doi.org/https://doi.org/10.1111/jeb.13047

Ross, L., Mongue, A. J., Hodson, C. N., & Schwander, T. (2022). Asymmetric inheritance: the diversity and evolution of non-Mendelian reproductive strategies. *Annual Review of Ecology, Evolution, and Systematics*, *53*, 1–23.

Schurko, A. M., Neiman, M., & Logsdon, J. M. (2009). Signs of sex: what we know and how we know it. *Trends in ecology & evolution*, *24*(4), 208–217.

Simion, P., Narayan, J., Houtain, A., Derzelle, A., Baudry, L., Nicolas, E., Arora, R., Cariou, M., Cruaud, C., & Gaudray, F. R. (2021). Chromosome-level genome assembly reveals homologous chromosomes and recombination in asexual rotifer Adineta vaga. *Science Advances*, *7*(41), eabg4216.

Stankowski, S., & Ravinet, M. (2021). Defining the speciation continuum. *Evolution*, *75*(6), 1256–1273.

Suren, A. (1990). Microfauna associated with algal mats in melt ponds of the Ross Ice Shelf. *Polar Biology*, *10*(5), 329–335.

Wang, Y., & Obbard, D. J. (2023). Experimental estimates of germline mutation rate in eukaryotes: a phylogenetic meta-analysis. *Evolution Letters*, *7*(4), 216–226.

Wilson, C. G., & Sherman, P. W. (2010). Anciently asexual bdelloid rotifers escape lethal fungal parasites by drying up and blowing away. *Science*, *327*(5965), 574–576.

Wolf, J. B., & Ellegren, H. (2017). Making sense of genomic islands of differentiation in light of speciation. *Nature Reviews Genetics*, *18*(2), 87–100.

Wu, C. I. (2001). The genic view of the process of speciation. *Journal of Evolutionary Biology*, *14*(6), 851–865.

Zhu, Y. O., Sherlock, G., & Petrov, D. A. (2016). Whole genome analysis of 132 clinical Saccharomyces cerevisiae strains reveals extensive ploidy variation. *G3: Genes, Genomes, Genetics*, *6*(8), 2421–2434.